Improving mine haul road performance through innovative material treatment using Nano-Modified Emulsions (NME's)

Bohlajana Qacha

Thesis presented in the partial fulfilment
of the requirement for the degree of
Master of Engineering(Civil Engineering)
at the University of Stellenbosch

Supervisor : Prof. Kim J. Jenkins

April 2022

DECLARATION

By submitting this thesis electronically, I declare that the entirety of the work contained therein is my own, original work, that I am the sole author thereof (save to the extent explicitly otherwise stated), that reproduction and publication thereof by Stellenbosch University will not infringe any third party rights and that I have not previously in its entirety or in part submitted it for obtaining any qualification.

Date : April 2022

ACKNOWLEDGEMENTS

I would like to express my gratitude and appreciation to the following individuals and organisations for their contribution in completing this thesis

- My supervisor and mentor, Prof. Kim Jenkins for his guidance, interest, and sheer dedication to ensuring that I am in the right direction. My sincere gratitude to Prof for always having the time to engage and enlighten me. This work would have not been possible without him.
- First Quantum Minerals Limited (FQML) for funding my studies, this work would have been impossible without thier sponsorship.
- Professor Jan Wium for his assistance with partly funding my living expenses during this research.
- Mr Colin, Gavin and Eric for their technical expertise and handy work in the laboratory.
- The laboratory manager, Guillaume Nel for his guidance and assistance with equipment operating procedures.
- My brother and mother, Sefako and 'Masefako Qacha, whose love and kindness remain endless.
- My friends Rorisang Morenammele, Learongoa Shale and Herline Van der Spuy for their insights and advice.
- My colleagues whom I have spent countless days in the PGRL for the insights, company, and jokes.
- Ruvimbo Zawu for the support and assitance
- My Lord and Saviour for carrying me throughout this research, proving me with the will and wisdom to complete it.

ABSTRACT

Mine haul roads require reliable riding quality for optimally low transport costs and truck maintenance. This is part of functional, structural, and pavement management systems. The extremely heavy traffic, environment (heavy rains), spillage of ore all contribute to the need of improving the design life of haul roads. Soil mineral phase analysis is a necessary test to understand the contribution of minerals within the aggregates to withstand the load-bearing requirements. More recently nanotechnology related to the stabilization of the load-bearing layers e.g., NME's (Nano-Modified Emulsions) have improved the strength and durability of haul road layers. The efficiency of the NME's depends on the mineralogy and requires chemical testing to evaluate the efficiency of the existing aggregate.

This study determines the effectiveness of organosilane compounds to improve mechanical properties, strength, hydrophobicity, and load-load bearing capacity of haul road base construction materials. Mechanical tests are key to understanding the performance of nano modified materials. For this project, mineralogy test samples include untreated and treated materials of both the crushed stone and Laterite aggregates from the Zambian Copperbelt. The expectation is to identify both primary and secondary minerals present in the aggregates and their composition. To evaluate shear strength and permeability of treated and untreated materials. This will enable the prediction of the aggregates' behaviour. The selected additives include nano silanes and modified bitumen and need to be benchmarked against untreated materials.

Research results indicate that organosilane compounds influence strength and water ingress in unbound granular materials particularly crushed stone. Small amounts of organosilane compounds offer optimum mix performance. Lime addition results in a decrease in tensile strength in all material mix designs. Mix components compatibility influences the effectiveness of stabilisation. Blending organosilane compounds into bitumen emulsion is an optimum incorporation mechanism, although this may depend on available equipment and aggregate types. There is decreased moisture ingress or hydrophobic properties on nano modified granular materials. In dry conditions natural aggregates and crushed stone show high strength.

Key words:
Haul Road; Pavement Materials; Nanotechnology; Mineralogy; Compatibility;
Nanosilane; Organosilane

OPSOMMING

Mynvervoer paaie vereis betroubare rygehalte vir optimaal lae vervoerkoste en onderhoud van vragmotors. Dit is deel van funksionele, strukturele en plaveiselbestuurstelsels. Die buitengewone swaar verkeer, Natuurelemente (swaar reën), mors van erts, dra alles by tot die verbetering van die ontwerp lewe van mynvervoer paaie. Kwalitatiewe ontleding van grondmineraal is 'n noodsaaklike toets om die bydrae van minerale in die aggregate te verstaan om aan die lasvereistes te voldoen. Meer onlangs het nanotegnologie wat verband hou met die stabilisering van die draende lae, bv.NME (Nano-gemodifiseerde Emulsies) die sterkte en duursaamheid van die vervoerpaaie verbeter. Die doeltreffendheid van die NME's hang af van die mineralogie en vereis chemiese toetsing om die doeltreffendheid van die bestaande aggregaat te evalueer.

Hierdie studie bepaal die doeltreffendheid van organosilaanverbindings om meganiese eienskappe, sterkte, hidrofobisiteit en die dravermoë van die konstruksiemateriaal van die padbasis te verbeter. Meganiese toetse is die sleutel tot die begrip van die werkverrigting van nano-gemodifiseerde materiale. Vir hierdie projek bevat mineralogie-toetsmonsters onbehandelde en behandelde materiale van beide die fyngemaakte klip- en Latreietaggregate van die Zambiese Copperbelt. Die verwagting is om primêre en sekondêre minerale wat in die aggregate en die samestelling daarvan voorkom, te identifiseer. Om die skuifsterkte en deurlaatbaarheid van behandelde en onbehandelde materiale te evalueer. Dit sal die voorspelling van die aggregaat se gedrag moontlik maak. Die geselekteerde bymiddels bevat nano-silane en gemodifiseerde bitumen en moet vergelyk word aan onbehandelde materiale.

Navorsingsresultate dui daarop dat orgaanosilaanverbindings die sterkte en die waterindringing beïnvloed in ongebonde korrelmateriaal, veral fyngemaakte klip. Klein hoeveelhede organosilaanverbindings bied optimale mengselprestasie. Die byvoeging van kalksteen lei tot die afname in trek sterkte in alle materiaalmengsels. Verenigbaarheid van mengkomponente beïnvloed die doeltreffendheid van stabilisering. Die vermenging van organosilaanverbindings in bitumen emulsies is 'n optimale inskakeling meganisme, alhoewel dit mag afhang van die beskikbaarheid van toerusting en aggregaat tipes. Daar is 'n verminderde vogindringing of hidrofobiese eienskappe op nano-gemodifiseerde korrelmateriaal. In droë toestande toon natuurlike aggregate en fyngemaakte aggregaat hoë sterkte.

TABLE OF CONTENTS

LIST OF FIGURES

LIST OF TABLES

LIST OF APPENDICES

LIST OF ABBREVIATIONS AND/OR ACRONYMS

MHR	Mine Haul Roads
NP	Nanoparticles
NME	Nano Modified Emulsions
BSM	Bitumen Stabilized Materials
XRD	X-Ray Diffraction
ITS	Indirect Tensile Strength
USBM	United States Bureau of Mines
RR	Rolling Resistance
RRI	Rolling Resistance Index
CBR	California Bearing Ratio
IRI	International Roughness Index
GVM	Gross Vehicle Mass
RDS	Roughness Defect Score
ESSV	Equipment Size Sensitive Variables
RPM	Revolutions Per Minute
CS	Crushed Stone
GCS	Graded Crushed Stone
SAPEM	South African Pavement Engineering Manual
TG 2	Technical Guideline 2
RBI	Road Building International
UCS	Unconfined Compressive Strength
DPP	Dry Powdered Polymer
PI	Plasticity Index
CNF	Carbon nanotubes
CNT	Carbon nanofibers
JNP	Janusparticle
TRH	Technical Recommendations for Highways
COLTO	Committee of Land Transport Officials
MDD	Maximum Dry Density

OMC	Optimum Moisture Content
UGM	Unbound Granular Materials
HVS	Heavy Vehicle Simulator
OB	Overburden
LA	Los Angeles
DSR	Deviator Stress Ratio
TSR	Tensile Stress Ratio
HPP	High Pressure Permeability
ANOVA	Analysis Of Variance

CHAPTER 1

INTRODUCTION

1.1 BACKGROUND

1.1.1 Mine haul Roads

Africa has significant global mineral reserves. The major mining countries in Southern Africa include Zimbabwe, Namibia, South Africa,Lesotho and Zambia. In most of these countries, the type of mining is an open pit, as a result, mineral transportation is a critical and central operation of these mines. To optimize the operation and sustainability of a mine, haul roads need improvement and customized solutions to their challenges.

Increasing traffic loading and varying extremities in climate conditions lead to an increase the demand for wearing course and base layers to perform and protect the underlying pavement. The haul road network in most open cast mine sites is unsurfaced and constructed using freely accessible material. The layers are not waterproof and barely water-resistant. The large dump trucks transfer ore from the pit to processing plants or dumpsites on constructed haul roads.

Thompson and Visser (1996) argue that the current haul road design approach, material quality, and operating performance are inadequate. The expansion of mining leads to the deployment of ultra-heavy dump trucks with payloads above 260 tons, yet the roads have been designed empirically, or not at all. This is because unlike public roads which has been designed and constructed by pavement engineers, haul roads are designed and constructed by mine officials whose core business is not road construction (Paige-Green and Heath, 1999). The recent mine haul road technology such as autonomous trucks and trolley lines necessitates innovation in haul road construction and material quality. There is minimum path wander and high channelized traffic per area, these will require a change in operating procedures, better materials, and a customized design solution for optimum performance.

Most haul roads construction in Southern African mines barely follows any engineering standard. Poor design and construction practices will lead to prohibitive running costs. Haulage costs are approximately 50% of the total costs incurred by a surface mine (Thompson and Visser, 1996), bound to surge with increasing truck size and conservative haul road design, construction, and maintenance systems. Existing pavement systems will be insufficient and costly concerning vehicle operating and maintenance costs.

Spillage of the payload is also a complicated challenge facing haul roads, it affects the tyre life significantly due to increased tyre penetrations. Tyre damage and penetration depend on the

spillage angularity and quantity on the road surface. Paige-Green and Heath (1999) mention that most tyre wear and tear result from dump trucks driving over fallen-off aggregate, forcing them to bounce severely, causing failure of suspension mountings. Although strategies are available to manage spillage, most vehicles ride over it before removal and destroy the tyres. It mostly occurs at curves or bends due to poor geometric design parameters such as small curve radius, it can potentially change wearing course properties and surface conditions. Visser (2015) explains that at one mine, a dump truck transported liquid mud to the loading point but it spilled along the haul road. This led to excessive dust during dry seasons, but it could also lead to extremely slippery conditions during rainfall seasons if not removed.

1.1.2 Pavement Materials

High-quality pavement materials are rarely available for the construction of haul roads given their scarcity and remoteness of mining sites. In addition, crusher activities are invariably set up for processing the mine material and not for crushing aggregates to provide accurate gradings for haul road pavements. Hauling high-quality rocks from distant areas is prohibitively expensive due to the low value-weight ratio. Tannant and Regensburg (2001) states 73% of 37 Canadian mine sites used local waste material for road construction, excluding the wearing course, while 9% used crushed stone. Furthermore, 82% of the mines used blasted crushed rock while only 9% used crushed sandstone.

Freely accessible materials lead to favorable construction costs. However, using these materials requires an understanding of their geology and petrology because of a higher risk of premature failure in pursuit of minimum costs (Paige-Green, 2003). The use of marginal materials is acceptable for lighter pavement structures. It is crucial to understand their long-term performance and durability in haul road construction. Potholes, rutting, and settlement are major challenges facing haul roads due to poor material quality, *ad-hoc* approach to construction, and lack of proactive attitude to change.

Rainy seasons are a threat to haul roads due to slippery conditions, so construction materials must provide satisfactory performance throughout all seasons. The response of road materials to traffic, water, and other environmental conditions is dependent on the material quality and soundness of construction practices. Marginal aggregates would need to be treated to offer exceptional performance under these challenges. Water ingress is the most calamitous distress condition in pavement construction (Paige-Green and Heath, 1999), therefore material quality and selection are critical to ensure minimum haul road deterioration. Aggregates must have the following attributes.

- Well graded for optimum particle interlock

- High bulk strength to resist shear and plastic deformation
- Sufficient aggregate strength to resist fracturing under wheel loads.

Compacted natural gravel, crushed stone, and gravel mixtures have been primarily used as construction materials for base and surface layers of haul roads. (Thompson and Visser, 2000*b*). The insufficiency of these materials next to a mining site leads to the use of marginal local materials, resulting in considerable improvement in maintenance frequency. Blading intervals increases to 7 days instead of 3-4 days for 45 kt dump truckload (Visser, 2015). Substandard materials lead to high defect progression scores on corrugations, rutting, and stoniness. These failure mechanisms influence riding quality and rolling resistance, ultimately an increase in rolling resistance results in energy and productivity loss. It is critical to note that marginal materials used at mine sites require agile modification to meet specifications, sustain ultra-heavy traffic loading and resist adverse climate conditions.

The load-bearing capacity of base layers needs to exceed the expected ultimate loading to avoid premature deformation or structural failures. A typical dump truck has a footprint area of approximately 1.13m^2, an equivalent diameter of 1.2m (Tannant and Kumar, 2000). Induced strains due to stress levels should be controlled to below the critical strain limit of 2000 microns (Thompson, 2009) for Category 2 haul roads to continue functioning as one structural unit. Blasted crushed waste rock is more appropriate as a base layer for considerable improvement in road performance.. The recommended design method for mine haul roads is a mechanistic-empirical approach. It has a relatively higher load-bearing capacity protecting the subgrade from deformation (Thompson, 2009)

1.1.3 Why innovate materials

The intention of introducing innovation to haul road materials is to improve haulage efficiency, ensure continuous growth of the mine, and increase productivity. Due to the increasing size of trucks (Thompson and Visser, 1996) and the expansion of mining activities, there is a need for a technological approach to revolutionize construction materials to meet the current needs of the industry. An example of an innovative approach to pavement materials is the use of nanotechnology in road stabilization. In this way, modified binders are developed to increase material durability, bearing capacity, water resistance, and road performance. The nanotechnology additives are mixed in either water or bitumen emulsions to form a new age binder known as Nano-Modified Emulsion (NME).

Compared to stabilization using neat bitumen, NME's use a small amount of residual binder content

(up to 2%), therefore cost-effective. They offer high strength at lower application rates, there is improved bitumen emulsion distribution throughout the pavement layer. In Gauteng, 0.3% to 0.7% of the polymer-modified emulsion was used to stabilize a G7 material. This leads to high strengths i.e. ITS and UCS results at a 0.7% application rate, equivalent to a C4 layer strength criteria (Jordaan and Kilian, 2016). The additives developed for use in soil stabilization so far are 100% organosilane.

Despite significant research done on the potential effect of NME's in pavement engineering, application of this technology to haul roads is limited. The focus has been narrowed to low-volume roads particularly in South Africa, Eswatini, and Namibia. Jordaan and Kilian (2016) explains that material enhancement technologies such as nanosilanes have had a narrow application in South Africa. Their successful tests and application in Limpopo and Gauteng have shown that they reduce water susceptibility, improve dispersion, surface coverage, and effectiveness of a bitumen emulsion.

Jordaan *et al.* (2017*a*) observe that local materials are defined as problematic or non-standard due to their inability to meet European or American standards. Nanotechnology products can reduce the negative impact of problem minerals in marginal materials. Load bearing capacity and durability of local waste rock and natural gravels used in haul road construction can potentially be increased through stabilization using NME or conditioning with organosilane treatments. Moreover, due to water resistance exhibited by this innovative material solution, it is possible that during wet conditions and rainy seasons downtime will be reduced as the roads may still be passable

In summary, innovative material solutions are necessary to meet increasing demands on pavements. These demands are in terms of increased traffic, increased axle loads or payloads, increased tyre pressure due to the advent of ultra-class trucks, and adverse climatic conditions. Emulsions are therefore modified to minimize the total cost of construction under these demands, increase material durability and resistance against adverse climate and reduce life cycle costs.

1.2 PROBLEM STATEMENT

Few specifications define appropriate haul road construction materials including Kaufman and Ault (1978); Paige-Green and Heath (1999); Thompson and Visser (2000*b*). However, these primarily consider using quality crushed stone instead of blasted crushed waste rock and natural gravel. Road stabilization using modified binders has been applied widely to public roads but barely to haul roads to meet pavement demands in a dynamic world and market needs. NMEs have been used to stabilize low-volume roads though there is still limited peer-reviewed research on their effectiveness in road construction generally. The research seeks to understand the feasibility of

NME's in haul roads and their effectiveness in improving the load-bearing capacity of materials.

Crushed mine waste rock and local natural gravels can be used as an alternative to high-quality crushed stone, provided that the marginal materials have the required mineralogy compatible with the treatment methods. A pure emulsion is usually used to stabilize these materials. Previous research has reported that local materials perform adequately but have not been used widely in Southern Africa because they do not meet European material standards. Investigations are needed to check the compatibility of the local materials with the treatment methods.

1.3 AIM AND OBJECTIVES

The primary aim is to determine the effectiveness of organosilane compounds to increase the mechanical properties, strength, durability, and load-bearing capacity of construction material of a haul road base. Aggregate materials considered for the study are lateritic soil and crushed waste rock. The research will assist in understanding the behavior of NME treated materials and their potential application as haul road construction materials. Objectives mentioned below will help reach the mentioned research aim.

- Characterize materials using standard laboratory tests and XRD in order to gain insights on compatibility of the material with respect to mineralogy for stabilisation
- Determine the optimum mix design of both laterite soil and crushed stone by varying both preblended emulsion and organosilane application rates. Lime will be the only active filler applied in preblended emulsion mixes. Performance evaluation of all the mixes will be carried out using Indirect Tensile Strength tests ITS.
- Conduct moisture susceptibility tests through soaking specimens in water and testing their ITS. Further, test the permeability of silane treated and untreated samples using high-pressure permeability tests to understand resistance to water ingress.
- Use different blending techniques and identify optimum approach depending on the material, performance, and ease of application
- Evaluate the shear properties through monotonic triaxial testing and resilient modulus using a dynamic triaxial test of NME treated materials to understand their response to loading.

1.4 RESEARCH SCOPE

The scope is narrowed characterizing both laterite soil and crushed stone aggregates using standard lab test and X-ray diffraction. It encompasses tests and analysis of laterite aggregate and crushed

stone mix design as treated materials and as NME stabilized materials. Optimum mix designs from ITS will be used to check performance through triaxial testing. Modified optimum mixes per material will also be tested for permeability under high pressure then benchmarked against control mixes.

1.5 SIGNIFICANCE OF THE RESEARCH

The research contributes to knowledge about the application of NME's on pavement engineering. It can influence more research on NME's application to marginal materials previously considered problematic and unfit for construction purposes. The study outcomes will assist pavement engineers at mining sites, designing haul roads considering innovative stabilization of local materials for better road quality and performance. The findings of this research may also assist in drafting technical guidelines for nano-modified treated materials in both public roads and haul roads.

1.6 RESEARCH LIMITATIONS

- Only two organosilanes have been selected for use due to time constraints, more organosilane additives will require more time.
- Blending organosilane in the bitumen was only considered using one cationic bitumen only. Using other emulsions would require more time and materials.
- The complex chemistry of preblended negative emulsion demands to be used as soon as possible due to an ongoing chemical reaction between the cationic additive and the anionic emulsion. Therefore low storage times.
- The optimum binder content will be kept constant throughout testing. The only variable will be the additive binder content, so the test will not be carried at an optimum binder content.
- There is a limited aggregates quantity to widen the scope of testing, so the available materials could only allow a few classification and performance tests.

1.7 CHAPTER OUTLINE

- Chapter 1: Introduction presents a brief background on mine haul roads, pavement materials, and the need for innovation. It introduces pavement materials common for use in haul roads and briefly highlights the current state of haul roads.
- Chapter 2: Literature Review gives a current perspective on haul roads and innovative materials. Common haul roads structural and functional challenges are defined. The chapter

introduces common materials for use in haul roads. Innovative materials, NME's, their application, and chemistry have been presented. Factors influencing the need for innovation have been included.

- Chapter 3: Methodology Demonstrates an experimental setup and explains which tests have been done and why they have been performed. Materials used in the study have also been presented and characterized here. Performance evaluation of all the mixes will be carried out using ITS. Other tests include high pressure permeability to test permeability and triaxial testing for shear properties and resilient modulus.
- Chapter 4: Results and Discussion outlines results from both classification tests and performance and discuss them comprehensively. Treated materials XRD results are also analyzed and benchmarked against untreated test samples results. These are interpreted for meaningful information for use in other phases.
- Chapter 5: Pavement Design and Analysis present optimum mix results from chapter five are used for pavement design to check the adequacy of treated materials as construction material and their performance under traffic and loading. The pavement design is analyzed to check sufficiency for application in haul roads.
- Chapter 6: Conclusions and Recommendations outlines research conclusions and recommendations for further research

CHAPTER 2

LITERATURE REVIEW

2.1 INTRODUCTION

Mine haul roads form an important network of gravel surfaced roads used to transfer ore and overburden from the pit to the dump area or a processing plant, particularly in a surface mine or an open-pit mine. Globalization has led to an increased demand for minerals in the market. The need for minerals as well as their accelerated consumption by the world, pressures mine sectors to upscale and expand production. This expansion does not happen in isolation but requires a considerable change within different mining operations. Increased productivity, profitability and mineral demand, requires optimally constructed mine transportation for efficient hauling performance.

Surface mine project expansion gives rise to the introduction of heavier machinery or haul equipment on the haul roads network. The size of trucks introduced in surface mines is enormous and can potentially cause detrimental damage if the mine pavement is not sufficiently balanced against the intensity of traffic. Thompson (2009) mentions that in pursuit of cost-effective mine operations, there has been a significant development in ultra-heavy highway truck class, capable of hauling up to 345 tons payloads. Unfavourable environmental and climatic conditions are also a major cause of road failures, coupled with empirically designed roads, poor road performance, and frequent maintenance are bound to occur.

Kidgell *et al.* (2019) state that most Southern Africa regions use problematic natural soils for haul roads pavement design and construction, which are of poor quality hence need to be stabilized to improve their load-bearing capacity and other necessary mechanical characteristics. The prohibitively expensive costs of haul road construction have the potential to be minimized by the employment of innovative and tested technologies. Nano-modified technologies can adequately improve naturally available materials to meet set specifications or requirements (Jordaan *et al.*, 2017*b*).

Nanotechnology refers to the design, construction and use of structures with the length of scale ranging from 1nm to 100nm (Steyn, 2009), to provide a fundamental and comprehensive understanding of materials science at the nano level and transition of nano effects to a macroscale (Mann, 2006). The use of nanoparticles potentially manipulates problematic materials, elevating them to high-performance compliant materials. This could be of significance in mine haul road construction and maintenance. Therefore, the focus is more on nanoengineering than on nanotechnology.

2.2 CURRENT PERSPECTIVE

2.2.1 Mine Haul Roads

The existing conditions of Southern African mine haul roads have not been sufficiently balanced with the high intensity of traffic and environmental conditions. Selection of the most appropriate base course and wearing course material has been sophisticated and increasingly critical, given the growing difficulty to access high-quality construction materials. Crushed stone and compacted natural gravel have been commonly used for the top layers of the mine pavement, and the selection of these materials is a key performance indicator for optimum haul road performance (Thompson, 2000).

Gravel and crushed stone mixtures are currently considered appropriate based on their low rolling resistance, high adhesion coefficient, economic viability, and workability (Thompson, 2010). Local materials are readily accessible and cost-effective though temporarily beneficial, on mine road networks, with time they lose strength and result in an inherently unsafe road with high maintenance frequency and costs.

As the use of ultra-heavy trucks surges, the rate of road deterioration increases, the available selected materials have insufficient strength to sustain the loading. Due to emerging technological advancements in off-highway vehicles and the ever-changing climatic conditions, the mine transportation system needs to be innovated to counteract these challenges. Thus, stronger, and durable materials are needed for optimum performance. Thompson (2000) indicates that MHR performance is intertwined with haul truck productivity since extreme surface irregularities may potentially lead to metal fatigue and haul truck frames.

There is a need for mine haul road engineers to appropriately design and formally construct haul roads, to avoid mediocre performance and premature road failure. According to Paige-Green and Heath (1999), there is a significant need for technical expertise in MHR construction since mine officials construct MHR based on empirical methods using poor quality materials. Thompson (2011*b*) strongly believes that these empirically designed MHR may still be safe and economically optimal however, should the safety or overall performance be inferior, it is uneasy to identify embedded deficiencies to account for the undesired behaviour and resulting accidents. In haul roads, transportation forms a central component of mining operations since mined ore needs to be moved from the pit to the processing area and dump rock or overburden to the dumpsite.

Lack of good quality materials within the mine site prompts mine pavement engineers to import appropriate materials which would then offer relatively higher road performance. Material hauling

is a costly exercise, based on the value to weight ratio of aggregates, the transportation costs are very high, as a result, haul roads are predominantly constructed using readily available poor-quality materials. This continues to show a serious need to improve the very existing locally available materials into high-performing construction materials to be able to sustain the ultra-heavy load and adverse environmental conditions. Thompson (2010) mentions that large modern surface mining operations compared to small-scale mining immensely requires high standards of road design to ensure optimum performance and safety.

Haul roads with poor rugged surfacing and structural defects breed accidents. According to Thompson (2011*b*), a coal surface mining-based study revealed that the most predominant accident causation was haulage trucks, accounting for 46 % of total accidents. Therefore, improvement of the current design, construction methods, and materials can potentially lessen the mining accidents statistics, due to fewer surface defects caused by traffic, water seepage, or other adverse conditions.

2.2.2 Innovative Material Solutions

The current haul road materials, design technology, and construction practices are being outperformed by the evolving surface mine equipment and operations. Materials with the potential to alter mine pavement performance are a critical innovative necessity. The innovative technology under consideration is nanoengineering, which encompasses the effective use of nanoparticles to enhance conventional material geotechnical properties and consequently, performance.

Nanotechnology in construction is a fairly new technology that has received limited research interest, but a narrow application based on doubts surrounding its sustainability, safety, reliability, and strength. There is a very limited understanding of nanoengineering hence the application of nano-products in Southern Africa mines remains unheard of. In the Southern Africa Region, the reluctance towards implementation of innovative technologies in pavement engineering goes beyond mine haul roads. Mann (2006) reports that despite compelling laboratory work and research projects, nanotechnology, particularly focused on materials, continues to face organizational resistance. The resistance to letting go of the skepticism and take a risk with the potentially beneficial road technology is deeply entrenched within mining organizations. Innovation should be regarded as a potential means to cost reduction.

The use of nanoproducts in mine pavement may likely result in dematerialization. This is due to their competitive nature and unique ability to improve geotechnical properties and material performance, a lesser quantity of the traditional materials would be required to be performance compliant. Leone (2012) mentions that nano-structured materials enhance development within the construction industry, high performance levels, low energy, and reduction in material costs are

achieved compared to traditional materials. In the development of durable and stronger materials, the use of nanoparticles allows reduction of required material quantities, meaning thinner pavement layers can provide the needed performance specifications at a reasonable construction cost.

To propel the mutation in the quality of life through nanoengineering products, private sectors in Japan, European Union, America, and other countries are competitive in pioneering nanoengineering technologies (Motlagh *et al.*, 2012). There has been an increasing research interest, based on applications of nanostructured materials, their commercialization and environmental hazards. However, it must be noted that there is little large-scale commercial application based on the poorly understood relevance of innovation in construction. This research aims to show the relevance and benefit of these improved materials.

2.3 HAUL ROAD CHALLENGES

These are challenges critical for haul road performance and durability. A mine pavement performance can only be optimal if all design aspects are adhered to holistically, each design criteria is mutually important. According to Thompson (2011*c*), designing and construction of the MHR are done effectively following an integrated approach. Thompson defines an integrated approach as correctly addressing each component of road infrastructure at the design stage so that no occurrence of premature failure because of a design deficiency in one design aspect.

A failure to follow an integrated approach in design will result in a poorly performing MHR. Distress conditions that occur lead to excessive damage that adversely affect productivity. These occurring defects can also be categorized as per design aspects, some affect layer works, others affect the surfacing and maintenance while others affect the geometrical design of the road. Underestimation of allowable loading and unclear understanding of construction materials' response to loading can be deadly to truck and mine operation efficiency. The occurrence of defects compromises the safety of mining personnel, equipment, therefore negatively striking an economic impulse.

Mine haul roads are designed formally in four different aspects as shown in Table 2.1. An integrated design approach assures that each design aspect is done appropriately. Mine road network serves varied functions (Thompson, 2011*a*). Constructing a road solemnly based on accessing one area from the other will result in a vastly deteriorated network destructively affecting the production fleet.

Table 2.1: Shows design aspects and definitions. Adapted from (Thompson, 1996)

Design Criteria	**Explanation**
Structural	The ability of the road to carry the imposed load without the need for excessive maintenance.
Functional	The ability of the road to provide a safe, economic and vehicle friendly ride.
	A selection of wearing course material
Maintenance	The gravelling frequency of wearing course material

2.3.1 Structural Design

The fundamental principles of structural design remain like those of flexible pavements. The most optimally performing selection of layers is done in cognisant of available material type, the intensity of loading, and reigning environmental factors. Unpaved haul roads are generally constructed using locally available mine material, whose costs are favourable.Thompson (1995) reports that in 1977, a research study based on structural-design aspects of MHR, conducted on behalf of the United States Bureau of Mines (USBM), concluded that a stable road base is a fundamentally important aspect of road design and construction. Therefore, a poorly constructed base, using poor quality materials is a liability to haul road optimal performance and a structural deficiency of a mine pavement. There is a lack of definitive material specification and limited structural design criteria concerning the construction of MHR. Preferential material specifications for unpaved haul road are shown in Table 2.2.

Table 2.2: Material Specifications for unpaved haul roads(Paige-Green, 1990*b*)

Index Description	**Specifications**
Maximum Size	75 mm - 100 mm
Oversize Index	10%
Shrinkage Product	100-365 (Preferably 240)
Grading Coefficient	16 - 34
California Bearing Ratio	15 @ 95% Mod AASHTO Compaction and 4 days soaking

Using a mechanistic design method, locally available construction materials are efficiently used. For unpaved haul roads, the mechanistic approach uses a single layer with a sufficiently high load spreadability as a base, made of appropriately selected blasted waste rock instead of alternating layers of base and sub-base (Thompson, 2011*a*). Visser (2015) points out that this is a much preferred structural design method compared to the CBR design method, no excessive vertical compressive strains were recorded in optimal mechanistic design compared to CBR-based design.

Furthermore, it is noted that surface deflections of CBR are slightly above those of mechanistic but under excessive loading, deflections may be worse with a high possibility of structural failure and accompanying defects such as rutting and wide depressions. The CBR-based design was primarily developed for use in airfield asphaltic pavements to sustain wheel loads not exceeding 4400 kN, yet its application in unpaved and stabilized haul roads is of questionable validity (Thompson and Visser, 1997*a*). Due to the inherent deficiencies exhibited by the CBR design-based method, the suitable recommendation is the use of the mechanistic-empirical design method to at least deliver an optimal design with less or no excessive deformations of compressive strain.

Therefore, since there are limited haul road design guidelines or lack of appropriate material properties and selection specification standards, particular to haul roads, any selected material that is compliant is eligible for use. The use of materials that follow the structural design specifications is of key importance to haul road optimal performance. As a result, improved materials can potentially exceed the set minimum specifications available and offer incredibly compelling performance. The selection of materials would have to be suitable to the category function of the road, category 1 roads require more durable materials than category 3 roads, as a result, the stabilization strategy can help strengthen base layers in permanent or semi-permanent haul roads. Figure 2.1 demonstrates the typical mechanical layer structure of haul roads.

It is important to tailor the structural requirements of a road to its structural design life since that has a major contribution to the road's functional performance, longevity, and contribution to mining operation success. Different roads serve a variety of functions and are in use for different periods. As a result, the structural requirements of a temporary road will differ from those of a permanent road. The expected performance of a permanent road is much higher than that of a temporary road, therefore the permanent road will have to be weather impassable, possess high structural integrity, and always accommodate maximum traffic until the end of its structural period. Should heavy-class contemporary haul trucks be adopted on a mine site, permanent haul roads should be designed to accommodate such types of trucks to minimize potential complications. Table 2.3 shows a summary of haul road categories.

Table 2.3: Summary of haul road categories. Adapted from (Visser, 2015)

Haul Road Category	**Daily Traffic Volume (kt)**	**Regulated performance Index**	**Description**
Category 1	>25	7-9	Permanent high-volume main roads from ramps to tip. Operating life at least 20 years
Category 2	8-24	5-6	Semi-permanent ramp roads, in and ex-pit hauling roads on blasted rock on in-situ, medium traffic volumes. Life of 10 years
Category 3	<7	>4	Temporary in and ex-pit roads, low traffic volumes. Usual operational for less than 3 years

Specifications for the selected blasted rock exist, in terms of the maximum size of the blocky material being less than 50 % of the layer thickness. Darling (2011) indicates that the material should not contain excessive amounts of fines and clay, also the typical modulus value for the selected blasted rock is around 3000 MPa.

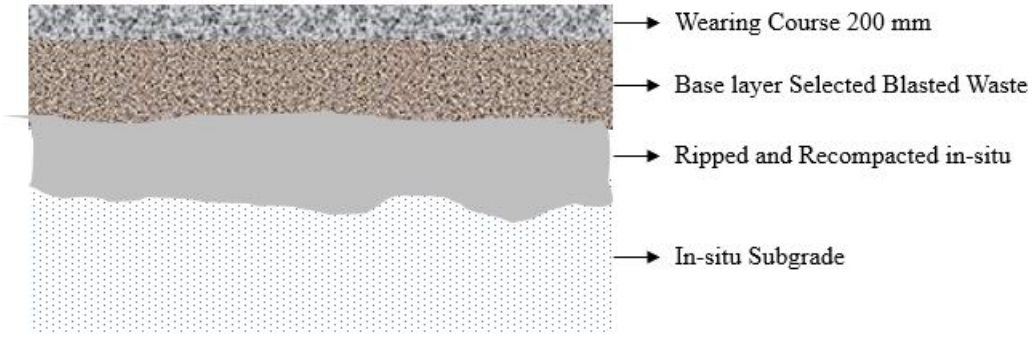

Figure 2.1: Mechanistic approach towards haul road structure

In Figure 2.1, the base material is tipped on the in-situ soil, beneath the wearing course. Therefore, in the case of mine haul road, the selected blasted rock is the most critical layer for optimal performance. Construction of a wearing course layer over a poor material with a low bearing capacity will prohibit efficient vehicle movement (Thompson and Visser, 1997*b*).

A study done on a pavement structure which had a nano-modified emulsion within its base and

sub-base resulted in exceptionally high ITS values, more so, it is reported that these are not unusual as other tested NME'S across Southern Africa proved to have a similar pattern (Rust *et al.*, 2019). Based on resulting low damage coefficients, the pavement materials seem to be insensitive to the loading to a noticeable extent. The use of appropriately selected rock modified with capable additives stands a chance to offer an unbelievably satisfying performance and comfortable truck haulage (Rust *et al.*, 2019). The thickness of the layers can potentially change, possibly leading to an earlier explained concept, dematerialization.

Stiffer upper layers of the haul road within the top 300 mm of the 2 metre pavement depth have the potential to improve the rolling resistance significantly. Thompson and Visser (1996) explain that the use of mine spoil rock in place of stabilized layer in the upper pavement structure results in a stiffer layer sufficiently reducing vertical strains in the layer underneath. A stiffer mine waste rock also means reduced layer thickness for the same load-bearing capacity.

2.3.2 Functional Design

The trafficability of a surface layer depends on the type of material used for surfacing. It is mainly a function of wearing course selection. According to Jones *et al.* (2003), performance of unsealed roads primarily depends on the gravel used as wearing course. Neglecting other influencing factors may result in poor riding quality, poor maintenance, and impassibility in wet conditions.

The wearing course material selection has also been detailed by Paige and Netterberg (1987) discussing requirements and properties for unpaved public roads. They recommended a fundamental aspect that carefully managed maintenance and proper maintenance scheduling can potentially result in a better performing road. This continues to demonstrate the importance of an integrated approach to a haul road design. According to Thompson and Visser (2000*b*), TRH20 wearing course material selection guidelines proved to be more suitable for use in mine haul road wearing course material specifications. However, these TRH20 guidelines were later enhanced to show variations in the occurrence of functional defects, resulting in Figure 2.2

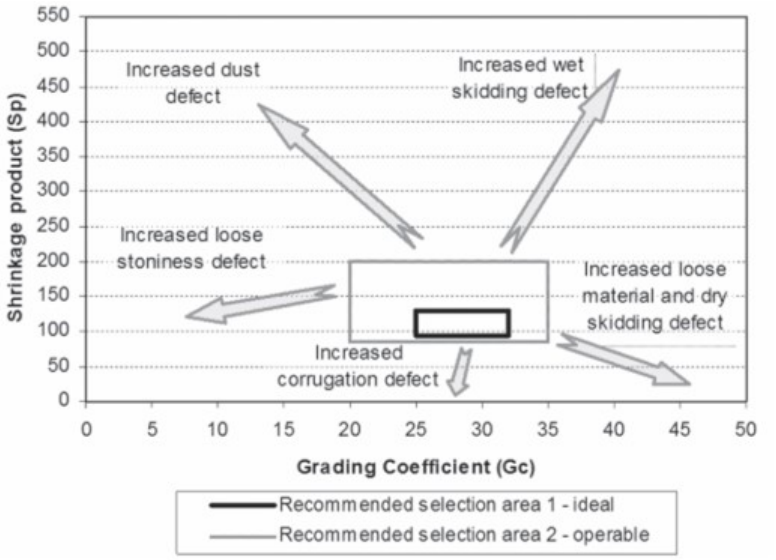

Figure 2.2: Wearing Course selection guideline. Adapted from (Thompson and Visser, 2000*b*)

To reinforce the importance of an integrated approach towards haul road design, the geometric design element can also adversely affect the functional performance. If the road curvature is very tight, meaning the radius of curvature is very small, there exists a high likelihood that this may result in shearing-off of the wearing course on the outside bend due to a smaller turning radius (Thompson, 2011*a*). In this case, the functional design would not be a primary cause of premature failure, but a poor geometric design would turn to be a root cause of surface damage, exposing the top of the base layer. The repetition of this will result in costly tyre damages.

2.3.3 Common Haul Road Challenges in Mines

Distress conditions are different in terms of their types, severity, and extent based on the traffic volume, load transported or tonnage, road function, and location. Therefore, mine haul roads are likely affected by severe distress conditions which could be unreasonably costly if not addressed. Routine maintenance work is a costly exercise for mining companies, this is a daily task depending on the functionality and the traffic volume of the road. A study carried out by Thompson (2000), considered haul road functional design of surfaced mine haul roads. It relates the severity of distress to haul road performance demonstrated by Figure 2.3. At high severity of defect expressed by defect score, haul road performance is poor.

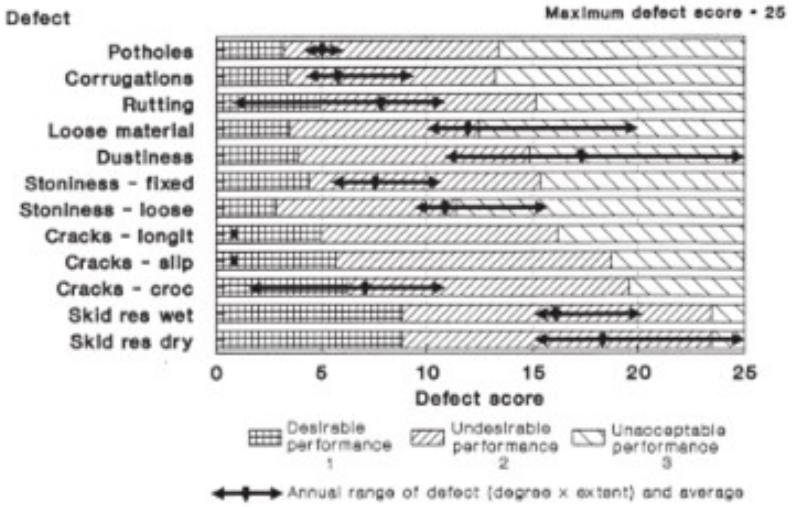

Figure 2.3: Road user data acceptability limits for haul road functional defects. Adapted from (Thompson, 2000)

Routine maintenance spans from spot re-graveling, shallow blading to re-sheeting, whose costs become exorbitant with time. Maintenance costs are not only limited to technical aspects of repairing the haul road but they extend to the overall vehicle and operating and maintenance costs. Deterioration is a result of high defect score distress conditions. Thompson (2009) explains that the optimum material to be used in haul road remains compacted gravel or crushed stone, however using a local mine material as an alternative would have favourable cost, though hard to predict if the local material would remain durable while offering optimum performance in the long term. To reduce material degeneration and dust, stabilization is often a viable option, a stabilized load-bearing layer means the layer is glued together, becoming less of a sacrificial layer which requires less frequent maintenance.

One of the biggest concerns about unsurfaced mine haul roads is dust generation. Wearing course fine particles becoming airborne, known as fugitive dust (Thompson, 2011*c*). This reduces air quality, drivers' safety due to impaired vision and consequently productivity. Tannant and Regensburg (2001) mention that watering maintains not only layer compaction but strength. It further reduces gravel loss, fine particles which act as a binder are lost resulting in degradation of a road surface. Dust management is, therefore, an important concept in ensuring less maintenance and lower roughness defect score. According to Barnes and Connor (2014), ambient particles less than or equal to 10 microns are a threat to human health as they cause respiratory health issues, cancer, and premature death.

Dust generation is also affected by the type of material the wearing course is composed of. According to Thompson (2011*a*) and Paige-Green (1989), material properties such as aggregate strength significantly influence dust generation. Paige-Green (1989) developed an annual gravel loss function (Equation 2.1) which is a function of traffic volume, grading, and climatic situation through Weinert N-value. The Weinert N-value shows the mode of weathering and indicates principle secondary minerals present such as those contained in silt and clay fines, which form a predominant part of generated dust. It further highlights the importance of in situ moisture content in unpaved roads

$$G_{LA} = 3.65[(ADT(0.059 + 0.0027N - 0.0006P_{26}) - 0.367N - 0.0017PF + 0.04774P_{26} \quad (2.1)$$

The amount emitted dust is a function of the ease at which the wearing course material is erodible; termed erodibility and the erosivity of the agents of erosion. To minimize dust generation mechanically, more resistant surface materials are an ideal selection. Paige-Green (1989) has shown a relationship between soil properties and wearing course performance, the selection chart shown in Figure 2.4 is described by two critical parameters: Grading Coefficient (G_c) and Shrinkage Product (S_p).

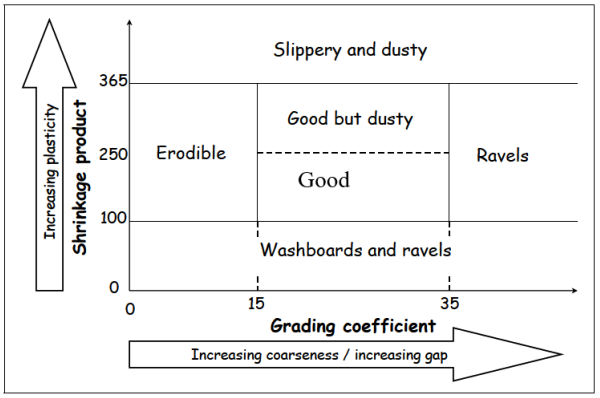

Figure 2.4: Material Selection Chart Adapted from (Paige-Green, 1989)

Dust management could have different aspects being chemical, mechanical, and administrative. Dust palliatives from part of a chemical approach are helpful in dust management and ensuring dust suppression, however, the effectiveness of dust suppression according to Tannant and Regensburg (2001) depend on the type of palliative, wearing course, traffic volume, environmental conditions. Some palliatives are highly active at certain temperatures and humidity levels while some are not, as a result, their success in suppressing dust is hugely dependent on the mentioned factors. Dwayne further mentions that field trials were carried out to evaluate the effectiveness of

different chemical dust suppressants shown in Figure 2.5.

Chemical	Unit Cost ($/l)	Application Rate(L/m^2)	Cost/km application (1986$)
Asphalt Emulsion	0.26	1.8	11700
Calcium Chloride	0.11	2.2	6000
Calcium Lignosulfonate	0.30	1.5	11300
Surfactant	2.95	0.009	650
Water	-	-	35

Figure 2.5: Application rate and cost of dust control. Adapted from (Tannant and Regensburg, 2001)

The data shows the unit cost of each dust suppressant, application rate, and total cost per kilometer application along a certain width. Although availability or ease of access and use may influence the dust palliative selection, economical constraints may also be a critical factor in the selection. A review of the tested chemicals, based on roads under constant use, showed that calcium chloride was cost-effective, its single application provided about 25% average control effectiveness over three weeks while water had to be applied every two hours to reach the same result (Tannant and Regensburg, 2001). The calcium chloride is most active at a relative humidity around 30% to 40% with increasing temperatures (Thompson, 2007), the intraparticle surface tension of water gets significantly increased thereby slowing evaporation and keeping the unpaved surface sufficiently moist and fines in place. Barnes and Connor (2014) states that the disadvantage of salts and brine is that they leach out of the soil during precipitation.

A water-based dust suppression approach is environmentally friendly and within the EPA regulations. In most cases, it is much more advantageous in terms of low cost and abundant water supply. Thompson (2007) developed Water-spray-based palliation performance models, establishing a relationship between dustiness and time; showing dust defect degree score and time after watering. Figure 2.6 illustrates the increase of dustiness with time while the haul road is under constant use. The duration in which the dust remains suppressed is less than 30 min, with a single spray of approximately 0.5 l/m2.

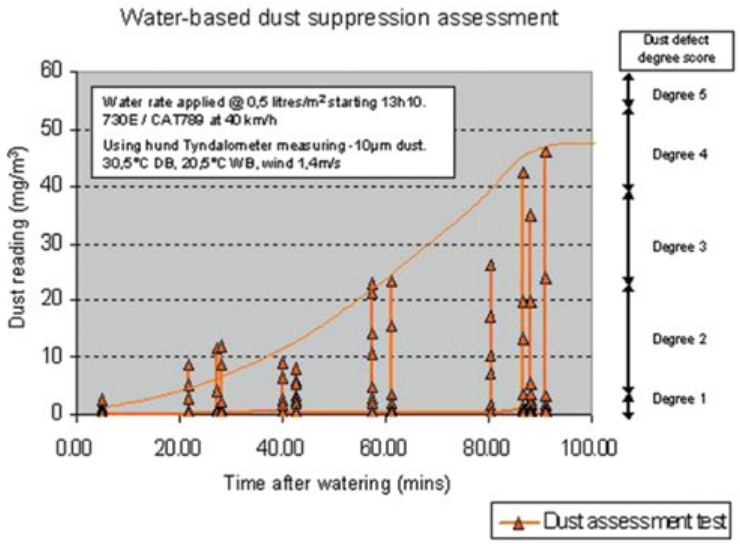

Figure 2.6: Water based dust suppression assessment. (Thompson, 2007)

If the haul road is left dry for a longer time, the degree of dust significantly increases, this rate of the increasing degree is hugely affected by the climatic conditions, traffic volume, and the type of the wearing course material. Different proprietary dust palliatives exist, meant to suppress dust on unpaved roads, Thompson (2007) concludes that in South African mine haul roads, dust generation is mostly dealt with on an ad-hoc basis, there has not been standardized methods for dust palliatives or sufficient constructive data collected to aid development and evaluation of dust management strategies.

Rolling resistance is defined as the resistance to motion that vehicles or haul trucks experience due to friction. A force needs to be exceeded to move the vehicle forward. The vehicle wheel must roll and moved with ease, the difficulty to do is an effect known as Rolling Resistance (RR). Thompson and Visser (2003) defines RR as an additional retarding effect experienced by a vehicle in motion, it is normally expressed using an International Roughness Index (IRI m/km), percent road grade, or resistance force as a percentage of gross vehicle mass (GVM) (Tannant and Regensburg, 2001). That total resistance experienced by a moving haul truck is a combination of rolling resistance and grade resistance, illustrated by Equation 2.2.

$$TotalResistance(\%) = Rolling\ Resistance(\%) + Grade\ Resistance(\%) \tag{2.2}$$

Thompson (2000) completed a study of pavement functional performance, developing a predictive model for change in rolling resistance with time. Factors that critically contributed to a higher defect

score associated with this model were identified as the wearing course material, traffic volume and speed. The model is defined by a function shown in Equation 2.3. It illustrates the relationship between roughness defect score based on degree and extent of existing distress conditions and rolling resistance.

$$RR = RR_{MIN} + RDS * e^{RRI} \tag{2.3}$$

RR_{MIN} is the minimum rolling resistance where RDS is zero. Rolling resistance Index (RRI), expresses the rate of change of rolling resistance with time show by Equation 2.4. Rolling resistance is influenced by several parameters related to road conditions, weather, vehicle tyre and operating systems.

$$RRI = -6.068 - 0.00385RDS + 0.0061V \tag{2.4}$$

V is the vehicle speed in km/h

The maintenance management strategy developed by Thompson and Visser (2003) through the use of an empirical modelling primarily applicable to haul roads. Cost parameters including fuel consumption, tyre wear, and road maintenance have also been related to RDS through empirical cost models. It was concluded that the rolling resistance increases with increasing RDS, an actual test data depicting the developed rolling resistance model is illustrated by Figure 2.7. Further explanation on this prediction model and vehicle operating cost models are provided by Thompson and Visser (2003). Given the different factors affecting RR and severity of defects, the accuracy of these empirical models and hence total resistance relies heavily on the inputs of variable factors such as material properties and traffic volume.

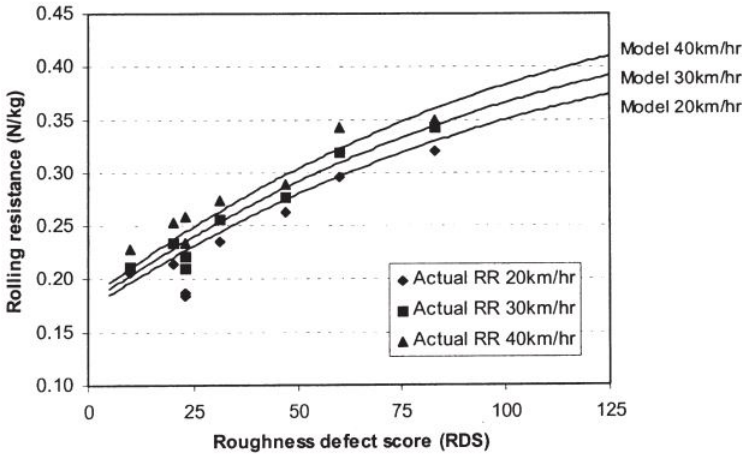

Figure 2.7: Rolling Resistance and RDS Model. (Thompson and Visser, 2003)

Increased rolling resistance harms haul road operation economics, particularly on fuel consumption, tyre wear, and vehicle operating costs. Increasing production demand in a mining industry pressures the use of an increased fleet of haul trucks with massive capacity, as a result, the cumulative cost associated with the fleet results in high energy consumption. Bozorgebrahimi *et al.* (2005) and Thompson (2009) points out that economics of scale have been a major concept adopted within the open pit mine industry, it is a function of (a) a merger between mining companies, (b)large scale mining operations and (c) use of ultra-massive mining equipment. The technology complexity and size have continued to rise for the past fifty years, currently, one 360 t truck is ten times 35 t trucks used in the mid-1900s. In a study of equipment size sensitive variables (ESSVs) effects on open-pit mining production and performance. In Equation 2.5, Bozorgebrahimi *et al.* (2005) developed a relationship between mining equipment size and overall production cost.

$$Z(Y_i, X) = F(\sum_{i=1}^{n}(Y_i(X))) \tag{2.5}$$

Where $Z(Y_i, X)$ the production cost function,(X) denotes the size of the equipment and $(Y_i(X))$ is the cost function of each ESSVs, and n is the number of considered EVs. Therefore, the production per equipment cost is a summation of all equipment size-related variables. Further details on this study are explained in Bozorgebrahimi *et al.* (2005).

The advent of ultra-heavy equipment necessitates haul road geometry adjustments. Small radii of curvature result in truck wheels making a three-point turn at curves, this is not only time-consuming, but it is a safety hazard, the wheels scrape off the surfacing causing stoniness, hence increased traction and rolling resistance (Visser, 2015). The large fleet does not only pose a threat to the haul road structural adequacy but Bozorgebrahimi *et al.* (2005) conclude that it significantly influences the milling cost which is a big-budget chunk. Larger mining equipment leads to coarser ore fragmentation, increasing the cost of comminution.

Tannant and Regensburg (2001) note that driving a mechanical drive haul truck CAT 793 at high rolling resistance segments would require a lower gear and lower speed compared to driving on a well-maintained smooth road, with a higher gear and higher speed. The same distance would be covered but a lower gear would have high energy demands. The same concept applies to haul trucks on a trolley line, there is a high amount of energy consumption or power delivered to the haul truck due to increased revolutions per minute (RPM) to overcome the total resistance. Visser (2015) studied the status of haul road design and management in South African coal mines and the impact on cost-effectiveness. Savings of approximately 1 million liters of diesel were made with no adjustment to payload or tonnage hauled but through haul roads geometry optimization such as

adjustments in curve radii and gradient.

Permeability of a pavement layer influences the longevity and durability of a haul road. Highly permeable layers or materials allow water to seep into deep road layers weakening the entire road structure. High permeable materials provide little protection of the subgrade against water damage.A less permeable layer adequately protects the layers beneath against water ingress, almost maintaining their dry strength.

The top layers must protect lower layers against water ingress, it is understandable that permeability of material on-site does not only depend on the nature of the material but also the road geometry, a key parameter in surface water drainage. Other factors include interconnected voids, nominal maximum aggregate size, and compaction (Venter, 2019). Since a whole haul road network is barely entirely surfaced, it would be beneficial for the base layer to be impermeable.

Darcy's law, Equation 2.6 governs fluid motion principles, it defines that the velocity of the homogeneous fluid in in a permeable material increases with increasing pressure gradient but decreases if the fluid is more viscous (Lock *et al.*, 2012).

$$q = -\frac{kA}{\mu}\frac{dP}{dL} \tag{2.6}$$

Where:
q is the flow rate (m^3/s)
A is the cross-sectional area exposed to water (m^2)
μ and dp/dL are fluid viscosity and gradient of pressure loss
k is the coefficient of permeability

2.4 HAUL ROAD PAVEMENT STRUCTURE

Based on the size of the surface mine, the length and width of the permanent haul road vary. Permanent roads require sound construction methods and materials while temporary roads can be constructed using naturally available suitable materials. The Gross vehicle mass (GVM) of large dump trucks can be more than 4000 kN, a Komatsu 860E-1K rock truck has a GVM of 448013 kg and a tyre pressure greater than 720 kPa. Permissible vertical strain limits are 1500 for permanent haul roads classified as Category I and 2500 for temporary roads such as ramps, classified as Category III (Thompson and Visser, 1996). This implies that construction materials used for haul roads should provide adequate bearing capacity and stiffness to sustain this ultra-heavy equipment.

A need for new age modifiers to increase materials strength by improving their chemistry or physical properties arises. Haul road layers can be constructed using naturally available rocks, blasted overburdened rocks, gravel, and crushed stone. These materials have also been briefly discussed in the following sections.

2.4.1 Laterite

Laterite is a reddish, tropically weathered material ranging from fresh rock to a sesquioxide (hydroxides) -rich pedogenic material(Gidigasu, 1974). It is a residual soil type commonly found in most sub-tropical zones such as Southern and Western Africa, the term laterite may mean something different from lateritic soil depending on different users and composition (Netterberg, 2014) as seen in Figure 2.8, but its generic properties include those listed. However, in this research project, such terms have been used interchangeably

- Rich in aluminium and iron oxide ($Al_2O_3 + Fe_2O_3$)
- Kaolinite is the dominant clay mineral ($Al_4Si_4O_{10}(OH)_8$)
- There is reduced silica content (SIO_2)

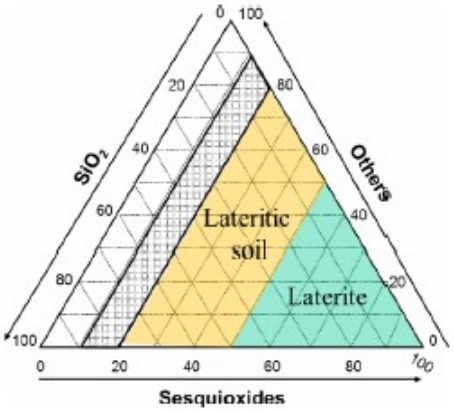

Figure 2.8: Composition of laterite and Lateritic Soil.(Netterberg, 2014)

Lateritic samples are freely available as natural aggregates in most areas where high-quality rocks or aggregates are not available and the material hauling economics are not viable. Available lateritic material ranges from soft soils easily crushed by the hand to large hard boulders with sound quarzitic gravel. Gidigasu (1974) mentions that studies in West Africa, Nigeria, and Thailand, revealed that the field performance of laterite soils as road construction materials is hugely influenced by specific gravity, water absorption, and aggregate strengths. Furthermore, well-graded, optimally compacted

lateritic soils with adequate drainage and strength performed satisfactorily under repeated traffic loading.

Contrarily, Sudla *et al.* (2018) points out that in Thailand, laterite soils have a higher content of fine particles with unsuitable properties responsible for its intensive shrink and swell behaviour, due to its water sensitivity, the swelling and shrinking become worse. As a result, it can only be considered as a subgrade material instead of a potential aggregate for upper layers. It is for these challenging problems that this research seeks to improve the performance of this marginal material through new-age additives, which are applied in little dosages to increase material strength and impart water repellence features.

A stabilization method commonly considered is blending weaker aggregates with suitable high-quality material thereby enhancing particle interlock upon compaction. This is known as mechanical stabilisation and is cost-effective since it achieves adequate mechanical properties in pavement layer construction. (Sudla *et al.*, 2018) concluded that blending laterite with a non-plastic high-quality crushed stone (CS) decreases plasticity with increasing CS application rates; from as little as 10 % content, CS blends also results in increased durability since it has low LA abrasion loss value. Coarse grains of laterite break easily during compaction increasing the fines content, subsequently swelling in wet conditions. Therefore, the blend has a lower fines content due to CS resistance to breaking under compaction. This material solution does not improve the chemical nature of the material but the mechanical performance of the bulk mix, it is a bigger challenge in locations that lack high-quality crushed stone, as a result, new-age material additives are worthy of exploration as aggregate modifiers.

The suitability of laterite as a common material for pavement use is hugely dependent on its degree of weathering and genetic properties such as morphological characteristics, secondary minerals content, and type. Laterite material is not viewed as a potential road building material in South Africa, most pedocretes except silcrete do not provide the potential for use as either surfacing stone or base course for moderately trafficked and low volume pavements (SAPEM). This limited application as a pavement material is explained by Netterberg (2014):

- Failure to meet specifications such as grading; the little coarse fraction of the fine aggregates hence gap graded and high plasticity in the range 15-20 and relatively low CBR values.
- Unusual mineral type and content renders them inappropriate for use, however, quartz gravel contained in some laterite may influence performance in pavement application depending on quartz gravel content.
- Lack of available documentation guideline particularly related to laterite as a potential road

material or appropriate tests that accurately indicate laterite behaviour based on origin.

- Unsuitable current methods that do not adequately indicate future mineralogical and textual state, Gidigasu (1974) mentions that historical research showed some laterite passed the standard test but with time under chemical weathering, it exhibited some durability issues

2.4.2 Crushed Stone

These are normally high-quality stone materials classified according to the TRH14 Manual as G1 to G3, with G1 being the highest quality and G3 being secondary to G1 and G2. It is usually extracted from selected quarries with the appropriate stone type. Most of the crushed stones do not contain any clay minerals, as a result, they are non-plastic. The basic pavement material for most pavement structures is crushed stone due to its load-bearing capacity and relative strength and resistance to adverse environmental conditions.

Since grading is a critical factor in the mix designs and consequently, road construction, the crushed rock is screened into different sizes. Ultimately, a well-graded crushed stone blend is achieved depending on the target grading per project. Thompson and Visser (2000*b*) note that for haul road construction, compacted natural gravel and crushed stone have widely been used as a base and wearing course materials. This is because they offer exceptional water resistance and increased load-bearing capacity as UGM's, provided tight construction methods are followed, they are capable of an optimal particle interlock forming an aggregate matrix representative of an intact parent rock (Kleyn, 2012). Grading is of utmost importance and given the heavy loading of trucks and other equipment, it is generally resistant to loading impact and the non-plasticity helps avoid the negative effect on the shear strength, clay minerals may affect the particle interlock and consequently contribute to shear deformation.

Theyse (2002) reported on HVS testing done in South Africa to evaluate the effect of traffic loading on the stiffness of the crushed stone, which was slightly higher than that of natural gravel, the increase in stiffness was accompanied by an increase in the bulk stress. He further states that in most South African pavements, stiffness decreased due to increasing traffic and moisture ingress. The effective stiffness of the base layer aggregate was recorded to reduce from 800 MPa to 400 MPa under wet conditions, showing the extent to which water ingress or moisture presence can affect the stiffness of a UGM.

To offer relatively higher performance, the UGM's are normally stabilized using bitumen emulsions. This increases stiffness, bond strength due to the present binder, and a relatively higher resistance towards water ingress compared to an untreated layer. Therefore, emulsion-treated materials are

part of haul road construction material.

2.4.3 Overburden Blasted Rock

Technical, economical, and environmental needs influence the use of selected blasted waste rock as a potential aggregate for a base or subbase layer depending on the rock's nature, physical characteristics, and load-bearing capacity. The application of this material will be dependent on the overburden rock type, it is hugely dictated by the strength of the overburden rock at the mining facility. In a diamond mine, basaltic rocks are used as road aggregates while in a copper mine, iron-rich dump rock may be applicable. Not only blasted waste rock can be used as a road material but also suitable mine tailings.

Thompson (2011*c*) reports that under the mechanistic design method for unpaved roads, both the subbase and the base are replaced by blasted waste rock. It is normally tipped on the marked road area then using a large, tracked dozer, dozed into the road layer to form the necessary road profile, it is preferable to shape and compact the upper 300 mm of the blasted waste rock to accommodate mine traffic. Apart from the vibratory or large impact roller, compaction is mostly done by haul trucks and other wheeled equipment.

Mallick *et al.* (2017) assessed coal mine overburden material as a potential aggregate for mine haul road construction material, the untreated overburden material showed low CBR values in the range 1.7 -2.1% which is very low and was rendered unsuitable as subgrade material. In both the UCS and tensile strength test, the overburden did not show appreciable strength values; 56.2 kPa to 71.2 kPa, it showed little load resistance for external loading hence limited potential as a haul road subbase. This further shows commercial additives are required to improve the CBR and other engineering index properties of overburden to consider it as a potential aggregate material.

Using overburden material for haul road construction is not a new phenomenon. In the Indian coal mine industry, murrum (normally known as lateritic soil) is usually used for haul road construction, a cementitious stabilizer known as Road Building International Grade 81 (RBI-Grade-81/RBI) was used on the murrum soil at increasing application rates, resulting in increased mechanical properties such as CBR, UCS, and dynamic Young's Modulus. The use of an optimum content of 6% RBI resulted in the highest strength gain due to an effective cementitious gel formation. Moreover, in terms of strength gain, RBI proved to be a better stabilizer compared to lime (Mallick and Verma, 2020).

Koner and Chakravarty (2016) carried out a study aimed at characterizing mine overburden dump material and evaluating it for pavement construction application through standard laboratory test-

ing. The resulting cohesion values from the direct shear test for nine out of eleven mine sites did not exceed 20 kPa while the friction angle for all for the overburden material from all mine sites was well below 50 °C. The overburden material through its geotechnical parameter showed that it is expansive as per ASTM standards, it would result in significant distress conditions in rainy conditions and under massive repeated loading.

In some mine sites, mostly copper mines and diamond mines, the overburden consists of a rocky material known as blasted rock waste, which could potentially be used as a suitable base layer. However, in some mine facilities, OB has a low bearing capacity and would result in an exceedingly poor functional performance.

2.4.4 Case Study: Kansanshi and Kalumbila Haul Roads

Copper Mines in Kansanshi and Kalumbila, both in Zambia are considered in this study, in terms of material aggregate used on their haul road networks and tested in this research project. Kansanshi Mine has a daily production of about 200×10^6 kg per day and 70×10^6 kg of overburden. This material is hauled using enormous dump trucks including the Komatsu 860E and Liebherr T284. The tyre life as a function of road conditions in these mine sites ranges from 7500 hours to 10000 hours in exceptional circumstances.

In Kansanshi, the base is constructed by a 150 mm thick layer of crushed rock on top of a 2 m rock fill. The stone base has been crushed using an impact crusher and compacted using an impact roller. However, the grading of the crushed stone is variable due to high fines content, more than 36 % passing the 0.425 sieve. There are also larger aggregates materials with a size of more than 40 mm, the blend of these materials creates an adequately graded crushed stone.

At the ramp and trolley, the pavement can carry up to six electric trucks; channelized traffic, most trucks are dual-powered, they both use fuel and electricity through installed trolley lines. The surfacing at this section is an SS60 emulsion (2.6 % RBC) treated base, the grade of the ramp is 10 %. At some sections, there is a well-performing double seal (made from 32 mm and 19mm stone) which has performed relatively well, with tack coat, cover spray, and a fine slurry. Upon application of emulsion and there is some pick up by tyres hence it would be worthwhile to explore thixotropic additives to emulsions. At an old ramp, that is not active with a trolley line, the base has a variable emulsion content, some sections have experienced isolated cracking which could be as a result of shear failure in areas of weak support. There is also a haul road constructed from laterite material.

In Kalumbila mine, which is situated 140 km north of Kansanshi, the length of the haul road

network is more than 50 km, the width of some of the ramps at Kalumbila is 53 meters and the width of the permanent haul roads is three times the width of the largest dump truck. The daily production is 450kt using 400t trucks (make CAT and Liebherr).

At an active trolley ramp with a grade of 9.7%, the base is constructed from a crushed stone with a maximum size of 40 mm to 50 mm. The top layer is an SS60(2.4% RBC) emulsion stabilised base that experiences a considerable amount of spillage. However, this section is planned to be surfaced with appropriate wearing course material.

The surfacing at a brake test ramp is a large cape seal made of 32mm and 19 mm stone, with coarse slurry. The application rate of the CSS65 emulsion used is 1.2 l/m2. There is some wear-off visible on the ramp surfacing but there is no shearing of material from the surface, the possible cause of wear is the brake shear forces of empty trucks. The adjacent road to this brake test ramp is surfaced using a triple seal with 32mm,19mm, and 9.5mm of stone, it shows a remarkable performance. The surfacing comprises 0.8 l/m2 of a prime coat and 1.2 l/m2 of CSS65. Application of emulsion sometimes results in surface runoff, mist sprayers with lighter application rates to reduce surface erosion could be a potential solution.

There is an inactive trolley ramp with no surfacing at all. The base is from crushed rock with a maximum stone size of 75 mm. However, there is a binding layer overlain by a crushed stone so that these large stones and boulders are not protruding. Figure 2.9 illustrate this structure at trolley 1A at the mining site.

Generally, an optimum base layer design of 100 mm thick continuously graded crushed stone with a maximum size of 26 mm would perform well. A double seal surfacing on both the trolley ramp and brake test ramp would potentially perform well, comprised of a 32 mm and 19 mm stone and slurry. In surfaced roads, mud carried over into the paved network from unpaved haul roads will be reduced significantly, increasing safety during wet seasons. Large mechanical brooms are necessary to sweep off dust and some spillage, they need to be adapted for usage on haul roads.

A statement released by First Quantum Minerals Ltd (FQML) Zambia on investing in the design and management of haul roads in their Kansanshi mine showed cost savings of approximately US5 million (R 72246250.00). Due to innovative maintenance strategies and their world-class haul operation systems, tyre life has dramatically increased, trolley faults decreased, and safety enhanced. It is reported that from 2018 to 2020, tyre life showed a 25% increase from 6000 hours to 7000 hours, this is worth US5 million cost savings and to a further 10000 in exceptional circumstances. Visser (2015) conclude that it is through adherence to such principles mining operations have become effective and financially benefited.

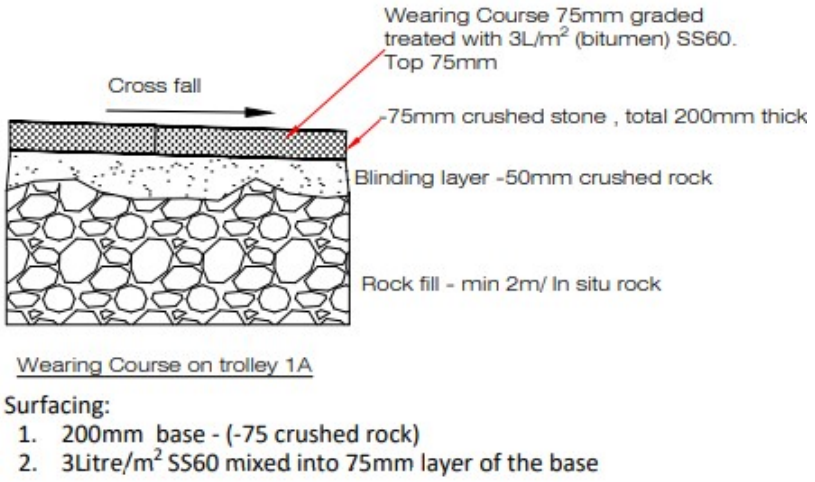

Figure 2.9: Pavement Structure on trolley 1A

2.4.5 Pavement Material Properties

Material Parameter	Range		Impact on Functionality
	Min	Max	
Shrinkage Product	85	200	Reduce Slipperiness but prone to raveling and corrugation
Grading Coefficient	20	35	Reduce erodibility of fine materials, but induces tendency to ravel
Dust Ratio	0.4	0.6	Reduce dust generation but induces raveling
Liquid Limit (%)	16	26	Reduce slipperiness but prone to dustiness
Plastic Limit (%)	12	17	Reduce slipperiness but prone to dustiness
Plasticity Index	4	9	Reduce slipperiness but prone to dustiness and raveling
CBR at 98% Mod AASHTO	80	-	Resistance to erosion, rutting and improved trafficability
Max Particle Size (mm)	-	20	Ease of maintenance and vehicle friendly ride

Figure 2.10: Wearing course material selection parameters. (Thompson and Visser, 2000*a*)

Lateritic gravel for heavy duty pavements			
Grading	**Sieve Size**	**% Passing (Target Grading)**	**% Passing Range**
	37.5	100	100
	19.0	80	72-1000
	9.5	57	50-78
	4.75	43	38-58
	2.36	31	25-44
	1.18	23	18-35
	0.60	18	13-28
	0.425	15	11-25
	0.30	13	9-22
	0.15	9	6-17
	0.075	7	4-13
	0.0135	4	2-9
Liquid Limit (%)		<25	
Linear Shrinkage (%)		<2	
Max Dry Compressive Strength		>2300	
CBR Soaked		>80	
Dust Ratio		0.3-0.7	

Figure 2.11: Lateritic gravel specifications for heavy duty pavements. (Netterberg, 2014)

2.5 INNOVATIVE MATERIAL SOLUTIONS

Innovative material solutions include technologically enhanced materials to meet the current challenges in the road construction industry, as they outweigh the traditional construction methods. This is a strategic necessity to improve safety and operational effectiveness to ensure that road infrastructure commensurate with hauling or productivity needs. These additives are blended either in water or bitumen then mixed with aggregates. It is imperative to understand their behaviour and evaluate their performance and decide if they deliver optimally.

2.5.1 Bitumen Stabilized Materials (BSM's)

BSM's are granular materials treated with either bitumen emulsion or foamed bitumen. The design mix includes less than **1%** of active filler, cement, or lime depending on which one provides optimal performance under testing (Collings *et al.*, 2020).

The stabilization of materials improves material strength and further reduces moisture susceptibility. In this research, the focus will be confined to the bitumen emulsion stabilizing process that includes and further modifying it to accelerate its performance.

Bitumen emulsion is a dispersion of tiny bitumen droplets in water kept in separation by an appropriate emulsifier/surfactant. The charge of the bitumen emulsion droplets depends on the

charge of the emulsifier. The bitumen emulsion can either be cationic or anionic meaning positively charged or negatively charged, respectively.

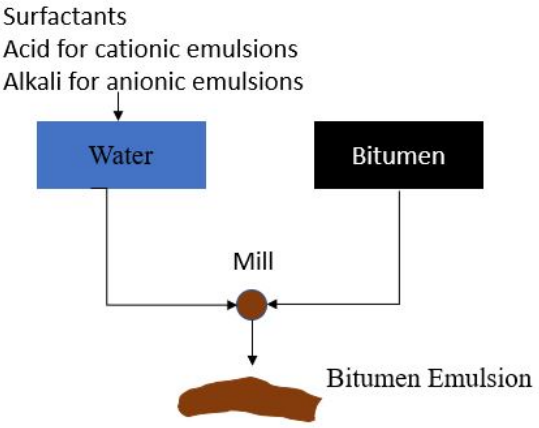

Figure 2.12: Bitumen emulsion manufacturing process

Figure 2.12 shows the blending of bitumen, water, and surfactant to manufacture a bitumen emulsion (Collings *et al.*, 2020). The surfactant consists of a long hydrocarbon chain whose end could either be positive or negatively charged, its charged ions orient themselves to the bitumen droplet surface, thereby forming a suitably firm bond. The acid is poured in to regulate the concentration of hydrogen ions until the needed pH is obtained (Read and Whiteoak, 2003). Acid is applied in cationic emulsions while alkali is added in anionic emulsions.

Binder Surface Run-off behaviour

Materials that are suitable to be stabilized with bitumen emulsion range from G1 to G5 materials. G5 quality natural gravels extracted from laterite, dolomite, limestone can also be stabilized with bitumen emulsion. BSM classification is done in two categories, being BSM1 and BSM2. The classification is greatly influenced by the quality of the parent rock (Collings *et al.*, 2020).

Mine haul road networks are not particularly popular for their gentle slopes, due to the common mining methods and conventional open-pit mining, the applicable transport system is the ramp truck haulage system. The road networks have steep sections where the application of low viscous materials would be challenging due to the possibility of a significant runoff. According to Kashaya (2013) distress mechanisms could be caused by a binder runoff, from the surface on which it has been applied leading to uneven binder thickness along the surface area, consequently resulting in raveling at the upstream section and bleeding downstream. For significant mine haulage truck productivity and efficiency, the recommended maximum ramp gradient ranges from 8 % to 10 %, (Thompson, 2011*a*). Furthermore, the camber of the ex-pit roads also should be kept to about 2 % to 3 %.

Figure 2.13: Dust suppressant running off upon application

Figure 2.13 shows an ex pit ramp of a gradient well below 10 %, however, the addition of a dust suppressant also drains down along the road section. Therefore, an insufficiently viscous liquid will also trickle down the steep road surface under poor surface material texture and unsuitable binder spray rates. The binder type and application viscosity contribute to surface runoff. It further highlights that an occurrence of a thixotropic reaction during bitumen emulsion application prevents the emulsion from quick flow, as a result, a higher binder application rate can be achieved compared to standard binder application, without the possibility of run-off.

High viscosity emulsions are applicable at relatively steep gradients such as mountain terrains, viscosity is a critical factor that must be customized as per the pavement application and set in line with the type of slope or grade (Ronald and Luis, 2016). The 10 % slope is very steep and comes with a high possibility of binder runoff, while 2 % camber is acceptable, meaning there is less likelihood of the applied binder to runoff. Highly viscous and modified binders can be used to mitigate runoff on steep slopes. Kashaya (2013) mentions that polymer-modified binders are more viscous and less likely to run off compared to unmodified binders, runoff is a function of gradient, texture depth, and application rate, it is directly proportional to the spray rate. Therefore, to add modified binders on a steep gradient, it would be critical to use low spray rates should spraying application methods be used. On a relatively smooth surface like a slurry seal, runoff is more likely to be higher than a surface with a higher rolling resistance or much larger stone size.

2.5.2 Organosilane

Organosilane compounds comprise silane coupling agents whose reactivity types include inorganic and organic in the same molecule. These compounds typically have one organic substituent and

three hydrolyzable parts (Antonucci *et al.*, 2005). They alter the surface of inorganic particles such as sand and aggregates for improved interaction and bonding with the binder, therefore, their use as an anti-stripping additive and bonding agent leads to enhanced moisture sensitivity and bonding tack coat.

Nano-silica

It is imperative to facilitate a clear understanding of silanes by defining silicon, which is the most common chemical element found in sand and rocks. Pure silicon is too reactive to be freely found in nature, hence it widely exists as a compound. It easily bonds with other organic materials and should it be attached to some reactive molecules, such molecules bond firmly to organic polymers. Hence its suitability for use in different functional chemicals. Monomeric silicon chemicals are referred to as Silanes while a silicon monomer means a basic group of other three atoms or molecules joined to Silicon. Monomers may also be joined to form polymeric silicon which is known as siloxane (Okamoto *et al.*, 2011).

2.5.3 Nanomaterials commonly used in construction

A silane that contains at least one carbon-silicon bond structure is referred to as an organosilane. Carbon and silicon chemistry can result in unique properties which could potentially render material behaviour competitive in terms of performance. Jordaan and Steyn (2019) report that the nanosilane technology solutions offer improved properties when used in bitumen emulsions. They are adhesion promoters for aggregate and stabilizing agents and provide hydrophobicity to aggregates. The adhesive nature is reliant on the strongest silicate chemical bonds in the aggregates to form a siloxane as shown in Figure 2.14. The use of these solutions dates as back as the 1820s, since then, some research has been conducted leading to developments of silicon-based products such as silanols, alkylakoxi-silanes, and organo-silanes which protect structures against adverse climatic effects and pollution.

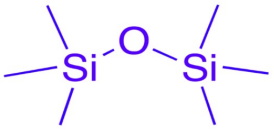

Figure 2.14: Siloxane Bond

Table 2.4: Nanomaterials used in construction materials. (Mohajerani *et al.*, 2019)

Application	**Area**	**Nanoparticle Type**	**Major Applications**
	Concrete	Silica	Reinforcement in mechanical strength, Rapid Hydration
	Concrete	Titania	Self-cleaning, Increased degree of hydration
	Concrete	Carbon	Crack Prevention, Mechanical durability
	Asphalt Concrete, Timber	Aluminium Oxide	Increased compressive strength, Increased serviceability
Construction	Bricks mortar	Clay	Increased compressive strength, Increased surface roughness
	Concrete	Iron Oxide	Abrasion-resistant
	Steel	Copper	Weldability,Corrosion resistance; Formability
	Asphalt concrete	Zycosil	Increased fatigue life, Higher compaction

Organo-silane compounds are well known for their potential to enhance the adhesion of organic polymers and inorganic substrates. They contain an organic functional group, R-, and a hydrolyzable alkoxy group, -OR, hence the general formula R-Si-OR. When used as a coating additive, upon application, the silane moves towards the interfacial region, reacting with the absorbed moisture at the hydrophilic (hydrophilic) surface of the substrate, thereby producing silanol groups which in turn bond firmly to the surface (Khitab and Tausif Arshad, 2014).

Carbon Nano Tubes (CNT)

These are long hollow cylinders of monolayer or multi layer graphene sheets whose diameter extends from 1nm as shown in Figure 2.15. An electron is confined to one dimension(1-D) in reciprocal lattice space, giving rise to quantum effects which in turn affect the material chemistry (Strano *et al.*, 2009). Carbon nanotubes have widely gained popularity in application to construction materials and material science, because of their exceptional effect in binder modification. An increase in loading has led to standard binders not being able to deliver optimal performance. These are ideal additives in construction due to their strength, weight and surface to volume ratio. .

Figure 2.15: The structure of a carbon nanotube (CNT). (Mann, 2006)

Carbon Nanotubes can exist in two different forms whose effectiveness in performance enhancement is different. The two different existential states single tubes or coaxial tubes are both explained below:

- Multi-walled Carbon Nanotubes (MWCNT): These have more than one wall. In Egypt, Amin *et al.* (2016) investigated the effect of MWCNT's as an additive to bitumen, results reveal that high failure temperature and rutting resistance of bitumen increased significantly. The enhancement of high temperature from 64°C to 76°C means an increased resistance to permanent deformation, making the modified material compliant to set requirements. Similarly, adoption of this technology in the Southern African regions can possibly improve existing local materials properties to meet set specifications.

  Carbon nanotubes differ in quality and have five times Young's modulus and eight times the strength of steel while being 1/6 of the density (Mann, 2006). Therefore, they are eligible for use in material modification for major infrastructural projects in the construction industry. Once introduced in the mix or soil, the inter-particle spacing reduces and the soil becomes nano-reinforced, resulting in the construction of an incredibly stiff soil matrix and subsequently, an improvement in the mechanical properties of the soil. MWCNT's are not, however, easily dispersed homogeneously, compromising the effectiveness of their intended effect and performance, therefore, a surfactant is necessary to promote dispersion (Correia and Rasteiro, 2016). These nanoparticles are corrosion resistant (Steyn, 2011), further making them ideal candidates for innovative material enhancement.

- Singled Walled Carbon Nanotubes (SWCNT): These are more effective than Multi-Walled Carbon Nanotubes (NWCNT's) due to their relatively high aspect ratios and small diameters (Makar, 2011). This feature makes them desirable to work with. Ahmad *et al.* (2018) further

points out that in as much as they are not easy to work with, they exhibit much higher strengths and stiffness compared to the MWCNT's at the right optimum content when appropriately dispersed. In bitumen mixtures, these materials, with an optimum content of 0.05% improved Marshall Stability and rigidity flow (Shu *et al.*, 2017). Niyogi *et al.* (2002) also points out that utilization of these carbon nanoparticles pushes the limits of science, their low strength-to-weight ratio and carbon to carbon bond in its conjugated form, is the strongest, giving rise to a material whose elastic modulus exceeds that of a diamond.

According to Sobolev (2016), a new material with approximately 50% of the reactant's strength was developed. This was due to 10 % of SWCNT mixed into a high performance fibre, Zylon. Furthermore, SWCNT reinforced fibers exhibited a significantly high amount of strength when tested, nearly 1.8 GPa. This further reinforces the notion that the incorporation of these additives in materials potentially results in superior mechanical performance and durability. Underlying chemical interactions at a quantum level result in novel macro properties.

2.6 NANO MODIFIED EMULSIONS(NME'S)

Bitumen is a hydrocarbon product obtained by removing light fractions, with a relatively low boiling point in a fractional distillation of crude oil. Additionally, the basic residual product is normally termed "straight run" bitumen. Its compositions could be different since it is affected by the origin of crude oil. Bitumen may have regional variations in terms of the molecular weight of hydrocarbons and physical properties (Read and Whiteoak, 2003). To achieve desired performance in field applications, bitumen can be blended to form emulsions, stabilized by an emulsifier. An emulsion is a mixture of two or more liquids that are immiscible, it is a dispersion of small; droplets into one liquid of another liquid (James, 1998). A Nano Modified Bitumen Emulsion (NME) is a bitumen emulsion that has been further modified using nano additives, these have lower surface tension and viscosity at the correct shear force, thereby resulting in a separation of bitumen droplets (Jordaan *et al.*, 2021*b*).

Bitumen emulsions can be classified into different categories depending on their composition. It is possible to use different material additives to blend with basic bitumen emulsion to develop a customized bituminous product for a specific task. The two categories can be explained as:

- Standard Emulsion: This refers to a conventional emulsion, it could be an oil-in-water(O/W) emulsion, water in oil emulsions (W/O), and water in oil in water (W/O/W) emulsion (James, 1998) It is possible to have multiple-phase emulsions where the dispersed droplets carry some

droplets of the liquid, they are dispersed in. These standard emulsions can either be negatively charged or positively charged. They have no additives to improve their performance or enhance their properties, other than emulsifiers and chemistry to balance the emulsions.

- Modified Emulsion: These are enhanced emulsions, there normally exists a wide variety of additives to improve emulsions performance, such include polymers, contemporary nano additives, and other available adhesion promoters. According to Jordaan *et al.* (2017*b*), the nano additives are classified as organosilanes since such a classification offers a better technical description. Their adoption in pavement engineering, particularly in bitumen emulsions is still in an infancy stage.

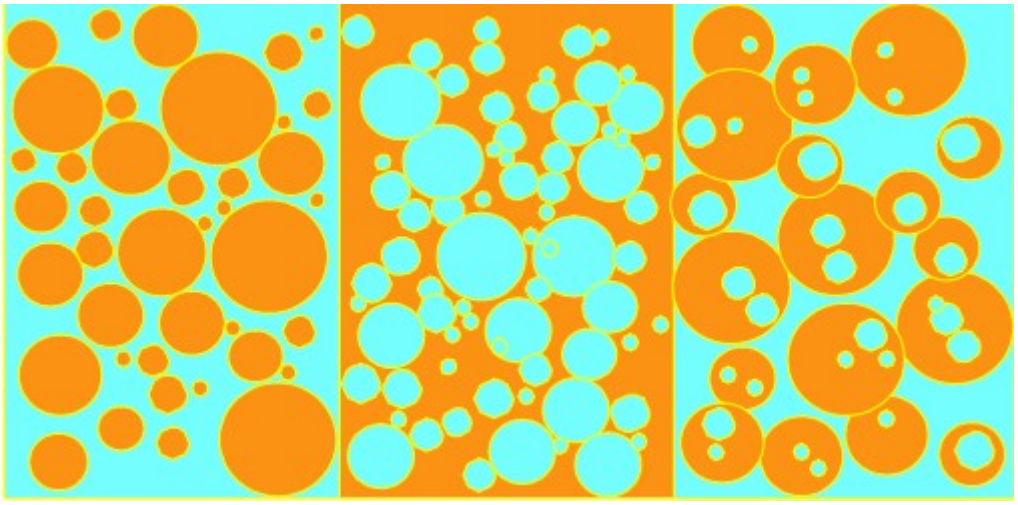

Figure 2.16: Different phases of standard bitumen emulsions

A high-quality graded crushed stone with a high level of emulsion will have properties like those of asphaltic concrete (Bullen, 1998). Additionally, a marginal material with a low emulsion application will have its performance slightly improved, this is representative of the South Africa and Australia experiences. A relationship exists between material quality and bitumen emulsion quantity with a link to performance. To date, numerous chemical additives have been on trials to modify bitumen, these include polyphosphoric acid (PPA), silanes, nanocomposite modified bitumen, and others (Porto *et al.*, 2019), only a few have been practically applicable. Ebels and Jenkins (2007) mention that these modifications, particularly in bitumen emulsions are challenging since the compatibility of all involved additives needs to be balanced for optimum strength. Proper metering of additives is critical for the quality of the emulsion therefore a controlled procedure will lead to efficient product manufacturing and less errors.

Since the 1990s, there has been significant growth in the adoption and application of nanotechnology

in different fields such as science, medicine, electronics, materials, and construction (Abdullah *et al.*, 2015). This demonstrated an increasing need to match the level of increasing technological demands in each industry and accelerate service delivery and product quality. Most research evaluating the use of nanoparticles has been geared towards nanoengineering, a nano manipulation of materials and processes at the nanoscale to modify the behaviour of materials and consequently performance.

There is dearth of research explaining how the scale and geometry of nanoparticles affect their interaction with soil/aggregate particles, further curtailing agile implementation in the field of civil engineering or particularly, pavement engineering. Nanotechnology application in pavement has been considered since 1990's (Zhu *et al.*, 2004). Its development has been accelerated in different fields including electronics and devices, medicine or drug delivery, and surface coatings. There has been a very narrow application of nano modified products in the construction industry, it is important to note that significant research has been carried out about the inclusion of nanoparticles in concrete (Steyn, 2009). The construction industry and industrial sectors have lagged due to different reasons like funding thereby hindering developmental progress.

2.6.1 Types

- Bitumen Based NME

Bitumen Emulsions are further blended with nanoparticles to modify the physicochemical properties of the bitumen and consequently performance upon application. Blending bitumen and asphalt with nano additives is one of the contemporary techniques of binder modification and the newest approach in the road construction industry (Ghoreishi *et al.*, 2020).

Use of bentonite in bituminous binders and mix designs increases adhesion and mix performance. According to Van De Ven *et al.* (2008), unmodified clay is highly hydrophilic and therefore incompatible with most naturally occurring traditional materials, the modification, therefore, makes it organophilic and provides a large surface area in the bitumen emulsion. The findings showed that the modified bituminous binders have an improved softening point, ductility, and increase in viscosity depending on the structure and dispersion of nanoclay additives (Ganesh, 2012). The binder resistance to permanent deformation and rutting has been recorded to be much higher for modified asphalts compared to base asphalts.

Like the effect nanoclay has on bitumen, Crucho *et al.* (2019) reports that modified nano-silica binder showed an increase in both softening point and viscosity. In South Africa, Rust *et al.* (2019) showed that the addition of nanosilane particles to a composite material forms a protective layer that reduces the susceptibility of the bulk composite material to water, henceforth rendering it

water repellent. Rust *et al.* (2019) further evaluated stabilization of base and subbase layers using an anionic SS60 NME, at 1% to 1.5% by mass of aggregate, the heavy vehicle simulation test revealed that the modified pavement layers were to some extent, insensitive to the magnitude of wheel load, no cracking was observed at test sections. The nanosilane additives also provide the pavement layers with hydrophobic effects, as a result, the pavement remains dry with a low rate of deterioration due to decrease or no significant water ingress.

The effectiveness of Nano additives, given the correct chemistry, optimum dosages, and suitable materials or mix components, enables the use of lower residual bitumen application rates (Jordaan and Kilian, 2016), bitumen is an expensive commodity. The use of little dosages to gain needed strength results and considerable cost savings reinforces a common ideology that good things come in small packages.

Laboratory results of untreated G5 materials are shown in Figure 2.5. Akhalwaya and Rust (2018) mention that NME stabilization of this G5 material show improved performance compared to standard bituminous materials, indirect tensile strength values showed a 23 % increase in dry conditions and a 338 % increase in wet conditions. It can further be observed that the NME materials exhibit better performance in wet conditions, as a result, have an improved hydrophobicity compared to standard bituminous materials. The significant performance increases were achieved with 0.7 % per mass of standard SS60 anionic bitumen emulsion, achieving higher increases in unconfined compressive strength (UCS). Little amounts of nano additives validate the cost-effectiveness of this stabilization approach.

Table 2.5: Material properties of an untreated G5 material.(Akhalwaya and Rust, 2018)

Material		**Atterberg Limits**		**Compaction**	
Type	Granular	Liquid Limit (%)	20	Max dry density (kg/m^3)	2132
Classification	G5 (COLTO,1985)	Plastic Limit (%)	17	Optimum moisture content(%)	6.4
Treatment	None	Plasticity Index (%)	3	98 % Mod AASHTO CBR	55
pH	8.3	Grading Modulus	2.26	% Swell	0.01

Their tensile strength is 100 times stronger than steel (Pacheco-Torgal and Jalali, 2011; Firoozi *et al.*, 2016), furthermore the addition of CNTs reduces inter-particle spacing leading to a strong and stiff soil matrix. Following an improvement in mechanical properties, these NPs further increase the tensile strength of the mix, decrease brittleness, and increase Young's modulus, thus higher resistance to permanent deformation (Pacheco-Torgal and Jalali, 2011).Zhu *et al.* (2004) adds that a CNT composite is six times stronger than a conventional carbon fiber composite, they are relatively more flexible and do not easily fracture under compression.

According to Steyn (2011) the massive economical production of CNTs to accommodate the multi-scale nature of structural engineering projects remains unrealistic currently. To overcome the existing production scale constraints, understanding the transition from molecular processes to larger-scale processes should be effective and sufficient (Buehler and Ackbarow, 2007), for optimum performance of potentially new novel structural materials.

- Polymer-Based NME

These are nano polymeric composites, they exhibit a significant prospect towards material science, in pavement technology. According to Yang and Tighe (2013), they are a recent noble discovery, whose physical and chemical properties are magnificently enhanced with the addition of nano clay to a polymer given that the dispersion of nanoclay is optimum. In this case, bitumen has been modified with a known polymer, then it is further modified using a secondary agent that further improves its mechanical properties or engineered purpose. Nanoclays have been added to an SBS copolymer Modified Asphalt, increasing its storage stability, performance properties, rutting resistance (Yang and Tighe, 2013).

Application of PNME resulted in increased indirect tensile strength, with the advent of nanoclay modifying agents. Through optimization of nano additives used and effective pavement materials selection, in cold weather climatic conditions, nano-modified materials show reduced susceptibility to moisture or water. This prospect is vital given that, a significant number of pavements have their major causation of distress conditions as exceedingly high moisture content or water. Therefore, cold regions are highly likely to survive freeze and thaw, snow-related defects, and others.

Polyolefinic plastomers or thermoplastics blended into bitumen generally result in increased bitumen stiffness and improved rutting resistance (Porto *et al.*, 2019). Modified bitumen is characterized as a two-phased system comprising the asphaltenic matrix and the polymeric matrix. The latter is normally investigated for complex interaction mechanisms that occur due to the additive and the potential effects the additive has on the rheological properties of bitumen.

The secondary modification of polymer-modified bitumen with nano additives requires absolute care to address design and application specificity. The ultimate performance is driven by the underlying chemistry and polymer matrix morphology which are predominantly controlled by surface chemistry, size, and shape of applied nano additives. According to Porto *et al.* (2019), unique interactions develop when the nano additive size is approximately equal to the length of a single polymer coil, this approach leads to optimal control of mechanical properties.

The fundamental aspects in the effectiveness of the polymer-based NME include the polymer matrix, nano additive, and the interfacial region amongst these components. The cross-linking of

polymer chains, i.e. polymer networks, exhibit long-term resistance to mechanical loads and show increased temperature resistance (Crosby and Lee, 2007). These networks, such as epoxies, under modification with nanoparticles, develop secondary networks which control the polymer matrix mechanical properties at high deformation. Key to the performance of the nano additive is three aspects, chemistry, size, and shape.

Lesueur (2011) reports that the chemistry of each component affects its mechanical properties, but the most iconic property is the size, which is predominantly responsible for the nano effect in the polymer-based nanocomposite. The surface-to-volume ratio significantly affects the grain-to-grain contact of components at the nanoscale, the interfacial region then controls newly developed structural arrangements. As a result, the more the interfacial region the higher the potential of unique physio-chemical properties (Crosby and Lee, 2007). It must be noted that the effectiveness of the bond strength within the components interface and a polymer matrix depends extensively on the dispersion of the filler within the polymer matrix. Poor dispersion of a filler will not result in the most favourable and desired interactions within the polymer matrix, consequently poor end-product.

An important concept to consider when blending these different components to achieve a well-designed, novel and optimized structure is the compatibility of the components amongst one other. According to Zhu *et al.* (2014) plastomers have a relatively lesser elastic component than thermoelastic elastomers, as a result, due to their ability to gain strength quicker, they are more susceptible to permanent deformation and brittle failure. Their non-polar nature and tendency to crystallize results in incompatibility problems with bitumen (Porto *et al.*, 2019). Thermoplastic elastomers are preferable as bitumen modifiers because they can stretch upon loading and recover thereafter (Porto *et al.*, 2019), making them more resistant to permanent loading.

However, Jordaan *et al.* (2021*a*) carried out a study to understand materials used in the construction of base layer directly above the subgrade, he states that an elastomer modified binder exhibits a major disadvantage since it has a high possibility of entrapping moisture within a newly constructed or rehabilitated base layer thereby accelerating pavement failure due to moisture accumulation. The high moisture build-up just below the surfacing will potentially lead to bleeding and rut deformation. Since entrapped water cannot evaporate, it is possible for the surfacing to be detached from the base, weakening the adhesive strength of the interfacial bond. Figure 2.17 illustrates this concept; stripping (Oliviero Rossi *et al.*, 2017), where the bitumen film has retracted from the stone aggregate due to entrapped water. The phenomenon may further be exacerbated by seasonal moisture variation within the base.

Depending on the target final properties, it is important to select compatible materials for a suc-

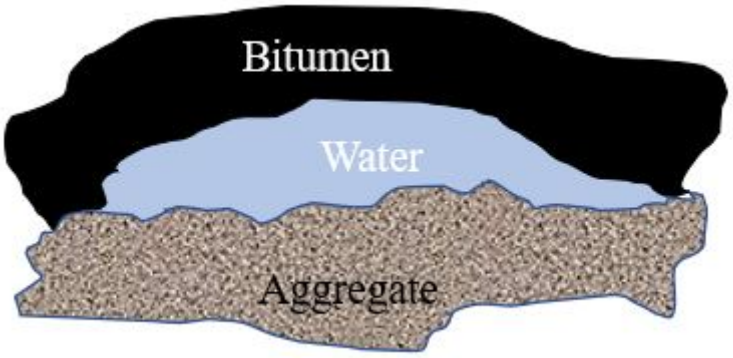

Figure 2.17: Water trapped between bitumen and aggregate

cessful optimum product. Material-compatible nano-based additives can neutralize any adverse effects of secondary minerals (Jordaan *et al.*, 2021*a*), such as layered silicates or clay which are by-products of chemical weathering. Similarly, Jordaan and Steyn (2019) mention that the concept of compatibility is not limited to components within one type of bulk material, however, some aggregate materials have mechanical property deficiencies, and it is important to test if such materials are compatible to be stabilized with PNME's. Polymeric nanocomposites, therefore, present a possibility of intelligently designed materials. The addition of the nano additive leads to a better dispersion of the polymer in a mix (Yang and Tighe, 2013; Porto *et al.*, 2019) and a better product.

2.6.2 Benefits

The use of nanomaterials in construction provides a possibility of a wide array of benefits, although the advantages of the application of nano additives have not been widely researched, and field application has been limited. Previous tests results showed improved physical, mechanical, and chemical properties. Exemplary benefits of nanoparticle addition within the construction industry are listed.

- Nanoparticles atoms are impeccably ordered, as a result, material dimensions transition from macro size to the nano-sized, this causes a significant change in the material properties and macro behaviour/performance, resulting in decreasing energy consumption (Mohajerani *et al.*, 2019) and material quantity. Furthermore, the use of nano-silica (NS) as a filler in calcium silicate hydrate (C-S-H) increases interparticle bond strength within concrete and cement paste.
- With a significant decline in ease of access to high-quality construction materials, the use of nanoparticles in construction provides a prospect of using local/traditional soils which have no

developed standard or guidelines, through this pavement technology, sustainable development can be promoted, and cost-effective material solutions employed with a low value to weight ratio.

- According to Mohajerani *et al.* (2019), the durability and efficiency of modified materials are enhanced depending on the measure of the interfacial tension amongst voids, aggregates, and other mix particulates. The built environment sector produces less waste from conventional materials use, focus then lies on environmental protection coupled with innovation competitiveness. Concrete gets its self-cleaning property from Titanium Oxide nanoparticles due to their high surface area of particles and ability to break down dirt in concrete surface into harmless water and carbon dioxide.

There is narrow research in terms of the long-term adverse effects of the application of nanoparticles on the environment and human health. The concern arises due to a recent increase in the use of these materials and their less understood chemical and functional complexity. It is important to know which components in the nanoparticles are toxic or which nanoparticles could be toxic to human health and the environment with time. However, it is unlikely that all nano additives a free from toxicity therefore, most proprietary additives may still be rendered unsafe for extensive practical use. Available information on their toxicity could be insufficient in characterizing nanomaterials due to the lack of existing universally accepted methods for hazards, and long-term exposure evaluation.

2.6.3 Formulation

There are different ways in which mixing components are added to the bitumen but the most effective one depends on the suppliers' application guidelines, according to Jordaan *et al.* (2017*a*) and TOSAS, there are three different mechanisms to incorporate the silanes into the mixture.

- Recycler Method: Terrasil+ treated water is injected into the water separately from the bitumen emulsion, this approach enhances silane attraction to the aggregate material.
- Water and Terrasil+ mix, water is mixed with Terrasil+ or Terrasil+ then the bitumen emulsion is diluted depending on the set design parameters or suppliers recommended proportions, usually one part of bitumen emulsion to 10 parts of Terrasil+ treated water.
- Mixing the aggregate first with the Terrasil+ treated water and shortly thereafter including the emulsion into the system.

Using a preblended modified emulsion from the supplier eliminates the need to incorporate the organosilane inside the mix as an end-user. The setup followed under this approach is like that of bitumen emulsion, where stabilizers, emulsifiers, and acid are added in the mixing chamber

that then mixes all the constituents at appropriate temperatures in a colloidal meal, Figure 2.18 illustrates the concept.

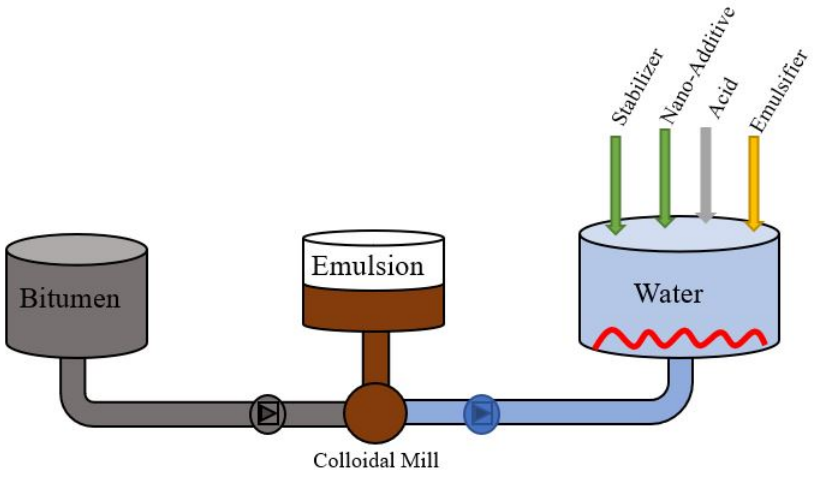

Figure 2.18: Nano additive incorporation into the mix chamber

2.6.4 Application

According to Jordaan and Kilian (2016), the NMEs are available in South Africa and have undergone successful laboratory and field trials. They have been tested under variable climatic conditions on several road sections made from different materials, particularly in Gauteng and Limpopo. Jordaan *et al.* (2017*a*) further states that the availability of these NMEs is not limited to South Africa but extends to the global market, it is important to classify the raw material to which the NME will be applied, for successful modification. Akhalwaya and Rust (2018) studied the nano-modified G5 base and subbase material(see Table 2.5) used at a site in Johannesburg, results showed that the NME modified material significantly outperformed standard bitumen stabilized materials. An amount of 0.7 % by mass of dry material resulted in a 23 % increase in the strength of Dry ITS test specimens and 338 % for wet ITS test specimens. An SS60 emulsion was used for modification, the treated material was then classified under NME2, which for clarification is equivalent to BSM2.

Rust *et al.* (2020) studied the performance of new-age technologies on the D1884 road near Mayerton and K46 road in Johannesburg, both in South Africa, various percentages, inter alia, 0.7%, and 1.25% silane-modified emulsion were used to stabilize an imported G5 material. The severity of cracks on the D1884 was high with a significant water ingress damage coupled with high problematic mica content of approximately 36.1% while K46 had also undergone a massive deterioration. Upon stabilization, it is reported that based on results from accelerated pavement testing of permanent deformation, the NME stabilized base and subbase of the D1884 road performed exceedingly well

according to the Heavy Vehicle Simulator (HVS) testing protocol. Furthermore, laboratory testing showed a significant increase in strength, particularly for test specimens tested under wet conditions.

Practical application of emulsion technology is not only popular in the pharmaceutical sphere, paint industry, and agriculture but it also goes into the bitumen industry. Standard bitumen emulsions have been widely used in mainstream pavement engineering applications but further modifications of such emulsions for use in the Southern Africa mine sites for haul road stabilization have not been effectively realistic. Tannant and Kumar (2000) state that one stabilizer that was used in one Canadian coal mine around 1999 was fly ash, it showed potential for haul road stabilization given stresses induced in the base layer are well below 0.65 MPa, this was a novel approach in 1999 but given the technological revolution and economy of scale in haul truck operations, a more befitting material solution is necessary.

There are fewer publications about stabilizing agents used in Southern Africa mines. Safety is a pivotal aspect of mine operations and almost all mine operations are geared towards maximum productivity, as a result, less effort and use of modified emulsions as a pilot approach towards long-lasting and weather passable haul roads is an existential reality.

Kidgell *et al.* (2019) evaluated the effect of NMEs on the properties of Dolomite, which is also characterized as a problematic material based on its mineral phases and behaviour in the presence of water. It is pointed out that upon stabilization, with two curing periods of 4 days and 4 months, both the ITS and UCS test results rendered the stabilized material as NME1 according to NME classification, also showed in Figure 2.19. The stabilizing agents are hugely involved in the chemical modification of materials, the dolomite is reported to have further changed from the plasticity of 7 to being non-plastic, the expansiveness of dolomite was therefore significantly reduced, consequently, its performance at low plasticity index would be relatively better than at a high PI. These results show the existing potential of nanosilanes to adequately stabilize problematic materials, given the chemistry amongst all mix constituents is correct and the negative influence of mineralogical composition on natural material strength can be neutralized.

NMEs had also been approved as an innovative material solution in Thohoyandou, South Africa, Jordaan *et al.* (2017*b*) points out that using 0.7 % of silane-modified SS60 anionic emulsion with polymer additive by mass of aggregate was used to stabilize a G7(draft TRH14, 1987) base layer material. Upon stabilization, the stabilized material resulted in an ITS strength that exceeds minimum strength requirements for BSM1 detailed in TG2 2020. Jordaan *et al.* (2017*b*) further mentions that the same technology was approved by the Swaziland Ministry of Public works and Transport, a road to North of Manzini was considered for an upgrade, the initial design had a good quality G1 stone as a base layer underlain by a cemented C4 subbase. An alternative design that

included a local G6 natural stone stabilized with 0.5 % of the silane-modified SS60 was selected as an optimum and cost-effective design relative to an initially recommended traditional design approach.

There are countries where the nanosilanes have been applied on low volume roads especially in rural areas where traffic is not massive and the loading is not extreme, these include Brazil, Malawi, Namibia, and the Democratic Republic of Congo. However, there is barely published literature on the effect and durability of the applied nanosilanes on the stabilized roads in the named countries.

2.7 NME CLASSIFICATION

The use of controlled matter at a smaller scale has become a colossal improvement not only in material science but in a wide variety of industries dealing with the application of colloidal and or innovative materials. Sobolev (2016) describes nanoengineering as the manipulation of materials at the nanoscale to develop new materials with novel physicochemical and mechanical properties including self-healing and self-cleaning. Particle properties drastically go under significant changes at a quantum scale, therefore, understanding the structural arrangements of nanoparticles at their nanoscale is an important aspect to effective strategies necessary in tailoring desired products whose functional characteristics would be fit for purpose. The need to produce nanomaterials reliably is based on the increasing demands of macro materials, their structural and compositional complexity, the possibility to address this demand is based on the ability of nanoparticles properties to be manipulated through their size, composition, and structural order (Caruso, 2001).

2.7.1 Classification of NME's

Innovative materials have also received some interest beyond Southern Africa. In Norway, pavement design materials detail acceptable limits and requirements for unbound granular materials use in unbound layers, primarily to avoid any premature failure or distress conditions which include cracking, potholing, stoniness. The developed requirements or limits involve grain shape, flakiness index value, Los Angeles (LA) Value, and others (Barbieri *et al.*, 2020).

Furthermore, in a study of the effectiveness of polymer-based nano additives and lignosulfonates on their practical use, Barbieri *et al.* (2020) tested the aggregates using thin-section microscopy to image mineralogy and grain sizes, and X-Ray Diffraction (XRD) to identify present mineral phases and composition. Chemical tests contribute hugely to material classification and allow a precise prediction of material performance. Identifying mineral phases of rock allows the determination of primary or secondary minerals, their contribution on aggregate to bitumen interaction or compat-

ibility. Therefore, it is critical not to consider the mechanical characterization of materials alone for classification but also chemical analysis or geological characterization.

Similarly, the South Africa pavement industry has also proposed specifications for the newly adopted NMEs. The approach to the specifications is a concept like that of TRH 14:1985. First-class materials are denoted "1", which is the best performing material that meets the top criteria. Therefore, NMEs are classified into four classes ranging from NME1 to NME4. However, Jordaan *et al.* (2017*a*) has also included NM-EG5, which caters for a stabilized poor materials G5-G6. It is reasoned that these materials could be modified with sufficient nano additives to be water repellent and possess significantly high CBR95 values thereby making them conform to specifications and requirements and of equivalent G5 Class.

Generally, there is a lack of universally developed engineering standards for use for developed and use of NMEs laboratory setting or practical application. Figure 2.19 presents material requirements for NME1 until NME4, it should be noted that the chemical classification in terms of X-RD scans is included within the classification parameters. Further basic explanation of NME classes is explained by Jordaan *et al.* (2017*a*)

Material [1]	Material Classification			
	NME1	NME2	NME3	NME4
Minimum material requirements before stabilisation and/or treatment (Natural materials)				
Material [1] specifications (minimum)				
Un-stabilised material: Soaked CBR [2] (%) (Mod. AASHTO)	CS/GS/NG/SSC	>45 [2] (95%) ACV < 30%	>25 [2] (95%)	>10 [2] (93%)
Grading Modulus (GM)	NG	>1.8	>1.5	-
Sieve analysis: % < 0.075 mm ($P_{0.075}$)	ALL	<20%	<25%	<35%
XRD scans:				
- Total sample	ALL	√	√	√
- 0.075 mm fraction ($P_{0.075}$)	ALL	√	√	√
NME stabilisation with micro-meter (µm) emulsion particle sizes				
% Material passing 2 µm ($P_{0.002}$) (e.g., Clay & Mica & Talc) as a % of Material (with Talc < 10%) (XRD-scans of the material passing the 0.075 mm sieve is used to determine the % clay, mica and talc in the material—In this case $P_{0.002} = P_{0.075} \times (P_{clay\,etc.}$ in $P_{0.075})$, or % Silt and Clay	ALL	<15%	<15%	<15%
	NME stabilisation containing micro-scale as well as nano-scale particles (adjusted according to material grading)			
	ALL	NA	<35%	<35%
	NME stabilisation with emulsion containing nano-scale and pico-scale particles (grading adjustments) together with technologies addressing workability of materials on site			
	ALL	NA	<35%	<35%
Material specifications after stabilisation and/or treatment				
In-situ density to be required after stabilisation and compaction (mod. AASHTO) (%) (minimum)	Base	>100%	>100%	>98%	>97%
	Sub-base	NA	>98%	>97%	>95%
DCP (DN mm/blow) (Quality control) (stabilised and compacted)		NA	NA	<2.6	<3.5
Mod. AASHTO density (%) (for laboratory testing)		>100%	>100%	>100%	>100%
* UCS_{wet} (kPa) (150 mm Φ Sample)	**Design** [3]	>2500	>1500	>1000	>750
	Construction [4]	**>2200**	**>1200** [5]	**>700** [5]	**>450** [5]
Retained Compressive Strength (RCS): (UCS_{wet}/UCS_{dry}) (%)		>85	>75	>70	>65
RCS in relation to minimum $UCS_{wet(criteria)}$ ($RCS_{effective}$) (%)		>100	>100	>100	>100
* ITS_{wet} (kPa) (150 mm Φ Sample)	**Design** [3]	>240	>200	>160	>120
	Construction [4]	**>220**	**>180** [5]	**>140** [5]	**>100** [5]
Retained Tensile strength (RTS): ITS_{wet}/ITS_{dry} (%)		>85	>75	>70	>65
RTS in relation to minimum $ITS_{wet(criteria)}$ ($RTS_{effective}$) (%)		>100	>100	>100	>100

[1] CS—crushed stone; NG—natural gravel; GS—gravel soil, and SSC—sand, silty sand, silt, clay; ACV—Aggregate Crushing Value; [2] CBR only used as reference to traditionally used test procedures as a broad first indicator; * Definitions: (UCS = Unconfined Compressive Strength) (ITS = Indirect Tensile Strength); UCS_{dry}; ITS_{dry} = testing after rapid curing; UCS_{wet}; ITS_{wet} = testing after rapid curing and 4 h in water; $(RCS_{effective}) = (RCS \times (UCS_{wet}/UCS_{wet(criteria)}))$; $(RTS_{effective}) = ((RTS \times (ITS_{wet}/ITS_{wet(criteria)}))$; **Design [3] = Minimum criteria to be met in the laboratory during the design phase; Construction [4] = Minimum criteria to be met during construction as part of quality control;** [5] Criteria based on Technical Guideline TG2 [24].

Figure 2.19: Minimum recommended standard specifications for New-age (Nano) Modified (NME) stabilised materials (Jordaan *et al.*, 2021*a*)

2.8 MATERIAL CHEMISTRY

An important aspect is the influence of nanoscale chemical interactions on macro behavior of materials. The complexity of this concern is proportional to the decrease in the level of material granularity. A study has been carried out by Jordan comparing different emulsifying agents on anionic bitumen emulsions, the study further highlights the effect of nanosilane modification on bitumen emulsions, however, does not detail the chemistry of each component in the modified product and the accompanying chemical processes. Rust *et al.* (2020) explains that making an NME requires a high shear mix to adequately blend a nanosilane-based additive, bitumen, water, and a surfactant. In this case, the bitumen emulsion acts as a carrier of both the bitumen and the nanosilane to cover the aggregate surface and provide sufficient particle coating, thereby promoting bitumen-aggregate adhesion.

Akhalwaya and Rust (2018) mentions that to form NME the nanosilane-based additives could either be added to cationic or anionic charged bitumen emulsions. The neat bitumen emulsions are stabilized by an emulsifying agent, Figure 2.20 A illustrates a representative form of an emulsified bitumen droplet. It is further highlighted that the compatibility of the nanosilane modifier is based on its compositional chemistry, therefore, a poor nanosilane selection with unsuitable chemistry will consequently fail to attach to a silica-based aggregate imparting hydrophobic properties as shown in Figure 2.20 B and anti-stripping.

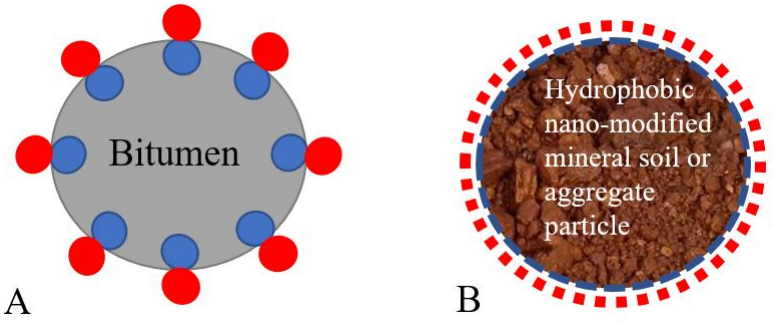

Figure 2.20: Representative particles of bitumen and aggregate

Figure 2.20 A shows a bitumen droplet kept separated by a surfactant represented by a Janus particle (JNP). These JNPs normally dominate interfaces and modify phase stability, attached to the inner walls of the bitumen droplet is a nonpolar tail and the other part at the bitumen droplet surface is a polar ionic portion (Jordaan *et al.*, 2021*b*). Orientation of the JNPs is based on the charge of the bitumen droplet surface, therefore varies from product to product. Figure 2.20 B demonstrates a typically treated aggregate particle, the molecular water depicted by the blue color

evaporates with the water included within the bitumen emulsion, leaving the nano organosilane coating attached to the mineral aggregate.

2.8.1 Surface morphology and interaction

One of the critical aspects primarily responsible for the success of nanosilane interaction is their surface properties and size. In Pavement Engineering, the effectiveness of nanosilane-modified emulsion is that the aggregate interface is also influenced by the physical properties of the nanosilane. One critical property is the size of the nanoparticles, they have a high surface to volume ratio compared to bulk materials, this property makes them more chemically reactive as they have a higher presence per surface area with decreasing size.

Jordaan *et al.* (2021*b*) also ascertains that surface coverage of 1000 litres of bitumen with 4 μm particles size is equivalent to that of one liter nanoparticles with a 4 μm size. There is a high percentage of atoms per unit surface thereby increasing the surface forces, high surface-to-volume ratio can lead to unique chemical, optic, and physical properties. Table 2.6 shows an example demonstrating the increase of surface-to-volume ratio with decreasing size calculations using nanometre (nm) as a unit length.

Table 2.6: Example calculations of surface to surface to volume ratio

Nanoparticle Diameter(nm)	**Nanoparticle Diameter**(nm)	**Volume** (mm^3)	**Surface Area** (nm^2)	**SA: Vol Ratio** (nm^2/nm^3)
1	0.001	0.524	3.14	6
10	0.01	524	314	0.6
100	0.1	523598	31416	0.06
1000	1	5.24×10^8	3.14×10^6	0.006
10000	10	5.24×10^{11}	3.14×10^8	0.0006
100000	100	5.24×10^{14}	3.14×10^{10}	0.00006
1000000	100	5.24×10^{17}	3.14×10^{12}	0.000006

Incorporating nano additives into traditional construction materials is aimed at manipulating the dominating bulk behaviour through molecular level modification, change and improve the dominant behaviour. Ultimately, failure mechanics and fracture mechanisms of bulk materials are altered in terms of, inter alia, occurrence, and intensity. The rate of permanent deformation of materials is relative, loading response is dependent on their make-up at a molecular or atomic level. The origin of material deformation emanates from underlying atomic mechanisms (Buehler and Ackbarow, 2007).

Therefore, improved resistance to loading through nano modification and higher bond strength at contact zones present a potential for increased material durability under traffic damage, moisture, and temperature-related defects.

2.8.2 Aggregates, Bitumen and Water

According to Baldi-Sevilla *et al.* (2017), the stone aggregates are generally polar compared with bitumen, as a result, as water percolates into the aggregate-bitumen interface during a spring-thaw season. A significant amount of stone gets wetted, an adhesive bond failure between aggregates and bitumen occurs. In explaining the structure of bitumen and its interaction with mineral aggregates, Oliviero Rossi *et al.* (2017) mentions that bitumen is a colloidal material characterized by a low chemical affinity to aggregates that possess a strong water affinity. This is due to the degree of interfacial energies amongst the surface of each material. Bitumen polar functionalities have different adsorption capacities, therefore, the adhesive strength would be dependent on the polar nature of each polar functionality.

Some aggregates are super hydrophilic and have very high surface energy resulting in a low contact angle. This results in good wetting of the material aggregates, the increasing surface energy or decreasing surface tension are accompanied by a decrease in contact angle, this means the wetted area of an aggregate particle is greater at smaller contact angles for hydrophilic materials. This indicates that the ability of water to percolate into the material is much easier for some type of hydrophilic aggregates, the water ingress will ultimately lead to premature moisture damage on pavement layers. It is useful to understand the relationship between water, binder, and aggregates, the effect of water on different aggregates with variable material properties, and how such effects can be mitigated through modified or new age binders.

2.8.3 Aggregates and Water

Through a review of past and present research on fundamental concepts related to stripping and premature pavement failure, Bagampadde *et al.* (2004) outlined important factors shown in Figure 2.21 affecting pavement stripping potential, factors include both bitumen and aggregate properties. Bitumen affinity to the aggregate surface is also dependent on bitumen chemical composition, most strongly adsorbed polar functionalities such as carboxylic and sulfoxides within bitumen are water susceptible, hydrophilic. Apostolidis and Scarpas (2020) add that not only do these functional groups affect the overall affinity but also active surface sites of minerals are critical as they are available for reactivity. The chemical thermodynamics of the surface phenomena remains a complex subject that is uneasy to control due to multiple chemical processes that occur amongst

bulk components.

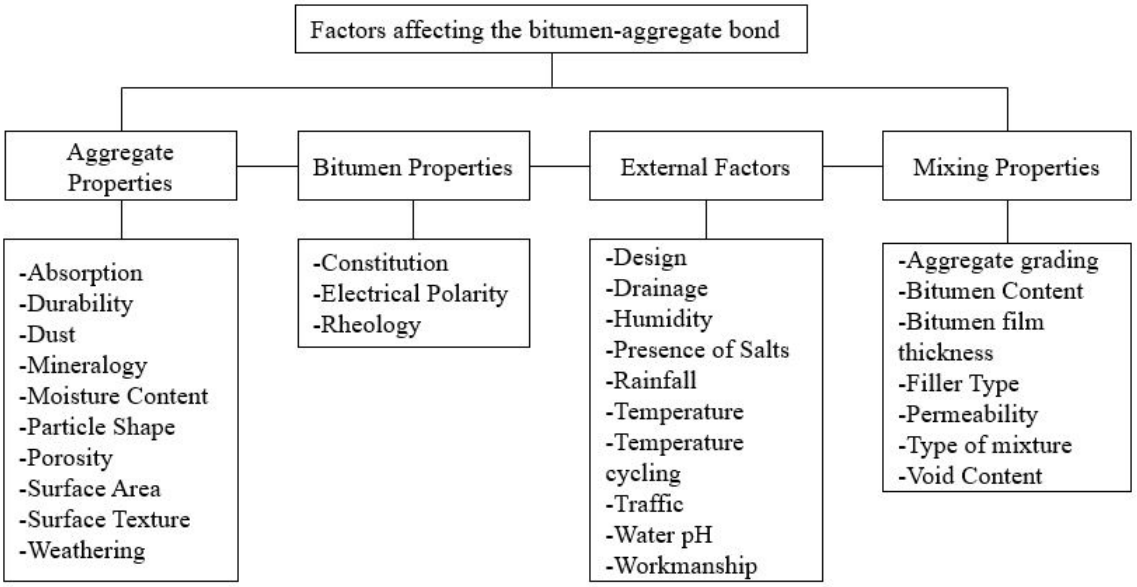

Figure 2.21: Factors affecting bitumen-aggregate bond.(Tarrer and Wagh, 1991)

Effective adsorption of bitumen droplets of the aggregate surface is also affected by the aggregate chemistry (Bagampadde *et al.*, 2004), active surface sites are available for interactions with polar bitumen parts. This chemical reactivity is also hugely affected by the mineral phases present on the aggregate surface, that is, if the present mineral is not compatible with the asphalt binder, there will be weaker chemical reactivity, adhesion, and high stripping potential.

Similar to poor mineralogy, the physical properties of aggregates can potentially lower the striping resistance if aggregates do not have a rough texture to provide binder interlock. Very porous aggregate that may potentially entrap water and adsorbed coatings preventing effective actual contact between bitumen and the aggregate, such inhibitors include too much dust on an aggregate surface (Bagampadde *et al.*, 2004).

Tarrer and Wagh (1991) ascertain that the key to the insensitivity of asphalt pavement to stripping includes aggregate mineralogy and chemical composition. Acidic aggregates contain high amounts of silica hence are more hydrophilic and susceptible to stripping compared to low silica containing carbonate rocks which are relatively hydrophobic. To demonstrate the occurrence of stripping of aggregates in the presence of water Figure 2.22 has been used as an illustration.

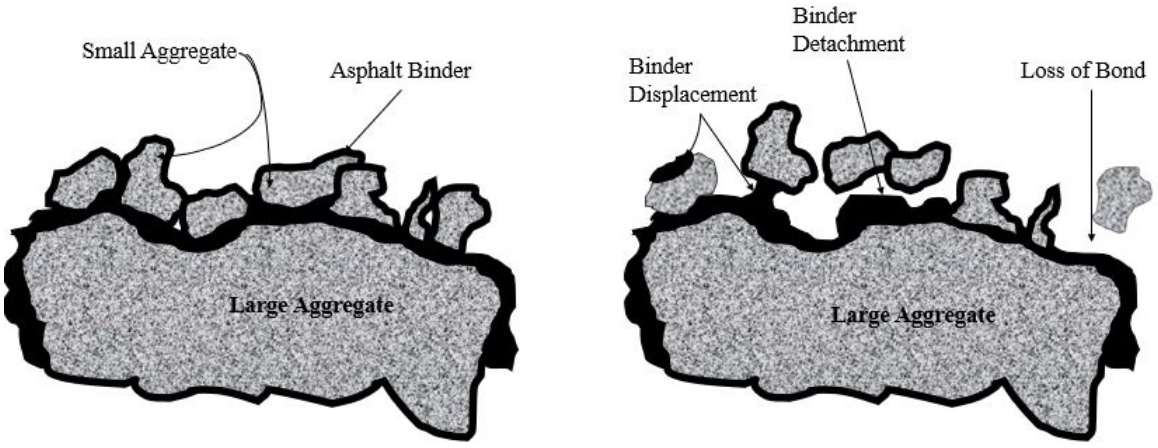

Figure 2.22: Illustration of stripping.

To explain this phenomenon thermodynamically, Bagampadde *et al.* (2004) explain that upon bitumen coating the aggregate, the total free energy emanates from the contributions of bitumen, aggregate, and the interface. Should water percolate the system, the composition, and the interfacial area are prone to change. If the percolating water has low free energy, it replaces the binder from the aggregate resulting in a stripped surface. Water percolating reduces the aggregate surface free energy more than bitumen, resulting in a thermodynamically stable condition of minimum surface energy (Majidzadeh and Brovold, 1966). Therefore, in a three-phase system of bitumen, aggregates, and water, the aggregate surface has more affinity towards water than bitumen. There are different stripping mechanisms as listed below, explained in detail by Tarrer and Wagh (1991), but common to all is the presence of water at the aggregate to bitumen interface, ultimately leading to loss of adhesion.

- Detachment
- Displacement
- Spontaneous Emulsification
- Pore Pressure
- Hydraulic Scouring

2.8.4 Nano-Additives, Bitumen and Water

This section is a precursor to a comprehensive understanding of nano-additives reactions and effects on bitumen and aggregate surface. Understanding the chemical and physical properties of nanomaterials, their size and quantum effects lead to enhanced awareness and modeling of the

interfacial chemistry and properties between the bitumen binder and material aggregates (Steyn, 2011). The knowledge on nanosilane chemistry or interrelationships between matter is more of a chemistry focal point than an engineering interest, however, a sufficient understanding of chemistry is necessary to comprehend the behaviour of nanosilanes for a better practical use (Steyn, 2011). According to Jordaan and Steyn (2019) nanosilanes as stabilization agents in bitumen emulsions imparts a dual impact:

- Increase the adhesiveness of the bitumen particle to the stone aggregate or silica particle surface.
- Imparts hydrophobic properties of the aggregate surface thereby preventing water ingress that may have an adverse effect in contact with secondary minerals such as clay.

Guo *et al.* (2019) mention that the addition of NHSS to an asphalt mix significantly increases the shear strength of the aggregate-bitumen interface by approximately 30 % at -10°C temperature, this can be attributed to the NHSS contribution to asphalt viscosity. Furthermore, for temperatures above, the tensile strength of NHSS modified asphalt specimens was slightly higher than that of unmodified specimens.

Steyn (2011) stipulates that organosilanes are adhesion promoters with a hydrocarbon chain that has an affinity for a bitumen particle on one end and a polar silane end group that attracts inorganic surfaces. It is further pointed out that the low concentrations added in bitumen emulsions help increase the wettability of the aggregate. The silanes promote adhesion between the bitumen droplet and material aggregate surface due to the hydrocarbon chain functionality, through the formation of a monolayer that resides at the aggregate-bitumen interface. Figure 2.23 illustrates the active adhesion at the interface due to the decreased surface energy due to hydrocarbon orientation and functionality.

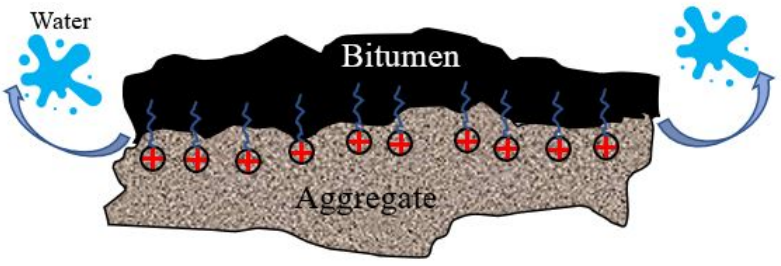

Figure 2.23: Bitumen to aggregate interface strength.

Material nature varies in terms of compatibility, surface properties, and chemical reactivity, making it hard to attain a high adhesion strength between the two dissimilar materials, Pape (2011). Ac-

cording to Matinlinna *et al.* (2018), the adhesion strength of silane is material dependent, therefore different materials will have adhesiveness based on their type. Silica is the most favourable material exhibiting the strongest adhesive strength forming a strong siloxane (-Si-O-Si-) bond upon silane treatment. It links with hydroxyl groups on the substrate surface. A limited amount of hydroxyl groups on the mineral aggregate surface results in a weak silane bond hence poor adhesion strength. If a material with a low concentration of hydroxyl (-OH) groups bonds with silane, there is a high likelihood of premature adhesive bond failure on the silane-surface aggregate interface.

The contribution of silanes as adhesion promoters at the interface region involves complex physical and chemical processes, Pape (2011) explains that water tends to weaken the adhesive bond however, unique physicochemical properties of nano-organosilanes result in approximately 40 % of increased flexural strength, ensuring an enhanced bond strength and resistance to environmental hazards. According to Pape (2011), the fundamental chemical principle is that the nanosilane firmly attaches to the bitumen molecule upon mixing with material aggregates, reactive bonds of the silane ensure a strong bond between bitumen particles and aggregate minerals.

The surface is of the aggregate material changes to hydrophobic upon stabilization with the alkoxy silane modified binder. Jordaan *et al.* (2021*b*) maintains that the extent to which the material repels water is dependent on the size of the alkyl group attached to the silicon atom. The hydrophobicity degree ranges from the superhydrophobic material to a super hydrophilic material as shown in Figure 2.24. This most hydrophobic material is characterized by a large contact angle, has a low water affinity producing a lotus effect upon water contact.

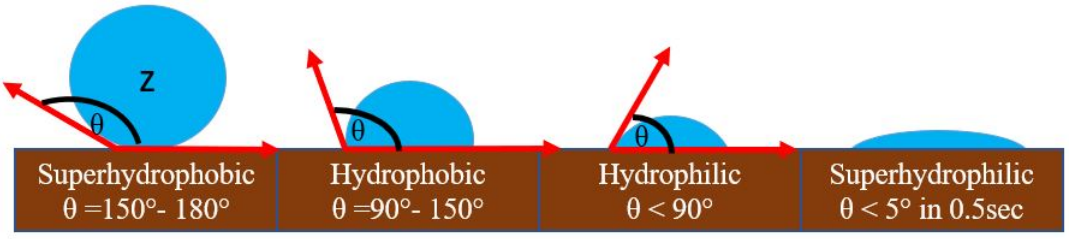

Figure 2.24: Levels of material hyrophobicity

Organosilane is a polymer-based ultraviolet and heat-stable product that is not leachable concerning its safety evaluation tests. According to Barbieri *et al.* (2020), it is made of two components (organic and inorganic), with the chemical ability to change the hydrophilic silanols on a silicate surface of the aggregate materials. Moreover, the newly formed water repellent layer of alkyl siloxane on the silica aggregate has a size around 4 to 6 nm, the functional groups are therefore not only essential in combining with hydroxyl groups of the inorganic substrate but they extent to organic polymers

strengthening the interfacial bonding.

It is essential to understand how a silane modifies a substrate surface, it is a four step process from hydrolysis to bond formation.Rahman and Padavettan (2012) explain that alkoxy silanes undergo hydrolysis in the presence of water, hydrolyzed silane self-condense then deposit on the silica surface forming a siloxane bond with silanol groups. After condensation to oligomers, then hydrogen bonds with hydroxyl groups of the substrate. When water is driven off the substrate during the curing process, a covalent linkage forms with the substrate. There is one bond extending from each organosilane silicon atom to the substrate surface in their interfacial region. The two silanol groups are freely available or condensed while R groups remain available for covalent reaction with other phases (Arkles, 2011). Figure 2.25 illustrate the process.

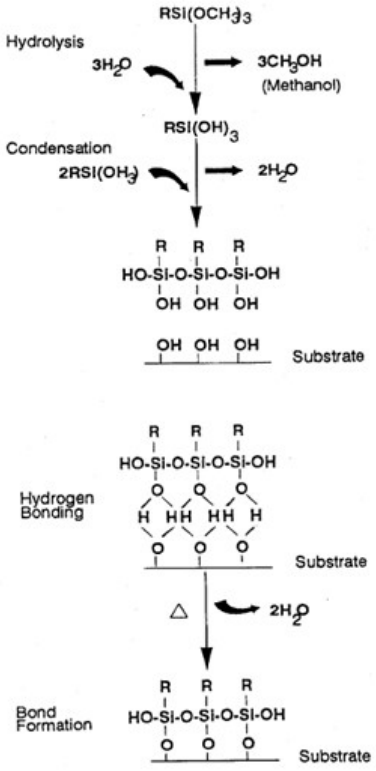

Figure 2.25: Reaction Process of alkoxy silanes. (Witucki, 1993)

It is critical to consider the mechanism of nanomaterials in soil strength improvement at a microscopic level. Huang and Wang (2016) define this through modification of the soil pore spaces occupied by fluids. Due to particles nano-size, different structures at that scale, functional groups, and bond strength, they can efficiently disperse in the pore spaces among aggregate soil grains. Huang and Wang (2016) further explain that for nano additives added in the mix through incorporating them in water, the rheological water suspension properties influence the effectiveness of the

additives towards efficient soil stabilization, hence strength improvement. According to fundamental laws of physics on collisions of carrier fluid particles, water or bitumen generate forces which due to Brownian movements are greater than gravitational forces experienced by the nano additive particles (Jordaan *et al.*, 2021*b*), therefore, they form a colloid in water.

Additionally, the viscosity of the nano additive-water suspension steeply increases, thereby forming a gel, which upon getting in contact with aggregate pore fluids, transforms the zero shear resistance fluids into shear resisting colloidal fluids (Huang and Wang, 2016) .This improves the cementation of the aggregate matrix and the general shear strength of the soil. The NME stabilized layer then repels water due to a series of chemical reactions that have occurred between mineral aggregates and the modifying agent, thereby resulting in an accelerated drying and strength development in the layer (Jordaan *et al.*, 2021*a*). The water chased away covers the surface of the aggregate and does not percolate into the bulk material, if it does permeate, it does not go further than a few millimeters because of the action of the silanols on the surface of the aggregates. This indicates that under wet conditions the dry condition material strength and stiffness are retained.

2.9 FACTORS AFFECTING EFFECTIVENESS OF NME'S ON SUBSTRATES

2.9.1 Dispersion

Inadequate dispersion of the nano additive in the mix means that not all aggregate particles will be coated with the organosilane in the additive. The aggregate surface area will be coated by a non-homogeneous additive carrier. It is imperative to ensure a homogeneous mix through an effective dispersion of the organosilane in water or bitumen emulsion depending on the selected nanosilane incorporation mechanism. To achieve maximum dispersion of additives, Abdullah *et al.* (2015) advocate that mechanical mixing methods are insufficient for an ultimate homogeneous mixture, but depending on the chosen nano additive, a thermodynamic driving force is necessary to separate silicate layers into primary silicate sheets. This phenomenon applies to nano additives such as nano clay, a surfactant that reduces surface tension on particle surfaces is used, keeping them in suspension or colloidal state to avoid agglomeration.

The surfactant essentially contributes to the effective dispersion of additives in a carrier liquid, provided it is compatible with the binder or carrier liquid. It is also probable that compatible surfactant will not only enhance dispersion but also the bonding of the additive with aggregate surfaces. Murphy *et al.* (2019) point out that from application of nanosilane on a 150 mm base layer, effective distribution was achieved with application rates as little as 0.75 % NME, the stabilized layer was compliant to specifications set for both indirect tensile testing and unconfined

compressive strength. Though much smaller percentages would be considered almost impossible to be effectively and entirely mixed using standard emulsions, a suitably modified emulsion with an optimally dispersed nanosilane is attainable.

2.9.2 Aggregate Quality

Compaction is one of the most prime aspects of construction, providing a dense structural unit with appropriate particle interlock depending on the compaction effort, material type, and water content. Good compaction offers lesser material permeability and lower porosity. de Bono and McDowell (2020) define material porosity as a ratio of the volume of voids to the total material volume. Aggregate materials with a lower particle interlock are relatively less dense and have a high voids space per given volume. Since porosity is directly proportional to the void's space, such materials are rendered porous. Essentially, the quality of aggregates influences the effectiveness of nanosilane stabilizers, tougher aggregates with a higher crushing and degradation resistance will have their surfaces sufficiently modified by nano ilanes, aiding a proper adhesion between aggregate and binder.

Coating poor quality aggregates with low crushing resistance with a liquid anti-stripping agent can potentially result in the additive extensively percolating into the aggregate sample, compared to spreading evenly over the surface thereby lowering additive content per surface area. Therefore, it is essential to note that the success of the additives depends on the material type, porosity, and optimum amount of additive for sufficient coating. An optimum amount of modified binder should wet the aggregate samples and also possess the appropriate rheological properties to penetrate pores and other openings efficiently. The effectiveness of alkoxy silane modification also depends on the quality of the material. Lack of an active water repellent layer on the entire aggregate surface results in a relatively weak barrier towards the water, hence the surface does not become superhydrophobic, water damage may still be a significant impairment. The ability of a nanosilane additive to modify aggregate into hydrophobic surfaced materials is dependent on the extent of surface coverage given how widely dispersed the nanosilane is in the carrier liquid, nano-silane distribution on the substrate remains a crucial factor for a functional end product.

2.9.3 Compatibility

Incompatibility of the mix constituents leads to a poor performing end-product. It is essential to ensure every additive or surfactant put into the mix is compatible with other mix constituents. Compatibility is principal in these different scenarios:

- Compatibility with mineralogy

- Compatibility of stabilizing agent and other proprietary additives
- Compatibility of modifier to aggregate surfaces

According to Jordaan and Steyn (2019), standard material classification tests characterizing mixing materials do not adequately reflect the most scientific material properties. The adhesive bond at the aggregate–bitumen bond can potently be affected by the aggregates chemical composition (Rossi *et al.*, 2016). Jordaan and Steyn (2019) further state that chemical testing is necessary based on location and respective weather conditions, the Southern Africa weathering and material degradation are much severe than in the Northern Hemisphere where standard material tests are adequate. Therefore, it is crucial to identify mineral phases in naturally available materials that may have been chemically affected by weathering. Jordaan *et al.* (2021*b*) adds that a proper nanosilane selection is influenced by primary and secondary minerals identified because some silanes have significant limitations should they be in contact with secondary minerals.

The importance of compatibility in mixing has further been amplified by Murphy *et al.* (2019) in studying the influence of characteristics of emulsifying agents on the stabilization of granular materials using NMEs. It is reported that despite the lack of materials specifications about emulsifying agents in South Africa, surfactants could impact the performance of NME's. Eight different anionic emulsions from five suppliers were used to stabilize a G5 quality Granite material in Gauteng, the minimum resultant ITS_{DRY} value using 1.2 % anionic NME was 291 kPa and the maximum was 400 kPa. The difference could be attributed to emulsifying agents' different application percentage rates and bitumen emulsions manufacturing processes. The differences in ITS strength were significant, indicating that stabilization of a relatively poorer quality in-situ material could potentially result in poor ITS results primarily depending on the selected surfactant type and amount.

The strength of interface bonding due to nanosilane additive is firmly influenced by the minerals available in the pavement material, the inconsistent results in ITS highlighted above may also be influenced by the unsuitable selection of stone/aggregates and an appropriate nanosilane additive. Engineers must be familiar with mineral phases present in aggregates samples, for a successful introduction of silanes into pavement materials and improved load capacity design aspects. Silane effectiveness on inorganics is not only dependent on the type of substrate being modified, but factors also influencing optimum silane modification extent to (Arkles, 2011):

- The concentration of surface hydroxyl groups
- Type of surface hydroxyl groups
- Hydrolytic stability of the bond formed.

- Substrate features

Surface modification is most effective if the above factors are satisfied appropriately, effectiveness is proportional to the surface hydroxyl groups content. Jordaan and Steyn (2019) mentions most nanosilanes' effectiveness is curtailed if the substrate contains small quantities of silica. As a result, Arkles (2011) explains that substrates such as graphite and carbon black are the poorest compounds to be modified by nanosilanes, Figure 2.26, demonstrates the extent of the effectiveness of nanosilanes from carbonate materials to silicate materials. Modifying a substrate with a non-suitable additive will result in a poor-quality product, rendering the silane-aggregate interaction incompatible.

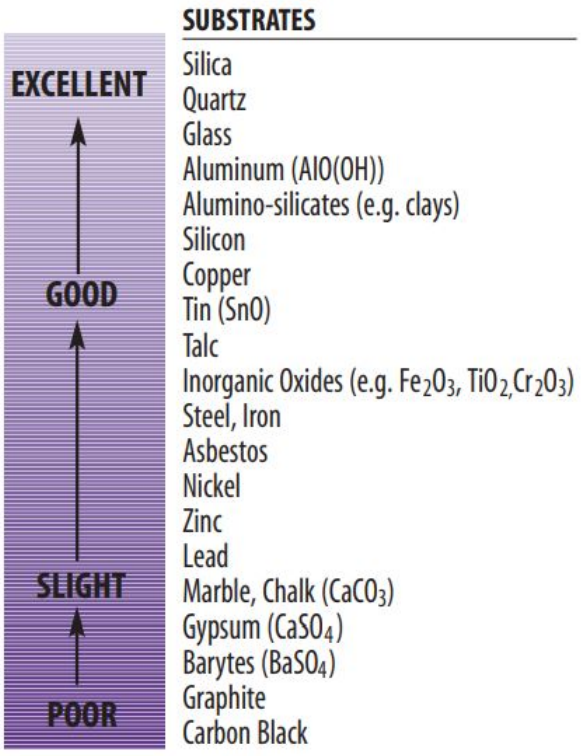

Figure 2.26: Silane effectiveness on organics. (Arkles, 2011)

Generally, the silica content is inversely proportional to aggregate-bitumen affinity. Therefore, a suitable nano modifier is essential for optimum pavement design using innovative NMEs. In summary, the selection of the nanosilane is influenced by:

- Compatibility with the bitumen and surfactant in the bitumen emulsion
- Mineralogical nature of the material aggregates
- The end properties expected by the user

2.9.4 Mineralogy

To understand the chemical composition of aggregates more comprehensively, Figure 2.27 illustrates their chemical composition and trends in mineral content. Mineral ranking from high silica content to low is as follows: Orthoclase feldspar > Quarts>Plagioclase feldspar > Pyroxene > Olivine. On the left side of Figure 2.27 minerals with low silica content are depicted, characterized by poor adhesion problems as aggregates. Sufficient modification of these materials would require high amounts of suitable adhesion promoters. In essence, the higher the silica content in a material, the lesser nanosilane is needed for adhesion promotion. Significantly deviating from the silane optimum dosage, which is dependent on silica content may potentially result in the mix impairments such as disturbed binder rheology.

Orthoclase Feldspar contains approximately 60-70 % of Silica, quartz is also mainly silica with a significant percentage, about 65 %. Most of these mineral composition ranges are hugely affected by climatic factors such as weathering, seasonal rainfall, and high temperatures. It is therefore imperative to decide on the suitability and compatibility of material for stabilization also considering mineralogy. Minerals considered problematic in road construction and material stabilization include (Jordaan and Kilian, 2016; Jordaan and Steyn, 2019)):

- Mica Minerals
- Clay Minerals such as Smectite, Illite, Kaolinite
- Cohesionless sands
- Sand containing crushed shells or pulverized coral reefs
- Calcretes and Soluble salts

Paige-Green (2003) states that despite costs and environmental impacts reduction, increasing the use of marginal materials increases the risk of premature distress conditions. In order to use them optimally, it is necessary to understand their long-term performance and durability. Mineralogy, pavement structure traffic, and conditions form requirements to understanding durability and long-term service. Excessive amorphous silica content, inter alia, leads to cementation in lime-treated materials, compaction and density problems.

Micas pose little or no threat to construction as long as their quantity remains below 10% though some weathered biotite may exhibit compaction problems. However, considerable construction problems such as swelling and particle disintegration arise from weathered rocks containing smectite. In situ weathering of granites also leads to collapsible soils. Phyllosilicates consist of all clay minerals, characterized by low shear strength and volumetric instability, their presence in road

construction may be a threat depending on type and quantity.

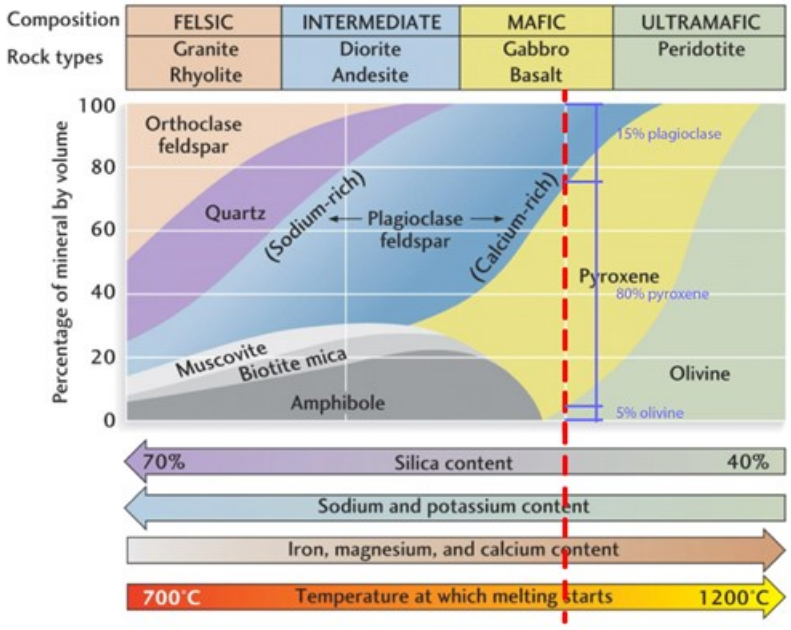

Figure 2.27: Mineral composition of rocks found of different rock types.

More examples of secondary minerals which are a major component in the problematic nature of materials are shown in Table 2.7.

Table 2.7: Major secondary phyllosilicates in soil and specific problematic rocks groups. Compiled from (Nanzyo and Kanno, 2018; Paige-Green, 2003)

Secondary phyllosilicate	**Problematic Rock Groups**
Kaolinite	Basic igneous rocks
Halloysite (1 nm)	Arenaceous rocks
Halloysite (0.7 nm)	Mudrocks
Montmorillonite	Diamicitites
Beidellite	Pedocretes
Nontronite	
Vermiculite	
Illite	
Mg Chlorite	

In regions with alternating dry and wet climates, soils with excessively high amounts of smectite exhibit an intensive shrink and swell behaviour (Nanzyo and Kanno, 2018). In dry conditions, significantly deep vertical, horizontal and diagonal cracks are formed on such soils, in wet climatic regions with rainfall seasons the water penetrates through the cracks previously formed into the lower pavement layers. All areas affected by moisture will slowly begin to swell, upper layers lifted

by the swelling force then show an undulated surface. The shrinking and swelling due to water escape and ingress, respectively, leads to more cracks and deteriorated roads with poor riding quality, this is reflective of how naturally available aggregates with poor mineralogy may affect the ultimate performance of the pavement.

The compatibility concept amongst mix constituents is closely related to the mineralogy of the materials in the mix. Qualitatively measuring the mineral composition in the material aggregates is crucial, it has a direct influence on the effectiveness of nanosilane modification. Most aggregates contain silica though less attention goes to the silica content per material, which is key to siloxane bonds formation with organosilanes. Jordaan and Steyn (2019); Oliviero Rossi *et al.* (2017) emphasize that the expected performance of NME modified materials is dependent on the material mineral composition of the material. Primary and secondary minerals should be identified since the extent of weathering particularly in Southern Africa, has a direct influence on material mineralogy causing unreliable alkoxy silane bond strength modifications.

In most Sub-Saharan African countries, standard road building material classification tests do not include mineralogy testing yet unexplained premature pavement failure of naturally available local materials may be a consequence of unsuitable minerals present (Jordaan *et al.*, 2017*b*), not necessarily poor construction methods. In pavement layer stabilization it is a rare exercise to carry out mineral identification tests to gauge the composition of both primary and secondary minerals, whose effect on performance may be adverse. Jordaan *et al.* (2017*b*) further points out that this is due to old empirical tests such as CBR which were not customized to entirely characterize problematic or natural Southern Africa materials.

The aim is not to invalidate or question the basic material classification tests' significance (Jordaan and Steyn, 2019), their inadequacy to fully aid in understanding and optimization of pavement design aspects remains a concern. Scientific tests such as X-Ray Diffraction (XRD) are a prerequisite to understanding basic geology and material mineralogy, which is key in the accurate selection of compatible stabilizing agents and optimal use of local materials available for road building (Jordaan and Kilian, 2016). Some materials fractions have a fine clayey nature, XRD studies are useful in revealing their composition. Despite some materials such as fieldspars exhibiting no problems as road construction aggregates, XRD studies of different basalt and granite showed presence of some kaolinite and sericite. (Paige-Green, 2003).

Chemical deterioration of road construction materials is accompanied by secondary minerals formation, identification, analysis, and classification of such minerals, and understanding of their impact on road-building materials performance will aid engineers to avoid premature pavement failure and manipulate them through chemical interaction with nanosilanes at a micro-scale. In summary, the

successful use of nanosilane technology will require a basic understanding of scientific data, road building materials mineralogy, and its influence on the aggregate strength of stabilized road layers (Jordaan and Steyn, 2019).

The impact of minerals on the mechanical properties of rocks could be described by piecewise linear relationship, within a certain range of mineral content, there is no significant increase in mechanical strength however where the mineral compositions make up the framework of the bulk material, there is a noticeable effect of mineralogy on aggregate mechanical properties (Pan *et al.*, 2016). High strength minerals such as quartz have a much higher effect on mechanical properties but low strength minerals such as clay minerals, at low compositions barely have a significant impact on rock mechanical properties.

Paige-Green (2003) agrees that mineral type and quantity are crucial, materials with high kaolinite quantity would behave differently in service to those with low smectite component. Most previous investigations have given a wide scholarship on the relationship between quartz content and rock strength, however, the relationship is very material dependent, and derived correlations are generally not universally definitive of all materials, since mineralogy is also a complex aspect affected by geography, weathering, and heterogeneity of formation.

Understanding silicate and non silicate minerals is a key aspect in NME selection and design. High content of poor mineral phases as shown in Figure 2.26 will require different modification to attain high strength bonding of the stabilizing agent (Jordaan *et al.*, 2021*b*). Ozturk *et al.* (2014) concludes that inconsistencies in correlating mineral content with tensile strength or mechanical properties partly remain a reason the relationship between the two parameters has been challenging to quantify sufficiently. However, not only mineralogy affects strength but grain size, shape, textural characteristics also influence engineering performance.

2.10 FACTORS INFLUENCING NEED FOR HAUL ROAD INNOVATION

2.10.1 Problematic Materials

In open-cast mines, the most common haul road construction materials for a base and wearing course layers are compacted natural gravel, crushed stone, and gravel blends (Thompson, 2000). The selection of such materials is based on an optimal functional design to mitigate the extent of poor functional performance manifesting through excessive dust, increased tyre wear, and other impairments. The selection of an appropriate locally available wearing course material could be a tricky exercise depending on the in-situ material at the mine site. An overburden blasted rock type considered for a base layer under a mechanical - empirical design, is hugely dependent on ore type

at a mine site, basalt and some kimberlite form part of a blasted rock at a diamond mine while in a copper mine, a naturally available lateritic rock would be considered for road base material. The durability of all these different materials therefore differs.

Netterberg (1994) explains that standard materials meet specifications such as ASSHTO, ASTM, or TRH14 in South Africa, in terms of PSD or PI. However, non-standard materials are those not in accord with any material specifications, but they may be used successfully given their suitability in terms of aggregate durability. Waste dump rock and some mine tailings could potentially be used in haul roads construction. These have barely made it to highway road construction due to extreme processes of gaining industry acceptance. The low political and engineering acceptance of risk has therefore confined utilization of these marginal materials, including mine waste to a local scale (Netterberg, 1994). Their main problem is not only incompatibility but also high susceptibility to deterioration under adverse environmental conditions and continued traffic, such as fatigue cracking from ultra-heavy loads.

The aggregate type, condition, and extent of weathering effects play an important role in material suitability and durability. A comprehensive understanding of material durability as a function of material type is pivotal in understanding further the likelihood of nanotechnology products revolutionizing material science. It is crucial to know standard materials behaviour and factors affecting their effective performance. This preliminary knowledge will aid in understanding how organosilanes will neutralize the harmful effect of secondary minerals in problem soils. Paige-Green (2004) provides extensive information on the engineering geology of roads in South Africa.

2.10.2 Rainy Seasons and Hydrophobicity

The most destructive distress condition in road design and construction is due to water ingress. It weakens the layers and makes them more susceptible to further deterioration like frost heave. Traditionally, this is counteracted by proper drainage systems and a sufficient cross fall on a road surface (Paige-Green and Heath, 1999). Water percolation weakens the road's structural integrity, leaving it cracked and impassable during wet climatic conditions. Dispersive clay soils have high exchangeable sodium ions, their fine fractions exhibit high surface electrical repulsive force causing them to be eroded easily in suspension by moving water (Paige-Green, 2004).

In rainy seasons or stormy weather conditions, depending on the wearing course material response to the rate of precipitation, haul roads become too slippery. As a result, it is difficult for dump truck operators to work efficiently and deliver an optimum daily tonnage. Paige-Green (1990a) points out that in wetter Southern Africa areas experiencing prolonged rainfall and arid zones with short but intense thunderstorms, unpaved roads are faced with severe drainage issues. The resulting

excessive water content percolates into the base, and other bottom layers causing premature and chronic distress conditions such as load-bearing capacity loss, a capillary rise of water due to suction also increases the water content.

Ugwu *et al.* (2013) investigated the use of nanotechnology as a preventative engineering solution to high-level quality-oriented problems relating to construction procedures materials and other aspects. Different soils, including problematic laterite and clay, showed an increase in engineering properties but more importantly, the long alkyl chain in the added nanosilane altered the water repellent nature of aggregates at a molecular level, making them hydrophobic. The extent of hydrophobicity is seen through the beading effect (Jordaan *et al.*, 2021*b*), which is a visual effect visible through the contact angle of water with the treated material, water behaviour on a treated surface is visible through this effect.

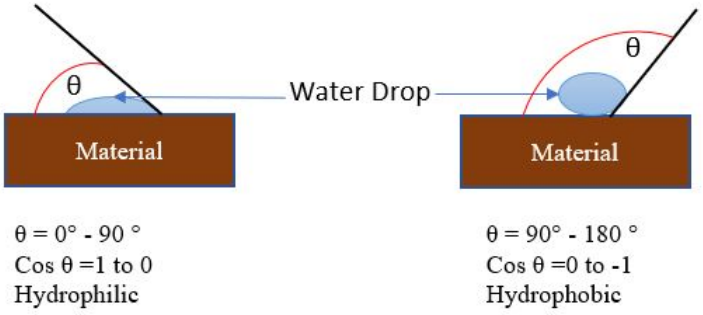

Figure 2.28: Shows a water repellent zone on a treated surface.Adapted from (Jordaan *et al.*, 2021*b*)

Figure 2.28 illustrates the beading effect, showing that if a water drop on a surface covers a larger area, resulting in a contact angle less than 90 °, materials are susceptible to water ingress. Jordaan *et al.* (2021*b*) further mentions that for a sample not entirely immersed in a water bath, a positive absorption rate is seen due to water capillary rise since the wetness of the material goes over the initial water line. For a hydrophobic test specimen, the contact angle is greater than 90° extending to 180°, there is a negative capillary rise denoted by negative Cos (θ), where θ is in the range 90°-180°. A minimum area is covered by the water drop on the treated surface since the formed surface layer is water repellent.

Hydroxyl groups make the soil surface hydrophilic, upon contact with nanosilane molecules, a hydrophobic zone forms at a molecular level. The newly formed siloxane bonds act as a protective monolayer to the particle surface. The modified surface maintains breathability, the pores allow vapors to escape but prevent water ingress.

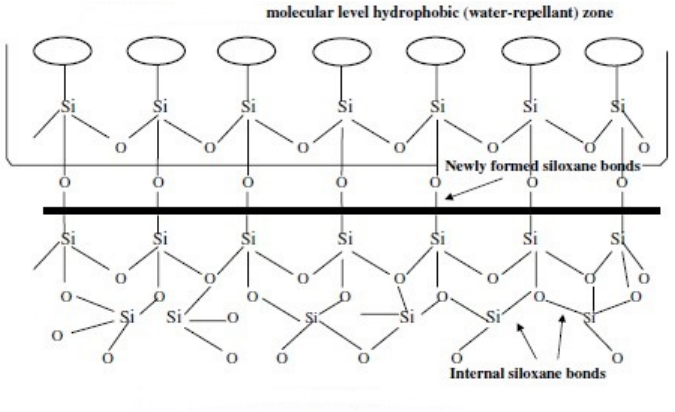

Figure 2.29: Soil surface modification. (Ugwu *et al.*, 2013)

Paige-Green (1990*b*) emphasizes that consideration should be given to the effect of water ingress on unpaved roads due to absence of seal to offer sufficient water protection. Resisting water infiltration into the pavement surface mitigates moisture-related damage of pavements significantly. Moisture damage is a prime cause of stiffness loss, strength loss, and durability issues.

In a study evaluating ZycoSoil nano additive, increased filler content led to higher fatigue life while decreased air voids resulted from ZycoSoil aggregate coverage (Mohajerani *et al.*, 2019). Stabilization using the silane-modified emulsion showed that base and subbase layers relatively retained dry strength. Simulating wet conditions through continuous water addition both on the surface and in-depth of the layers coupled with 80 KN dual wheel load traffic condition, both the base and the subbase layer showed optimal performance (Rust *et al.*, 2019).

The material pores without being clogged, are sufficiently coated with a layer of hydrophobic film, resulting in decreased electrostatic force between water and aggregates. Kim and Moore (2009) reports that two aggregate mixtures, both with 0.1 % ZycoSoil showed Tensile Stress Ratio (TSR) values of 0.99 and 1.00 compared to 0.85 and 0.82 for the control mixture. A significant improvement in moisture resistance was recorded. According to TG2, when TSR values are above 80 %, treated material can be rendered relatively moisture insensitive or less susceptible to moisture damage.

2.10.3 Cost Aspects

There are many factors affecting production costs, the focus is on cost impacts of poor haul road design, construction, and maintenance. Exploring how material solutions may be a strategic way towards cost-effective transport-related mine operations. According to Thompson and Visser (2003), directly related to the road condition are the two most important aspects of road user costs; vehicle operating costs (VOC) and maintenance costs. Therefore, haul road design, construction, and

Figure 2.30: Cost impacts of poor haul roads.

maintenance strategies should be aimed to optimize all the cost elements shown in Figure 2.30, to minimize the cost of operations related to hauling roads.

Modeling VOC is a relatively complex process due to its different components, models within the context of haul road transportation predict the impact of such components on the VOC specific to the equipment type and haul road conditions or material type. Prediction models include those of:

- Fuel Consumption
- Tyre Usage
- Maintenance-Plant and Labour

An ideal haul road maintenance strategy results in minimum total costs (Thompson and Visser, 2003). A suitable maintenance approach geared towards optimum road performance will ultimately be cost-effective due to the continued optimization of cost elements shown in Figure 2.30.

Using an alternative NME design allows the use of locally available materials (G7/G8), which in most cases are free, modified with application rates as little as 1.0 % to 1.5 % residual bitumen content. Alternative NME design enables dematerialization, haulage savings, time, and effort reduction, and not only a water-resistant layer but also a smooth riding quality (Jordaan *et al.*, 2021*b*). This is due to better stone orientation during compaction since bitumen acts as a lubricant in the NME.

2.11 SUMMARY

The chapter introduces haul road networks and innovative material solutions, it presents a current perspective on both topics. Less attention is given to haul road design, construction, and maintenance practices yet the load size increases with increasing truck sizes. Mine officials barely consider haul road construction as an important aspect of mine operations. Innovative road materials are used widely in low volume roads but have a limited application in haul roads. Structural, functional, and other common haul road challenges are explained, there include potholes, stoniness, frost heave, spillage, and dustiness. These challenges are discussed in detail, the extent to which they affect the performance of the road is highlighted.

Common haul road construction materials include crushed stone, blasted dump rock and natural aggregates such as laterite. Freely accessible materials such as laterite have variable mechanical properties and as such, pavement engineers often preclude them as construction materials, yet they offer satisfactory performance where they have been used. The chapter briefly discusses a case study of Kansanshi mine and Kalumbila mine haul roads, it describes the pavement structure at different sections including ramps, construction materials used and binder content. Untreated bitumen emulsions are normally used to stabilize some haul roads layers, modified emulsions are barely applied on mine haul road networks. This chapter introduces common organosilanes used in construction, it discussed NME types, benefits, formulation, and application. Organosilane compounds have been used on low volume roads in a few Southern Africa countries, they resulted in a good performance at low dosages with reasonable costs savings on construction and materials. Nano-modified emulsions classification criteria based on standard laboratory, chemical and performance testing is presented. Chemistry is an important aspect of effective stabilization, the chemistry among aggregates, organosilane, binder and water is discussed. Factors affecting the effectiveness of an NME such as compatibility of either binder, organosilane and aggregate are discussed. Incompatible mix components will not result in an optimum mix due to poor chemistry between the components.

Mineralogy is discussed in detail, aggregates with high content of poor minerals such as swelling clays and muscovite tend to be less durable and offer poor performance with time, particularly in wet conditions. Materials with high quartz content are more compatible with organosilanes than carbonate rocks. Organosilane influence on strength improvement and hydrophobicity depends on their compatibility to mineral types. Factors influencing the effectiveness of nano-modified emulsions on substrates have been explained, these include the dispersion of the nano additive in the emulsion and their chemistry. Substandard materials, shortage of high-quality materials around

mine sites, environmental conditions, increasing traffic and high haulage costs prompt mining sectors to develop innovative materials that would not only be durable but increase production and safety. Given that organosilanes as innovative material solutions have performed well in low volume roads, there is a potential of a significant influence on haul road performance.

CHAPTER 3

METHODOLOGY

The experimental design and methodology present both preliminary testing procedures and performance tests aimed at understanding the behaviour of NME treated materials compared to untreated materials. The preliminary tests include standard tests indicative of material properties and determine the suitability of stabilization. Mineral identification tests of natural aggregates and treated mixes for all three selected materials are detailed. The chapter discusses different organosilane mixing approaches and procedures followed in each organosilane incorporation mechanism.

The effect of NME treatment on the different aggregates was measured using indirect tensile strength and shear properties from triaxial testing, a difference in test results reflected an effect on an additive or parameter change. A high permeability pressure testing was carried out on all materials to evaluate the extent of hydrophobicity or water ingress susceptibility. All performance tests results were compared against the minimum criteria to check their compliance. A pavement design and analysis is done based on an optimum mix and selected design input parameters. Figure 3.1 shows an experimental setup followed for material classification and engineering evaluation of NME effect on material properties and performance.

3.1 BACKGROUND OF MATERIALS

Natural materials have been used extensively in road construction such as laterite, which is used commonly in low volume road base and subbase layers. According to (Queiroz *et al.*, 1991), laterite colours range from yellow to red, denoting iron oxide content. The dominant clay mineral is kaolinite, the silica/sesquioxide ratio is less than two. Laterites form from weathering in tropical and subtropical regions, not primary soil formation processes such as sedimentation and metamorphism (ARAYA *et al.*, 2021). Its use in road bases depends on location due to varying material properties. As a result, it is necessary to derive empirical specifications (Paige-Green *et al.*, 2015).

Bitumen is considered the first product to be adopted by humankind around 3800 BC as both an adhesive and a waterproofing material (Deepa *et al.*, 2019). Bitumen emulsions have been in use since the early 20th Century, however, currently, the extent of their usage depends on location. About 10 % of available paving grade bitumen is used as bitumen emulsions, with the United States being the biggest producer of 3 million tons per year and a consumer of bitumen emulsion (James, 2006). Other countries such as South Africa, France, Brazil, Mexico are also significant producers and users of bitumen emulsion.

In the early 21st century, a huge interest in nanotechnology and nanoscience developed. In the

United States, Feynman's concept of nanoengineering played an important role in aligning the American National Science priorities (Bayda *et al.*, 2020). In other words, the subject of manipulation of matter at an atomic level became a gateway to wide research in the field of nanotechnology. This is where the application of nanotechnology in a variety of industries began.

3.2 MATERIALS

The investigation and selection of materials required for research, as well as the binders and additives, require knowledge of the material options available and their behaviour.

Several bitumen emulsion types ,the unmodified CSS60 and an anionic SS60 and a preblended SS60 were procured by Tosas. These were all prepared in the Republic of South Africa and used as fresh as provided. The unmodified bitumen, particularly CSS60, was manually blended in the laboratory using different nano silane additives at different application rates.

The anti-stripping agents or nano silane additives included a Terrasil plus(T+) and a Zycobond(Z) dust suppressant, all 100% organosilane compounds. These were both prepared and supplied by Advanced Polymers. The additives were applied in three application rates as a percentage of bitumen. The supplier's recommendation gives the dosage per volume of the soil, however, for clarity and understanding, such dosages have been converted and expressed as a percentage of the unmodified bitumen emulsion.

Copper Mines operated by First Quantum Minerals Ltd Zambia, aim to provide safe and efficient haul roads. The aggregate materials used include a reddish material sourced from Zambian Copperbelt, Kansanshi at Solwezi known as Laterite, a 26 mm Graded Crushed Stone (GCS) also from Kalumbila, and a different crushed stone (CS) with a maximum size of 40mm from Kansanshi Mine site. FQM Ltd Zambia supplied all aggregate materials.

Table 3.1: Characteristis of Laterite aggregates

Textural Group	**Color and macrostructure**	**Origin and State at Excavation**	**Nature of coarse particles**
Laterite Rock	Reddish brown, dark brown. Red colour denotes high iron oxide content Indurated conglomeratic	Zambian Copperbelt. Residual soil. Ranges from very soft material breakable under finger pressure to relatively harder rocks	Irregular quartz particles of different sizes depending on site and depth of extraction.

Table 3.2: Types and properties of the Bitumen Emulsions

Bitumen Emulsion Type	Bitumen Content	pH	Components
Cationic Slow Setting	61%	2.0	Water,Bitumen,Surfactants
Anionic Slow Setting	60%	11.2-12	Water Bitumen,Surfactants
Nano-Modified Anionic Slow Setting	60%	Alkaline	Water,Btumen, Surfactants, Zycotherm,Terrasil,Zycobond

Table 3.3: Properties of nanotechnology products

Properties	Terrasil+	Zycobond DS
Form	Liquid	Liquid Acrylic co-polymer
Colour	Pale Yellow/Red ochre	White
Flash Point	>80 °C	Not flammable
Explosion hazard	Not known	Hazardous polymerization will not occur
Density	1.01 g/ml	1.01-1.02 g/ml
Freezing Point	5 °C	Not known
Solubility	Highly soluble in water	Dispersible in water
pH Value	10 % solution in water neutral or Slightly acidic	6.5-8
Viscousity	0.1-0.5 Pa s	Not known
Composition	65-70% Hydroxyalkyl-alkoxy-alkylsilyl compouns, 25-27% Benzyl alcohol, 3-5% Ethylene Glycol	Acrylic co-polymer based composition in water

3.2.1 Experimental Framework

The evaluation of nano modification effect on selected materials was based on standard tests indicative of material properties. The mineral identification of natural aggregates was compared against that of treated mixes for all three selected materials. The effect of the treatment with NME on the different aggregates was measured using indirect tensile strength and shear properties from triaxial testing, a difference in test results reflected an effect on an additive or parameter change. A high permeability pressure testing was carried out on all materials to evaluate the extent of hydrophobicity or water ingress susceptibility. All performance tests results were compared against the minimum criteria to check their compliance. Figure 3.1 shows an experimental setup followed for material classification and engineering evaluation of NME effect on material properties and performance.

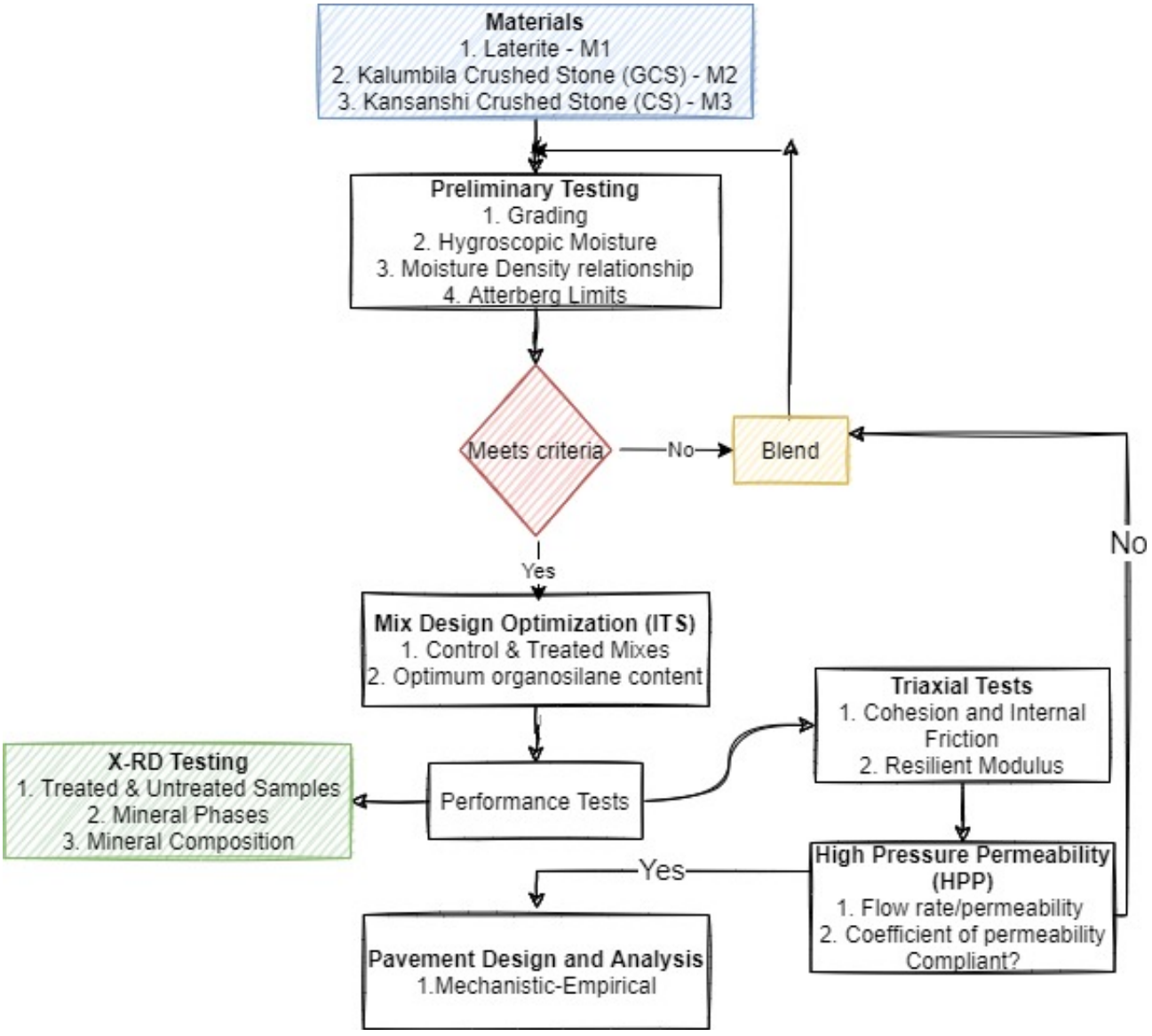

Figure 3.1: Experimental Design

3.3 SAMPLE PREPARATION AND TESTING

The objective of the laboratory testing carried out in this project research comprises two major phases, to define material classification and existing interaction mechanism amongst the mix constituents, bitumen, nanosilanes, water, and aggregates. One other crucial phase was to evaluate the influence of nano additives on the mix performance through a series of tests. A standard laboratory testing regime inclusive of X-Ray Diffraction (XRD) was performed for material classification. Chemical analysis of materials through mineralogy enabled both material characterization and a comparison between treated and untreated material suitability.

Sieve analysis was done to describe the nature of particle size distribution and determine the target grading. Atterberg limits were conducted to describe material plasticity and characterize fine-grained soil fractions. Indirect Tensile Testing (ITS) was done to indicate the performance of selected untreated and treated materials in both dry and wet conditions, since it is a mathematically derived empirical value, both monotonic and triaxial testing were both carried out to determine shear properties and resilient modulus, respectively. These parameters describe materials better due to the simulation of field conditions through stress applications in directions reflective of field conditions.

The water repellent characteristics of the mixes are of importance since one of the major components offered by the NME includes the hydrophobicity of materials. Evaluation of the water resistance of treated materials apart from simulation of wet conditions before ITS testing was extended to permeability testing.

3.3.1 Material Crushing

The laterite material used for the sample had a variable particle size distribution with huge fractions above 40 mm. Due to a limited quantity of the material available for testing, it was necessary to scalp off fractions greater than 20mm, crush them using the jaw crusher to smaller aggregate samples. The crushing was followed by mixing the crushed aggregate fractions with the natural aggregate to enable a homogeneous mix, subsequently, reliable material characteristics.

Although laterite is known to be an extensively weathered material, depending on geological occurrence, depth of extraction and the extent of weathering, the particle size of the aggregate samples do differ. Relatively big boulders were fed into the jaw crusher set with a 20mm gap. Given the influence of particle size on the mechanical behaviour of unbound granular materials (UGM), the 20mm restricts the presence of larger aggregate particles to influence the reliability of results. A jaw crusher uses a compressive force to break down the material fed through the top part into the

crushing chamber, upon being crushed by the two jaws, the material goes out through the narrow exit at the bottom, this setup is demonstrated in Figure 3.2.

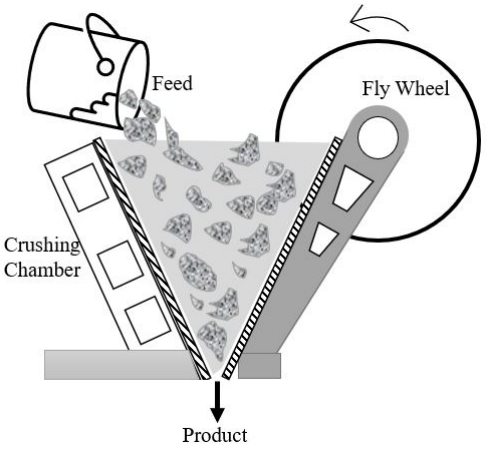

Figure 3.2: Schematic illustration of a jaw crusher

3.3.2 Sieve Analysis

Sieve analysis or particle size distribution was done following SANS 3001-AG1:2014, refer to Appendix A. The preferred sieve diameter sizes ranged from 20 mm to 0.075 mm. It must be noted, for this research, it was not necessary to determine the PSD of fractions smaller than 0.075 mm. as a result, hydrometer testing was not carried out. Aggregate gradation refers to the distribution of particles sizes, fractions retained on each sieve are weighed and the percentage passing each sieve is determined. Grading is a standard test integral for defining and understanding the nature of the material. Before sieve analysis, selected material aggregates were air-dried until constant mass. This was done by distributing the material evenly over the floor surface in the laboratory, this was preferred over oven drying since it was reflective of field conditions. To ensure an optimum grain to grain contact amongst particles with minimum voids content, a well-graded mix is a critical aspect, it improves support leading to lower internal stress and increased load-bearing capacity.

Wet sieving was also called for, particularly for the laterite soil since it had a higher PI and a relatively higher cohesion amongst particles. This approach is beneficial when there is strong particle agglomeration, static charges are nullified, and particles aggregation reduces to allow most particles to pass through selected sieves. Wet sieving was done using three sets of 4 kg mass each, the method was done to remove fines that may potentially hinder differently sized particles' separation process. It is mostly recommended where selected aggregates have a relatively higher fineness content, the procedure is demonstrated in Figure 3.3.

Figure 3.3: Washing of crushed stone in preparation of sieving

Since the materials were to be stabilized with a new age modifier which is not classified with the BSM limits, it was not mandatory for the grading to follow that of BSM Specifications detailed in TG2, however, the guideline was still used for reference. Three sets of approximately 4kg mass were sieved (dry sieving) using a mechanical shaker as shown in Figure 3.4, more than one set was considered to get a reliable grading representative of the entire material.

Figure 3.4: Oven drying aggregates and sieving

The representative proportioning was done using five differently sized sieves, 0 mm,5mm, 7.1mm,10, and 14mm, the fractions retained on these sieves were stored in separate plastic bags upon sieving and later reconstituted according to the selected target grading in preparation for optimum water content, maximum dry density determination and mix regime for test specimens. Assessment of the materials was also done using the unified soil classification system (USCS) as per ASTM D2487-06.

This enabled determination of the coefficient of uniformity (C_U) and the coefficient of curvature (C_C) both shown in Equation 3.1 and Equation 3.2, respectively. Based on USCS, well-graded soils have a C_C ranging from 1 to 3 while their C_U exceeds 4.

$$C_U = \frac{D_{60}}{D_{10}} \tag{3.1}$$

$$C_C = \frac{(D_{30})^2}{D_{10} \times D_{60}} \tag{3.2}$$

A further determination of the characteristics of selected materials was considered through dust ratio (DR) and grading modulus (GM). Dust is a huge safety hazard on haul roads network exhibited by all materials from natural gravels to crushed stone mixtures used for a base course. Therefore it was essential to evaluate the DR using Equation 3.3, as per Australia (2003). Equation 3.4 was used to calculate the grading modulus.

$$DR = \frac{(P_{0.075})}{P_{0.425}} \tag{3.3}$$

$$GM = \frac{300 - (P_{2.00} + P_{0.425} + P_{0.425})}{100} \tag{3.4}$$

3.3.3 Optimum Moisture Content (OMC) and Maximum Dry Density (MDD)

One of the significant factors affecting the performance of UGM is the water content needed for optimum compaction and desired density. The optimum water content (OMC) and maximum dry density (MDD) were done according to SANS3001-GR30:2015 Edition, refer to Appendix A, through a moisture-density relationship. The resulting relationship showed a graph from which the maximum value on the vertical axis was the dry density and the corresponding moisture value on the horizontal axis represented an OMC, this was repeated two to three times per material, to get relatively reliable values.

Samples preparation for both laterite and crushed stone aggregates include 5 bags of a 7kg graded mix, these were mixed at different water contents per material type and compacted using modified AASHTO compaction effort. The choice of the number of specimens is based on how many points are necessary to draw the moisture density curve. TMH1(1986) Method A7 is a commonly used guide method to determine the OMC and MDD parameters throughout South Africa, the test and equipment are simple to use. The modified proctor involved five layers of soil being compacted in

standard 152 mm diameter steel mold, this was compacted using the automatic proctor hammer in equally distributed 55 blows per layer. The modified proctor compaction parameters are shown in Table 3.4, the setup in the Pavement Laboratory is illustrated by Figure 3.5.

Table 3.4: Modified Proctor hammer properties

Apparatus	**Value**
Mould	
Individual Internal Diameter(mm)	150
Average Internal Diameter(mm)	150
Height (mm)	95
Factor	43.2
Calculated Volume	100
Rammer	
Diameter (mm)	50
Drop (mm)	100
Mass(kg)	1.1
Energy per blow	7.94
Number of layers	5
Blows per layer	55

Figure 3.5: Modified Proctor hammer for compaction

3.3.4 Liquid Limit

Evaluating Atterberg limits and determining the plasticity of soils forms part of important soil characterization test methods. This method was done based on ASTM D 4318 –00 and further guidance by SANS 3001-GR10:2013 Edition 1.2. Liquid Limit is the percentage water content at which the soil mixed using a spatula in a Casagrande cup will flow together to the base of the cup, closing a cut made by a grooving tool with a 22 mm internal radius (SANS 3001-GR10:2013 Edition 1.2). The experiment is illustrated in Figure 3.6. Visually, fine fractions of most materials look similar. However, the performance when wetted can only be evaluated reliably using recommended test procedures instead of visual inspection. Therefore, it was significant to determine the liquid limit for a proper understanding of the material physical properties, classification, and performance indication.

The distance of the closed gap is dependent on the material, it was approximately 10 mm after 25 shocks of the Casagrande cup for laterite. This test, like other consistency limits, was performed on fine fractions retained on both the 0.425 mm and 0.075 mm sieve sizes. Small-sized soil mass samples are taken from the cup and placed in respective moisture cans, these are later placed in the oven and dried at 110°C until constant mass is reached. The water content is then determined. This is repeated with more samples at higher water contents to determine the liquid limit of the material.

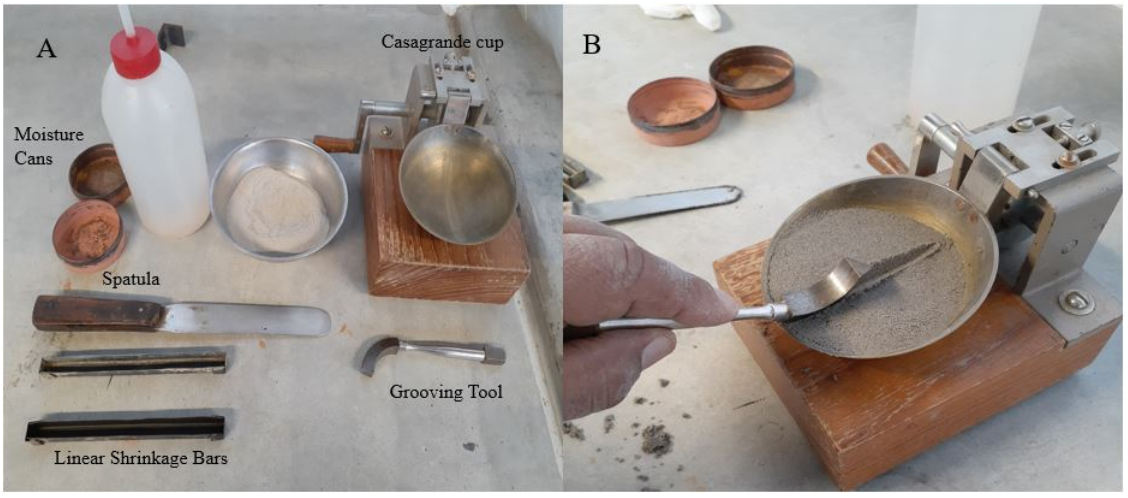

Figure 3.6: Performing consistency limits tests

The calculation of the LL follows Equation 3.5, the entire experimental procedure has been detailed in Appendix A

$$LL = \frac{Moisture\ content\ of\ soil\ sample}{Dry\ mass\ of\ soil\ sample} \tag{3.5}$$

3.3.5 Linear Shrinkage

Shrinkage Limit is a percentage of moisture content at which soil moves from a solid state to a semi-solid state. The test was done to indicate the selected soil behavior when wet, depending on aggregate types, soil exhibits some volume change upon moisture addition, but the extent or degree of the volume change varies depending on the soil's physical properties. Linear shrinkage helps understand the material susceptibility to volume change, by inspecting one-dimensional length change. The procedure was done based on TMH1 Method A4 which states that shrinkage limit is expressed as a percentage of the original dimension of the soil mass. Refer to Appendix A

The fine fraction, retained on both 0.075 mm and 0.425 mm were mixed individually with distilled water using a spatula, the mix was then filled into the shrinkage trough whose internal walls were brushed with paraffin wax to prevent cracking of the sample upon cooling. The filled shrinkage trough was then placed in a 105 to 110 °C oven until the shrinkage has dropped. Figure 3.7B and A show different materials filled shrinkage trough before and after oven drying. Equation 3.6 was used to calculate linear shrinkage.

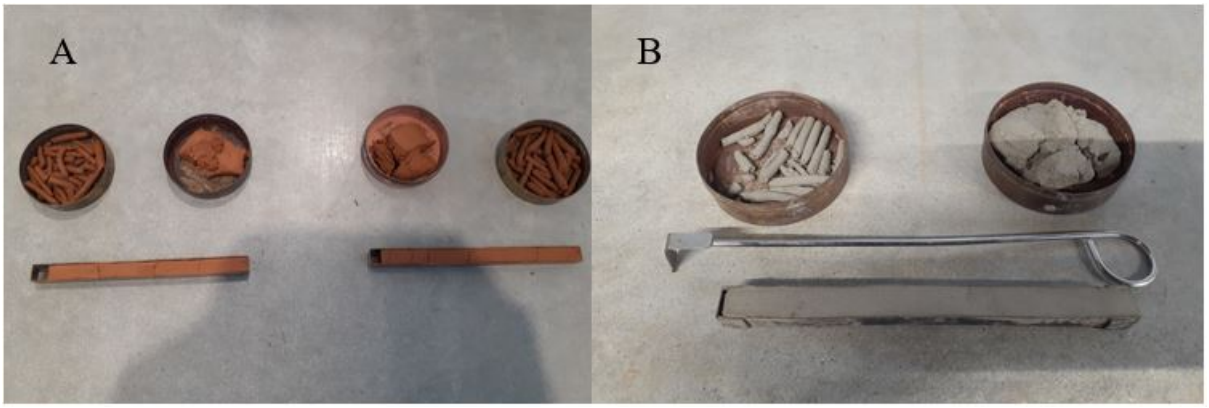

Figure 3.7: Linear shrinkage of Laterite and Crushed Stone materials

$$LL = \frac{Shrinkage\ of\ sample(mm)}{Length\ of\ original\ sample\ (mm)} \times 100 \tag{3.6}$$

This is a percentage of moisture content at which soil transitions from a semi-solid state to a plastic state. Similar testing guidelines as those stated under Liquid Limit and Linear have been used for reference. THM1 Method A3 also explains the determination of PL and plasticity index.

PL is the water content at which soil exhibits plastic deformation under vehicle loading. The PL determination was accompanied by the LL determination as both parameters were necessary for Plasticity Index (PI) calculation, which is one of the key parameters of material classification.

The test was carried on both the 0.425 mm and 0.075mm fractions. The response to the moisture addition of different fractions may slightly differ, depending on the physical characteristics, mineral type, and mineral content present. Small-sized soil mass samples were taken from the Casagrande cup and rolled into ellipsoidal specimens of approximately 3mm diameter. These were placed into the moisture cans as shown in Figure 3.6, weighed, and oven-dried until constant mass, usually 24hours at 105 °C to 110 °C. The calculation of the PL followed Equation 3.7

$$PL = \frac{(Mass\ of\ moisture\ driven\ off\ an\ ellipsoidal\ soil\ sample)}{Mass\ of\ the\ oven\ dried\ ellipsoidal\ soil\ mass} \times 100 \tag{3.7}$$

The plasticity index was calculated as the percentage difference between the liquid limit and the plastic limit as shown in Equation 3.8. This parameter is helpful to both pavement and geotechnical engineers to understand the plasticity of soil, from which strength and deformation predictions can be made.

$$PI = LL - PL \tag{3.8}$$

3.3.6 X-Ray Diffraction

Mineralogy was aimed to indicate which mineral phase is responsible for dominating material behaviour. To identify primary and secondary minerals present in both treated and untreated material samples then to link that to the ultimate performance of the material in terms of strength and moisture susceptibility. Some fractions, such as clay fines have a problematic relationship with water due to minerals they contain, mica, kaolinite, illite, etc.

The importance of this chemical characterization test has been emphasized in various publications; (Paige-Green, 2003; Jordaan *et al.*, 2017*b*; Rust *et al.*, 2019) . Jordaan and Steyn (2019) explain that some materials may exhibit unexplained failure not caused by poor construction practices but material-quality oriented problems due to problematic minerals present. Since new-age modifiers such as nano silane were selected for stabilization in this research project, it was important to identify all possible factors related to material properties that could potentially affect the effectiveness of stabilization. The effectiveness of NME stabilization could result from incompatible minerals or unsuitable mineral composition range.

The XRD test, contrary to XRF, provides phase identification instead of elemental identification and composition. Laterite is one of the pedogenic materials known to contain iron and aluminum

oxides but these neither identify mineral characteristics nor conclusively define the full nature of lateritic soils, hence a need for XRD analysis. The mineralogy test research flow is demonstrated in Figure 3.8.

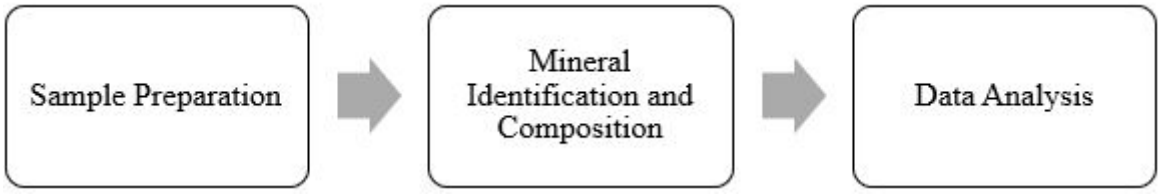

Figure 3.8: XRD testing flow chart

A total of nineteen samples from all three mixes were selected. Therefore, six material samples per material, a base test sample prepared per each material to benchmark all treated samples. These were oven-dried to get rid of moisture content. After sufficient curing, about 2 grams per mixed were weighed and placed in test tubes (Figure 3.9) to be tested.

Figure 3.9: XRD test specimens stored in test tubes

Base mix samples evaluate mineral identification in the natural state of aggregates while other samples will show the presence and mineral composition following treatment with proprietary nano silanes. The test samples were in a solid-state, fractions passing 0.075 mm sieve taken from laterite soil and crushed stone materials. Selection of samples for XRD testing was done as shown in Table 3.5.

Table 3.5: Selected mix designs for XRD analysis

	Mix Design		
Emulsion[1]	**Laterite (M1)**	**Kalumbila GCS (M2)**	**Kansanshi CS(M3)[3]**
None: Base Mix	0% Additive	0% Additive	0% Additive
Organosilane	0.5% T+ & Z	-	-
CSS60	1.2% Pure CSS60	1.2% Pure CSS60	1.2% Pure CSS60
	0.5% T+ & Z	0.5% Terrasil+	1.0% Terrasil+
	-	0.65 kg/m^3 Terrasil+ & Zycobond[2]	-
SS60	1.2% Pure SS60	1.2 % Pure SS60	1.2 % Pure SS60
SS60NME	1.2% SS60NME	1.2% SS60NME	1.2% SS60NME
			1.2% SS60+1%Lime
	A- (Mixing) Approach		

[1] Residual bitumen content constant at 1.2% by mass of aggregates.
[2] Terrasil+ dosage based on Approach 1.(kg/m^3 of aggregates).
[3] Organosilane content(%) in all Kansanshi mixes is by mass of bitumen emulsion.

Table 3.6: Properties and measurements of X-Ray Diffraction

Instrument		**Measurements**	
Manufacturer	BRUKER AXS	Tube voltage	40kV
Diffractometer	D8 Advance	Tube current	40mA
Measurements	Continous $\theta - \theta$ scan	Variable Slits	V20 Variable slit
Tube	Cu-Ka α radiation(λ Kα_1=1.5406$\mathring{A}$)	2θ range	0.5° to 130°
Detectors	LynxEye(Position Sensitive Detector)	Increment Δ 2θ	0.034°
		Measurement time	0.5 sec/step

Measurements are performed using a multi-purpose X-ray diffractometer D8-Advance from Bruker operated in a continuous $\theta - \theta$ scan in locked coupled mode with Cu-Kα radiation, Figure 3.10 A and B. The sample is mounted in the center of the sample holder on a glass slide and leveled up to the correct height. The measurements run within a range in 2θ defined by the user with a typical step size of 0.034 ° in 2θ. A position-sensitive detector, Lyn-Eye, is used to record diffraction data at a typical speed of 0.5 sec/step which is equivalent to an effective time of 92 sec/step for a scintillation counter.

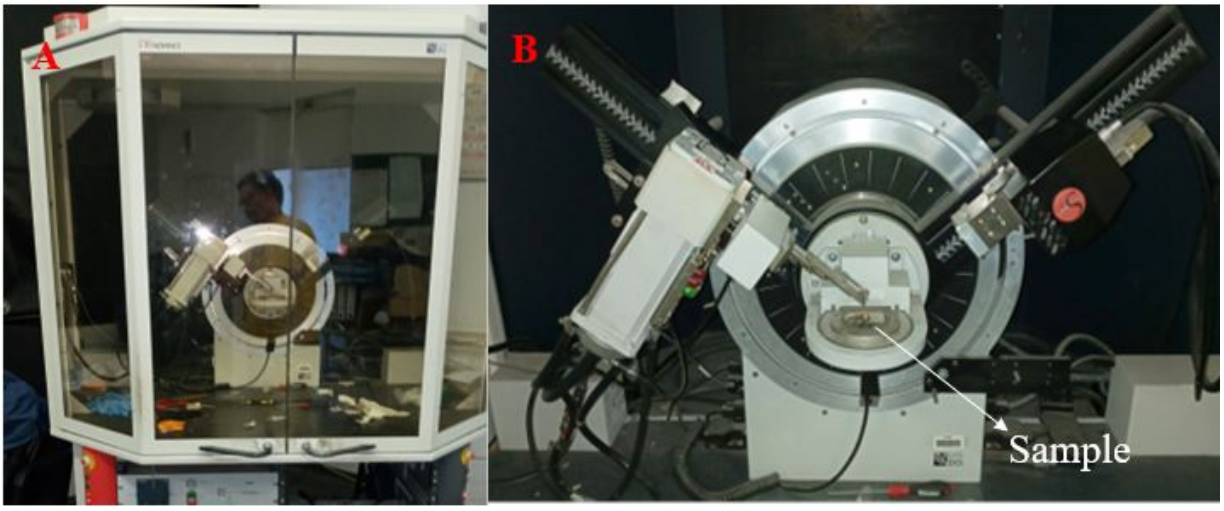

Figure 3.10: XRD Set up and sample under testing

Data are background subtracted so that the phase analysis is carried out for diffraction patterns with zero background after the selection of a set of possible elements from the periodic table. Phases are identified from the match of the calculated peaks with the measured ones until all phases have been identified within the limits of the resolution of the results. Refer to Appendix B for the results.

3.4 MIXING REGIME

3.4.1 Approach 1: Organosilane in water

The materials are treated with 1.2% compatible CSS60 and SS60 bitumen emulsions, this was an amount selected for all material stabilization in this study. Six samples were prepared per mix to determine the indirect tensile testing (conditioned and unconditioned). Table 3.7 shows three mixing categories developed per material. Mix C1 included stabilization with nano silanes only, a mixture of both Terrasil plus and Zycobond. Mix C2 had a preblended SS60NME as a binder while mix C3 included a CSS60 binder modified by Terrasil+ and Zycobond mixture. The mixing approach followed in all mentioned categories was mixing organosilanes with water at OMC, then mixed in aggregates followed by binder addition. Approach 2 explains this incorporation mechanism.

The supplier had pre-blended the SS60NME, as a result, lime was the only additive in Mix C2 at varying contents. However, during industrial emulsification of SS60, Zycotherm is added into the bitumen oil phase, then Zycobond and Terrasil (nano-tack) into the soap phase. A key remains as the water temperature and other factors requiring proper monitoring include water compatibility,

emulsifier, bitumen type, and polarity.

An active filler, lime, was applied to some mixes at different application rates ranging from 0.5%, 0.75%, and 1%, which is a maximum amount of active filler under BSM design. It is important to note that the BSM mix design was used as a reference, the treated materials do not form part of the BSM's but are categorized as NME stabilized materials.Cement as an active filler was not added into any of the prepared mixes

Table 3.7: A mix design matrix for all materials used

Category	**Emulsion Type**	**Additive**	**Content**	
	RBC[1]=1.2%	**Laterite (M1)**	**Kalumbila GCS (M2)**	**Kansanshi CS (M3)**
Mix C1[2]	Base Mix:No Emulsion	0	0	0
	Terrasil+ & Zycobond	0.65	0.65	-
		1	1	-
		1.35	1.35	-
Mix C2	Base Mix: Pure SS60	0%	0%	0%
	SS60 NME	0%	0%	0%
		0.5 % Lime	0.5 % Lime	0.5 % Lime
		1.0% Lime	1.0% Lime	1.0% Lime
Mix C3[2]	Base Mix: Pure CSS60	0%	0%	0%
	CSS60	0.65	0.65	0.25%
		1	1	0.5%
		1.35 +1% Lime	1.35+0.75%L	1%

[1] Residual bitumen content is 1.2% by mass of aggregates for all.
[2] Organosilane compounds dosage in kg/m^3 of aggregates except all Kansanshi mix designs.

In approach one, Terrasil+ and Zycobond mixture was blended in water in a 2:1 ratio. A calculated mass of or volume of Terrasil+ was poured in water at OMC while agitating, then Zycobond was added into the mix while stirring adequately to avoid any premature polymerization since it is a copolymer. Using them as a mixture most probably has more strength benefits than the individual application of each additive. Water temperature (25℃) and quality were critical for or a homogeneous mix with no early polymerization or Zycobond.

Terrasil+ was added into the water forming a clear to a translucent solution, a white to a turbid solution would indicate poor water quality. Therefore, distilled water was used throughout all experiments, since it did not contain contaminants and minerals. This blend was mixed in aggregates using a plate mixer then bitumen addition followed. The nano additives and their preparation are shown in Figure 3.11. Following mixing, vibratory compaction of specimen followed, all ITS specimens were compacted in two layers to a total height of 95 mm and a height of 150 mm.

Terrasil+'s quantity was calculated as per the supplier's recommendations. Equation 3.9 was used to calculate the additive amount in grams, taking into consideration the density of the soil and the CBR as a guide. It was recommended that aggregates with lower CBR need a higher organosilane amount than those with high CBR values. This recommendation was applied in approach 1 only.

$$Terrasil + Amount = \frac{Soil\ Mass(kg) \times T + Density(kg/m^3) \times 1000mg}{Soil\ Density(kg/m^3)} \times 100 \qquad (3.9)$$

Figure 3.11: Terrasil+, Zycobond dust suppressant and their preparation

All samples were cured in an oven for a minimum of 72 hours or until constant mass at 40° C, this rapid curing procedure followed TG2 2020. There is no widely accepted curing procedure particularly for NME treated materials, as a result, a BSM curing procedure was adopted, following this throughout all mix designs ensured consistency in experiments and test results reliability.

3.4.2 Approach 2: Organosilane in Bitumen

The techniques used to mix in nano silanes differ, for all the mixes previously performed, nano silane was incorporated into OMC water then mixed with aggregates. This is because nano silane additives used in this research are water-soluble reactive organosilane compounds. The addition of nano silane in water is a simple approach and easy to follow. The change in the incorporation technique may probably influence the behavior of the blend. Essentially, a second mechanism involved blending the nano silane into the unmodified bitumen emulsion instead of water. This involved using a high shear mixer operating at an optimum operating speed, at an optimum temperature, and for an

appropriate time to ensure a proper homogeneous mix of the nano silane and bitumen emulsion.

Table 3.8 shows some sensitivity design tests carried out to determine the optimum rotation speed and duration of blending using a high shear mixer. The intention was to monitor if the emulsion will still be fit for use and not broken after a certain number of revolutions per minute for a particular duration.

Table 3.8: Sensitivity tests for optimum mixing speed and time

Time(min)	**Revolutions per**	**minute(rpm)**	
	1000	2000	3000
10	B/NB	B/NB	B/NB
15	B/NB	B/NB	**B/NB**
20	B/NB	B/NB	B/NB
B=Break	NB =No Breaking		

Emulsification is a complex process, as a result, the addition of various modifiers requires utmost care. Typically, bitumen is heated to about 130 °C and soap 50 °C. In this study, bitumen emulsion was heated to about 70 °C to achieve appropriate mixing viscosity, a selected nanosilane was added through high shear mixing within the shortest time, Figure 3.12. The selected mixing duration was 15 minutes at 3000 rpm, from the sensitivity test in Table 3.8, the emulsion did not break at these parameters. Take care during high shear mixing, over-shearing the material may result in the opposite effect where a stable emulsion has its bitumen sheared out of suspension. Increasing the speed would not destabilize the emulsion through foam formation. It was important to obtain an optimum surface area of dispersion while dispersing nanosilane into materials.

Table 3.9: Approach 2 mix design matrix for all materials used

Category	**Emulsion Type**	**Additive**	**Content**	
	RBC =1.2%	**Laterite (M1)**	**Kalumbila GCS (M2)**	**Kansanshi CS (M3)**
Mix C4	Base Mix: Pure CSS60	0%	0%	0%
	CSS60	0.25%	0.25%	0.25%
		0.5%	0.5%	0.5%
		1.0%	1.0%	1.0%

The three materials shown in Table 3.9 were mixed with a bitumen emulsion modified using Terrasil+ only. There was a pure CCS60 emulsion base mix to compare against modified mixes. Each material was mixed with an emulsion containing 0.25%, 0.5%, and 1% organosilane.Terrasil+ quantity is expressed as a percentage of the bitumen emulsion. In Approach 1, the dosage was based on recommendations from the supplier and in Appproach 2, it was based on literature.

Figure 3.12: High shear mixing of bitumen and organosilane

In attempting to unleash the full potential of nano silanes as anti-stripping agents or nano modifiers, it is important to ensure proper dispersion, that is, the additive should be dispersed adequately in the unmodified binder for properly-mixed nano silane and bitumen binder matrix. The same concept applies when water is a carrier fluid for a nanosilane. Based on the ITS samples, the best mix design, meaning a mix design whose ITS results dominated others incorporated was selected for further performance testing.

3.5 STRENGTH TESTING

3.5.1 Indirect Tensile Strength (ITS)

This is an empirical test that determines a mathematical value indicating the performance of a material under both dry and wet conditions. It is calculated from the maximum load a test specimen can bear just before failure. It identifies a suitable mix design amongst a series of other mix designs with different application rates of active filler, bitumen, bitumen emulsions, and other additives. The tensile strength results from the binder's cohesive strength and the aggregate-bitumen interface bond strength. The resulting mix with a higher tensile strength due to an additive blended indicates

that it will have an increased long-term performance.

Jenkins *et al.* (2020) indicate that the ITS test is an appropriate tool to optimize mix composition variables. Each test specimen is 152 mm diameter by 95mm height. Active filler is selected, normally cement and lime both at 1% and 0%. Three samples are tested at each moisture conditioning variable: wet and dry. Upon selecting a suitable filler based on ITS results, an optimum amount of binder is also evaluated using different percentage rates, the binder content that results in the highest ITS value is selected as the optimum binder content. Throughout this research, the binder content was kept at 1.2% RBC, the variable was the nanosilane application rate.

SANS 3001-BSM4:201X, TG2, and BSM Cold Recycling Laboratory Handbook were used as reference guides to carry out ITS testing. Following mixing, test specimens were compacted using a vibratory hammer in two layers, where the mass of each layer was calculated using Equation 3.10 as per TG2.

$$Mass/Layer = \frac{Density \times Volume}{2} = \frac{[MDD + OMC(\%) \times MDD] \times \pi \times r^2 \times Volume_{Mould}}{2} \tag{3.10}$$

Compaction was done using Wirtgen WLV1 vibratory hammer(Figure 3.13) and BSM3:201X Edition 1 and TG2 as reference. A steel mold of 150 mm height was used, its walls were lubricated with a cooking spray to avoid test specimens attaching to them. This allows test specimens to be removed gently from the mold without being destroyed since they are fragile just after compaction.

The use of a vibratory hammer for compaction is to simulate field compaction (Jenkins *et al.*, 2020), it is most appropriate for crushed rock compaction capable of achieving greater than 100% Modified ASSHTO Density within 20 seconds, however much higher compaction energy is needed for high plasticity materials (Jenkins and Collings, 2017).

Figure 3.13: A vibratory hammer used for compaction

Accelerated curing was adopted to rid off moisture from the samples as per SANS 3001-BSM2-201X. The test specimens were placed in a 40°C oven for 72 hours until constant mass (Figure 3.14A). If the mass of the test specimen has not stabilized after 72 hours, it is oven-dried for a further 4 hours. The samples are removed from the oven and allowed to cool in a temperature-controlled environment, 25. The specimens were later tested dry in an ITS machine at 25. Other test samples were submerged in water(Figure 3.14C) for 24 hours upon which they were surface-dried and tested.

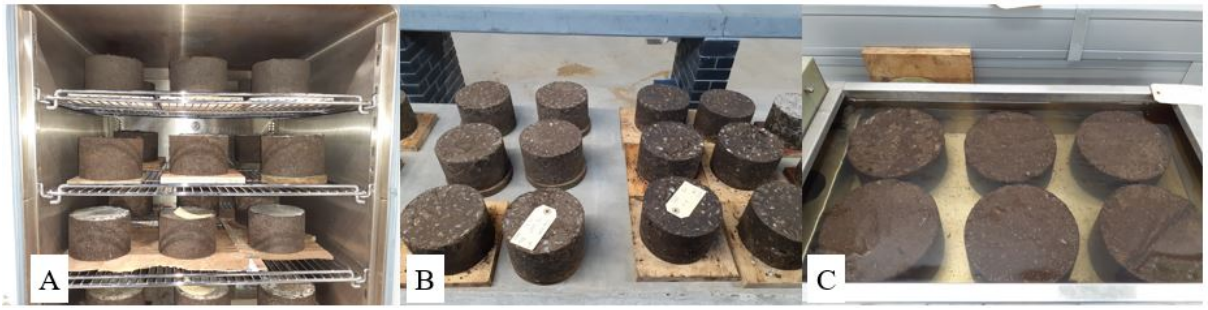

Figure 3.14: Curing and conditioning of ITS test specimens

Using the ITS machine, after curing test specimens and conditioning them to ambient temperature, a compressive force is applied at two points along the circumference of the specimen, along a vertical diametrical plane as shown in Figure 3.15A and B. The frame holding the specimen is moved by an adjustable metal plate controlled by computer software, so is the loading device. Refer to Appendix A.

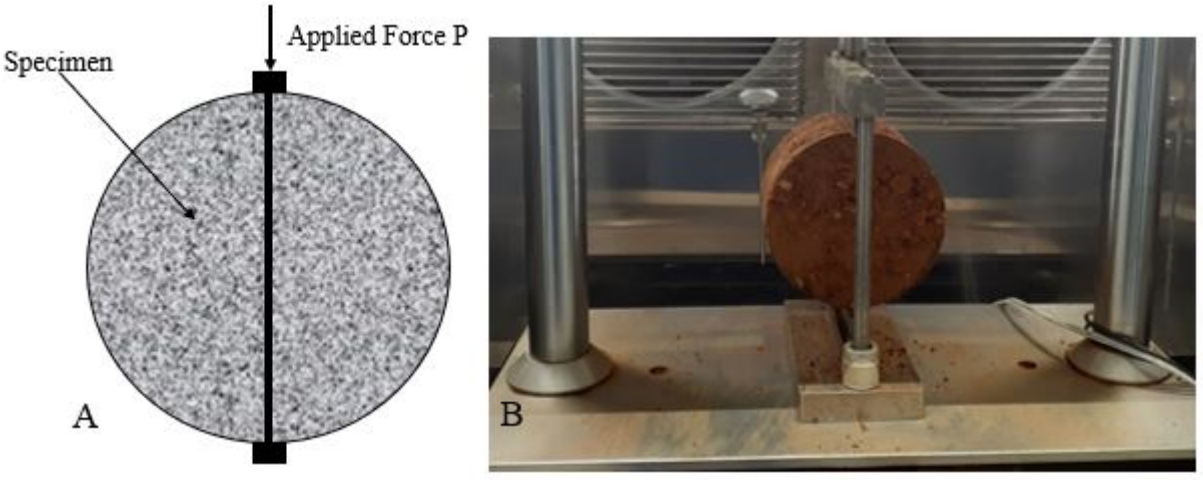

Figure 3.15: ITS testing set up

Based on ASTM D6931 – 12, the test specimens were placed on 19mm loading strips since their nominal diameter was 150mm with a tolerance of 2mm, where the length of the loading strips exceeded the test specimens' height. The setup and control parameters were set up, the loading rate was configured to 50.8 mm/min for constant deformation, test specimens were conditioned to 25°C temperature, these influence the resultant ITS values. A specimen was compressed until failure to get the maximum applied force. The internal temperature of the specimen and displacement were recorded. A sample mass per moisture conditioning variable per mix was weighed and oven-dried in a 110°C oven until constant mass to evaluate the moisture content at the break. The maximum force at failure was used to calculate ITS value per specimen using Equation 3.11. A mix design resulting in the highest ITS value was considered optimum and used for further performance tests.

$$ITS(kPa) = \frac{2 \times (Applied\ ForceP(N))}{(\pi \times height(mm) \times diameter\ (mm))} \tag{3.11}$$

Following this, different graphs per mix were plotted to show which mix type has the highest ITS value. The calculation of both the dry and wet ITS values was followed by the determination of a Tensile Strength Ratio (TSR), following Equation 3.12, this parameter indicates the mix's susceptibility to moisture or water ingress. A graph of mix type with different application rates

of additives was then plotted to show the trends in TSR with changing additive content. Refer to Appendix C.

$$TSR(\%) = \frac{ITS_{Wet}}{ITS_{Dru}} \times 100 \tag{3.12}$$

3.5.2 Triaxial Testing

Shear strength parameters are cohesion and angle of friction, obtained from a simple triaxial test. The stress sustained by specimens without failure was calculated from the failure force. The calculation of these parameters was based on the monotonic triaxial testing briefly explained below. The test was done at three confinement pressures and two specimens were tested per confinement pressure.

Monotonic Triaxial Testing

The monotonic triaxial testing results in shear parameters. The test makes use of a total of 10 triaxial specimens, 8 tested under dry conditions and 2 are tested under wet conditions. The TG2 indicates that the triaxial specimens should be 300mm high and 150 mm in diameter. The (Material Testing System) MTS equipment was used for testing, the displacement rate set at 3.00mm/min with confining pressures at 0 kPa, 50kPa, 100 kPa, and 200 kPa.

The compaction of test specimens was similar to that carried out under ITS testing, however, due to the 300 mm height of the triaxial test specimen, it was done in five layers. Equation 3.10 calculated the mass of each layer with adjustments in the specimen's height and material density. The mixes prepared for monotonic testing were done according to Table 3.10, it illustrates aggregate materials, binder and additives per mix.

Table 3.10: Mix design matrix for monotonic triaxial testing

Material	**Mix ID**	**1.2% Cross Emulsion**	**Additive**
Laterite	L1	SS60NME	0.5% Lime
	L2	CSS60	0.5% Terrasil+
Kalumbila GCS	KL1	CSS60	0.65 kg/m3 Terrasil+ and Zycobond (A1)
	KL2	CSS60	0.5% Terrasil+ (A2)
Kansanshi CS	KS	CSS60	0.5% Terrasil+ (A2)

The curing of the triaxial specimens is slightly different from the ITS curing procedure. It was done as per SANS 3001-BSM5:201X. The aim is to reduce the moisture content of test specimens to 60% to 70% of OMC which is approximately the equilibrium moisture content. A BSM guideline for carrying laboratory procedures with Wirtgen equipment was also used as a reference. After

the first curing phase of 8 hours, test specimens were wrapped (Figure 3.16B) using a cling-wrap instead of loose-fitting plastic bags, it was considered an effective way of preventing moisture loss.

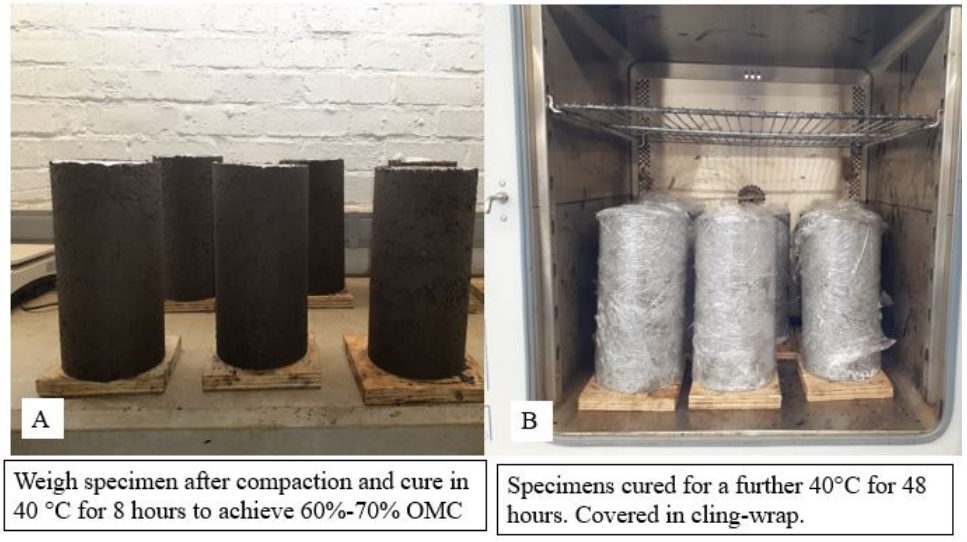

Figure 3.16: Curing and conditioning of triaxial test specimens

Test specimens were conditioned to temperature of 25 °C before testing, they were kept in a temperature chamber for 4 hours as seen in Figure 3.17A. A cylindrical test specimen was weighed and then put placed on the middle of a base plate and covered with a rubber membrane, encased in a metal casing fastened tightly. The fasted casing was then placed on the reaction frame adjustable using knobs connected to the MTS equipment. The top of the metal casing was covered using a thick metal plate with a small opening on the surface. The actuator position was adjusted until contact is made with the small opening on the top metal plate. This setup is demonstrated in Figure 3.17B.

Test parameters were set on the controlling software program, these include loading rate, strain rate. The required pressure was set, and the test started. The graph of applied force against time was a selected display, testing was stopped when the maximum force had been reached reflected by the decrease in the force with testing time. Data was automatically sent to the data logger in terms of a file text format, allowable maximum force values were copied from that file to a Microsoft excel sheet template for further analysis and determination of shear parameters.

The tested sample was removed from the reaction plate, unfastened, and taken out of the rubber membrane, its internal temperature was taken, Figure 3.17C. A representative mass of approximately 1000g was weighed and oven-dried to measure the moisture content as per TMH1 Method A7. The maximum allowable force was used to calculate the applied failure stress per test specimen,

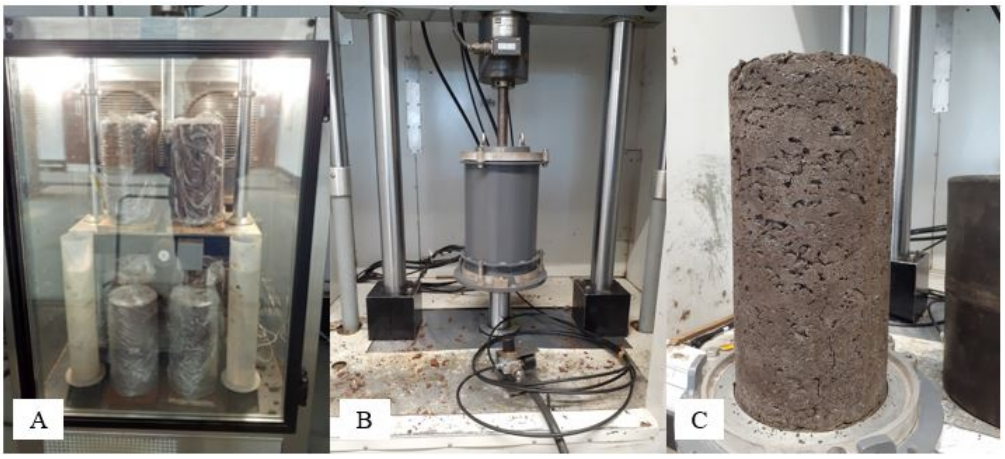

Figure 3.17: Monotonic Triaxial test setup

sigma 1(σ_1). This procedure is similar for all test specimens tested at both dry conditions and wet conditions.

$$FailureStress = \sigma_1(kPa) = \frac{Load_{Failure}}{Area} = \frac{P(kN)}{A(m^2)} \tag{3.13}$$

The applied failure stress was plotted against the corresponding confinement pressure. These are used to plot the Mohr-Coulomb circles from which the shear parameters are determined (TG2). The plot enables a straight regression line to be drawn tangential to all the circles. The line is known as the failure envelope, the y-intercept is known as a cohesion of the tested material while the angle between the line and the horizontal is an internal friction angle of the material.

As per TG2 2020, Appendix C, the regression line's intercept (B) and gradient (A) were used to calculate shear parameters using Equation 3.14 for the regression line, Equation 3.15 for Cohesion, and Equation 3.16 for an angle of friction. Refer to Mohr circles in Appendix C as well.

$$RegressionLine = A\sigma_3 + B \tag{3.14}$$

$$FrictionAngle(\phi) = sin^{-1}(\frac{A-1}{A+1}) \tag{3.15}$$

$$Cohesion(C) = B \times \left(\frac{1-2sin\phi}{2 \times cos\phi}\right) \tag{3.16}$$

According to Jenkins (2000), cohesion (C) and internal friction angle(ϕ) are important parameters

in determining the major principal stress($\sigma_{1,f}$). It is defined by relating the shear failure parameters and minor principal stress, sigma 3(σ_3) as shown in Equation 3.17

$$\sigma_{1,f} = \frac{(1 + \sin\phi)\sigma_3 + 2 \times C \times \cos\phi}{(1 - \sin\phi)} \tag{3.17}$$

3.5.3 Dynamic Triaxial: Resilient Modulus

This is a cyclic triaxial test from which resilient modulus (Mr) is determined. Resilient modulus can be defined simply as the material stiffness as measured in the unload cycle, indicating load spreadability. Similar to the monotonic triaxial test, MTS equipment was used for testing, the resulting resilient modulus is an important factor in the structural design, evaluation, and analysis of pavement, a key input parameter in the mechanistic-empirical design (Anochie-Boateng *et al.*, 2009).

Deviator stress and confining pressures have a major influence on the resilient behaviour of pavement layers (Anochie-Boateng *et al.*, 2009). These are very low stresses applied to the test specimen under dynamic triaxial testing (Jenkins, 2000), their selection allows the testing to be conducted in a single specimen. However, the stress levels selected were not representative of loading subjected to a haul road. There were no adjustments made to account for this, given the massive inflation pressures of haul truck tyres. It is expected that the Mr will aid in the understanding of materials quality.

The shear properties of the material are an input parameter in the determination of the resilient modulus, they were used to calculate the deviator stress ratios (DSR). The stress combinations: DSR and confining pressure are used in the MTS machine as inputs for the resilient deformation.

The testing was done at OMC/MDD conditions.The test specimen selected was based on an optimum mix design indicated by ITS testing. According to Anochie-Boateng *et al.* (2009), it is recommended that the test begins at the highest confining pressure with the corresponding low-level stress ratio to avoid failure of the specimen. The selected confinement pressure values were 200 kPa, 150 kPa, 100 kPa, 50 kPa. The transient load applied from these combinations was calculated and manually captured into the computer program.

The test specimen was placed on a base disc underlain by a base plate, covered by a latex membrane using a metal membrane stretcher. A loading cap was placed on the top of the specimen, covered with a membrane that was tightened with two O rings both at the top of the specimen and the bottom. The linear variable displacement transducers (LVDT's) were used to measure axial deformations, two LVDT holders placed 100 mm along the height of the specimen were used to hold three LVDT probes. These LVDT holders were tightly fastened with rubber bands ensuring

they make circumferential contact with the specimen. They were parallel such that LVDT probes secured by the bolts were vertically aligned and not skew. This is shown in Figure 3.18.

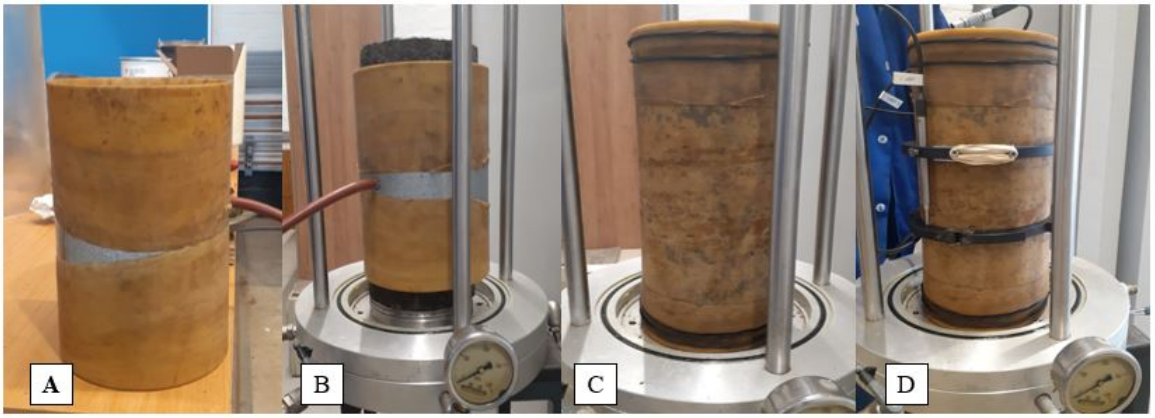

Figure 3.18: Resilient modulus test preparation

The tightened triaxial specimen was assembled into a pressure chamber. Steel braces were placed on the base plate and carefully aligned with the tie holes. The chamber was greased at the bottom and top surface area to ensure that it was airtight. This is an important check to ensure since it affects the testing regime, pressure will keep decreasing in the chamber if there is an air leak. The top cover of the pressure chamber was then tight on the top of the chamber such that the LVDT probes could be connected to corresponding cables that extrude out of the top cover, these were labeled to avoid confusion when connecting them. A detailed experimental procedure is found in the Appendix A.

The top cover was correctly placed on the pressure chamber casing and tightly fastened using tie rods anchored tightly to the base plate. The fastened LVDT setup up was then lifted onto the reaction frame with care given its relatively huge weight. The LVDT cables from the top cover were connected to the corresponding lead wires of the LVDT's. The loading ram was lowered so that it aligns with a steel piston inserted at the top of the cover. The test was performed at 25 °C temperature with a tolerance of 2 °C. Figure 3.19 shows a complete dynamic triaxial set-up ready for testing.

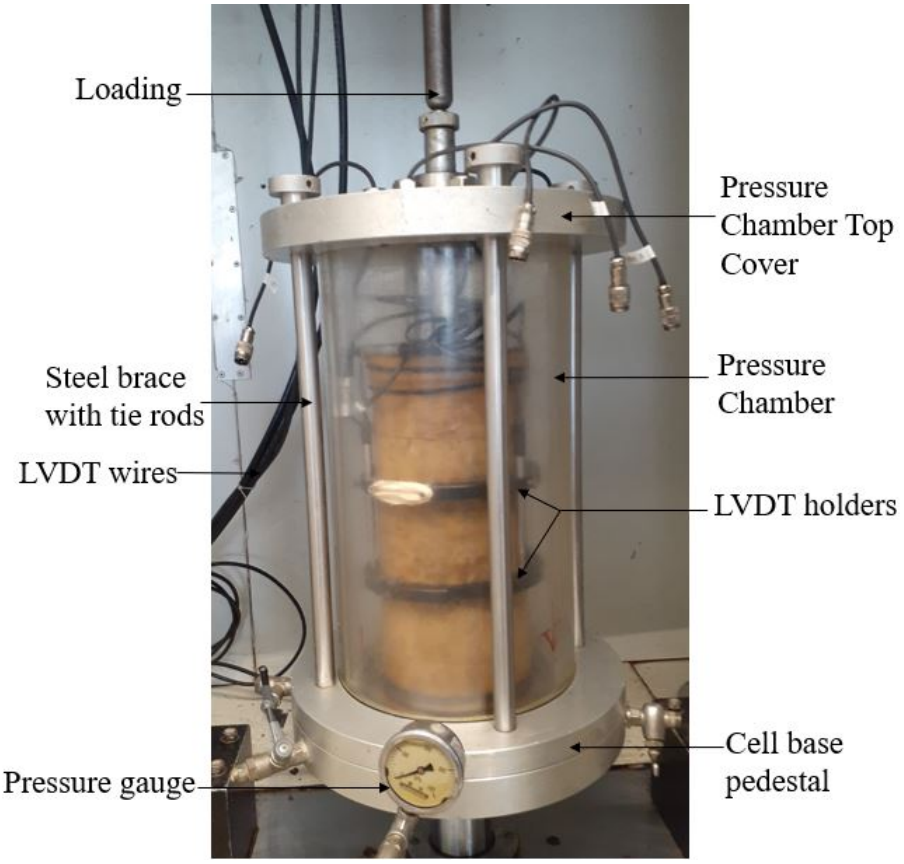

Figure 3.19: The pressure chamber for resilient modulus test

The load was applied to the specimen through a computer-controlled user-defined test program. Axial deformation was recorded by LVDT's connected to the computer set up. All data was captured and common Mr models were used to calculate the Mr of each material. Mr-θ model develops a power form trend line relating bulk stress and resilient modulus on a log scale. This relationship is used to calculate the effective resilient modulus per specimen

3.6 PERMEABILITY TESTING

The drainage characteristics of the treated mix were evaluated using permeability testing. This provides the coefficient of permeability through which the rate of flow of water through the material is known. The main drive towards permeability testing being a consideration was the ability of the nano silanes to impart hydrophobicity to materials, it was therefore important to evaluate the extent to which the nano additives improve the water repellent characteristic of the material.

It was decided to carry out permeability tests on all three materials, however, the Laterite material

seemed to fail under wet conditions in ITS testing, it was therefore indicative of failure under low pressures given the aggressiveness of the high permeability testing. The materials selected for this test are graded crushed stones; a 26 mm graded crushed stone and another graded crushed stone from a different mine site. They were selected because of their performance indicated by ITS results. Therefore, only optimum mix designs selected from the crushed stone materials were considered for testing.

3.6.1 High Pressure Permeability Testing

This test was developed in Stellenbosch University by a masters student, Mr.OR Grobbelaar in 2016 (Venter, 2019). The main objective was the evaluation of the permeability of chip seals under pressure. In this project, it has been applied to unbound granular mixes at low pressures. The setup shown in Figure 3.20 illustrates the apparatus of the HPP, the top shows a compressor adapter from which pressure is applied to the system. The is also a fitted funnel that aids with filling water into the apparatus. There is a water flow gauge that measures the water levels during testing.

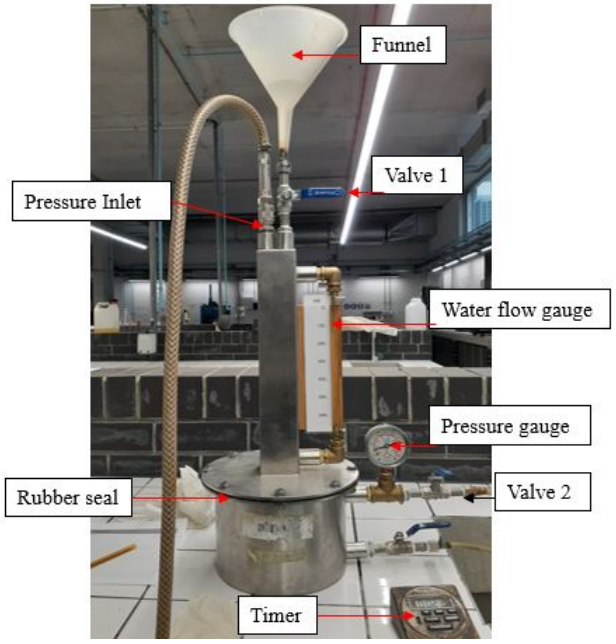

Figure 3.20: High pressure permeability test setup.

There are two sockets at the bottom section, the top one above the specimen contains a high-pressure valve that fills water into the system and a pressure gauge that monitors the internal pressure of the apparatus. The other socket below the sample contains a high-pressure valve used during testing to allow water to leave the system. A rubber seal is used to prevent water leakage

while it permeates through the specimen. It was inflated to 300 kPa to push against the internal walls of the steel encasement, preventing water from seeping past the test sample. Water was filled in the water gauge indicator and height is recorded at time intervals as it permeates.

The selection of confining pressure was influenced by the tested materials and the selected optimum mixed design. Given that the materials used are UGM, and the main objective is to test the extent of hydrophobicity imparted by nano silanes, the pressure was set to a lower value, 100kPa. The HPP apparatus is designed to accommodate test specimens with a 100 mm diameter and a maximum of 55 mm height. The height of the test samples was 52 mm because they would protrude beyond the rubber seal if they exceeded 55 mm. At this height, the rubber seal tightens samples sufficiently, water does not escape through the seal-sample interface region easily, Figure 3.21.

Figure 3.21: Shows test specimen inside a rubber sea;

The testing was carried out on different mix designs per two selected materials as shown by Table 3.11, 3 samples were prepared per mix design to find the average value of permeability per each mix design.

Table 3.11: Mix design selection for HPP testing

	Mix Design		
Emulsion	**Laterite (M1)**	**Kalumbila GCS (M2)**	**Kansanshi CS(M3)**
CSS60	-	1.2% Pure CSS60	1.2% Pure CSS60
	-	0.5% Terrasill+	1.0% Terrasill+
SS60NME	-	1.2 % Pure SS60	1.2 % Pure SS60
	1.2% SS60NME	1.2% SS60NME	1.2% SS60NME

3.6.2 Compaction and Curing

A Bosch GSH 11VC vibratory hammer (Figure 3.22) was used to compact samples to the desired height and density to achieve the 100% MoD AASHTO. This was done in a 100 mm diameter steel mold. Maximum dry densities of all materials were determined during MDD/OMC tests. The bulk density was calculated considering a selected height of 52 mm. Equation 3.10 calculated the compacted mass of each specimen with a change in samples dimensions and density of materials. Since three samples were compacted per mix design, appropriate masses were weighed and covered in plastic bags before compaction.

Figure 3.22: Vibratory hammer used to compact HPP samples

The same curing procedure as that in ITS testing was followed. Figure 3.23 illustrates specimens upon compaction and during curing.

In permeability calculations, the rate at which water passes through the sample volume is evaluated, amount water is recorded using the water level indicator and time is recorded at certain intervals. Permeability or flow rate was calculated (Equation 3.18 by determining water quantity passing

Figure 3.23: Compacted HPP samples and their curing.

through the sample per time taken to reach the next low lower level.

$$HPP_{Flowrate}(ml/min) = \frac{Volume_{Water}(ml)}{Time(min)} \tag{3.18}$$

3.7 STRUCTURAL DESIGN

There are different methods available for pavement design and analysis such as the AASHTO design method, CBR method, pavement number and mechanistic-empirical method. The mechanistic-empirical design method is selected suitable for haul pavement analysis in this research. It allows the evaluation of material effects on pavement performance or structural capacity. Furthermore, the material to performance relationship is developed and easier to understand under this method. Thompson and Visser (1997*b*) state that significant road deterioration is due to stresses and strains induced per layer, the method allows calculation of these stresses and strains and compares with the limiting strain criteria, which is 2000 μm for vertical strain values.

3.7.1 Mechanical-Empirical Design Method

The mechanical-empirical design follows a flow chart illustrated in Figure 3.24, it is an iterative process ensuring that an optimal haul road design is achieved given available input parameters such as applied load and tyre pressure, thickness and layer strength.

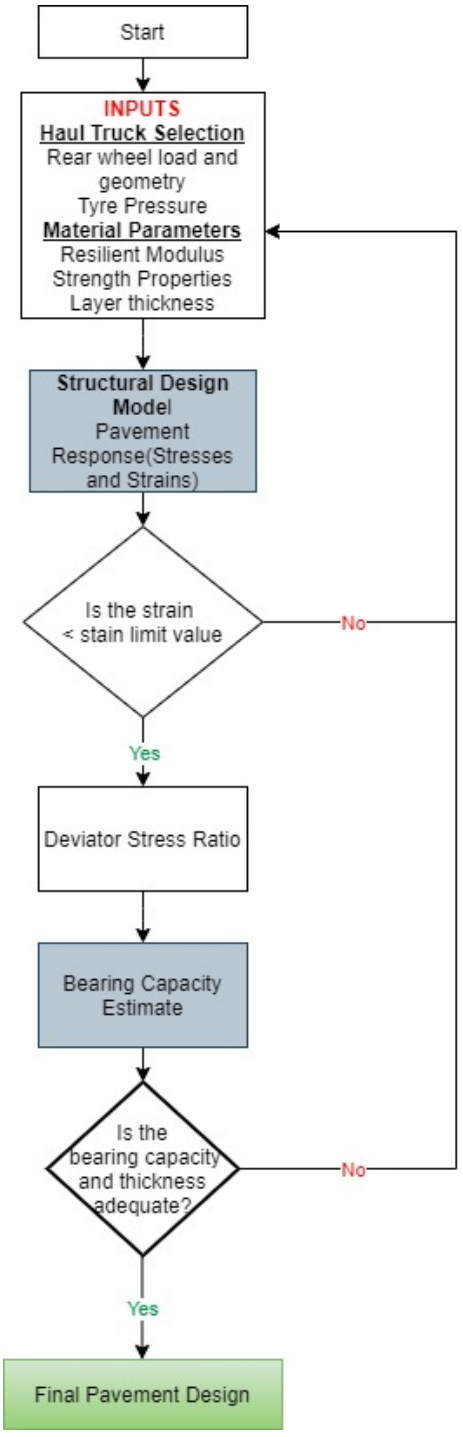

Figure 3.24: Flow chart of Mechanistic-Empirical Design. Adapted from (Theyse and Muthen, 2000)

3.8 SUMMARY

The chapter illustrates the experimental design methodology carried out in determining the effectiveness of NME stabilization using laterite, Kalumbila GCS and Kansanshi CS. The binders used include preblended SS60NME, unmodified CSS60 and Terrasil+ modified CSS60. All standard laboratory tests are carried out to determine material properties, tests include sieve analysis and Atterberg limits. The tests follow specifications and procedures explained in the chapter. Material classification tests are extended to mineral testing using X-ray diffraction. Mix design procedures are divided into two approaches, Approach 1 entails a nano additive being mixed in water and dispersed into the aggregate while mixing, this is a simpler method and easy to use when water is used as a carrier fluid. In Approach 2, Terrasil+ is blended into bitumen using a high shear mixer, this offers a high dispersion of the organosilane concentration. ANOVA is determined to support that organosilane addition and NME's have a significant statistical difference on material performance.

The different mixing approaches are done to evaluate any influence of organosilane application on mix performance. During ITS, the influence of Terrasil+ and Zycobond content on mix designs is evaluated on laterite, Kalumbila GCS and Kansanshi CS. Mixing processes such as compaction and curing are done as per relevant specifications. The triaxial specimens produced to measure the performance properties were prepared as guided by SANS 3001 BSM 5. Triaxial specimens are done for an SS60 and 0.5% lime modified laterite, CSS60NME modified laterite, Kalumbila GCS and Kansanshi CS. Shear parameters are developed from all monotonic testing. Dynamic triaxial testing is done on laterite and Kalumbila GCS materials, this test is used to measure the resilient modulus of the tested materials, axial deflections are measured on each transiently loaded sample encased in a triaxial chamber.

The high-pressure permeability testing procedure is originally developed for asphalt materials but to test the extent of permeability on Terrasil+ and Zycobond treated materials, it has been adopted. The procedure followed is briefly described in the chapter, the maximum pressure in testing is capped at 100 kPa due to the aggressiveness of the HPP testing. Modified and control mixes are tested to have a comparative permeability analysis. Finally, the chapter presents a pavement design approach to check the structural adequacy of the testes materials if used as haul base layers, pavement structures with different resilient moduli are analysed for stresses and strains which are benchmarked against literature specifications. Deviator stress ratios of all analysed pavements are finally calculated to indicate vertical compressive strain or the occurrence of accelerated permanent deformation with time.

CHAPTER 4

RESULTS AND DISCUSSIONS

4.1 INTRODUCTION

Materials that are used for haul road construction on two Zambian copper mines, namely Kanshansi and Kalumbila, have been evaluated at a research level for possibilities of performance enhancement. Laboratory testing of materials was carried out to define their characteristics, classification and performance. Widely published literature on using these materials in Southern Africa mines is not available, including their stabilization using new-age modifiers such as NMEs. A series of tests is used to evaluate the effect of NME's on the strength, stiffness, and water permeability of these haul road materials. Mix optimization of the modifiers, especially organosilane, can be evaluated in two different ways i.e. blending in water and blending in bitumen.

In addition to laboratory standard engineering tests, chemical tests i.e. XRD analyses characterized the materials, results from both treated and untreated samples were evaluated and linked to material performance. The research focused more on the material behaviour of haul roads, so the testing regime was designed to provide results that would show the usefulness of NMEs.

4.2 LABORATORY TESTING

4.2.1 Grading

Materials were all screened to remove fractions bigger than 20 mm. Particle size distribution curves represent dry and wet sieving per material. Although these materials are not BSM, the BSM grading limits have been adopted as a guide to decide on characterization and the suitability of the material stabilization. Generally, all tested materials fall within the BSM limits except washed Kalumbila GCS and laterite fractions less than 5mm, they are below the suitability zone. However, this does not have a significant effect since it changes by a very marginal percentage.

Laterite(dry) curve shows a sufficient PSD in all size ranges. It has a form of gap grading due to missing particles between 0.3 mm and 2 mm, medium to coarse sand aggregates. The absence of this fraction could contribute to the high moisture susceptibility of the material, fines fill in voids spaces within the bulk mix matrix, decreasing the high permeability of moisture or water ingress. However, this is consistent with what Gourley and Greening (1997) found in Southern Africa laterites, the shape of their grading envelope does not render the material insignificant, they can accommodate large grading limits. This further emphasizes why NME stabilization for this material does not present an enforceable grading specification but a reasonable guideline. Without modification and

stabilization, laterites would be unsuitable for road construction; experience durability issues.

Based on the Unified Soils Classification System USCS,, the C_C value of laterite is greater than 3(see Table 4.1), hence poorly graded. However, the C_U value is significantly higher than 6, rendering the soil well-graded, although both C_C and C_U conditions need to be met for a well-graded soil. There are fewer greater than 6 mm gravel fractions due to a higher percentage passing 10mm to 7.5mm, the curve is almost at the borderline of BSM limits. It shows a low potential occurrence of raveling and corrugation. However, the grading indicates that laterite is sufficient for stabilization since its curve falls within the chosen BSM specification guide.

Grading envelopes for crushed stone materials from both Kalumbila and Kansanshi are presented in Figure 4.1. Kalumbila grading curve fits perfectly within the BSM grading limits, the shape and steepness of the graph denote a well-graded material. There is a representation of all particle sizes in the material suitable for stabilization. Based on USCS, the C_C value of 0.68 is out of bounds for a well-graded material but, the C_U is 35.10 showing a well-graded soil since it is greater than 6. According to COLTO, a material with a GM ranging from 1.5 to 2.5 is categorized under the G6 class.

Similar to Kalumbila GCS, Kansanshi CS fits within the grading limits, the grading envelope shape represents a well-graded material. All fractions seem represented within the material, C_C and C_U values are within acceptable limits of a well-graded soil under the USCS. The grading modulus of 1.67 is also greater than 1.5 indicating a G6 material class as per COLTO. The grading is, therefore, suitable for stabilization using bitumen emulsion. This material had bigger particles larger than 28 mm not included in the testing procedure since they would influence performance. Coarse or gravel materials suitable for use in base layers should have a DR from 0.3 to 0.7 and a grading modulus above 1.5 (TRH14, 1985), all materials used in the study do meet these specifications. (see Table 4.1)

Table 4.1: Material assessment as per USCS in ASTM D2487-17 and COLTO

Material	**D_{10}**	**D_{30}**	**D_{60}**	**C_C**	**C_U**	**GM**	**DR**	**Sand Content (0.075mm-5mm)**
Laterite	0.20	2.31	6.50	4.11	32.50	1.56	0.30	46.04
Kalumbila GCS	0.23	1.14	8.21	0.68	35.10	1.48	0.33	40.07
Kansanshi CS	0.15	1.89	12.57	1.84	81.75	1.67	0.29	35.60

The dust ratio ranges from 0.29 to 0.3 for all materials. These will result in low dustiness since according to Thompson (2009), haul roads wearing course dust ratio range is 0.4 to 0.6, beyond which there is increased dust generation. Therefore all materials will result in less dust generation

though some raveling may occur if used as wearing course on unsurfaced haul roads. Percentage passing through the 0.075 mm exceeds 5% for all materials, this categorizes them as G4 under the TRH14 classification system. The grading envelopes of all materials fits within the specifications and, as a result, were selected as target grading. It is important to note that for NME stabilization, there are no existing grading limits so BSM specification grading limits are considered a guide.

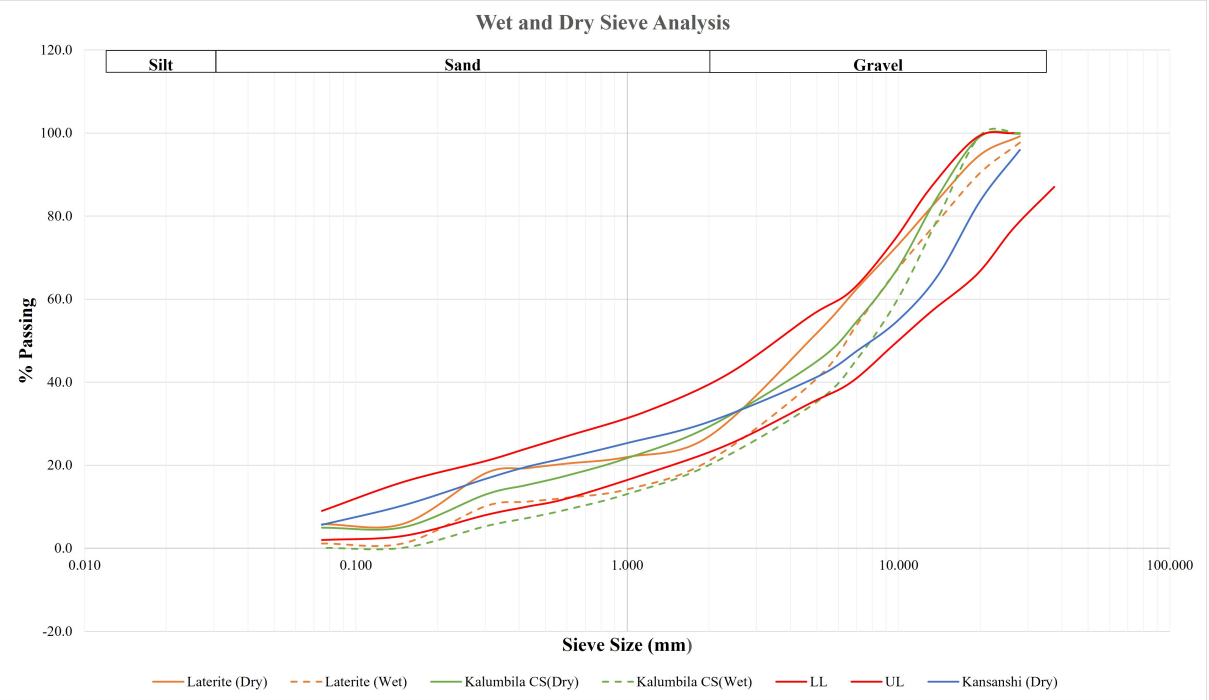

Figure 4.1: Wet and Dry Sieve analysis of all materials

4.2.2 Moisture and density relationship

The density and moisture content relationship of laterite and Kalumbila CS are shown in Figures 4.2 and 4.3, respectively. The value of R^2 denotes that the curves are the best-fit lines for the data provided. This relationship was determined using the modified Proctor compaction, it is understandable that most of the material compaction in haul roads is done by dump trucks or wheeled mining equipment instead of dynamic or vibratory compaction methods. However, this was selected as a standard testing method for all aggregates.

Two trials determined OMC/MDD of laterite at its natural state, both resulting in similar moisture content of 2190.2 kg/m^3. Trial 1 shows a slightly lower MDD value, but the difference is insignificant. The optimum moisture content corresponding to trial 2's MDD is 8.8%, as seen in Figure 4.2. Due to limited laterite quantity, fractions exceeding 20 mm were not discarded but crushed and blended

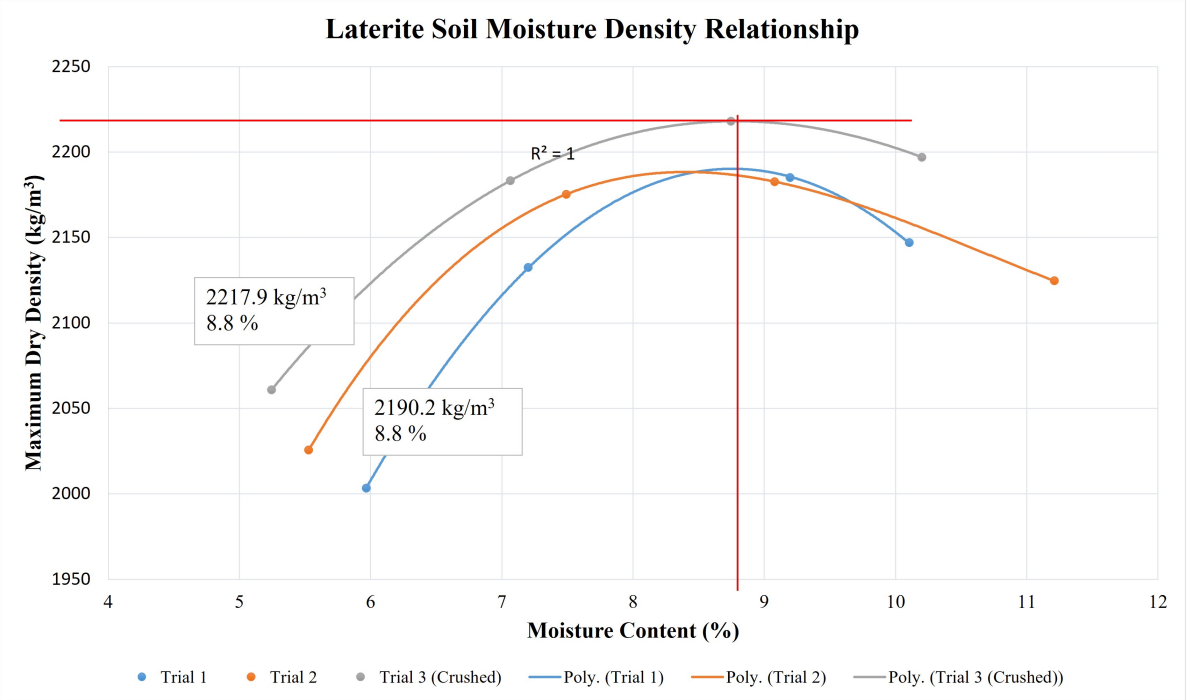

Figure 4.2: Laterite moisture and density Relationship

into the natural sample, the blend test results are shown by Trial 3. A significantly higher density is

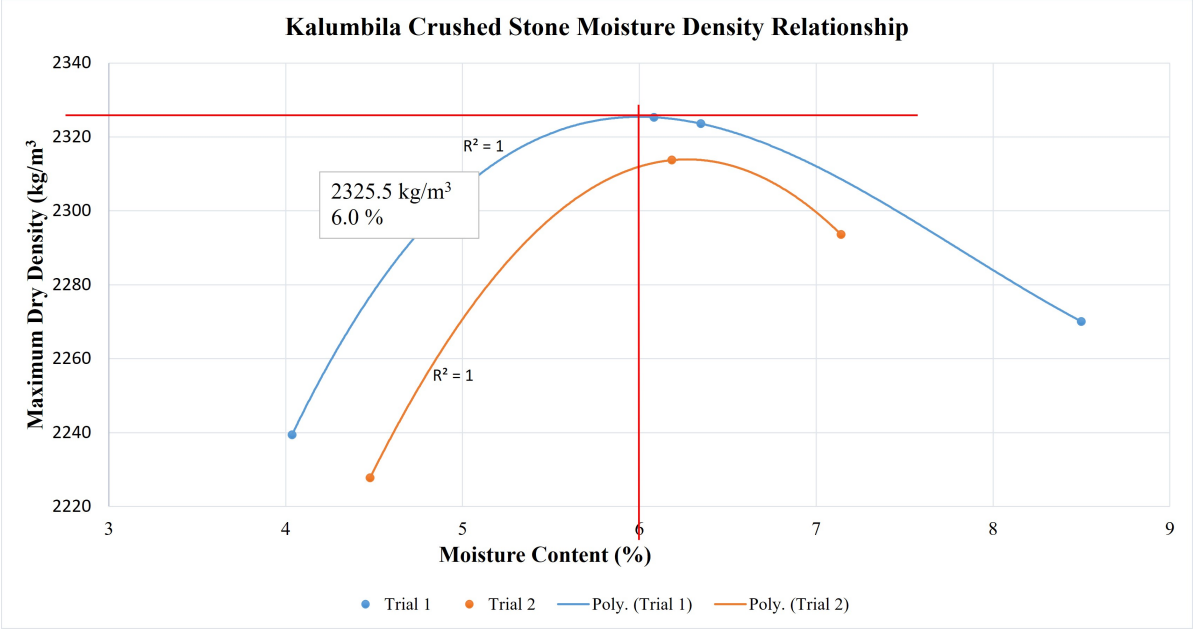

Figure 4.3: Kalumbila GCS moisture and density Relationship

shown, 2217.9 kg/m^3 at 8.8% OMC. This results from differently shaped aggregates due to crushing resulting in an optimum packing of particles and increased contact to contact area leading to an increase in density. Round particles have a relatively lower interfacial surface contact compared to angular aggregate particles. According to Vavrik *et al.* (2002), flat and elongated aggregates particles are hard to pack densely compared to cubical particles that pack in dense configurations.

In Kalumbila CS, two trials were performed to get reliable OMC/MDD results, Table 4.2 and Figure 4.3 show the results from both trials. The maximum dry density is 2325 kg/m^3 at 6.0% OMC in trial 1, and trial 2 resulted in an MDD of 2313.9 kg/m^3 at 6.3% OMC. The difference in MDD and OMC for both trials is marginal and would not have a significant impact on material performance, however, the chosen target density was that of trial 1 due to higher target density.

The author gathered from a mine site visit that construction procedures to attain a maximum dry density are barely followed, aggregates are compacted relatively dry in haul road construction resulting in a lower density. This will ultimately result in poor functionality, potholes, raveling, and excessive deflections with time under excessive loading. Poor construction methods using marginal materials will lead to costly maintenance due to a potentially high severity and extent of distress conditions.

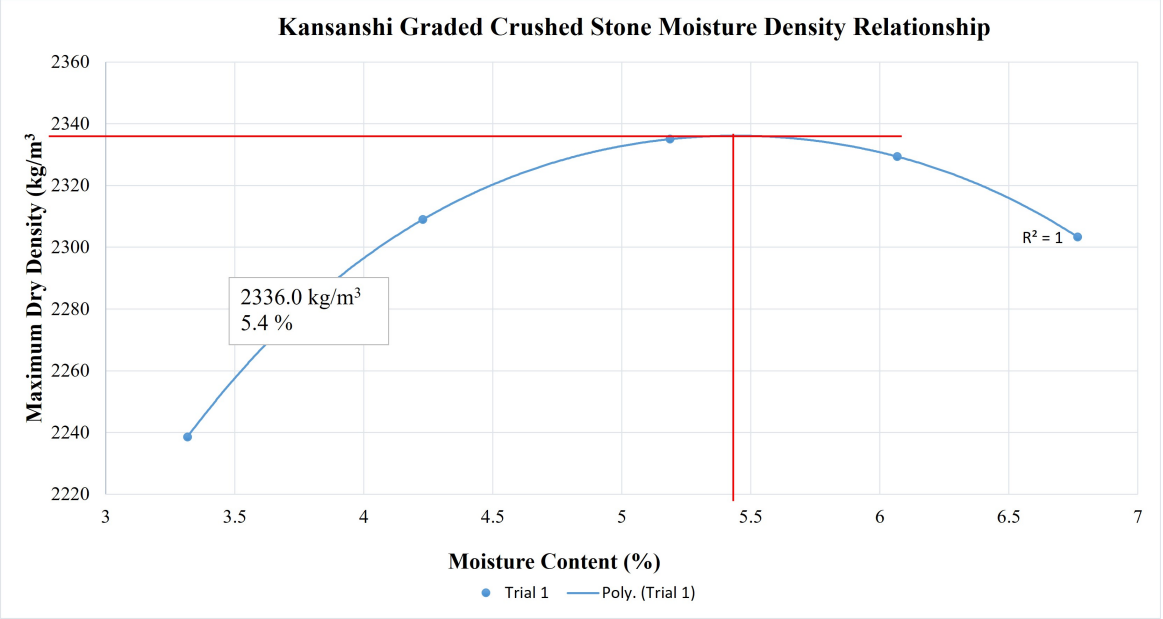

Figure 4.4: Kansanshi CS moisture and density Relationship

Table 4.2: Optimum moisture content and maximum dry density values

Material	Trial/Type	OMC (%)	MDD (kg/m_3)
Laterite	1/Crushed	8.8	2217.9
	2	8.8	2190.2
Kalumbila GCS	1	6.0	2325.5
	2	6.3	2313.9
Kansanshi CS	1	5.4	2336.0

There were fractions larger than 20 mm, with a maximum of around 40 mm, these were crushed using a jaw crusher due to lack of abundant material, reintroduced into original aggregates sample, mixed homogeneously, and tested. The particle shape and texture have likely contributed to a sufficiently higher density. Kansanshi crushed stone is well-graded (Figure 4.1), its particle size distribution was further helpful in attaining a maximum density of 2336.0 kg/m^3 at 5.4% OMC. Figure 4.4 shows the moisture to density relation of this crushed stone, it has a higher density than the other two materials from Kalumbila. However, its density is closer to that of Kalumbila GCS since they are both crushed stones though they may differ in chemical composition and specific material type.

4.2.3 Atterberg Limits

The plasticity of all materials was determined through a series of tests whose results are presented in Table 4.3 and illustrated by Figure 4.5. The report focuses on the liquid limit, plastic limit, plasticity index as well as linear shrinkage. It was decided to test the 0.075 mm fraction of all materials using the same testing procedure. Kalumbila GCS and Kansanshi CS 0.425 material fractions exhibit a non-plastic behaviour, the 0.075 mm fraction of Kalumbila GCS showed plasticity of 4.36. Non-plasticity indicates little to no clay and/or silt.

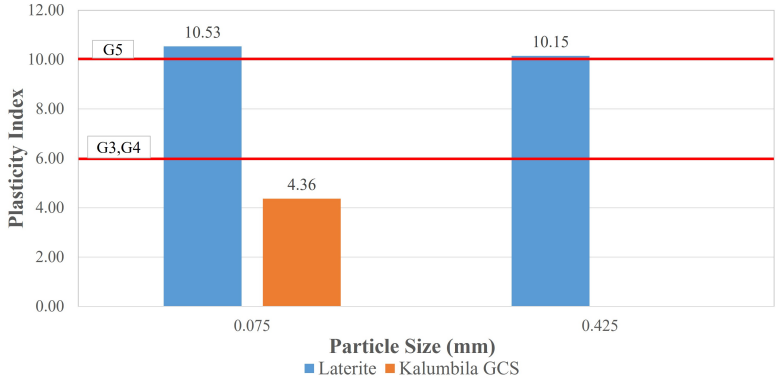

Figure 4.5: Plasticity Index of Laterite and Kalumbila CS

Table 4.3: Atterberg limits results summary and specifications. (TRH14, 1985) and (Thompson, 2009)

Soil Description	**Fraction**	**Liquid Limit**	**Linear Shrinkage**	**Plastic Limit**	**Plastic Index**
Laterite	0.425	30.65	5.33	20.50	10.15
	0.075	38.04	7.33	27.51	10.53
Kalumbila GCS	0.425	-	-	-	NP
	0..075	24.18	1.33	19.82	4.36
Kansanshi CS	-	-	-	-	NP
Material Specifications					
G3 and G4	0.425	25	3	19	6
G5	0.425	30	5	20	10
Wearing Course	0.425	17-24		12-17	4-8

Liquid Limit

The liquid limit, as shown by Casagrande, explores the transition of semi-solid to liquid behaviour of soil, based on increased moisture content. It characterizes the cohesiveness of the soil, it is one of the primary parameters to determine plasticity. Both laterite fractions showed a liquid limit above 30%, a 0.075 mm fraction results in 38.04%. These fractions are plastic, to gain a more comprehensive understanding of material plasticity, a reference should also be made to the plastic limit. These values go beyond limits provided by Thompson (2009), making lateritic soil susceptible to dustiness in unpaved surfaces. Considering the TRH14 specifications, the 0.425 mm laterite fraction shows a 30.65% that is 0.65% higher than the liquid limit for G5 materials. This is a marginal difference hence the material class would be G5.

Kalumbila and Kansashi crushed stone 0.425 mm fractions showed non-plasticity, testing was unsuccessful(See Figure 4.6). The mixed soil in the Casagrande cup did not make an appropriate groove upon being cut but sheared off to aside. 0.075 mm fraction of Kalumbila GCS showed a LL limit of 24.18%, but these cannot be benchmarked against any recommendations since the nominal fraction used is 0.425 mm. There is a high possibility that materials with high LL will perform sufficiently in service, consistency limits are tested on fines and the presence of a low component of high plasticity materials would not significantly impair adequate performance. The actual fines in the material might be low yet plastic.

Plastic Limit and Plasticity Index

Crushed stone materials exhibited no plasticity except the 0.075 mm fraction of Kalumbila GCS

Figure 4.6: Kansanshi CS in Casagrande cup, side view and top view

that had plasticity of 4.36%. This soil had low plasticity indicating a presence of silt and traces of low plastic inorganic clay. Kansanshi CS behaviour is also reflected by Figure 4.6, as a result, the testing was discontinued and material classified as non-plastic.

Laterite fraction both showed PI value around 10%, with a 0.425 mm fraction exhibiting 10.15% and 10.53% for a 0.075 mm fraction. There is little difference in the plasticity index values for these soils. The different fractions have no significant effect on the plasticity index specific to the tested laterite material. Soils with a plasticity index greater than 10% are considered to have medium plasticity and usually indicate a presence of a considerable amount of clay. Highly plastic materials require lime stabilization to reduce soil plasticity. Laterite would then be classified under G5 using the TRH14 classification system, however, the 10% maximum limit in the TRH14 was meant for sealed roads on the national network. Thompson (2009) recommends a maximum value of 8% PI to minimize skid resistance and dust resistance to ensure good functional performance. In terms of plasticity, the materials tested were out of acceptable ranges provided by both specifications mentioned.

Linear Shrinkage

Linear shrinkage forms a critical element in determining material functional performance because it is used to calculate the shrinkage product. Laterite has a relatively higher linear shrinkage compared to the crushes stone. The 0.425 mm fraction of laterite has 5.33% and the 0.075 fraction

has 7.33% SL. This maintains that the particle size distribution chosen did not have a significant effect on the Atterberg limits. The 0.075 mm Kalumbila GCS showed a linear shrinkage of 1.33%. Most available specifications specific to haul roads, defining acceptable limits of linear shrinkage present shrinkage with a relationship between shrinkage product and grading coefficient. Using TRH14 limits, the maximum value for G3 and G4 is 3% and 5% for G5, all 0.425 mm fractions tested are out of bounds rendering the materials undesirable.

The lower linear shrinkage values indicate that the materials tested have reduced slipperiness. There might be corrugations as these low values, however, haul roads are relatively better at less shrinking materials considering how wet the surface gets during rainy seasons. According to the TRH20, acceptable shrinkage product limits for unpaved haul roads range from 100 to 365 but a preferable value is any less than 240.

In summary, as seen from classification tests, all materials proved to be adequately graded for stabilization considering that all grading envelopes fit into the BSM grading limits. The plasticity indices of all materials on all fractions are relatively low, slightly above 10%. The maximum density of crushed stones is 2336.0 kg/m^3 at 5.5% OMC for Kansanshi CS and 2218 kg/m^3 at 8.8% OMC for Laterite. These indicate a relatively acceptable CBR value of above 30%. The TRH14 classification categorizes these materials in the range G4-G5 while Thompson (2009) material selection recommendations based on haul roads unlike TRH14 focused on public roads, are not sufficiently met. Therefore it is worthy to explore the improvement of these materials using innovative solutions to improve their suitability and functional performance.

4.3 MINERALOGY: XRD UNTREATED MATERIALS

Initially, three original samples were tested to characterize virgin materials' mineral phases. There were similarly prepared to all other XRD samples, though not treated. XRD testing was the readily available and cost-effective method to identify the mineralogy of road construction materials. Small soil particles with different lattices which change depending on water content and soils geography were analysed. Figure 4.7 demonstrates a diffraction pattern showing the angle of diffraction and peak intensity, individual patterns are shown in Figures B.1,B.2 and B.3, Appendix B. All the material patterns have been drawn on one plot and mineral compositions are shown in Table 4.4 per material.

Table 4.4: Mineral phases and composition of laterite and crushed stone materials

Laterite	**Kalumbila GCS**	**Kansanshi CS**
Mineral	**Mineral**	**Mineral**
Quartz	Albite low	Calcite
Hematite	Quartz	Quartz
Kaolinite(Iowa)	Microcline(Colorado)	Albite, calcian, ordered
Kaolinite 1Md	Ferro-richterite	Dolomite
Gibbsite	Muscovite	Illite
		Muscovite 3T
Primary Minerals		Secondary Minerals

This is a qualitative analysis, presenting diffraction patterns and identified minerals but not their concentration. This is due to the unavailability of Rietveld refinement methods together with a suitable structural database at a chosen facility

Figure 4.7 presents all three materials' diffraction patterns showing the number of X-rays observed at each angle on the x-axis. The peaks represent the intensity recorded as counts as seen, a pattern is distinct for every mineral phase. For similar samples, a relative intensity change between the mineral phases from one sample to the next reflects a relative decrease or increase in concentration between these samples.

The most critical aspect influencing pavement distress is the material quality which is also affected by the mineralogical nature of the material. The mineralogy significantly influences the material's mechanical performance. In the presence of agents of weathering, primary minerals in materials undergo alteration to secondary minerals whose problematic nature is the principal cause of poor material performance . Refer to colored cells in Table 4.4.

X-ray diffraction performed on laterite shows kaolinite emanating originally from Keokuk, Iowa. Samples revealed a presence of kaolinite 1Md usually known as dickite, a kaolinite polytype hence a clay mineral. Mica minerals are also present, high mica composition affects the quality of aggregates. Aggregates with high muscovite composition are unsuitable for haul road material selection since they absorb fluids and retain them (Kondelchuk, 2008). Laterite aggregates rich in muscovite would be detrimental during rainy reasons, exacerbated by elastic flakes contributing to poor packing. The low content here does not render them entirely substandard.

Laterite contains gibbsite ($Al(OH)_3$) predominantly occurring in tropical regions in extremely weathered aggregates, including lateritic soils. Gibbsite forms part of sesquioxides available in laterite soils at high concentrations. Quartz is also present at high concentrations in most samples, this is acceptable given quartz is the most bountiful mineral available in earth's crust. Hematite,

iron oxide (Fe_2O_3) is one of the primary minerals whose content in laterite is responsible for the reddish/pale yellow color of laterite soil. This confirms the visual inspection of laterite which characterized it as a reddish soil. This results are in agreement with previous finding on laterite soil mineralogy by Paige-Green *et al.* (2015); Netterberg (2014).

These tested materials have a greater potential to perform sufficiently as base layer construction materials based on referenced material selection specifications. Their mineral phases such as iron oxides (e.g haematite) offer self cementation properties, they perform sufficiently for marginal materials. There is a need for modification and guidelines to aid with application in different regions across Southern Africa.

The dominating mineral phase in Kalumbila GCS is albite low, it has a high composition shown by the peak with the highest intensity. Quartz is also identified though it is not a dominant mineral phase. A potassium-rich alkali feldspar mineral known as microcline is present, this is predicted to originate from Pike's Peak batholith, Colorado, USA. There some content of muscovite available, smaller amounts barely impair the material performance in road construction. At low content, it is unnecessary to relegate this material to a problematic materials category and deem it unsuitable for base layer construction.

Kansanshi CS has calcite as a dominating mineral mineral content shown by a high intensity peak. Calcite is a carbonate minerals while quartz is a primary silicate mineral. It is safe to refer to Kansanshi CS as a carbonate material given the high content of carbonate minerals. There is a presence of dolomite, if used as a predominant pavement material on subgrade layers, aggregates may exhibit the behaviour of dolomitic areas such as sinkhole formation and other related distress conditions. Besides illite, muscovite is available in aggregates. Mica and clay minerals have somewhat a similar structure, they are characterized by layered sheets which are sometimes not tightly bound allowing water molecules to enter their structure.

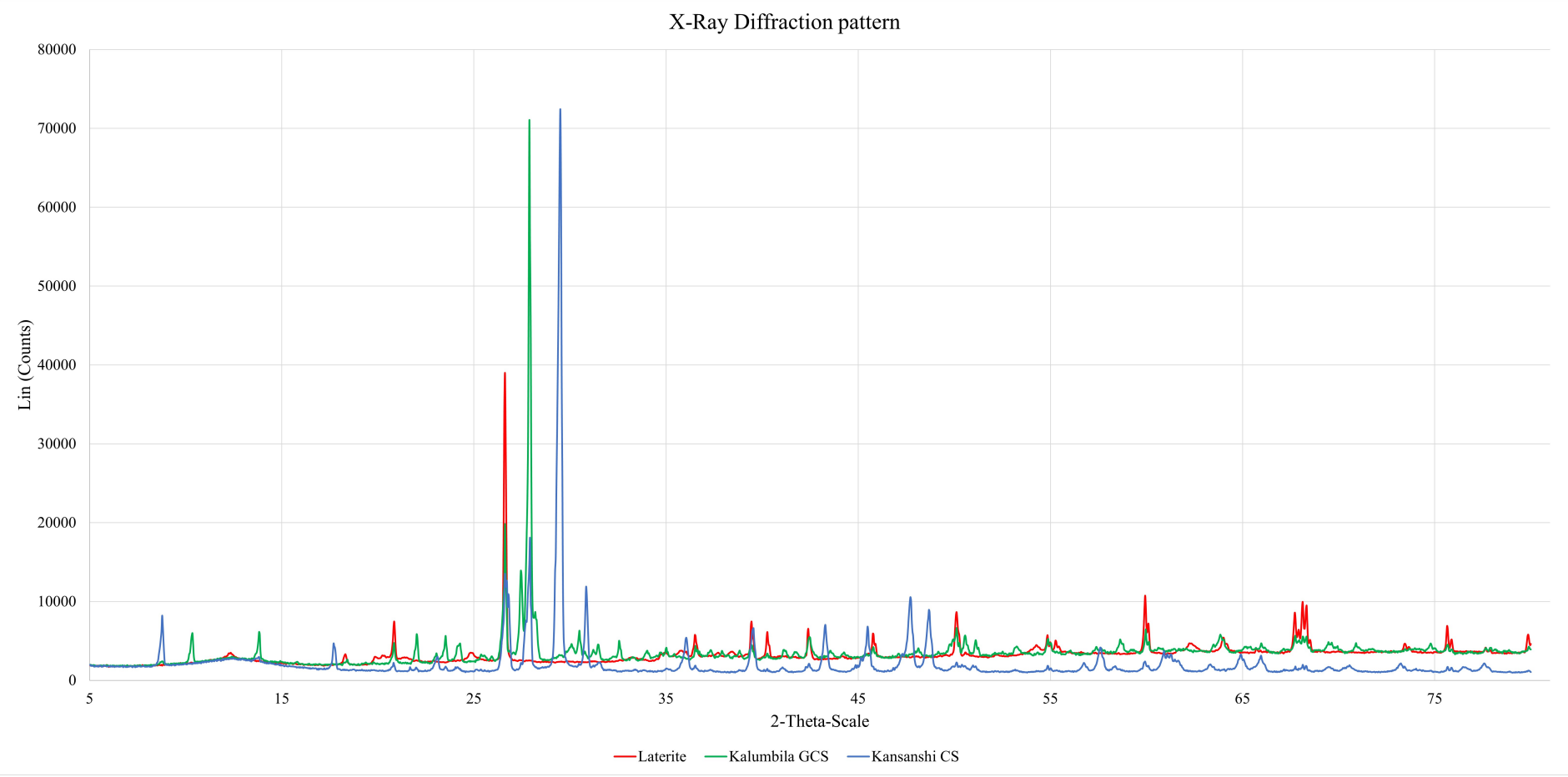

Figure 4.7: Diffraction patterns for laterite and crushed stone materials

Using mineral aggregates with high clay content with high plasticity will lead to premature failure such as swelling due to clay-water interaction. The results do not show any swelling clays such as montmorillonite, so the materials are likely not experience excessive swelling and shrinking with varying climatic conditions.

Table 4.5: Summary table of material characteristics and properties

Material	**Grading**	**OMC (%)**	**MDD (kg/m3)**	**PI(%)**	**Mineral Phases**	**Class**
Laterite	Gap-Graded Within BSM Limits	8.8	2217.9	10.15	Quartz, Hematite Kaolinite, Gibbsite	G5
Kalumbila GCS	Poorly Graded Within BSM Limits	6.0	2325.5	NP	Albite low, Quartz, Microcline Muscovite, Ferro-richterite	G4/G5
Kasanshi CS	Well Graded Within BSM Limits	5.4	2336.9	NP	Calcite, Quartz, Dolomite Illite, Muscovite 3T Albite, calcian, ordered	G4/G5

4.4 INDIRECT TENSILE STRENGTH TEST

An indirect strength test was carried out in two approaches, the difference was the mixing regime where the additive is blended in water in Approach 1 and bitumen in Approach 2. Further, ITS was used to indicate water sensitivity through the determination of Tensile Stress Ratio (TSR in %). ITS_{WET} is conditioned at 24 hours under water at 25 °C. BSM and NME limits have been denoted by red and green horizontal lines, respectively. An upper line of each colour represents ITS_{DRY} limit and a bottom line per colour indicates ITS_{WET} limit. Refer to Figure 4.8 to 4.9.

4.4.1 Approach 1

Nano-Additive only

The influence of organosilane additive on ITS of the mixture is summarized by Figures 4.8-4.9. The stabilization was limited to organosilane addition only, to understand the tensile strength of specimens without bitumen emulsion and evaluate the nano effect on test specimens. Since these

specimens did not have any bitumen emulsion, their performance has not been benchmarked against BSM or NME classification limits.

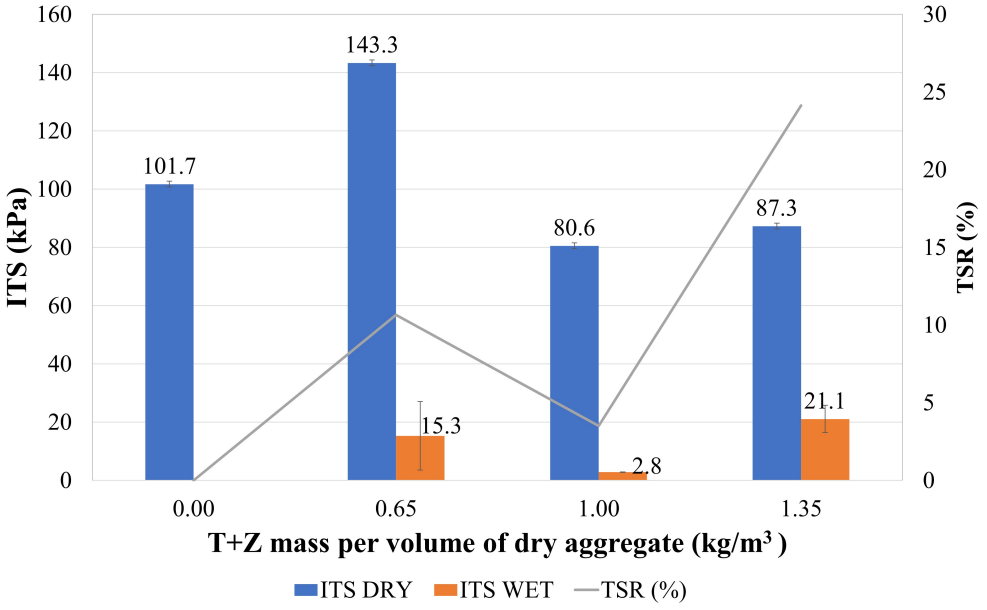

Figure 4.8: Laterite, Terrasil+ and Zycobond mixture ITS results

Figure 4.8 results indicate maximum ITS_{DRY} at 0.65 kg/m^3 Terrasil+ and Zycobond (T+Z) application rate. There is a steep decline in ITS_{DRY} from 0.65kg/m^3 to 1kg/m^3 followed by a very slight increase to 87.3 kPa at 1.35 kg/m^3. Therefore an optimum organosilane application rate based on dry specimens is 0.65 kg/m^3. However, the wet samples perform poorly and fail, the laterite base mix wet test specimens (at 0 kg/m^3) were destroyed while conditioned in water for 24 hours at 25 °C before testing (see Figure 4.9). ITS value of 2.8 kPa at 1kg/m^3 application rate indicates worst performance under wet conditions, also confirmed by low TSR value as seen. The nano-modified laterite samples show increased ITS_{DRY}, approximately a 40% increase from the base mix to the optimum mix.

Figure 4.9: ITS_{WET} laterite base mix test specimens disintegrated in water

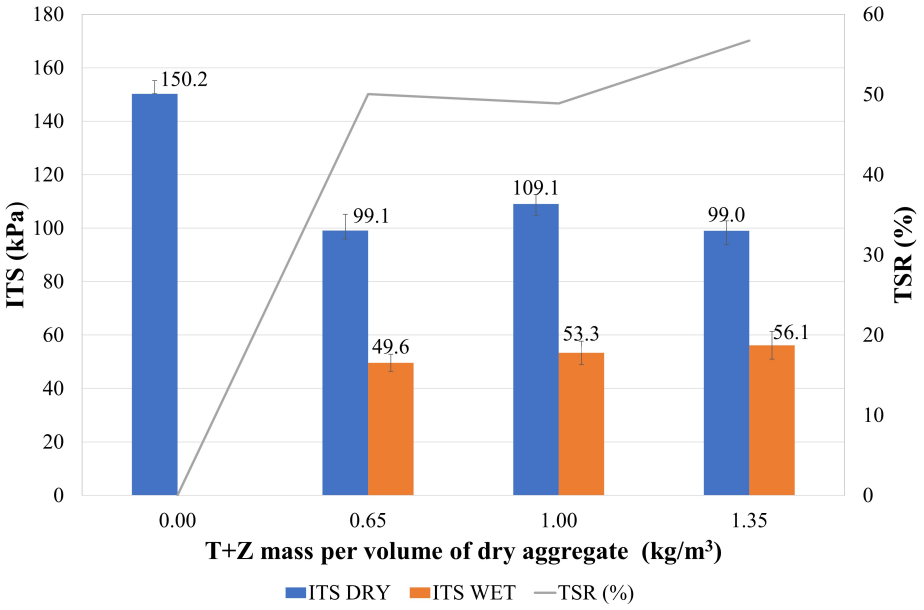

Figure 4.10: Kalumbila GCS, Terrasil+ and Zycobond mixture ITS results

Kalumbila graded crushed stone exhibited a higher ITS_{DRY} value (150 kPa) for an unmodified mix (See Figure 4.10). The introduction of the organosilane additives has led to an almost 50% ITS_{DRY} decrease from the base mix. At all organosilane application rates, there was no steep increase in ITS_{DRY} values, the maximum value is 109.1 kPa at 1kg/m^3 while the minimum is 99.0 kPa at 1.35 kg/m^3. This shows that the increase in organosilane content does not significantly influence Kalumbila graded crushed stone ITS_{DRY} due to minimum change in strength. The effectiveness of the nanosilane is highly dependent on the type of material being stabilized, therefore material characteristics may have likely influenced the result.

At 0 kg/m^3 Terrasil+ and Zycobond content (base mix), wet specimens fail and can not be tested further, shown in Figure 4.11. This indicates less water resistance by base mix samples and such a mix would be detrimental in regions with high rainfall. The addition of T+Z shows increasing ITS_{WET} from 0.65 kg/m^3 to 1.35kg/m^3 although the increase in strength with increasing T+Z content is minimal for this material.

Figure 4.11: ITS_{WET} Kalumbila GCS base mix test specimens disintegrated in water

In general, the increase in nanosilane content did not have a significant effect on ITS_{DRY}, however, it has increased the adhesion of the samples submerged in water since they did not disintegrate within 24 hours. The adhesiveness due to the nano effect is shown by Figure 4.11 where modified test specimens have not disintegrated in water like unmodified test samples. The TSR seems to increase with additive content, implying a decreasing moisture susceptibility with the increase. There is a minor decrease at 1.0 kg/m^3 but the general trend has a positive gradient.

In summary, the effect of the nanosilanes only, without the addition of bitumen in a mix has been reflected by the test specimens' water resistance since they remained intact in the water while unmodified samples failed. The increase in strength for dry test specimens did not remarkably increase with increasing additive content except for the laterite mix design at 0.65kg/m^3 application rate.

Pre-blended SS60 NME

The CSS60 is the most common product used with the organosilane due to its internal tails not reacting with the emulsion. However, the chemistry of the non-ionic (Zwitterionic) side has been altered, allowing SS60 modification with potential storage stability of up to a year. This explains the emulsification of cationic material (silane) with an anionic binder (SS60). The blend is best used while fresh because an irreversible reaction occurs destabilizing the emulsion with time. The modified SS60 emulsion, SS60NME, has been used for stabilization and ITS results are illustrated in Figure 4.12.

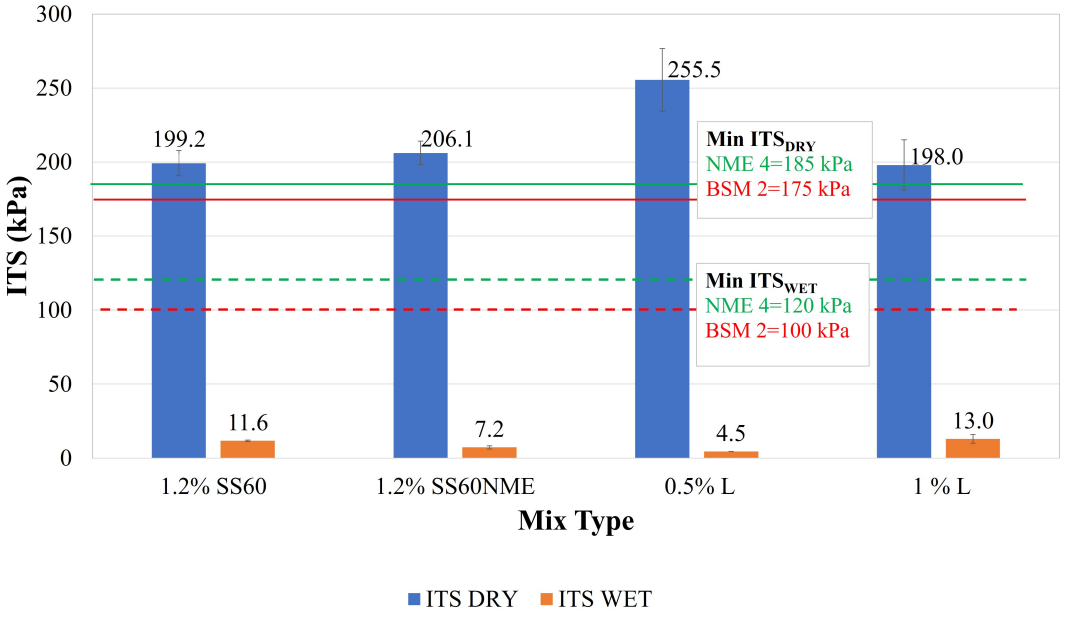

Figure 4.12: Laterite, Lime and SS60NME mixture ITS results

The influence of the organosilane effect on ITS results was evaluated by comparing the mixture with 1.2% SS60 NME with the base mixture (1.2% SS60) and other mixtures containing hydrated lime, as shown in Figure 4.12. The active filler purpose was to increase the binder dispersion, materials adhesion and further understand the behaviour of lime and NME treated material. ITS results were compared against BSM limits included in the TG2 and NME limits proposed by Jordaan and Steyn (2021).

All dry laterite test specimens at different application rates have similar average ITS$_{DRY}$ values except the mixture with 0.5% lime. Laterite samples show ITS$_{DRY}$ values exceeding BSM 2 and NME 4 minimum criteria. This enables a G4 or C4 equivalent performance to be achieved. The 0.5% lime mix has 255 kPa ITS$_{DRY}$ which meets the NME 3 minimum specification (229 kPa) and BSM1 limit. None of the wet specimens meet any set criteria, NME, or equivalent BSM. The lowest ITS for wet test specimens results from the same mix with the highest dry strength. This indicates that laterite soil stabilized with SS60NME does not result in a significant strength increase for dry specimens and also wet test specimens did not retain the dry strength at all.

The mixtures with hydrated lime were stabilized with 1.2% SS60NME, it is probable that the 0.5% lime was an optimum filler content yielding a good performing mix since ITS increased by approximately 50%. Laterite soil does not seem to perform well in wet conditions, indicated by the wet samples. Therefore, it would need to be used as a base or subbase layer to avoid exposure to

rainy conditions which would cause significant water damage.

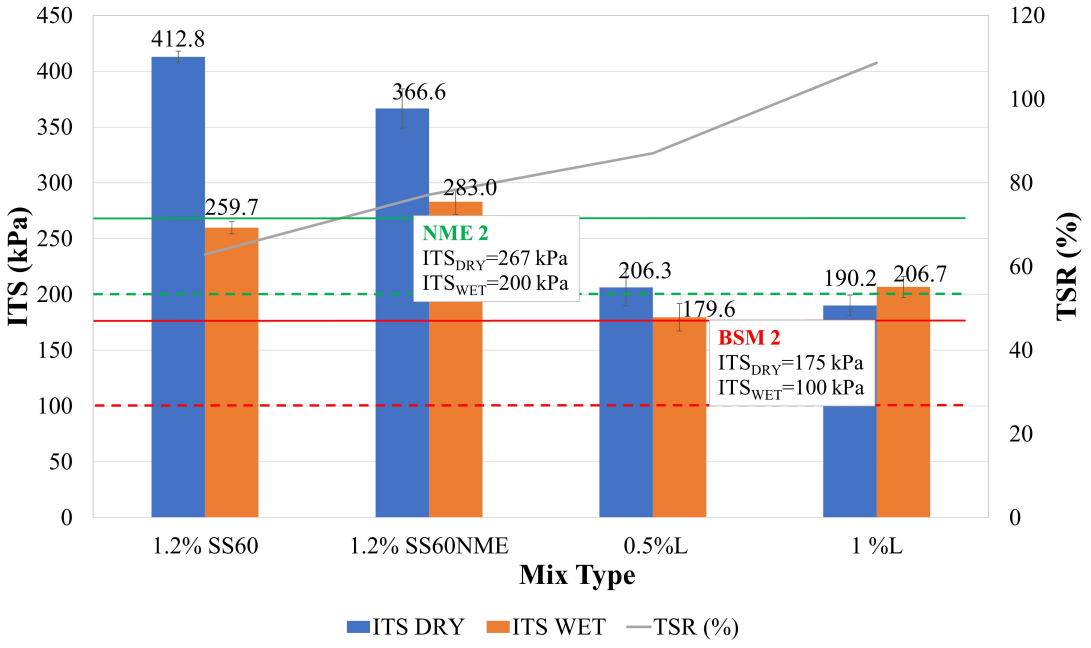

Figure 4.13: Kalumbila GCS, Lime and SS60NME mixture ITS results

Figure 4.13 summarizes ITS results from Kalumbila GCS stabilization using SS60NME. The dry specimens of the control mix (1.2% SS60) have significantly higher strength (412.8 kPa) compared to the NME mix with 366.6 kPa ITS$_{DRY}$. These meet BSM 1 (225 kPa) and NME 1(282 kPa) minimum specifications, indicating that the mixture is of high quality and suitable for use in upper pavement layers sustaining heavy traffic. Wet specimens from both the control mix and the nano-modified mix also meet the BSM 1 and NME1 specifications maintaining that the modified mixture can potentially offer performance typical of G1 or C1 material.

It is of interest that the ITS$_{WET}$ results of 1.2% SS60NME mix are sufficiently higher than that of the control mix by 23 kPa difference, about 9% strength difference. This implies that the additive in the SS60NME has led to some moisture resistance and increased adhesiveness, resulting in a higher ITS$_{DRY}$ value (283 kPa).

The addition of lime to the Kalumbila GCS mix, stabilized with SS60NME has not produced superior results than the control mix or the 1.2% SS60NME mix without lime. Lime addition leads to a decrease in dry specimen strength, a 16 kPa decrease from 0.5% lime content to 1%. However, there is somewhat an increase in the strength of wet test specimens from 179.6 kPa to 206.7 kPa. Both hydrated limes stabilized mixtures meet ITS$_{DRY}$ and ITS$_{WET}$ BSM 2 limits. The 1% lime stabilized mix wet samples meet the NME2 strength limit(200 kPa).

TSR increases with increasing lime content, the higher value being 108.7%, denoting that conditioned specimens have higher strength than unconditioned test samples. In wet regions, the material would perform much better using this mix design, though some durability tests would be necessary to ensure it sustains traffic and environmental conditions for a longer service period.

Unexpectedly, it is evident that lime stabilization results in low ITS_{DRY} and ITS_{WET} values in mixtures with NME's for this tested material. According to Ebels and Jenkins (2007), active filler on crushed rock BSM leads to higher cohesion levels and strength values, NME stabilized materials behave contrary to that proposition. This shows that NME stabilized materials cannot be regarded as BSM's, therefore their performance should not be entirely predicted based on BSM's but actual laboratory and field testing is necessary.

Modified CSS60

A conventional CSS60 was modified using both Terrasil+ and Zycobond blend at different application rates. Figure 4.14 shows ITS results from laterite stabilization. There is no significant strength increase from the control mix to the 0.65kg/m^3 and 1.00 kg/m^3 dosage, both contents have a similar ITS_{DRY} values of averagely 229 kPa. Therefore, the 0.35 kg/m^3 dosage increase did not influence the dry strength of the test specimens. ITS_{DRY} results at both 0.65 kg/m^3 and 1.00 kg/m^3 application rates meet the NME 4 and BSM 2 specifications whilst wet samples at these dosages do not meet any minimum requirements from both specifications.

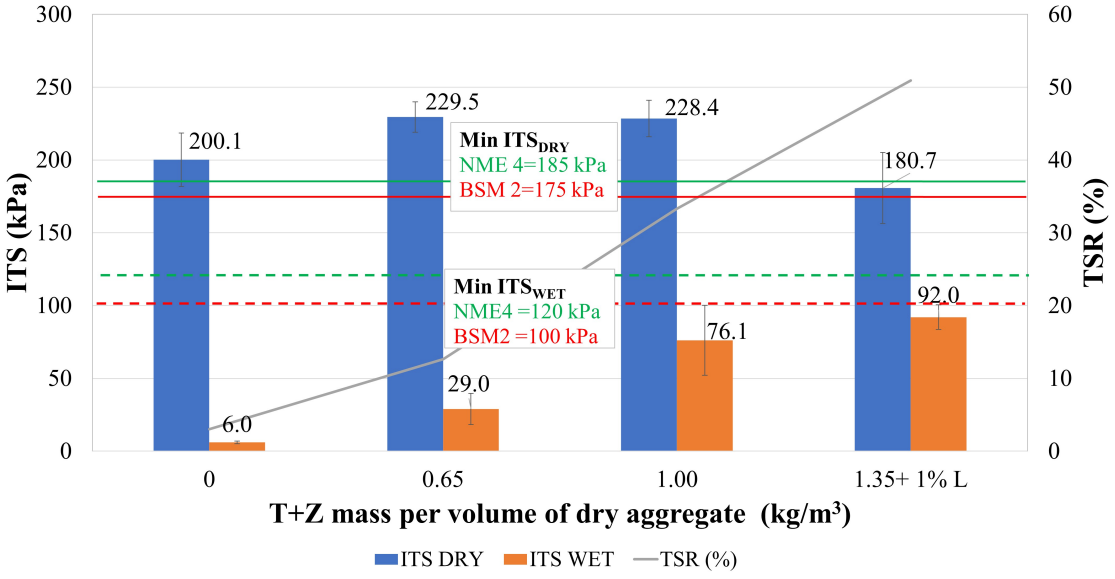

Figure 4.14: Laterite, Terrasil+ and Zycobond mixture ITS results

There is an approximately 60% ITS_{WET} increase from 0.65 kg/m^3 to 1.00kg/m^3 dosage, showing that the effect of increasing nanosilane content was significant on the wet specimens, unlike dry test specimens where the ITS_{DRY} results barely changed. These results indicate that the selected organosilane compounds are more effective on samples submerged in water for the chosen mix design and material type. Gauging treated wet samples against the control mix shows a significant strength improvement from 6kPa at 0.65kg/m^3 to a maximum of 76.1 kPa at 1.00kg/m^3. The additive has contributed to the bond strength of the bulk material such that it does not disintegrate in water.

The one mix design shown in Figure 4.14 has 1% hydrated lime and 1.35 kg/m^3 of Terrasil+ and Zycobond blend. The introduction of lime into the mix has led to about 50kPa decrease in ITS_{DRY}. This behaviour has been noted in previous mixtures and can probably be attributed to underlying chemical complexities occurring between lime, organosilane, and bitumen emulsion. Dry specimens in this mix design meet the BSM 2 limits but not NME4 limits. Wet test specimens have an increased strength though it does not meet any NME4 or BSM 2 limits for wet samples. This improvement may be due to the effectiveness of NME's in exhibiting resistance against water. The TSR has an increasing trend at 0 kg/m^3 to about 50% at 1.35kg/m^3 which does not meet NME 4 limit (65%).

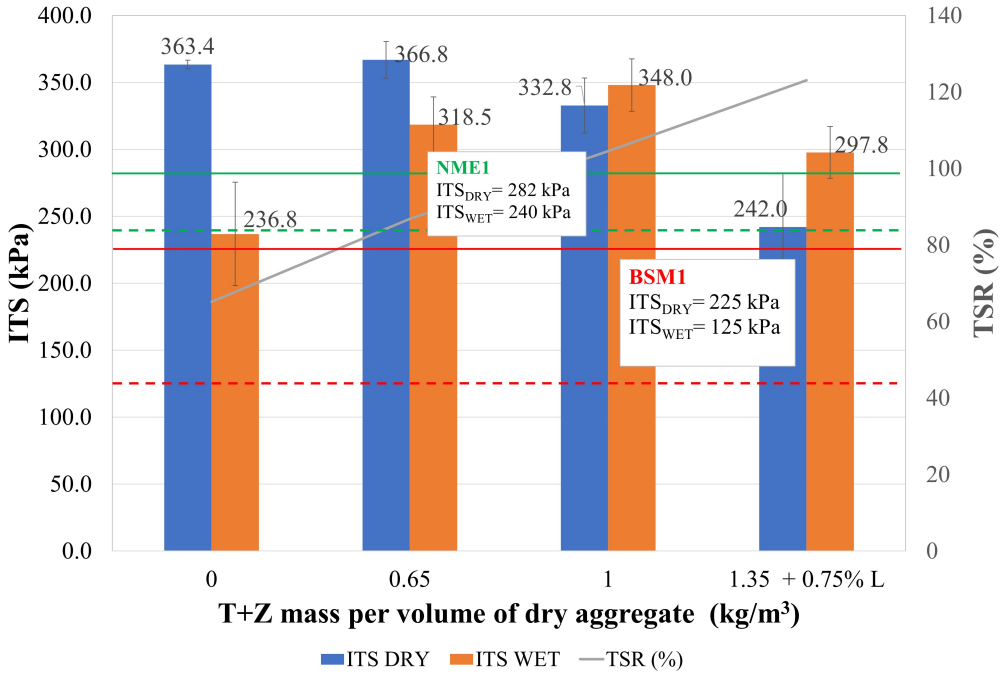

Figure 4.15: Kalumbila GCS, Terassil+ and Zycobond mixture ITS results

Kalumbila GCS ITS results are presented in Figure 4.15. The selected binder in this mix design

is an unmodified CSS60. The organosilane contents include 0 kg/m^3, 0.65 kg/m^3 , 1.0kg/m^3, and 1.35 kg/m^3 which also had 0.75% lime. All ITS$_{DRY}$ results meet both BSM1 and NME 1 minimum requirements except a mix design with 0.75% lime. All ITS$_{WET}$ results meet the BSM 1 and NME 1 limits though the control mix wet samples do not meet NME 1 limit (240 kPa) by a very small margin. The performance offered by this mix design is typical of high-quality materials such as G1.

The 0.65 kg/m^3 dosage is an optimum dosage rate due to the highest performing mix amongst others, high ITS$_{DRY}$ values can indicate a brittle material susceptible to cracking. It is essential to work with values around 300 kPa or slightly below to avoid premature cracking from brittle materials. The influence of the nano additive is visible again in wet samples due to a 35% ITS$_{WET}$ result increase from 236.8 kPa from the control mix (0 kg/m^3). Increasing Terrasil+ and Zycobond content leads to an increase in ITS$_{WET}$ values except for a mixture containing 0.75% lime. This is seen until 1.0kg/m^3 dosage whose test specimens recorded an average ITS$_{WET}$ of 348 kPa. Therefore the maximum effect is seen on wet samples than dry test specimens. Interestingly, the lime stabilized wet specimen has performed much better than a dry one with an ITS strength of 297 kPa, a 23% difference in dry and wet strength, the mix design with 1.0 kg/m^3 also has a similar trend.

Unpredictably, in terms of strength improvement, 0.65 kg/m^3 dosage does not result in higher strength, ITS$_{DRY}$ has increased by 3.4 kPa to 366.8 kPa which is minimal. A different trend occurs with increasing the organosilane content where the ITS$_{DRY}$ value decreases to 332.8 kPa from 366.8 kPa. The organosilane effect continues to be more evident in wet specimens than dry specimens regarding strength improvement. The ITS results are much higher than previous mixtures containing both SS60 and SS60 NME, this maintains that selected organosilane compounds favour the CSS60 emulsion due to their internal tails not reacting with the emulsion. The cationic material is more stable and the surfactant in the emulsion creates a neutral environment in which the organosilane thrives. With all additives, Kalumbila GCS performs best, in both dry and wet conditioning.

4.4.2 Approach 2

The additive content in the second mixing approach was calculated as a percentage of the cross bitumen emulsion content. Laterite ITS results from mixing approach 2 are summarised in Figure 4.16. Increasing the Terrasil+ content leads to a slight increase in strength, however, increasing the dosage beyond 0.5% leads to a decline in ITS$_{DRY}$ as seen at 1% dosage results. Terrasil+ does not seem to increase the laterite material strength significantly, it is seen that the control mix has average ITS$_{DRY}$ of 200.1 kPa yet 0.25% and 1% Terrasil+ dosage results in a strength value close

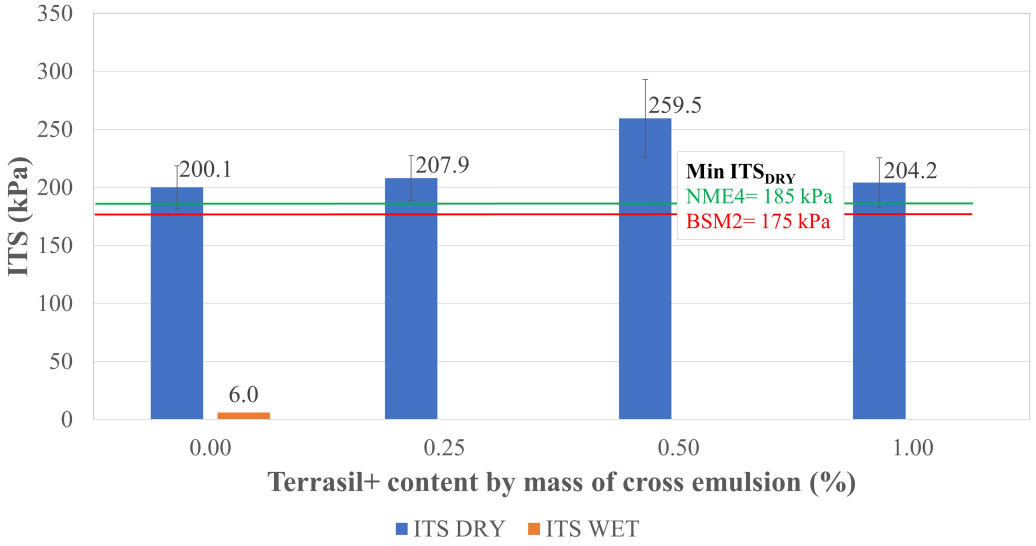

Figure 4.16: Laterite and CSS60NME ITS results

to that of the control mix. The maximum ITS_{DRY} value (259.5 kPa) emanates from a mix with 0.5% Terrasil+ content. It is evident that too little and too much nanosilane content is not an ideal application rate but it is important to determine the optimum content as seen in Figure 4.16.

All the dry test specimens meet the BSM2 and NME4 specifications however, all NME treated materials wet samples fail. NME 4 materials are suitably stabilized but do not offer high-quality performance against high tyre pressures. In this approach, the bitumen emulsion seems to suffocate the nano additive since no strength improvement or adhesion is present in wet samples, they just disintegrate upon being removed out of the water bath from which they were in for 24 hours at 25 °C.

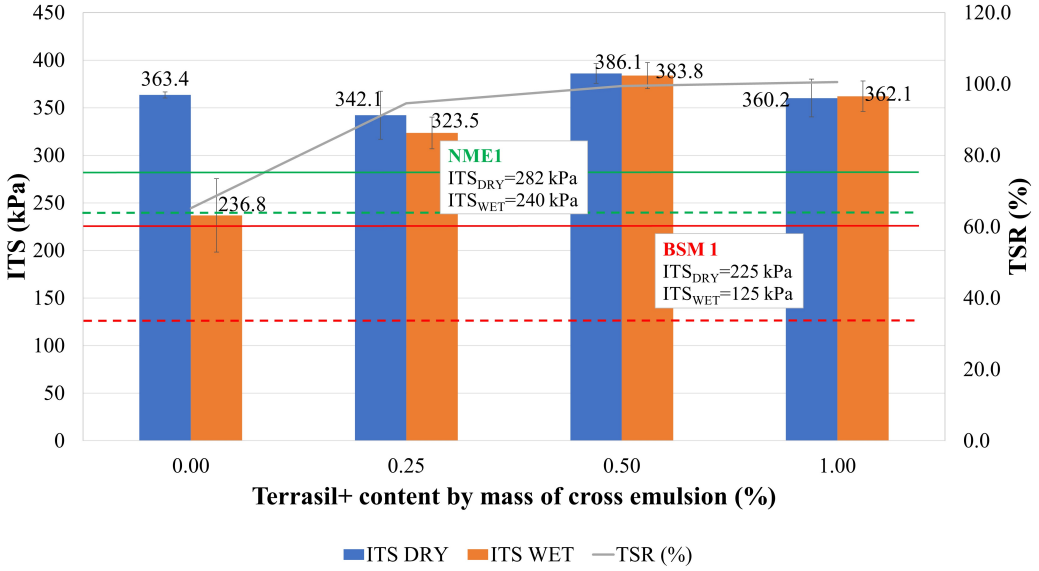

Figure 4.17: Kalumbila GCS and CSS60NME mixture ITS results

Kalumbila GCS responds sufficiently well to a nano-modified CSS60 as shown in Figure 4.17. All dry specimens meet the minimum requirements of both BSM1 and NME4 specifications. The maximum ITS_{DRY} value (386.1 kPa) recorded is at 0.5% Terrasil+ content, which is slightly higher than the average ITS_{DRY} value of the control mix by 22.7 kPa. Terrasil+ content increase does not translate to an increasing ITS of treated specimens, this is seen by a decline in dry strength at 0.25% followed by an increase at 0.5%. It is apparent that within a range of little organosilane content lies an optimum amount as illustrated by Figure 4.17.

All treated specimens ITS_{WET} values meet BSM1 and NME 1 specifications with average strength at 1% being slightly higher than ITS_{DRY}. Generally, almost all treated wet samples retain their dry strength. ITS_{DRY} values are all above 300 kPa, which is a good sign showing the effectiveness of the nanosilane compound, this may also indicate a brittle mixture prone to cracking.

The increasing Terrasil+ content leads to an increase in ITS_{WET} values except at 1.0% nanosilane content. This shows that the nanosilane is active against water and resists it very well, the TSR value at 1.00% Terrasil+ content is 100.5% and 99.4% at 0.5% Terrasil+ content, which exceeds the NME 1 limit set at 85%. The good performance of this mix can also be attributed to the material type and quality, compatibility of silane and bitumen emulsion, and dispersion levels. Kalumbila GCS responds well to the second mixing approach in which the silane is dispersed in the bitumen emulsion.

The increase in strength of treated wet specimens compared to the control mix (236.8 kPa) is about 20% at the optimum Terrasil+ content. The environment was ideal for the nanosilane to thrive and exhibit hydrophobicity. Figure 4.18 presents a broken sample which shows that water did not penetrate the sample more than 10 mm after being submerged in water for 24 hours as per ITS specification.

Figure 4.18: Treated wet specimens unaffected by water (very low penetration).

Kansanshi CS SS60NME Mix

SS60NME was used as a binder Kansanshi crushed stone stabilization with ITS results are presented in Figure 4.19. All dry specimens treated with Terrasil+ and lime have ITS lower than the control mix only modified with a conventional 1.2% SS60. The preblended SS60NME did not improve both the dry and wet ITS, decreasing to 382.7 kPa from 481.7 kPa for a control mix. The addition of 0.5% lime decreases the strength of dry specimens further, as seen on previous mixtures with both laterite and Kalumbila crushed stone. Increasing lime content to 1% slightly increases the ITS value of dry test specimens, it does not result in a significant strength change where it has been used in silane treated materials.

Nanosilane and lime-treated wet test specimens have low strength values compared to the base mix, a 0.5% lime and SS6ONME treated mix show 143.8 kPa ITS value, which is 226 kPa from the base mix and 44.3 kPa from the 1.2% SS60NME treated samples.The 1% lime-treated wet samples have the lowest ITS value of 128 kPa.

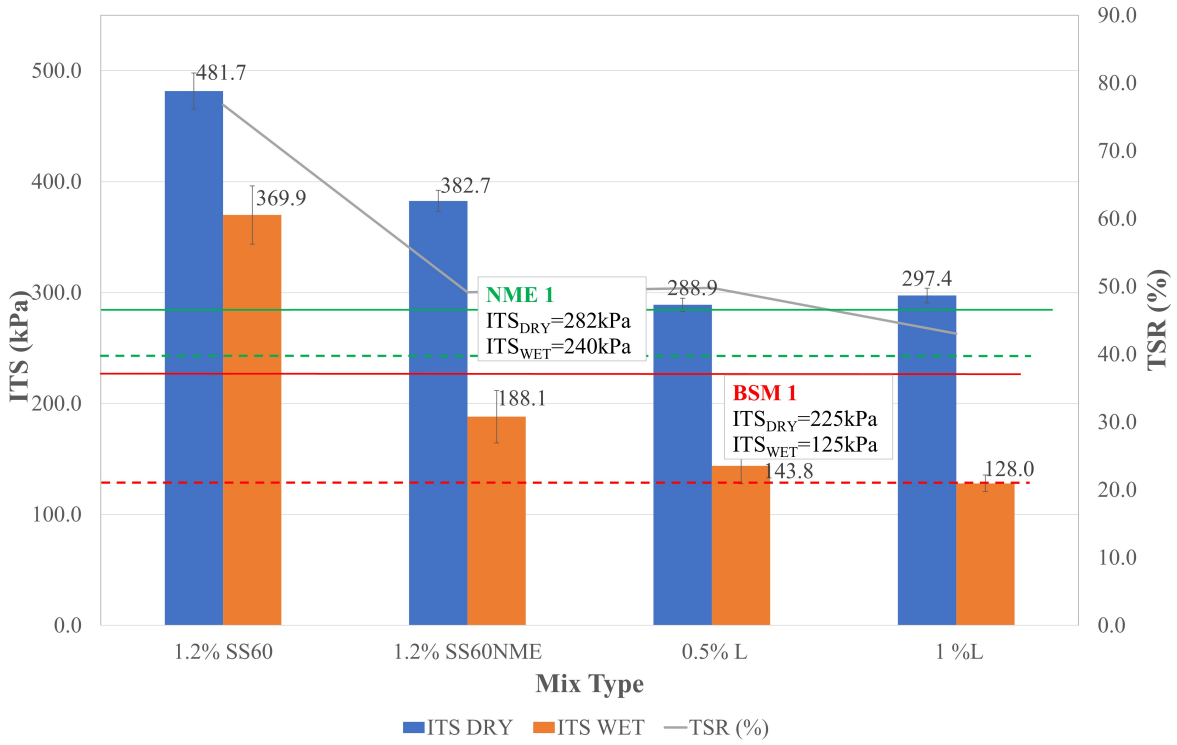

Figure 4.19: Kansanshi CS and SS60NME mixture ITS results

All ITS$_{DRY}$ values meet the NME 1 and BSM1 minimum specifications and hence they can offer a high-quality performance typical of high-quality G1 materials. This design applies to base layers subjected to high tire pressures such as mining environments or areas subjected to massive loading, given the durability of materials allows long-term service. The wet specimens all meet BSM 1 specifications, but not NME 1 limits, TSR values for almost all treated materials are below 60% which is less than 85% for NME 1 materials.

In summary, Kansanshi crushed stone was not sufficiently stabilized by lime, although ITS values seen are adequate for design, organosilane content and blends with varying lime content in the preblended emulsion did not result in a remarkable strength increase.

Kansanshi CS CSS60NME Mix

Figure 4.20 shows the Kansanshi crushed stone ITS results. The second mixing approach was selected for this material type (crushed stone) since the Kalumbila GCS performed remarkably well under mixing approach 2. Terrasil+ was the only chosen additive, the soil stabilization and dust suppressants have different functionalities and, therefore, application rates.

All ITS_{DRY} results meet NME 2 (267 kPa) and BSM1 minimum specifications but not NME 1. The maximum ITS_{DRY} of 377.7 kPa is seen from the 1% Terrasil+ content, though this indicates a very brittle mix that would easily crack. Therefore, 0.5% Terrasil+ content could be considered optimum dosage due to suitable ITS results representative of a good mix. Interestingly, increasing Terrasil+ content for Kansanshi stone results in decreasing ITS_{DRY} values. The control mix shows a 407.0 kPa dry strength while 0.25% Terrasil+ content shows 325.7 kPa. The increase in Terrasil+ content starts increasing ITS_{DRY} value at 0.5% to 1% application contents, 1% Terrasil+ content results in 377.7 kPa.

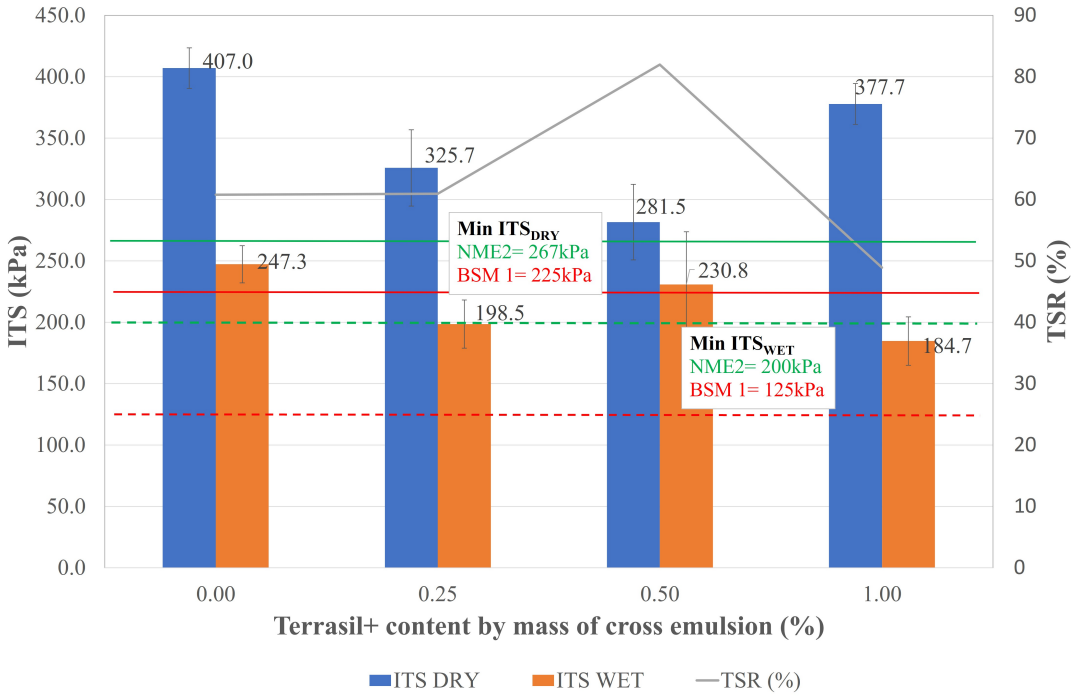

Figure 4.20: Kansanshi CS and CSS60NME mixture ITS results

Wet specimens also meet all minimum specifications set for both NME2 and BSM1, except the average ITS_{WET} at 0.25% Terrasil+ content by a marginal amount. Moisture susceptibility in treated samples with reference to TSR increases from 60% at 0.25% Terrasil+ content to 82% at 0.5% Terrasil+ content, then plunges down to 49% at 1% Terrasil+ content.

The control and modified mixtures have high ITS_{DRY}.However, the control mix seems to be highly susceptible to moisture damage relative to the mix at 0.5% additive content. This indicates that 0.5% additive content is an optimum content in terms of ITS and moisture susceptibility as shown by TSR values.

4.4.3 Comparison of Approach 1 and 2

Only CSS60 treated samples are considered in this case. ITS_{DRY} values are relatively high in Approach 2, though the strength difference is not a significant amount, the maximum difference of 31.1 kPa occurs at 0.5% application rate, the average strength difference is 25.4 kPa (see Figure C.1, Appendix C). However, the main difference in mixing regimes is visible on wet ITS specimens, those compacted based on Approach 2 fail before testing while those from Approach 1 do not fail but perform poorly upon testing. Therefore, in Approach 2 mix, bitumen suffocated the nanosilane, precluding water-repelling and adhesion features of the nanosilane additive. Laterite ITS_{DRY} from both mixing approaches meet NME 4 and BSM 1 specifications but not any higher limits, therefore changing the mixing regime did neither relegate the mix to a lower performance class or higher such as BSM1 or NME 1. The regime change has however had a significant effect on wet samples, in which the adhesion of the sample was reduced disintegrating test specimens while in water.

Kalumbila GCS perform sufficiently well, it has a satisfactory response to the NME, all ITS_{DRY} values exceed 300 kPa strength except those treated with 1% lime from Approach 1. However, the maximum ITS_{DRY} of 386.1 kPa occurred in Approach 2, the maximum difference in strength is 53.1 kPa occurring at 1% Terrasil+ content. Both mixing approaches perform well probably because the material type is of high quality than laterite and that the nanosilane thrives in a cationic binder material.

Kalumbila GCS wet samples perform better in Approach 2 though the strength difference is minimum, around 40 kPa at 1% nanosilane content and 20 kPa at 0.5% nanosilane content. Blending organosilane in bitumen performs better for crushed stones indicated by their high ITS_{DRY} and ITS_{WET} values. Kalumbila GCS strength results both mixing regimes meet both BSM1 and NME1 specifications. The mixing approach does not seem to have a very significant influence on mix performance per this material type, all test samples meet strength limits. Figure C.2 and C.3 Appendix C illustrate Kalumbila GCS ITS_{DRY} and ITS_{WET} results from both Approach 1 and 2.

The effectiveness of the nanosilane incorporation mechanism is influenced by factors such as material type and available equipment. In some applications, directly incorporating it into the mix is a much easier method because of known parameters such as application rate, OMC, test evaluations, and simulations. By incorporating it into the bitumen (Approach 2) there are obstacles such as storage stability and shelf life where organosilane reacts to itself in the elongated presence of oxygen.

4.4.4 Statistical Analysis

A statistical approach is followed to determine the organosilane influence on the strength of dry and wet test specimens in all materials. The quantitative method allows checking if there occurs any significant statistical difference with a variation of one parameter, organosilane content. Therefore one way ANOVA is used. A p-value is a statistical parameter typically set at 0.05, below which resulting values are statistically significant. It indicates how the independent variable; organosilane content influences ITS strength.

The p-value was determined for each mixture category and compared against the limit of 0.05. There are higher values of the p-value for dry test specimens and lower values for almost all wet test specimens, indicating that dry samples are least affected by increasing organosilane content. CSS60NME modified Kansanshi CS wet samples, CSS60NME modified Kalumbila GCS dry samples, and CSS60NME modified laterite dry samples are beyond 0.05 indicating that there is no significant statistical difference. This implies that the increase in organosilane content has the least influence on the ITS strength of mentioned mix categories. The low p-values shown for most mixture categories provide support for the influence of organosilane content on ITS. Generally, increasing organosilane content increases ITS_{WET} results in most mix designs, hence the smallest p-values shown in Figure 4.21.

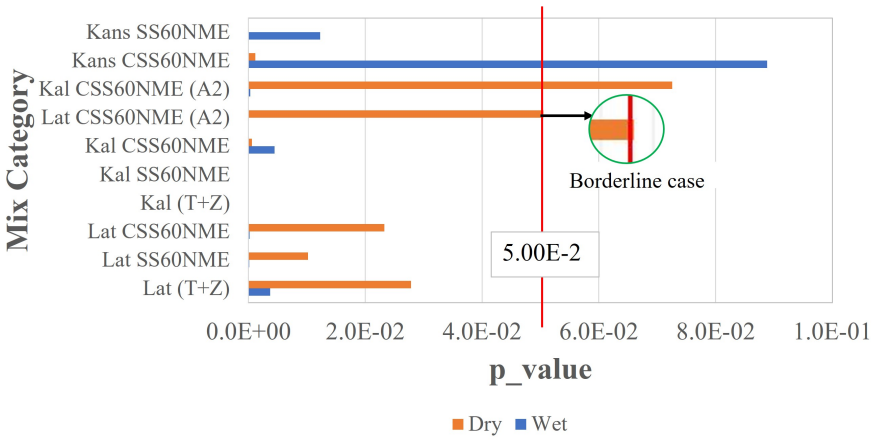

Figure 4.21: p - values from influence of organosilane content on dry and wet ITS samples

4.5 HIGH PRESSURE PERMEABILITY

The performance of NME treated material was studied as a function of organosilane concentration added at variable application rates. The ITS testing indicates moisture susceptibility of tested samples through TSR (%), it is evident that organosilane effect is more pronounced in wet test

specimens strength improvement than dry test specimens. Although the HPP test was initially developed for asphalt layers, it allows understanding of permeability of materials, in this case NME treated materials. The selected testing pressure was kept constant throughout the test as 100 kPa.

4.5.1 Laterite

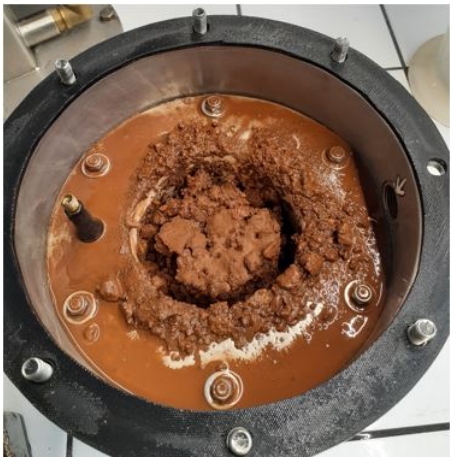

Figure 4.22: Laterite HPP results at 100 kPa

The high pressure permeability test was applied on laterite aggregates and the test fails as seen in Figure 4.22. Increasing the maximum applied pressure beyond 100 kPa would have similarly destroyed the treated sample. The laterite samples were treated with 1% Terrasil+ modified CSS60. The HPP is an aggressive test hence the laterite results. Being an unbound granular material, it fails to be resistant to water ingress at the set pressure. This indicates that laterite soil is not suitable as a surfacing layer, it could have the potential as a base layer or subbase layer, as long as it has a top protective layer.

Laterites are generally very permeable, especially those with pseudo sands. Haselsteiner *et al.* (2014) mention that laterites contain highly permeable layers beneath surface clay layers, evident through massive water loss during in situ water pressure tests. Their permeability ranges from k= 10^{-4} m/s to 10^{-11} m/s. This explains the behaviour of the selected laterite under HPP, it is very permeable at 100 kPa and disintegrates during the permeability test as illustrated in Figure 4.22.

4.5.2 Kalumbila GCS

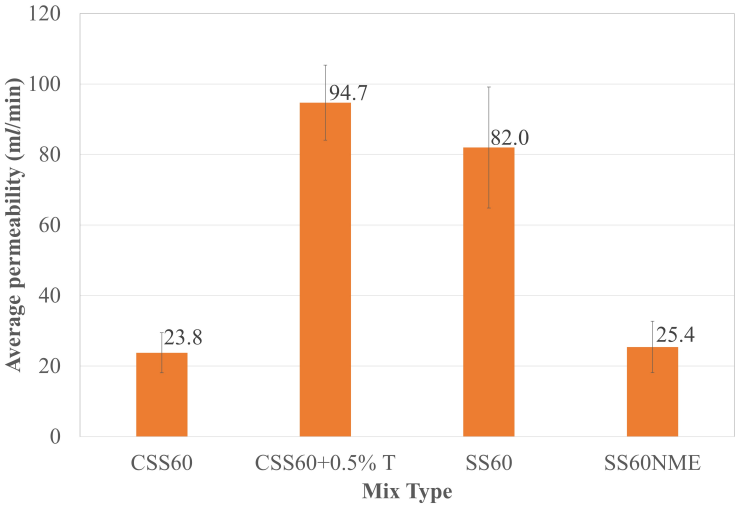

Figure 4.23: Permeability results of Kalumbila GCS at 100 kPa

Figure 4.23 illustrates the HPP results of Kalumbila GCS. The modified CSS60 shows the highest average permeability amongst all mix types, while the untreated CSS60 shows the minimum permeability amongst all mix types. The 0.5% Terrasil added in the CSS60 does not lower the permeability of the sample but increases it from 23.8ml/min to 94.7 ml/min, this might be due to other factors such as the air voids, presence of finer fractions without which the permeability increases.

The use of SS60NME has results in a significant permeability decrease, a mix with an untreated SS60 emulsion shows 82.0ml/min while the treated one shows 25.4 ml/min, indicating a 224.4% permeability difference. SS60NME shows an extremely low permeability compared to the control mix, therefore it shows that the nano additive is active in making a mix relatively impermeable. The CSS60 and SS60NME modified mixes show similar and lowest permeability amongst all the mix types. This indicates low voids space and the presence of an optimum grading.

4.5.3 Kansanshi CS

Kansanshi CS has the highest permeability when treated with a conventional CSS60 (see Figure 4.24), the highest error bar may also represent some test inconsistencies or material deficiencies regarding some finer fractions of finer aggregates, subsequently, increased void space and permeability. Adding 0.5% Terrasil + significantly lowers permeability to 101.3 ml/min. It is crucial to note that the permeability of the CSS60 treated Kansanshi CS mix is also very high. The SS60 emulsion shows the lowest average permeability of 42.9ml/min while SS60NME shows an increased average

permeability. Using CSS60 and organosilane blend seems to be effective in lowering permeability per the tested material while the SS60 NME is not effective.

Given both crushed stones have been tested using the same binders and additives, permeability issues stem from aggregate materials. The results show different trends on both materials when using modified binders, the HPP results are therefore inconclusive.

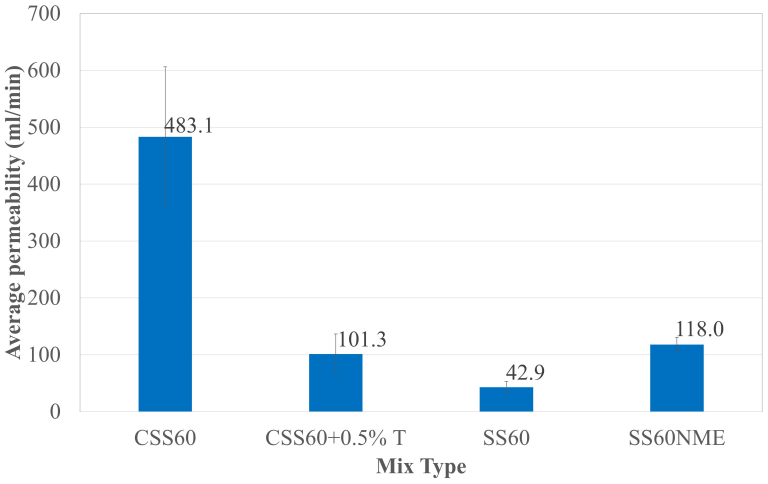

Figure 4.24: Permeability results of Kansanshi CS at 100 kPa

4.6 MINERALOGY: XRD TREATED MATERIALS

Mineral phases of untreated and treated samples were identified, compared against each other to determine if the organosilane addition influences the mineral phases, the occurrence of new mineral phases, or improvement of existing ones. Nineteen test specimens, three of which are untreated control samples were selected for testing are defined in Appendix B, Table B.1.

4.6.1 Laterite

Untreated laterite(sample 1) did, however, show the presence of a set of small peaks for samples 3, 4, 5, 6, and 7 but not in sample 1. It is as if these peaks appeared in the processed samples and allude to the presence of new phase(s). Red squares illustrate the position of these peaks in Figure 4.25. This effect remains particular to samples of group 1, as no such effect could be observed for the other two groups (Kalumbila GCS and Kansanshi CS). These extra peaks were difficult to assign a mineral phase and remained unidentified and marked by a black arrow. Ultimately, trying to assign a mineral phase to these peaks, yields unconvincing results which could be considered questionable. The extra phases were: Muscovite, Gismondine, Anorthite and Laumontite. Anorthite is commonly

found in soil samples, so it would be considered a possible match if it were not for the intensities not matching the measured peaks

Questionable matches occur if some of the lines indicated by the reference patterns do not coincide with any measured peaks, then the proposed phase is questionable. Unfortunately, in such a case, no better match is determined.

The x-ray diffraction analysis shows that all treated and untreated laterite samples consist of quartz (SiO_2), kaolinite-$Al_2Si_2O_5(OH)_4$, hematite (Fe_2O_3), and gibbsite ($Al(OH)_3$). The dominant mineral is quartz followed by the clay component, kaolinite. All the mentioned minerals are common across all laterite samples. However, all test samples (4 and 6) without nanosilane have traces of muscovite ($KAl_3Si_3O_{10}(OH)_2$), predicted to have Panasqueira, Portugal origin. Muscovite has been identified,its significant distribution in a material precludes that material from being considered suitable for road construction due to its problematic nature.

Sample 3 (SS60 NME treated laterite) and 5 (0.5% Terrasil+ and Zycobond treated laterite) do not have traces of the muscovite, the presence of nanosilane may have contributed to the alteration of mineral structures leading to no muscovite mineral detected. Micas are diverse and some flaky with poor cleavage hence their absence in a bulk material influences material strength.

Sample 7 (CSS60, Terrasil+ and Zycobond treated laterite) further shows different minerals identified as gismondine and anorthite. These minerals availability and identification may partly be due to the chemical compatibility between the nanosilane and CSS60, leading to an effective NME. Literature has mentioned that effective stabilization using nano silanes is also dependent on silica content in the material. Laterites have silica (quartz) as a dominating mineral phase, therefore all these factors favor a suitable and effective NME treatment.

4.6.2 Kalumbila GCS

Mineral distribution and crystallographic phases have an impact on the strength of the material. Kalumbila GCS has the dominant mineral as albite low ($Na(AlSi_3O_8)$ in the untreated specimen, all treated test specimens show a similar trend with different intensities as reflected by the XRD pattern. Additional samples common in all materials include ferrorichterite, syn ($Na_2CaFe_5Si_8O_{22}(OH)_2$), muscovite 3T - ($KAl_{2.89}Si_{3.11}(OH)_2O_{10}$), microcline ($KAlSi_3O_8$) - from Pike's Peak batholith, quartz (SiO_2). The mineral phases with the highest intensities at close 2θ ranges are quartz and albite low, although albite low has a significant distribution within the 2 θ range. There is also a relatively high mineral distribution of microcline within a notable 2θ range.

Traces of problem minerals such as swelling clays will not severely influence material strength,

the absence of clayey minerals denotes no swelling and plasticity, consistent with Atterberg limits. Identified minerals, such as microcline feldspar, a common rock-forming mineral phase whose presence does not lead to premature pavement failure. Microcline albite and quartz are mineral phases normally found in road construction materials. XRD patterns for all treated Kalumbila GCS are shown in Figure B.6, Appendix B.

Generally, the XRD patterns of the control sample and all treated soil samples from 8 to 13 are similar. The mineral phase distribution and intensity are close regarding XRD data. There are traces of muscovite along the entire 2θ range, it seems to have the least intensity amongst identified minerals. Nanosilane addition did not influence the availability of mineral phases or the identification of others uncommon to all samples.

4.6.3 Kansanshi CS

Kansanshi crushed stone test specimens have a similar XRD pattern as seen in Figure B.3, Appendix B. The most dominant mineral phase is calcite($Ca(CO_3)$). Other identified minerals include quartz SiO_2, dolomite $CaMg(CO_3)_2$, illite-2M1$(K,H_3O)Al_2Si_3AlO_{10}(OH)_2$, muscovite, vanadian barian - $(K,Ba,Na)_{0.75}(Al,Mg,Cr,V)_2(Si,Al,V)_4O_{10}(OH,O)_2$ and albite, calcian, ordered $(Na,Ca)Al(Si,Al)_3O_8$. All these minerals are identified throughout all samples with calcite having higher intensities within the 2θ range. The XRD patterns for all treated Kansanshi CS are shown in Figure B.7, Appendix B.

Traces of muscovite and illite are identified although muscovite has a much higher intensity than illite across the 2θ range. The absence of clay minerals in this type of material denotes no swelling and clay-related problems. Less content of low plastic clays is allowable in road construction materials. High mica content is a problem, however, if the muscovite mica is unevenly distributed within the entire material at low concentrations, the material may be considered for road construction. Traces of problem minerals do not signify a problem but a high concentration value indicates a potential problem in service.

Mineral compatibility with mix constituents is not only limited to organosilane application but also bitumen, bitumen adhesion is more effective on mica and quartz than alkali feldspar (Lyne *et al.*, 2013) such as microcline. However, concentration values of mica should be minimum to ensure durability of material in service. Dolomite and albite also occur in traces since they have very low intensities within the selected 2θ range. The effectiveness of NME stabilization is poor with carbonate rocks such as calcite, however, a suitable nanosilane that is compatible with calcite can be applicable. Added nanosilane and lime do not seem to influence available mineral phases in the sample since all materials have similar diffraction patterns.

4.6.4 Mineralogy and Performance

Gao *et al.* (2018) point out that water is the root cause of debonding at the mineral-bitumen interfacial region, the mineral type also influences the extent of debonding. The mineral-water-bitumen interface bond strength of microcline and albite showed to be stronger than that of quartz and calcite weakened by permeated water (Gao *et al.*, 2018). The degree of weakness is also influenced by molecular structure and water-mineral adhesion force.

Laterite has a higher percentage of quartz. The ITS_{WET} specimens exhibited a poor performance (loW values) which indicated weaker adhesion force with water molecules. There are low atomic interacting forces between quartz and bitumen, the organosilane addition barely influences quartz content because high-intensity peaks reflect across all treated samples but organosilane addition seemed to increase wet samples strength (see Figure 4.14), indicating increased adhesion due to reduced water ingress.

Albite was a dominant mineral in Kalumbila GCS. In some instances, such as the CSS60NME mix, wet specimens retained ITS_{DRY}, leading to a TSR (%) exceeding 100%. A significant distribution of microcline and albite in Kalumbila is partly responsible for the stronger atomic interactions with bitumen. Organosilane treated compatible bitumen emulsion such as CSS60 preserves bond strength and improves the force of adhesion. Water ingress into an untreated mineral-bitumen aggregate would weaken the bond, but the introduction of the silane repels the water(see Figure 4.18). High ITS_WET values illustrative of this behaviour are shown in Figure 4.15 and 4.17. A cumulative effect of appropriate minerals and suitable organosilane leads to an increased material strength.

Calcite is a dominant mineral in Kansanshi CS, the mineral-water-bitumen interface had a higher adhesion force when compared to quartz. Gao *et al.* (2018) mention this may be due to unsymmetrical calcite molecular structure with calcium ions. High ITS_{DRY} and ITS_{WET} values implied a better bond strength which increased with organosilane addition at selected dosages.

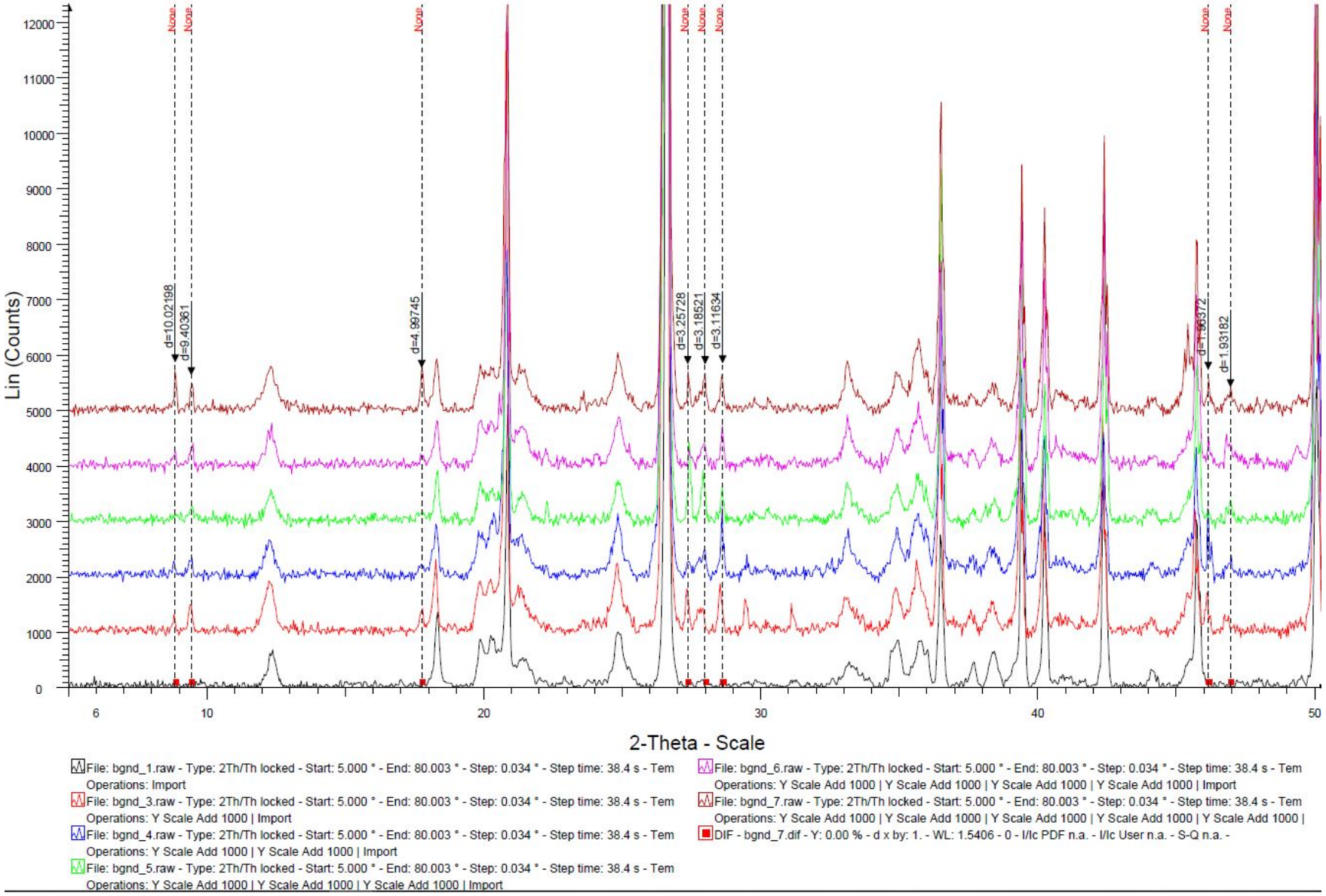

Figure 4.25: XRD pattern for treated and untreated laterite materials

4.7 TRIAXIAL TESTING

4.7.1 Shear Parameters

The shear parameters indicate the strength of materials and binder functionality. All treated specimens in mix designs are based on performance optimization from ITS results, an optimum mix design is used for triaxial test specimens. Although lime stabilized materials did not perform optimally from ITS results, it was decided to consider it for triaxial testing because some laterites may contain high plastic clays that would need lime modification. All crushed stone aggregates were stabilized with Terrasil+ and Zycobond modified CSS60.

Table 4.6: Summary of shear parameters from monotonic testing of all materials

Material	**Mix ID**	**C(kPa)**	ϕ°	**RC (%)**	$\mathbf{R^2}$	**m**	**b**
Laterite	L1	266.3	49.6	31.3	0.99	7.375	1446.5
	L2	221.4	44.3	68.9	0.96	5.643	1052.1
Kalumbila GCS	KL1	49.9	53.2	49.4	0.95	9.041	300.11
	KL2	51.7	54.5	49.2	0.99	9.749	323.08
Kansanshi CS	KS	136.5	44.2	77.8	0.99	5.592	645.77

The monotonic triaxial test summary in Table 4.6, for laterite treated with L1 (SS60NME and 1% Lime) yields a cohesion value of 266.3 kPa and 49.6 °friction angle. These parameters all meet BSM 1 specification requirements. Figure 4.26 shows a slightly different friction angle (49.3 °), because it has been determined graphically instead of mathematical equations provided in TG2. Regression lines on which these equations are based are provided in Appendix C, Figure C.4,C.5 and C.6. There are no published NME specification requirements for triaxial limits, so BSM limits detailed in TG2 will be considered as guidelines. The high cohesion value and adequate friction angle imply that SS60NME treated laterite would be a suitable base layer material given there is a sufficient cover against water.

L2(CSS60 and 0.5% Terrasil+) modified mix shows slightly lower shear parameters relative to L1, cohesion value decreased to 221.4 kPa and the friction angle is 44.3 °, these meet the BSM 2 limits. The retained cohesion for the 0.5% Terrasil+ modified mix is 68.9%, this is 37.6% higher than retained cohesion in the L1 mix. The effect of the nano additive against water ingress or moisture susceptibility is reflected by the higher cohesion value of this mix, water was unable to penetrate the sample extensively while in a water bath, preserving its cohesion. The retained cohesion value also meets the minimum BSM2 specification set at 65%.

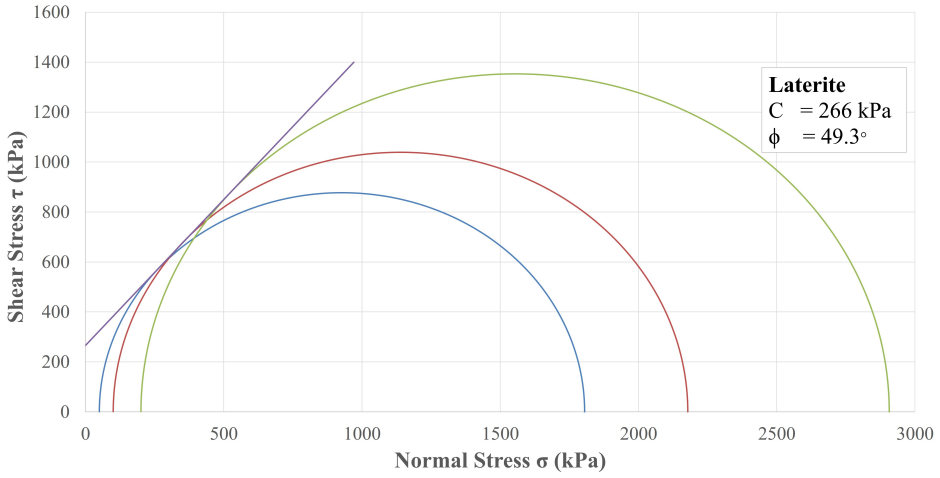

Figure 4.26: Mohr-Coloumb circles and failure envelope for L1

According to Paige-Green *et al.* (2015), the typical selection for laterite gravel based on shear parameters require a cohesion value greater than 85 kPa. However, values between 45 kPa and 30 kPa may also be acceptable given the friction angle exceeds 60 °. The criteria applies to low volume roads, haul roads selection criteria require high shear strength, haul truck tyre loading normally exceeds the allowable load capacity thus soils with low cohesion values and friction angles will result in an unstable base layer (Thompson, 1995). Therefore, 226 kPa treated laterite cohesion and 49.3 °friction angle can be considered suitable for a haul road base layer.

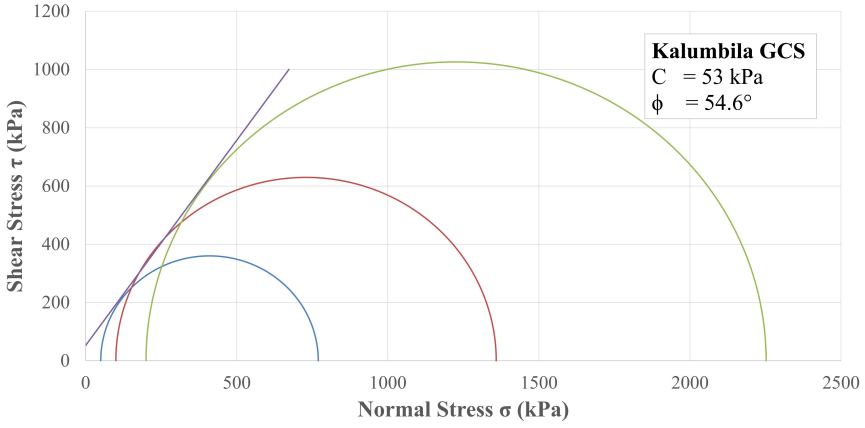

Figure 4.27: Mohr-Coloumb circles and failure envelope for KL1

Kalumbila graded crushed stone material mixes (KL1 and KL2) show similar shear parameters with a slight insignificant difference between each measured parameter. Also, the retained cohesion has barely changed since the difference is 0.2%. Since KL1 followed mixing Approach 1 (A1) and

KL2 followed Approach (A2), at similar application rates, it is maintained that the mixing regime per Kalumbila CS did not have a significant bearing on shear parameters or mix performance. The friction angles from both mixes are 53.2°and 54.5°, this is higher than all friction angle limits provided for BSM's. However, this mix is not regarded to have any BSM equivalent performance based on one parameter.

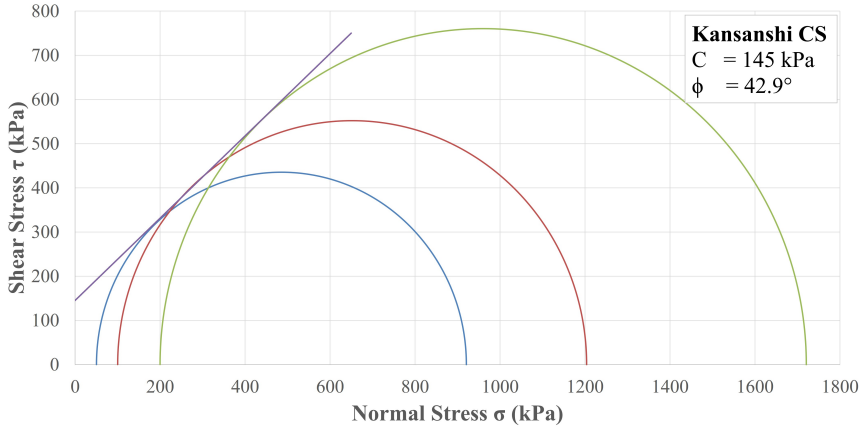

Figure 4.28: Mohr-Coloumb circles and failure envelope for KS

Kansanshi CS performed relatively well compared to the Kalumbila GCS, it was characterized as a well-graded material, its response to CSS60NME showed indicated a compelling performance. The cohesion value for this material is 136.5 kPa which is significantly higher than the Kalumbila GCS but lower than any BSM specification requirements. Figure 4.28 shows a higher cohesion value of 145 kPa, this results from determining shear parameters graphically. The friction angle is 44.2°, the retained cohesion is 77.8%, which are both above BSM limits. The higher retained cohesion further shows that the material responded well to the 0.5% Terrasil+ mixed in the bitumen emulsion. Figure 4.28 shows Mohr circles and the tangential failure envelope of the Kansanshi CS. The failure envelope was used to determine the parameters shown on the graph.

4.8 RESILIENT MODULUS

Different models are available to determine the resilient modulus of the material, although they are primarily developed for granular base materials their application can be extended to BSM's (Jenkins *et al.*, 2004). The bulk stress-resilient modulus (Mr-θ) and bulk stress DSR (Mr-θ-σd/σd,f) models show fairly good correlation coefficients. These were deemed suitable compared to other models because they describe the resilient response of the treated materials relatively better. Treated laterite and Kalumbila GCS materials and tested using a dynamic triaxial test. Kansanshi material was not tested due to limited material quantity.

4.8.1 Bulk stress-resilient modulus (Mr-θ)

According to Anochie-Boateng *et al.* (2009), Mr of a material increases with increasing stress, stress dependency of granular materials is commonly described using this model. Laterite and Kalumbila GCS are stress-dependent materials shown by the increase in Mr with increasing bulk stress. The best fit data is represented by the regression line whose R^2 indicates if the data fits perfectly. Laterite has an R^2 of 0.984 while Kalumbila GCS has an R^2 of 1.0. The higher R2 values imply that the model is a suitable representation of the treated materials stress dependency. If the data was scattered it would imply that the model does not adequately represent the bulk stress-Mr relationship, Figures 4.29 and 4.30 illustrate that data points are along the best fit line.

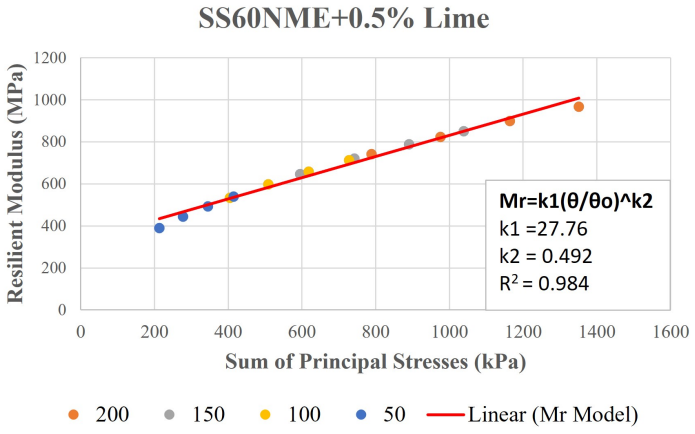

Figure 4.29: Resilient Modulus of laterite

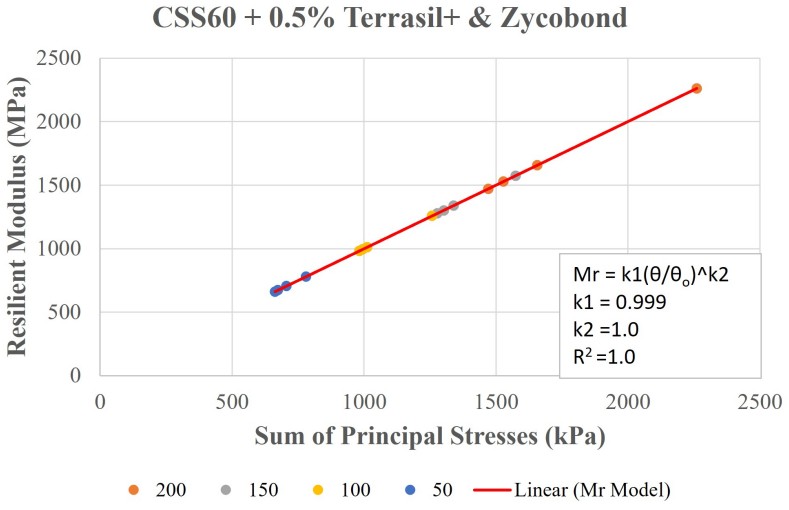

Figure 4.30: Resilient Modulus of Kalumbila GCS

4.8.2 Bulk stress-resilient modulus (Mr-θ-σd/σd,f)

This model characterizes Mr using both bulk stress and DSR. The deviator stress component takes into consideration the shear behaviour of the material, unlike in the (Mr-θ) model whose parameters do not reflect the shear effect. It is an extension of the (Mr-θ) model, it considers the DSR whose increase leads to stress stiffening. Figure 4.31 shows the laterite best fit line using this model, the correlation coefficient is 0.802. This indicates a relatively poor model describing the laterite material resilient modulus. All data points are scattered around the best fit line, the Mr is not suitably characterized by this model. Kalumbila GCS is perfectly described by this model due to less scattered data points and a high R^2 (0.9873). Mr -θ model also showed the best-fit line for Kalumbila material and a higher R^2.

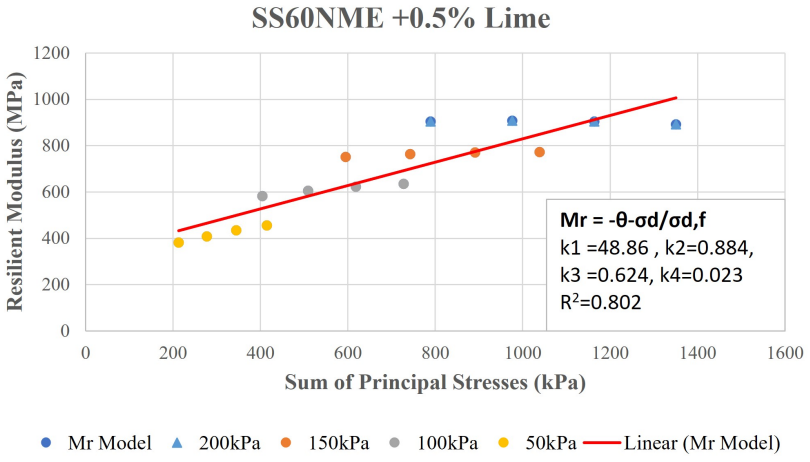

Figure 4.31: Resilient Modulus of laterite

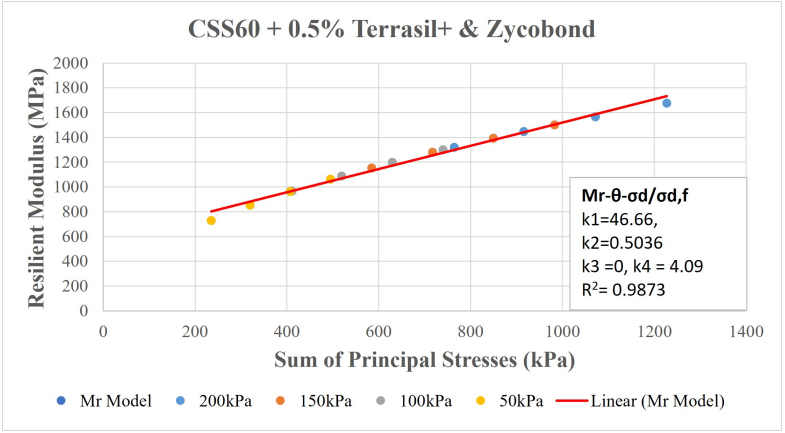

Figure 4.32: Resilient Modulus of Kalumbila GCS

4.8.3 Best-fit model

The two selected models shown relatively have a higher correlation coefficient hence they are deemed suitable for resilient modulus determination. The model that best describes stress dependency is based on R^2, the difference between measured and calculated Mr is squared and the physical accuracy of the data points. The models are best-fit models, although one model is selected to describe that material.

Mr-θ and Mr-θ-σd/σd,f models are used to model Laterite Mr, the Mr-θ model having the highest R_2 than the Mr-θ-σd/σd,f. Therefore, the model with high R^2 describes the stress dependency of laterite accurately. The Mr-θ-σd/σd,f model has a low R^2 and the data points are scattered around, the model does not sufficiently describe the material behaviour. Therefore the chosen model is Mr-θ.

$$Mr = 27.76 \times \left(\frac{\theta}{\theta_d}\right)^{0.492} \tag{4.1}$$

Two Mr-models best represent Kalumbila GCS due to their high correlation coefficients. Mr-θ model has a high R^2 of 1, while the (Mr-θ-σd/σd,f) model has 0.9873 but it has a k3 of 0, implying that the DSR does not influence the resilient modulus. The best fit model is therefore chosen as the Mr-θ model.

$$Mr = 0.999 \times \left(\frac{\theta}{\theta_d}\right)^{1.0} \tag{4.2}$$

4.9 SUMMARY

Laterite, Kalumbila GCS and Kansanshi CS are graded, and their grading envelopes fit within the BSM grading limits used as guidelines. Both wet and dry sieve tests are carried out although the wet sieves graphs of finer particles grading were slightly below the BSM lower grading limit. Laterite is identified as gap graded while the crushed stones do not meet all criteria to be classified as well graded when using the Unified Soil Classification System (USCS). All materials dry sieve analysis grading envelopes indicate suitability for stabilization. The moisture-density relationship is done for both crushed and not crushed aggregates for laterite and Kalumbila GCS. Bigger stone sizes are crushed and mixed homogeneously with other fractions. Crushed materials result in higher maximum density than not crushed aggregates, this behaviour is similar for both laterite and Kalumbila GCS. This is due to good packing influenced by differently shaped crushed aggregates.

Atterberg limits show that the crushed stone materials had no plasticity from the tested 0.425 mm fraction. However, laterite has a plastic limit of 10% from both the 0.075 mm and 0.425 mm

fractions. Little or no plasticity indicates a very low clay and/or silt content. Laterite PI results reveal that changing soil fraction from which consistency limits are determined did not influence the PI. Atterberg limits results from all materials were compared against literature values for haul roads, these were out of the ranges proposed from literature. The mineralogy of the samples is determined using X-ray diffraction. Qualitative results show the presence of minerals common in construction materials such as quartz, microcline, and calcite.

Primary and secondary minerals are also identified to be present in all materials indicated by the low-intensity peaks. These included kaolinite and gibbsite in laterite, muscovite in Kalumbila GCS and dolomite, illite in muscovite in Kansanshi CS. Mineralogy of treated samples is also tested to identify any changes under treatment with NME's. There are newly developed phases in the treated laterite material, the new phases may be due to the effective NME treatment. Most Kalumbila and Kansanshi treated material show similar results.

In NME treated materials traces of muscovite did not show meaning, the addition of organosilane may have contributed to a reduction in muscovite. New mineral phases were seen on NME treated material, implying effective stabilization using NME's, therefore new and improved phases were seen.

Indirect tensile strength testing is done to indicate optimum performance amongst design mixes. All ITS_{WET} samples for laterite and Kalumbila GCS failed as they disintegrated while submerged in water. ITS_{DRY} samples of nano-modified laterite and Kalumbila GCS maintained adhesion in the water showing effectiveness of the nano additive in the aggregate material. Optimum organosilane content is 0.5% of cross bitumen content or 0.65 kg/m3 of material aggregates. Preblended SS60 shows low laterite ITS_{WET} values not meeting both BSM and NME specifications, but dry specimens perform well and meet NME4 specifications. Kalumbila GCS ITS_{WET} samples meet NME2 and BSM2 requirements, all samples perform significantly well at 1.2% SS60NME content meeting NME 1 limits.

CSS60NME slightly increases laterite ITS_{DRY} and wet with an optimum content at 0.65 kg/m3 of aggregate. Kalumbila GCS responds significantly well to CSS60NME with almost all specimens meeting NME1 limits and some ITS_{WET} exceeding ITS_{DRY}. Approach 2 mix approach is more effective for crushed stones but less for laterite, compared to Approach 1. Kansanshi CS is mixed using Approach 2, ITS_{DRY} meet NME1 when treated with preblended SS60NME, while ITS_{WET} are BSM1 equivalent. CSS60NME treated Kansanshi CS meets shows high ITS results both at 0.25% and 1% of Terrasil+ content, meeting NME1 limits.

In some applications, directly incorporating organosilane into the mix is a much easier method

because of known parameters such as application rate, OMC, test evaluations, and simulations. By incorporating it into the bitumen (Approach 2) there are obstacles such as storage stability and shelf life where organosilane reacts to itself in the elongated presence of oxygen.

Laterite fails under high-pressure water permeability; this behaviour is indicated by ITS results. Kansanshi CS and Kalumbila GCS treated with a Terrasil+ modified CSS60 do not show significantly low HPP values. SS60 NME treated Kalumbila GCS have low permeability than the control mix. Terrasil treated CSS6O in Kansanshi CS shows significantly low permeability compared to the control mix. SS60 NME and lime treated laterite has a high cohesion of 266 kPa and a friction angle of 49.6°. All Kalumbila GCS mixes have cohesion and angle of friction around 50 kPa and 54 °, respectively. 0.5% Terrasil+ treated Kansanshi CS shows a good cohesion of about 136 kPa. The resilient modulus of Kalumbila crushed stone is higher than that of laterite and the simple Mr θ model is selected to calculate the material stiffness.

CHAPTER 5

STRUCTURAL PAVEMENT DESIGN AND ANALYSIS

This chapter presents a pavement structural design and analysis using a mechanistic-empirical method. Loading and haul road network pavement structures are selected in terms of typical dump truck, and common haul road layer works for analysis. A base layer is selected for analysis, its resilient modulus is determined from established models and tests. Stresses and strains are calculated based on the selected loading and other pavement design method input parameters. A strain profile is used to show the change in strain with depth and classify the category of the haul road depending on strain levels.

Providing a safe cost-effective hauling operation entails ensuring optimum haul road performance. The haul road pavement structure should sufficiently sustain heavy truck loading, environmental conditions and protect the subgrade against these high stresses and strains consequently providing a durable haulage platform. Softer layers provided less protection of the subgrade but stiffer layers, particularly at the top of the pavement provided more load spreadability and protect the in-situ subgrade. In a structural design, construction methods are as important as material selection, therefore an adequate design used tested materials following suitable construction standards.

5.1 DEVIATOR STRESS RATIO (DSR)

The concept of the deviator stress ratio is shown in Figure 5.1. It summarizes factors influencing the determination of deviator stress ratio such as shear properties obtained from a simple triaxial test. At high deviator stress ratios, the rate of strain accumulation can accelerate, leading to permanent deformation or failure. At failure, the critical DSR is exceeded and the equilibrium state of plastic strain becomes unstable (Jenkins and Collings, 2017).

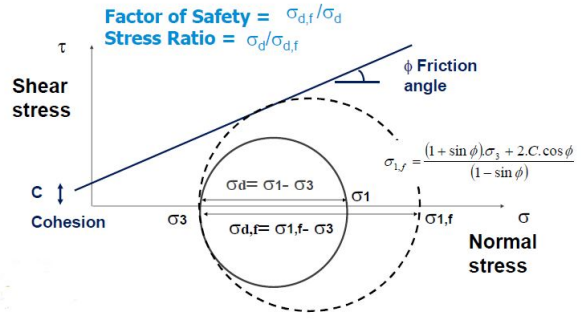

Figure 5.1: The concept of deviator stress ratio.(Jenkins and Collings, 2017)

At low deviator stress ratios, a material performs well and is less likely to fail, acceptable DSR

values are approximately 30% and below. DSR varies depending on the type of material i.e. critical DSR of fine gravel is different to that of granular materials due to their variable stress thresholds. Pavement life is a function of deviator stress ratio

5.2 STRESS AND STRAIN CALCULATIONS

It is essential to evaluate stress and strain at critical positions within the pavement structure. The structural capacity of a pavement structure is defined by its weakest point, which could be anywhere within the pavement structure. Analysis locations are directly under the wheel loading and at overlapping strain fields. Figure 5.2 illustrates a layer elastic model adopted for a mechanistic-empirical model analysis locations and critical parameters.

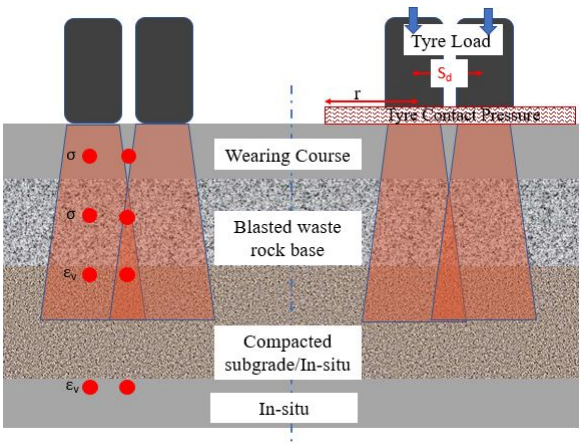

Figure 5.2: Analysis positions and critical parameters

Haul roads do not have as many layers as national road networks. Therefore, relevant layers have been shown. Haul road network surfacing is barely asphalt or seal layer, therefore stress conditions at the wearing course are not considered critical as the layer has an insignificant influence on the structural capacity of a haul road structure. Critical parameters are three-dimensional stresses at the mid base layer and vertical compressive strain at the top of the subgrade as shown in Figure 5.2.

5.2.1 Dump truck selection and material properties

Applied loading and material characteristics are key inputs in the mechanistic-empirical design inputs. A 789D Caterpillar mining haul truck with a GVM of 324 319kg is chosen for loading conditions (Table 5.1) and pavement response. According to the Original Equipment Manufacturer(OEM), 67% of the load is distributed to the rear axle group when laded. A single axle with

dual tyes (SADT) is chosen, it is assumed that there is a 10% load variation with 65 km/h speed, therefore the load per wheel slightly decreases. Centre to centre distance (CC_d) between the dual wheel is assumed to be 1500 mm. The tyre pressure is 650 kPa and the load per wheel is 450 kN, 37.00-R57 standard tyres are considered. The contact radius is calculated using Equation 5.1, and a circular tyre imprint is assumed.

$$Contact\ Area = a(m^2) = \sqrt{\frac{Wheel\ Load(kN)}{Tyre\ Pressure(kPa) \times \pi}} \tag{5.1}$$

Table 5.1: Haul truck specifications and loading conditions

Haul Truck Specifications		**Axle Groups**		**Wheel Load**	
Type	C789D	Type	SADT	Load (kN)	480
GVM (kg)	324 329	Tyre Width(m)	1.044	Contact Area(m^2)	0.485
CC_d(m)	1.260	Tyre Pressure(kPa)	650	Contact Radius(m)	0.392

5.2.2 Resilient modulus iteration

The stiffness of a layer is a critical input parameter in the mechanistic-empirical design of roads. The response of a pavement layer to loading is influenced by the stiffness of the pavement layer beneath it. Therefore each layer within the pavement structure has a different resilient modulus, the load spreadability is different per layer.

Resilient modulus models are used to evaluate the resilient modulus used in the mechanistic-empirical design, it is important to note that modified granular materials resilient modulus is modelled similar to granular materials. An iterative approach is used to determine the modified base layer resilient modulus. Critical confinement and principal stresses evaluated in the middle of the base layer are used to calculate the bulk stress, a parameter in the selected resilient modulus model (Table 5.2). The newly calculated resilient modulus is used to calculate stresses which calculate resilient modulus, this process continues until the resilient modulus value converges.

Table 5.2: Resilient modulus models

Base Mix	**Model**	**k1**	**k2**
Laterite + SS60 + 0.5%Lime	Mr = k1 θ^{k2}	27.76	0.492
Kalumbila GCS + CSS60 + 0.5% (Terrasil+ and Zycobond)	Mr = k1 θ^{k2}	0.999	1.0

After the resilient modulus value has converged, the value is used for stress-strain calculations at critical analysis points of the pavement structure. The iterations to calculate resilient modulus

are done for a series of pavement structures with varying subgrade stiffness. The quality and stiffness of subbase and subgrade have a significant influence on pavement performance. As a result, six pavement structures (Table 5.3), each at 200mm and 300 mm thick base, are considered for sensitivity analysis in determining the base layer resilient modulus. The increment of thickness from 200mm to 300mm is to understand the extent to which a thicker layer can mitigate induced vertical strain and vertical stress levels at analysis points and consequently the DSR.

Table 5.3: Six analysed pavement structures

	Structure 1	Structure 2	Structure 3	Structure 4	Structure 5	Structure 6
G3/ G4	Base 200 mm 300 mm v= 0.35	Base 200 mm 300 mm	Base 200 mm 300 mm	Base 200 mm 300 mm	Base 200 mm 300 mm	Base 200 mm 300 mm
G5	Blinding Layer t= 250mm E=150 MPa v=0.35	Blinding Layer E=250 MPa	Blinding Layer E= 350 MPa	Blinding Layer E= 150 MPa	Blinding Layer E=250 MPa	Blinding Layer E= 350 MPa
G5	Blinding Layer t=250mm E= 100 MPa v=0.35	Blinding Layer E=400 MPa	Blinding Layer E= 400MPa	Blinding Layer E= 100 MPa	Blinding Layer E=400 MPa	Blinding Layer E= 400 MPa
G5	In-situ t=500 mm E= 400 MPa v=0.35	In-situ t = 500 mm E= 400 MPa	In-situ t = 500 mm E= 500 MPa	In-situ t=500mm E= 200 MPa	In-situ t=500mm E= 200 MPa	In-situ t=500 mm E= 200 MPa
G5	In-situ t=1000 mm E=500 MPa v=0.35	In-situ t= 1000 mm E= 500 MPa	In-situ t=1000 mm E= 500 MPa	In-situ t= 1000 mm E= 300 MPa	In-situ t=1000 mm E= 150 MPa	In-situ t= 1000 mm E= 300 MPa

The Poisson ratio is assumed to be 0.35 throughout all materials. Critical parameters for the base and sub-layered binding layer are vertical stresses at the middle of these layers. The critical parameter within the in situ subgrade is the vertical compressive strain at the top of the subgrade, 0.2 mm from the top interfacial region (Refer to Figure 5.2). The resilient modulus of the base must be neither very high nor very low to ensure a balanced pavement. High resilient modulus values attract more stresses while lower stiffness barely attracts stresses to distribute to the bottom layers, therefore sufficient load spreadability is an essential aspect of pavement balance. Results of the calculated base resilient modulus are shown in Table 5.4.

The resilient moduli of structures 1 and 4 are the lowest among the analysed six pavement structures. The stiffness of the in situ layers in structure 4 is low, 200MPa and 300MPa as seen in Table 5.3. The low stiffness of the lower values leads to a slightly lesser base layer resilient modulus compared to other structures. However, the base resilient modulus in structure 1 is also low, due to relatively less stiff support of a 150MPa blinding layer. The supporting layer influences the performance of a layer above it, hence the low resilient modulus of the base in structure 1. Structure 3 has the highest resilient modulus, indicating a good stress distribution into the deep layers. Structure 3 has good support with sufficiently stiff layers denoting higher load spreadability amongst the pavement layers.

Table 5.4: Structure 1 to 3 base layer resilient modulus

		Thickness	
		t =200 mm	t= 300 mm
Mix Type	Structure	Mr (MPa)	Mr (MPa)
Laterite + SS60 + 0.5% Lime(L1)	1	928	842
	2	961	885
	3	984	906
Kalumbila GCS + CSS60	1	1219	1004
+0.5% Terrasil+ and Zycobond	2	1332	1116
(KL1)	3	1408	1173
	Ref	2767	

5.2.3 Stress and Strain

Mohr-Coulomb circles are used to plot the principal stresses for structures 1 3 and 4. Major principal stresses and applied stress at failure (parameter in DSR calculation), are shown. The principal stresses produce Mohr circles well below the failure criterion. This is only done for a base layer thickness of 200mm. Figure 5.3 and 5.4 show laterite and Kalumbila GCS structure 1, respectively. Structures 3 and 4 are presented in Figures D.2 to D.5, Appendix D

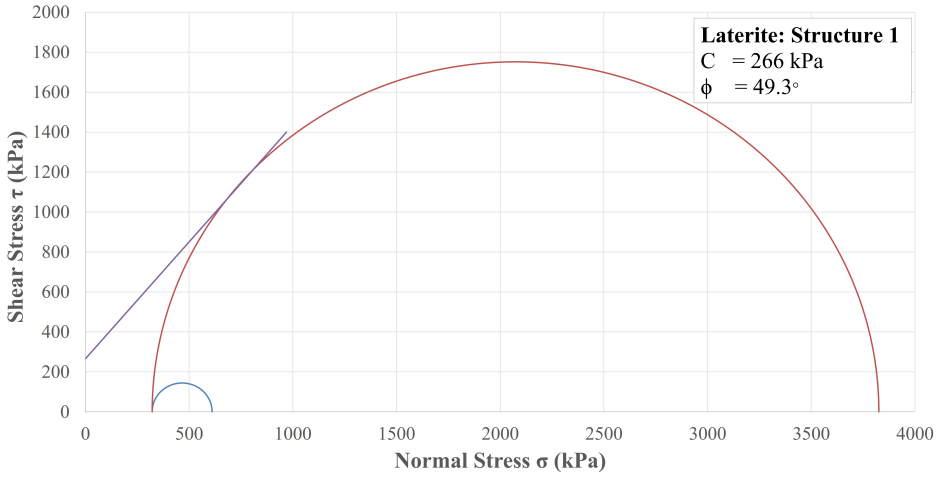

Figure 5.3: Mohr circle for laterite Structure 1

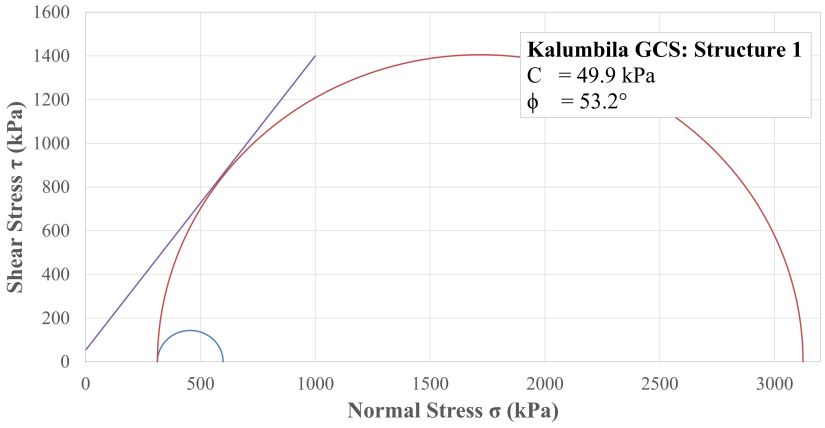

Figure 5.4: Mohr circle for Kalumbila GCS Structure 1

The deep haul road structure, with stiffer layers such as blasted dump rock, exhibits high base layer resilient modulus both at 300 mm and 200 mm thickness, vertical stresses and vertical compressive strains are well below the critical strain limit. A 200 mm base layer meets the strain limit (2000 microstrains), therefore the base layer thickness can be kept at 200mm and not increased to accommodate more stresses. This implies that using stiffer layers with good support at the top of the pavement can lead to a decreased layer thickness. Given the haul roads width of approximately 40 m, dematerialization would be economical.

The compressive vertical strain changes because of the different layer moduli and thickness used in the pavement structures. Figure 5.5 shows the vertical compressive strain profile with depth for structure 4. It further illustrates that haul road category 2 and 3 limiting design criteria were

not exceeded since the maximum resulting strain is below 1000 microstrains. Structures 1 and 3 had lower strain values due to slightly higher layer stiffness layers, structure 4 is identified as the weakest structure, high stress induces higher vertical compressive strains as seen in Figure 5.5.

Table 5.5: Haul road vertical compressive strain limit per category.(Visser, 2015)

Haul road category	Daily traffic volume (x100 kg)	Strain Limit
Category 1	>25	900
Category 2	8-24	2000
Category 3	<7	3000

Laterite vertical compressive strains induced directly below the wheel are just above 900 microstrains (Table 5.5) which is a strain limit value for category 1 haul roads. The strains between the wheels within the layers are also increased by the overlapping strain fields due to dual tyre loading.

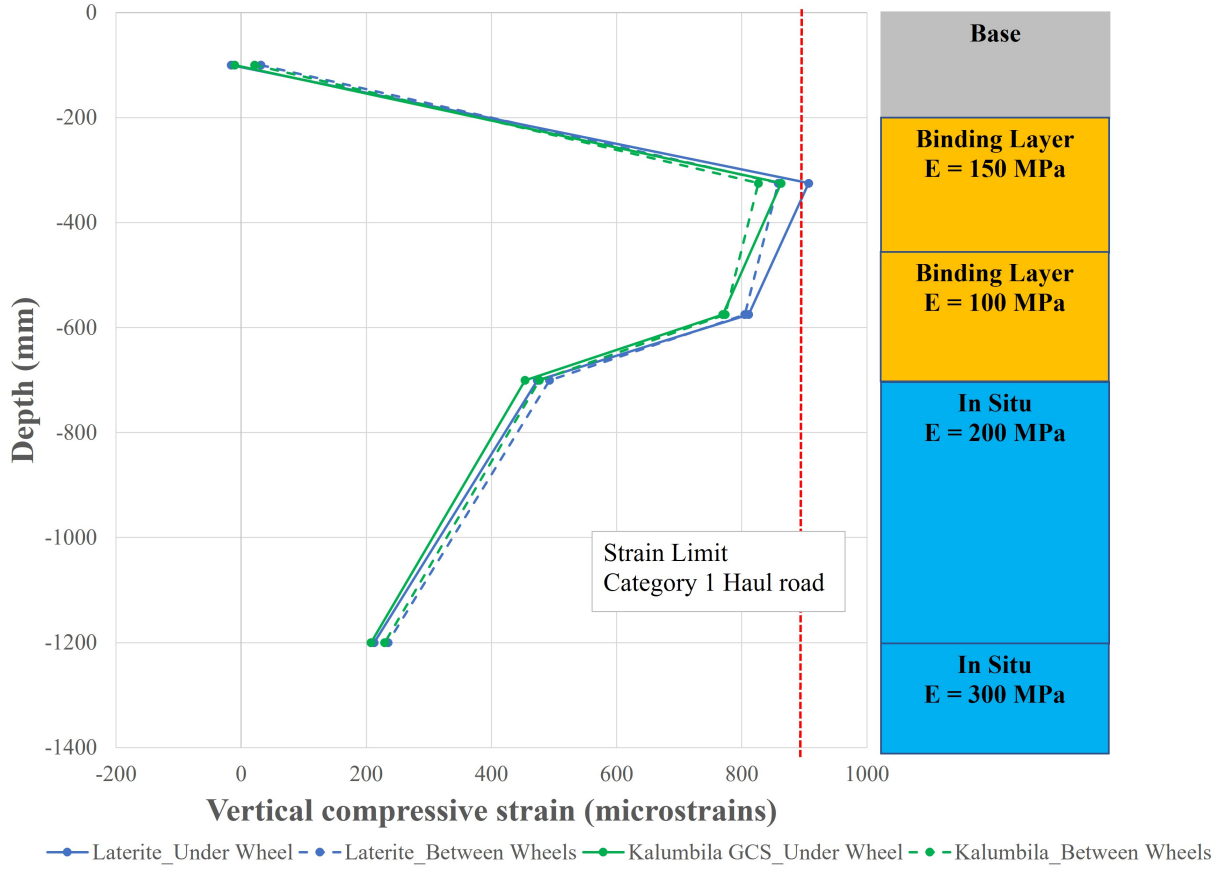

Figure 5.5: Vertical compressive strain profile for structure 4.

The pavement structure should limit the stresses and strains induced in the subgrade layers. The higher stiffness of the top layers of the pavement structure protects the magnitude of stresses and strains at the bottom layers. It is important to note that higher strains develop at the overlapping strain fields, therefore stiffer top layers sufficiently decrease the magnitude of vertical compressive strains at bottom of the pavement. Structure 3 is the stiffer pavement structure, Kalumbila GCS results indicate that a quality blasted rock layer as the base may provide a stiff layer that would significantly influence the structural capacity of the pavement. The induced strains in pavements structure indicate the performance of category 1 haul road, at assumed thicknesses and resilient modulus values, strain values for every layer remain below 1000 microstrains.

5.3 PAVEMENT LIFE

Estimation of structural capacity is based on DSR, all pavements structures are evaluated for DSR's and compared against the reference structure to estimate the performance of the base layer per structure and also the structure as a unit. Resilient modulus increase results in decreasing deviator stress ratio (See Figure D.1, Appendix D). Low stiffness of top layers may result in the poor pavement due to high stresses in the subgrade. The sufficiently high stiffness of top layers results in lesser stresses within the subgrade, leading to a sound pavement with the load sufficiently distributed to layers.

Table 5.6: DSR values of both laterite and Kalumbila GCS

Thickness mm	**Structure**	σ_1 kPa	σ_3 kPa	**Mr** MPa	$\sigma_{1,f}$ kPa	σ_d kPa	$\sigma_{d,f}$ kPa	**DSR** %	**C** kPa	θ °
	Mix: Laterite + SS60+0.5% Lime									
200	1	610.1	322.0	928.0	3825.8	288.7	3503.9	8.24	266.3	49.6
	3	636.4	395.0	984.1	4365.6	241.4	3741.4	6.08	266.3	49.6
	4	605.4	371.1	956.9	2817.8	234.3	2817.8	6.14	266.3	49.6
	Mix: Kalumbila GCS + CSS60+0.5% Terrasil+ and Zycobond									
200	1	598.8	312.5	1220.0	3124.3	286.3	2811.8	10.18	49.9	53.2
	3	628.1	399.3	1408.3	3908.4	228.8	3509.1	6.52	49.9	53.2
	4	591.4	362.0	1299.4	3571.3	229.4	3209.2	7.15	49.9	53.2

The low values of DSR indicate a good material performance. Low deviator stress ratios indicate low vertical stress within the structure, as a result, the critical strain limit is not exceeded. At low DSR values, accelerated deformation is unlikely.The low DSR values indicate sufficient confinement pressure. The depth of the pavement and stiffness of the layers has contributed to the low DSR values.

5.4 SUMMARY

The pavement design follows a mechanistic-empirical approach. Mix types analysed are made from laterite and Kalumbila graded crushed stone. Laterite is stabilized with SS60 emulsion and 0.5% lime while Kalumbila GCS is stabilized with CSS6 emulsion and 0.5% Terrasil+ and Zycobond. These are analysed as pavement construction materials for a haul road base layer. The mechanistic-empirical design follows guidelines from both the SAPEM and Thompson and Visser (1996). Rubicon Tools software is used to calculate critical parameters at evaluation positions, these are vertical compressive strains at the top of subgrade layers and stresses mid unbound granular base layers. The concept of deviator stress ratio is used to indicate pavement performance and stabilized base layer behaviour.

The mechanistic-empirical method requires load conditions and material characteristics as main inputs. The load conditions used are for a 789D Caterpillar laden dump truck with 67% of the load distributed to a rear axle group. A single axle dual tyres axle group with 480 KN wheel load and 650 kPa tyre pressure is used. Six pavement structures were analysed, varying the stiffness value per structure and the thickness of the base layer from 200mm to 300 mm. In all six pavement structures, the base is underlain by a sub layered blinding layer. The stiffness of the blinding layer second sublayer and all layers below is varied to determine the dependence of base layer performance on subgrade stiffness or support with varying stiffness. The stiffness of the base layer is determined through iteration until it converges and the lowest resilient modulus within the six structures was considered. Pavements 4 and 1 have the least resilient modulus to relatively poor base layer support.

Following haul truck selection and material characteristics, actual stresses and strains are calculated to determine applied stress at failure. All pavement structures undergo vertical compressive strain well below category 1 to category 3 haul roads. The maximum strains induced in pavement 4 are below the category 1 haul road strain limit (1000 microstrains). Applied stress at failure is used to calculate the deviator stress ratio which indicates that a material undergoes accelerated deformation at high DSR values but a steady plastic strain at low values. A higher deviator stress ratio denotes a higher vertical compressive strain. All analysed pavement structures have DSR values well below 30%, the haul road base layer deep support and confinement influence the low DSR values.

CHAPTER 6

CONCLUSIONS AND RECOMMENDATIONS

6.1 CONCLUSIONS

This chapter provides conclusions from material properties, their performance through tests and the pavement structure. Materials used included laterite, graded crushed stone from Kalumbila mine and a standard crushes stone from Kansanshi mine. It is advantageous to characterize a material before application on the road to avoid expensive rehabilitation and construction costs should an inherently deficient material prematurely fail.

Upon selection of optimum materials establishments are made on performance of selected tests based on developed testing regimes. Suitable materials are used for road construction following a selected design approach. All three types of aggregates are tested for material properties, they were then mixed at different organosilane application rates and constant binder application rate following two mixing approaches. Optimal mix designs are selected and used for test specimens. Material performance is concluded based on the performance tests. A structural design of laterite and Kalumbila GCS material is carried out.

The primary aim of the research was to determine the effectiveness of organosilane compounds to increase the mechanical properties, strength, durability, and load-bearing capacity of haul road base construction materials. The following conclusions can be drawn from the research:

Standard Tests

- Laterite showed a gap graded grading envelope while Kansanshi CS was well-graded meeting most USCS specifications. Grading envelopes of all materials met BSM grading limits used as guidelines and therefore were rendered suitable for stabilization.
- The PI of the materials was done on both the 0.425 mm fraction and 0.075mm fraction. Laterite had a PI of approximately 10% on both fractions, fraction size did not significantly influence PI.
- Mineralogy tests showed the availability of minerals common in most construction materials and some traces of secondary minerals such as kaolinite and muscovite.

Mix Design

- • A silane incompatible with the bitumen emulsions does allow homogeneous dispersion of all binder constituents, bitumen settles to the bottom due to undesirable chemistry.
- Approach 2 was a better mixing mechanism. The effectiveness of the nanosilane incorporation

mechanism is influenced by factors such as material type and available equipment, chemistry, ease of use, storage stability and NME shelf life.

- Laterite material failed in water indicating poor performance in wet conditions and durability issues, however, most ITS_{DRY} specimens met BSM2 and NME4 specifications.
- Lime additive does not increase the strength of NME materials, almost all mix designs with the addition of increasing hydrated lime content have shown a decrease in ITS values.
- In NME treated materials traces of muscovite did not show meaning, the addition of organosilane may have contributed to a reduction in muscovite. New mineral phases were seen on NME treated material, implying effective stabilization using NME's, therefore new and improved phases were seen.
- Kalumbila GCS had the highest ITS results amongst all the materials, indicating a high potential if used to construct NME modified haul road base underlain by good support.

Shear parameters and resilient modulus

- • SS60 and lime treated laterite showed a high cohesion of 226 kPa, from ITS test this material can be appropriate for a base layer provided there is sufficient cover against water ingress and other environmental conditions. Kansanshi CS has a higher cohesion that Kalumbila GCS.
- Resilient modulus of laterite and Kalumbila GCS was modelled using Mr-θ model instead of Mr-θ-σd/σd,f , it represented dynamic triaxial results well due to a higher coefficient of correlation. This says the material behaviour or response to loading was similar.

Permeability

- Laterite failed under high-pressure permeability testing, Kalumbila GCS showed lower permeability for control samples and high for samples treated with a Terrasil+ modified CSS60. Kansanshi CS permeability was low for NME treated samples. NME contributed to samples being tested and not just falling apart.

Pavement life

- Pavement life analysis reveals that weaker subgrade layers result in maximum strains within the pavement structure. However, a good base layer support with high stiffness attracts more strains and protects the subgrade.
- Low deviator stress ratio values in all structures imply a relatively good haul road performance with a steady rate of low plastic strain. Results indicate low permanent deformation with time.

6.2 RECOMMENDATIONS

It is recommended that further research is done on these topics:

- The durability of NME treated materials used as base layers in both low volume roads and mine haul roads.
- The cost-effectiveness of NME treated materials in haul road construction and influence on haulage costs.
- The influence of storage stability of nano modified emulsions on effectiveness of organosilane and mix performance
- Field application of organosilanes or NME's and monitoring their behaviour during both wet and dry conditions.
- Influence of organosilane incorporation mechanisms on different haul road construction materials, particularly natural aggregates, and blasted dump rock
- Determine the chemistry between lime and NME's and the relationship between lime content and NME compatibility.

REFERENCES

Abdullah, M.E., Zamhari, K.A., Buhari, R., Kamaruddin, N.H.M., Nayan, N., Hainin, M.R., Hassan, N.A., Jaya, R.P. and Yusoff, N.I.M. (2015). A review on the exploration of nanomaterials application in pavement engineering. *Jurnal Teknologi*, vol. 73, no. 4.

Ahmad, N., Nasir, M.A., Hafeez, M., Rafi, J., Zaidi, S.B.A., Haroon, W. *et al.* (2018). Carbon nanotubes (cnts) in asphalt binder: homogeneous dispersion and performance enhancement. *Applied Sciences*, vol. 8, no. 12, p. 2651.

Akhalwaya, I. and Rust, F.C. (2018). Laboratory evaluation of road construction materials enhanced with nano-modified emulsions (nmes).

Amin, I., El-Badawy, S.M., Breakah, T. and Ibrahim, M.H. (2016). Laboratory evaluation of asphalt binder modified with carbon nanotubes for egyptian climate. *Construction and Building Materials*, vol. 121, pp. 361–372.

Anochie-Boateng, J., Paige-Green, P. and Mgangira, M. (2009). Evaluation of test methods for estimating resilient modulus of pavement geomaterials. In: *Proceedings of the 28th Southern African Transport Conference, pp245*, vol. 248.

Antonucci, J.M., Dickens, S.H., Fowler, B.O., Xu, H.H. and McDonough, W.G. (2005). Chemistry of silanes: interfaces in dental polymers and composites. *Journal of research of the National Institute of Standards and Technology*, vol. 110, no. 5, p. 541.

Apostolidis, P. and Scarpas, A. (2020). Numerical study of sorption of asphalt binders on minerals. *Construction and Building Materials*, vol. 259, p. 120392.

ARAYA, A. *et al.* (2021). Monitoring performance of laterite base trial section: A case of addis ababa, ethiopia. *Journal of Construction Project Management and Innovation*, vol. 11, no. 1, pp. 63–78.

Arkles, B. (2011). Hydrophobicity, hydrophilicity and silane surface modification. *Gelest Inc, Morrisville*.

Australia, M.R.W. (2003). A guide to the selection and use of naturally occurring materials as base and subbase in roads in western australia. retrieved september, 2008.

Bagampadde, U., Isacsson, U. and Kiggundu, B.M. (2004). Classical and contemporary aspects of stripping in bituminous mixes. *Road materials and pavement design*, vol. 5, no. 1, pp. 7–43.

Baldi-Sevilla, A., Aguiar-Moya, J.P., Vargas-Nordcbeck, A. and Loria-Salazar, L. (2017). Effect of aggregate–bitumen compatibility on moisture susceptibility of asphalt mixtures. *Road Materials and Pavement Design*, vol. 18, no. sup2, pp. 318–328.

Barbieri, D.M., Hoff, I. and Mørk, M.B.E. (2020). Organosilane and lignosulfonate as innovative stabilization techniques for crushed rocks used in road unbound layers. *Transportation Geotechnics*, vol. 22, p. 100308.

Barnes, D. and Connor, B. (2014). Managing dust on unpaved roads and airports. Tech. Rep., Alaska University Transportation Center.

Bayda, S., Adeel, M., Tuccinardi, T., Cordani, M. and Rizzolio, F. (2020). The history of nanoscience and nanotechnology: from chemical–physical applications to nanomedicine. *Molecules*, vol. 25, no. 1, p. 112.

Bozorgebrahimi, A., Hall, R. and Morin, M. (2005). Equipment size effects on open pit mining performance. *International Journal of Surface Mining, Reclamation and Environment*, vol. 19, no. 1, pp. 41–56.

Buehler, M.J. and Ackbarow, T. (2007). Fracture mechanics of protein materials. *Materials Today*, vol. 10, no. 9, pp. 46–58.

Bullen, F. (1998). Development of a guide for the design of cold mixed granular materials. In: *Road Engineering Association of Asia and Australasia (REAAA), Conference, 9th, 1998, Wellington, New Zealand*, vol. 2.

Caruso, F. (2001). Nanoengineering of particle surfaces. *Advanced materials*, vol. 13, no. 1, pp. 11–22.

Collings, D., Hefer, A., Jenkins, K. and Johns, F. (2020). Technical guideline tg2: Bitumen stabilised materials: A guideline for the design and construction of bitumen emulsion and foamed bitumen stabilised materials.

Correia, A.A.S. and Rasteiro, M.G. (2016). Nanotechnology applied to chemical soil stabilization. *Procedia engineering*, vol. 143, pp. 1252–1259.

Crosby, A.J. and Lee, J.-Y. (2007). Polymer nanocomposites: the "nano" effect on mechanical properties. *Polymer reviews*, vol. 47, no. 2, pp. 217–229.

Crucho, J., Picado-Santos, L., Neves, J. and Capitão, S. (2019). A review of nanomaterials' effect on mechanical performance and aging of asphalt mixtures. *Applied Sciences*, vol. 9, no. 18, p. 3657.

Darling, P. (2011). *SME mining engineering handbook*, vol. 1. SME.

de Bono, J.P. and McDowell, G.R. (2020). On the packing and crushing of granular materials. *International Journal of Solids and Structures*, vol. 187, pp. 133–140.

Deepa, P., Laad, M., Singh, R. *et al.* (2019). An overview of use of nanoadditives in enhancing the properties of pavement construction binder bitumen. *World Journal of Engineering*.

Ebels, L.-J. and Jenkins, K. (2007). Mix design of bitumen stabilised materials: Best practice and considerations for classification. In: *Proceedings of the 9th Conference on Asphalt pavements for Southern Africa (CAPSA'07)*, vol. 2, p. 5.

Firoozi, A.A., Olgun, G. and Mobasser, S. (2016). Carbon nanotube and civil engineering. *Saudi Journal of Engineering and Technology*, vol. 1, no. 1, pp. 1–4.

Ganesh, V.K. (2012). Nanotechnology in civil engineering. *European Scientific Journal*, vol. 8, no. 27.

Gao, Y., Zhang, Y., Gu, F., Xu, T. and Wang, H. (2018). Impact of minerals and water on bitumen-mineral adhesion and debonding behaviours using molecular dynamics simulations. *Construction and Building Materials*, vol. 171, pp. 214–222.

Ghoreishi, A., Koosha, M. and Nasirizadeh, N. (2020). Modification of bitumen by epdm blended with hybrid nanoparticles: Physical, thermal, and rheological properties. *Journal of Thermoplastic Composite Materials*, vol. 33, no. 3, pp. 343–356.

Gidigasu, M. (1974). Degree of weathering in the identification of laterite materials for engineering purposes—a review. *Engineering Geology*, vol. 8, no. 3, pp. 213–266.

Gourley, C. and Greening, P. (1997). Use of'substandard lateritic'gravels as roadbase materials in southern africa. *TRL, United Kingdom*.

Guo, W., Guo, X., Li, J., Li, Y., Sun, M. and Dai, W. (2019). Assessing the effect of nano hydrophobic silane silica on aggregate-bitumen interface bond strength in the spring-thaw season. *Applied Sciences*, vol. 9, no. 12, p. 2393.

Haselsteiner, R., Schuetz, H.-G., Osan, C. and Somdalen, B. (2014). *Lateritic Soils for Dam Foundations and Dam Cores-Two Case Studies and Their Typical Properties*. na.

Huang, Y. and Wang, L. (2016). Experimental studies on nanomaterials for soil improvement: a review. *Environmental Earth Sciences*, vol. 75, no. 6, p. 497.

James, A. (1998). Asphalt emulsions (chemistry and concepts). In: *2nd Asphalt technology conference of the Americas, Austin, Texas*.

James, A. (2006). Overview of asphalt emulsion. *Transportation Research Circular E-C102: Asphalt Emulsion Technology*, pp. 1–15.

Jenkins, K. and Collings, D. (2017). Mix design of bitumen-stabilised materials–south africa and abroad. *Road Materials and Pavement Design*, vol. 18, no. 2, pp. 331–349.

Jenkins, K., Robroch, S., Henderson, M., Wilkinson, J. and Molenaar, A. (2004). Advanced testing for cold recycling treatment selection on n7 near cape town. In: *Proceedings of the 8th Conference on Asphalt Pavements for Southern Africa (CAPSA'04)*, vol. 12, p. 16.

Jenkins, K., Rudman, C. and Bierman, C. (2020). Delivering sustainable solutions through improved mix and structural design functions for bitumen stabilised materials. *Advances in Materials Science and Engineering*, vol. 2020.

Jenkins, K.J. (2000). *Mix design considerations for cold and half-warm bituminous mixes with emphasis of foamed bitumen*. Ph.D. thesis, Stellenbosch: Stellenbosch University.

Jones, D., Paige-Green, P. and Sadzik, E. (2003). Development of guidelines for unsealed road assessment. *Transportation research record*, vol. 1819, no. 1, pp. 287–296.

Jordaan, G. and Kilian, A. (2016). The cost-effective upgrading, preservation and rehabilitation of roads-optimising the use of available technologies. Southern African Transport Conference.

Jordaan, G., Kilian, A., Du Plessis, L. and Murphy, M. (2017*a*). The development of cost-effective pavement design approaches using minerology tests with new nano-technology modifications of materials.

Jordaan, G., Kilian, A., Muthivelli, N. and Dlamini, D. (2017*b*). Practical application of nano-technology in roads in southern africa. In: *Proceedings of the 8th Transportation Technology Transfer (T2) Conference, Lusaka, Zambia*, pp. 8–10.

Jordaan, G. and Steyn, W. (2019). Testing of granular/soil characteristics for the optimisation of pavement designs using reactive stabilising agents including "new-age" nano-technologies. In: *12th Conference on Asphalt Pavements for Southern Africa (CAPSA), Sun City, South Africa*, pp. 13–16.

Jordaan, G.J., Broekman, A. *et al.* (2021*a*). Evaluation of cost-effective modified binder thin chip and cape seal surfacings on an anionic nano-modified emulsion (nme)-stabilised base layer using accelerated pavement testing (apt). *Applied Sciences*, vol. 11, no. 6, p. 2514.

Jordaan, G.J. and Steyn, W.J. (2021). Nanotechnology incorporation into road pavement design based on scientific principles of materials chemistry and engineering physics using new-age (nano) modified emulsion (nme) stabilisation/enhancement of granular materials. *Applied Sciences*, vol. 11, no. 18, p. 8525.

Jordaan, G.J., Steyn, W.J. *et al.* (2021*b*). Fundamental principles ensuring successful implementation of new-age (nano) modified emulsions (nme) for the stabilisation of naturally available materials in pavement engineering. *Applied Sciences*, vol. 11, no. 4, p. 1745.

Kashaya, A.A. (2013). *Surface run-off behaviour of bitumen emulsions used for the construction of seals*. Ph.D. thesis, Stellenbosch: Stellenbosch University.

Kaufman, W.W. and Ault, J.C. (1978). *Design of surface mine haulage roads: a manual*, vol. 8758. Department of the Interior, Bureau of Mines.

Khitab, A. and Tausif Arshad, M. (2014). Nano construction materials. *Reviews on advanced materials science*, vol. 38, no. 2.

Kidgell, M., JvdM Steyn, W. and Jordaan, G. (2019). Effect of nano-modified emulsions (nme)(nano-silanes) stabilizers on the properties of dolomite. Southern African Transport Conference.

Kim, J. and Moore, J.R. (2009). Laboratory evaluation of zycosoil as an anti-stripping agent on superpave mixtures. *Unpublished, Auburn, AL: NCAT*.

Kleyn, E. (2012). Successful g1 crushed stone basecourse construction. *SATC 2012*.

Kondelchuk, D. (2008). *Studies of the free mica properties and its influence on quality of road constructions*. Ph.D. thesis, Luleå tekniska universitet.

Koner, R. and Chakravarty, D. (2016). Characterisation of overburden dump materials: a case study from the wardha valley coal field. *Bulletin of Engineering Geology and the Environment*, vol. 75, no. 3, pp. 1311–1323.

Leone, M.F. (2012). Nanotechnology for architecture. innovation and eco-efficiency of nanostructured cement-based materials. *J. Architec. Eng. Technol*, vol. 1, pp. 1–9.

Lesueur, D. (2011). Polymer modified bitumen emulsions (pmbes). In: *Polymer modified bitumen*, pp. 25–42. Elsevier.

Lock, E., Ghasemi, M., Mostofi, M. and Rasouli, V. (2012). An experimental study of permeability determination in the lab. *WIT Transactions on Engineering Sciences*, vol. 80, pp. 221–230.

Lyne, Å.L., Redelius, P., Collin, M. and Birgisson, B. (2013). Characterization of stripping properties of stone material in asphalt. *Materials and structures*, vol. 46, no. 1, pp. 47–61.

Majidzadeh, K. and Brovold, F.N. (1966). Effect of water on bitumen-aggregate mixtures.

Makar, J. (2011). The effect of swcnt and other nanomaterials on cement hydration and reinforcement. In: *Nanotechnology in civil infrastructure*, pp. 103–130. Springer.

Mallick, S.R. and Verma, A.K. (2020). Performance of rbi"" stabilized coal mine overburden material for haul road pavement. *Arabian Journal of Geosciences*, vol. 13, no. 14, pp. 1–13.

Mallick, S.R., Verma, A.K. and Rao, K.U. (2017). Characterization of coal mine overburden and assessment as mine haul road construction material. *Journal of The Institution of Engineers (India): Series D*, vol. 98, no. 2, pp. 167–176.

Mann, S. (2006). Report on nanotechnology and construction. *Institute of Nanotechnology European Nanotechnology. Gateway. available online at: http://www. nanoforum. org.*

Matinlinna, J.P., Lung, C.Y.K. and Tsoi, J.K.H. (2018). Silane adhesion mechanism in dental applications and surface treatments: A review. *Dental materials*, vol. 34, no. 1, pp. 13–28.

Mohajerani, A., Burnett, L., Smith, J.V., Kurmus, H., Milas, J., Arulrajah, A., Horpibulsuk, S. and Abdul Kadir, A. (2019). Nanoparticles in construction materials and other applications, and implications of nanoparticle use. *Materials*, vol. 12, no. 19, p. 3052.

Motlagh, A.A., Kiasat, A., Mirzaei, E. and Birgani, F.O. (2012). Bitumen modification using carbon nanotubes. *World Applied Sciences Journal*, vol. 18, no. 4, pp. 594–599.

Murphy, M., Jordaan, G., Modise, T. and Dryburgh, R. (2019). The influence of the characteristics of emulsifying agents on the stabilisation of granular materials using nano-silane modified bitumen emulsions. In: *12th Conference on Asphalt Pavements for Southern Africa (CAPSA), Sun City, South Africa*, pp. 13–16.

Nanzyo, M. and Kanno, H. (2018). Secondary minerals. In: *Inorganic constituents in soil*, pp. 37–58. Springer.

Netterberg, F. (1994). Low-cost local road materials in southern africa. *Geotechnical & Geological Engineering*, vol. 12, no. 1, pp. 35–42.

Netterberg, F. (2014). Review of specifications for the use of laterites in road pavement. *Contract: AFCAP/GEN/124). Crown agents, AFCAP and UKaid*.

Niyogi, S., Hamon, M., Hu, H., Zhao, B., Bhowmik, P., Sen, R., Itkis, M. and Haddon, R. (2002). Chemistry of single-walled carbon nanotubes. *Accounts of Chemical Research*, vol. 35, no. 12, pp. 1105–1113.

Okamoto, H., Sugiyama, Y. and Nakano, H. (2011). Synthesis and modification of silicon nanosheets and other silicon nanomaterials. *Chemistry–A European Journal*, vol. 17, no. 36, pp. 9864–9887.

Oliviero Rossi, C., Teltayev, B. and Angelico, R. (2017). Adhesion promoters in bituminous road materials: A review. *Applied Sciences*, vol. 7, no. 5, p. 524.

Ozturk, C., Nasuf, E. and Kahraman, S. (2014). Estimation of rock strength from quantitative assessment of rock texture. *Journal of the Southern African Institute of Mining and Metallurgy*, vol. 114, no. 6, pp. 471–480.

Pacheco-Torgal, F. and Jalali, S. (2011). Nanotechnology: advantages and drawbacks in the field of construction and building materials. *Construction and building materials*, vol. 25, no. 2, pp. 582–590.

Paige, P. and Netterberg, F. (1987). Requirements and properties of wearing course materials for unpaved roads in relation to their performance. *Traffic*, vol. 576, p. 625.

Paige-Green, P. (1989). *The influence of geotechnical properties on the performance of gravel wearing course materials*. Ph.D. thesis, University of Pretoria.

Paige-Green, P. (1990*a*). Some surface roughness, loss, and slipperiness characteristics of unpaved roads. In: *Surface Characteristics of Roadways: International Research and Technologies*. ASTM International.

Paige-Green, P. (1990*b*). The structural design, construction and maintenance ofunpaved roads. *Committee of State Road Authorities. Draft TRH*, vol. 20.

Paige-Green, P. (2003). The geology and petrology of road construction materials revisited. In: *Proceedings*, pp. 1–7.

Paige-Green, P. (2004). The geology and engineering geology of roads in south africa. *SATC 2004*.

Paige-Green, P. and Heath, A. (1999). Material selection and structural design, construction and maintenance of ramp roads in open pit mines. In: *Geotechnics for Developing Africa: Proceedings of the 12th regional conference for Africa on soil mechanics and geotechnical engineering, Durban, South Africa, 25-27 October 1999*, vol. 12, p. 49. CRC Press.

Paige-Green, P., Pinard, M. and Netterberg, F. (2015). A review of specifications for lateritic materials for low volume roads. *Transportation Geotechnics*, vol. 5, pp. 86–98.

Pan, R., Zhang, G., Li, S., An, F., Xing, Y., Xu, D., Xie, R. *et al.* (2016). Influence of mineral compositions of rocks on mechanical properties. In: *50th US Rock Mechanics/Geomechanics Symposium*. American Rock Mechanics Association.

Pape, P.G. (2011). Adhesion promoters: Silane coupling agents. In: *Applied plastics engineering handbook*, pp. 503–517. Elsevier.

Porto, M., Caputo, P., Loise, V., Eskandarsefat, S., Teltayev, B. and Oliviero Rossi, C. (2019). Bitumen and bitumen modification: A review on latest advances. *Applied Sciences*, vol. 9, no. 4, p. 742.

Queiroz, C., Carapetis, S., Grace, H. and Paterson, W. (1991). Observed behavior of bituminous-surfaced low-volume laterite pavements. *Transportation Research Record*, , no. 1291.

Rahman, I.A. and Padavettan, V. (2012). Synthesis of silica nanoparticles by sol-gel: size-dependent properties, surface modification, and applications in silica-polymer nanocomposites—a review. *Journal of Nanomaterials*, vol. 2012.

Read, J. and Whiteoak, D. (2003). *Shell Bitumen Industrial Handbook*. Thomas Telford.

Ronald, M. and Luis, F.P. (2016). Asphalt emulsions formulation: State-of-the-art and dependency of formulation on emulsions properties. *Construction and Building Materials*, vol. 123, pp. 162–173.

Rossi, C.O., Caputo, P., Baldino, N., Lupi, F.R., Miriello, D. and Angelico, R. (2016). Effects of adhesion promoters on the contact angle of bitumen-aggregate interface. *International Journal of Adhesion and Adhesives*, vol. 70, pp. 297–303.

Rust, F., Akhalwaya, I., Jordaan, G. and Du Plessis, L. (2019). Evaluation of a nano-silane-modified emulsion stabilised base and subbase under hvs traffic.

Rust, F., Smit, M., Akhalwaya, I., Jordaan, G. and Du Plessis, L. (2020). Evaluation of two nano-silane-modified emulsion stabilised pavements using accelerated pavement testing. *International Journal of Pavement Engineering*, pp. 1–14.

Shu, B., Wu, S., Pang, L. and Javilla, B. (2017). The utilization of multiple-walled carbon nanotubes in polymer modified bitumen. *Materials*, vol. 10, no. 4, p. 416.

Sobolev, K. (2016). Modern developments related to nanotechnology and nanoengineering of concrete. *Frontiers of structural and civil engineering*, vol. 10, no. 2, pp. 131–141.

Steyn, W.J. (2009). Potential applications of nanotechnology in pavement engineering. *Journal of Transportation Engineering*, vol. 135, no. 10, pp. 764–772.

Steyn, W.J. (2011). Applications of nanotechnology in road pavement engineering. In: *Nanotechnology in civil infrastructure*, pp. 49–83. Springer.

Strano, M.S., Boghossian, A.A., Kim, W.-J., Barone, P.W., Jeng, E.S., Heller, D.A., Nair, N., Jin, H., Sharma, R. and Lee, C.Y. (2009). The chemistry of single-walled nanotubes. *MRS bulletin*, vol. 34, no. 12, pp. 950–961.

Sudla, P., Horpibulsuk, S., Chinkulkijniwat, A., Arulrajah, A., Liu, M.D. and Hoy, M. (2018). Marginal lateritic soil/crushed slag blends as an engineering fill material. *Soils and foundations*, vol. 58, no. 3, pp. 786–795.

Tannant, D. and Regensburg, B. (2001). Guidelines for mine haul road design.

Tannant, D.D. and Kumar, V. (2000). Properties of fly ash stabilized haul road construction materials. *International Journal of Surface Mining, Reclamation and Environment*, vol. 14, no. 2, pp. 121–135.

Tarrer, A. and Wagh, V. (1991). The effect of the physical and chemical characteristics of the aggregate on bonding. Tech. Rep., Strategic Highway Research Program, National Research Council Washington, DC.

Theyse, H. (2002). Stiffness, strength, and performance of unbound aggregate material: Application of south african hvs and laboratory results to california flexible pavements.

Theyse, H.L. and Muthen, M. (2000). Pavement analysis and design software (pads) based on the south african mechanistic-empirical design method. *SATC 2000*.

Thompson, RJ* & Visser, A. (1995). An overview of the structural design of mine haulage roads. *Journal of the Southern African Institute of Mining and Metallurgy*, vol. 96, no. 1, pp. 29–37.

Thompson, RJ* & Visser, A. (2000). The functional design of surface mine haul roads. *Journal of the Southern African Institute of Mining and Metallurgy*, vol. 100, no. 3, pp. 169–180.

Thompson, RJ* & Visser, A. (2007). Selection, performance and economic valuation of dust palliatives on surface mine haul roads. *Journal of the Southern African Institute of Mining and Metallurgy*, vol. 107, no. 7, pp. 435–450.

Thompson, R. (1996). The design and maintenance of surface mine haul roads.

Thompson, R. (2009). Ultra-heavy axle loads: design and management strategies for mine pavements. In: *PATREC research forum 2009*. PATREC.

Thompson, R. (2010). Mine haul road design and management best practices for safe and cost-efficient truck haulage. In: *Society for Mining, Metallurgy and Exploration 2010 Conference Proceedings Pre-print*, pp. 1–10. Society for Mining, Metallurgy and Exploration.

Thompson, R. (2011*a*). 10.6 design, construction, and maintenance of haul roads. In: *SME Mining Engineering Handbook, Volume 1*, pp. 957–977. Society for Mining, Metallurgy, and Exploration.

Thompson, R. (2011*b*). Mine haul road design and management: a review of current practice. *Transactions Society of Mining, Metallurgy and Exploration (SME)*, vol. 328, pp. 474–484.

Thompson, R. (2011*c*). Mine haul road design, construction and maintenance management. *Curtin University, Australia*.

Thompson, R. and Visser, A. (1996). Towards a mechanistic structural design method for surface mine haul roads. *Journal of the South African Institution of Civil Engineers*, vol. 38, no. 2, pp. 13–20.

Thompson, R. and Visser, A. (1997*a*). An introduction to the integrated design of surface mine haul roads. *International Journal o/Surface Mining, Reclamation and Environment*, vol. 11, no. 3, pp. 115–120.

Thompson, R. and Visser, A. (1997*b*). A mechanistic structural design procedure for surface mine haul roads. *International Journal o/Surface Mining, Reclamation and Environment*, vol. 11, no. 3, pp. 121–128.

Thompson, R. and Visser, A. (2000*a*). Designing and managing unpaved opencast mine haul roads for optimum performance. *TRANSACTIONS-SOCIETY FOR MINING METALLURGY AND EXPLORATION INCORPORATED*, vol. 308, pp. 69–77.

Thompson, R. and Visser, A. (2000*b*). Selection parameters for mine haul road wearing course materials. *International Journal of Surface Mining, Reclamation and Environment*, vol. 14, no. 1, pp. 1–17.

Thompson, R. and Visser, A. (2003). Mine haul road maintenance management systems. *Journal of the Southern African Institute of Mining and Metallurgy*, vol. 103, no. 5, pp. 303–312.

TRH14 (1985). Guidelines for road construction materials. committee of state road authorities. *Pretoria, South Africa. (Technical Recommendations for Highways Series, TRH 14)*.

Ugwu, O.O., Arop, J.B., Nwoji, C.U. and Osadebe, N.N. (2013). Nanotechnology as a preventive engineering solution to highway infrastructure failures. *Journal of construction engineering and management*, vol. 139, no. 8, pp. 987–993.

Van De Ven, M., Molenaar, A., Besamusca, J. and Noordergraaf, J. (2008). Nanotechnology for binders of asphalt mixtures. In: *Proceedings of the 4th Eurasphalt and Eurobitume Congress Held May 2008, Copenhagen, Denmark*.

Vavrik, W.R., Pine, W.J. and Carpenter, S.H. (2002). Aggregate blending for asphalt mix design: Bailey method. *Transportation Research Record*, vol. 1789, no. 1, pp. 146–153.

Venter, C. (2019). *Asphalt permeability and moisture damage*. Ph.D. thesis.

Visser, A.T. (2015). Haul roads can make money! *Journal of the Southern African Institute of Mining and Metallurgy*, vol. 115, no. 11, pp. 993–999.

Witucki, G.L. (1993). A silane primer: chemistry and applications of alkoxy silanes. *Journal of coatings technology*, vol. 65, pp. 57–57.

Yang, J. and Tighe, S. (2013). A review of advances of nanotechnology in asphalt mixtures. *Procedia-Social and Behavioral Sciences*, vol. 96, pp. 1269–1276.

Zhu, J., Birgisson, B. and Kringos, N. (2014). Polymer modification of bitumen: Advances and challenges. *European Polymer Journal*, vol. 54, pp. 18–38.

Zhu, W., Bartos, P.J. and Porro, A. (2004). Application of nanotechnology in construction. *Materials and Structures*, vol. 37, no. 9, pp. 649–658.

APPENDIX A

PROCEDURES

A.1 DRY SIEVE ANALYSIS AND WET SIEVE ANALYSIS

Method A1 (b) from TMH1

1. Firstly, ensure the material has been air dried to rid it off excessive moisture content. This is achieved by sun drying the material for enough time prior to any classification tests.
2. Depending on which size of the material is to be scalped, place the appropriate sieve above the feed chute if the sample splitter. The splitter shall be equipped with two receptacles to hold the two halves of the sample following splitting.
3. Obtain a representative sample of the refilled bulk material and thoroughly dry in a 110 °C oven until constant mass.
4. Accurately weigh the dried mass and recorded its total mass, hereafter, be cautious to avoid any loss of the material since this will affect the reliability and accuracy of results.
5. Wash the oven dried sample over two sieves, the 0.075mm and preferably 1mm at the top, the sample is placed into the top sieve and distilled water is used to wash off the materials ensuring that there is no material is lost, the bulk material is washed until the water looks clear denoting that most of the fines have been washed way.
6. Dry the sample again in a 110 °C oven until constant mass, then weigh and record the mass.
7. Stack a series of sieves on a mechanical shaker, from the pan until the selected top sieve depending on what particle size was scalped. Place the material sample in the top sieve and activate the mechanical shaker to separate samples into individual sizes.
8. Ensure the shaking is done for a proper amount of time, and when necessary, agitate the sieves to ensure the shaking is effective. Upon completion, weigh and record mass retained on each sieve to the nearest 0.1 grams. **Note** for a dry sieving analysis, steps 5 and 6 are not applicable.

A.2 OPTIMUM MOISTURE CONTENT/MAXIMUM DRY DENSITY

SANS3001-GR30

1. The hygroscopic moisture of the sample is determined using SANS 3001- GR20:2010 Edition 1, the standard details determination of moisture content by oven drying.

2. Six 7 kg bags are reconstituted based on target grading from the representative proportions which were separated from the bulk samples following a selected number of sieves. Reconstituted samples are sealed in plastic bags to prevent moisture loss prior to mixing.
3. Adjust dry mass of the aggregate by subtracting mass of the in-situ moisture content, this entirely dry mass is considered as the new dry mass and used to calculate the mass of water to be added to find the optimum moisture content.
4. Each sample is mixed with water at different moisture contents, the water is poured into the mixer containing one 7 kg aggregate sample as it rotates to ensure homogeneous mixing.
5. Upon completion a moisture sample is scooped from different areas within the mix and put in a container of known mass then weighed. This is placed in the 110 °C oven overnight or until constant mass.
6. After mixing two samples at two different moisture content, approximate densities are evaluated, this is helpful in identifying if moisture content should be increased or decreased. Based on these approximate densities, other samples are mixed, and their approximate densities calculated.
7. A steel weighed steel mould is assembled to the modified proctor hammer, the mix is compacted in the steel mould in 5 layers, with each layer roughly made by two and a half scoops. Each layer is compacted evenly by 55 blows.
8. The mould and compacted wet mix are weighed when all layers have been compacted to determine mass of mould plus wet mass.
9. All samples scooped from each mix are oven dried at 110 °C until constant mass, these are weighed when dry and moisture content and actual density are calculated. A plot of actual density and moisture content is drawn whose maximum denotes the maximum dry density (MDD) at a moisture content considered to be optimum (OMC).

A.3 ATTERBERG LIMITS TEST

ASTM D 4318-00 Liquid limit

1. Take roughly $\frac{3}{4}$ of the soil and place it into the porcelain dish. Thoroughly mix the soil with a small amount of distilled water it appears as a smooth uniform paste.
2. Weigh four of the empty moisture cans with their lids and record the respective weights and can numbers on the data sheet.

3. Adjust the liquid limit apparatus by checking the height of drop of the cup. Practice using the cup and determine the correct rate to rotate the crank so that the cup drops approximately two times per second.
4. Place a portion of the previously mixed soil into the cup of the liquid limit apparatus at the point where the cup rests on the base. Squeeze the soil down to eliminate air pockets and spread into the cup to a depth of about 10mm at the deepest point.
5. Use the grooving tool carefully cut a clean straight groove down the centre of the cup
6. Turn the crank of the apparatus at a rate of approximately two drops per second and count the number of drops it takes to make the two halves of the soil pat come into contact.
7. Take a sample, using the spatula, from edge to edge of the soil pat. Place the soil into a moisture can. Immediately weigh the moisture can containing the soil, record its mass, place the can into the oven. Leave the moisture can for at least 16 hours.
8. Remix the entire soil specimen in the porcelain dish. Add a small amount of distilled water to increase the water content so that the number of drops required closing the groove decrease.
9. Repeat the three steps before this one for at least two additional trials producing successively lower numbers of drops to close the groove

   Data Analysis
10. Determine the water content from each trial.
    Water content $= \frac{Tws-Tds}{Tds-T} \times 100$
    Where Tws is the tare with wet soil, Tds is the tare with dry soil, T is the tare mass.
11. Plot the number of drops, N, (on the log scale) versus the water content (w). Draw the best-fit straight line through the plotted points and determine the liquid limit (LL) as the water content at 25 drops.

Plastic Limit

1. Weigh the empty moisture cans with their lids and record the respective weights and can numbers on the data sheet.
2. Take the remaining $\frac{1}{4}$ of the original soil sample and add water until the soil is at a consistency where it can be rolled without sticking to the hands.
3. Form the soil into an ellipsoidal mass. Roll the mass between the palm or the fingers and the glass
4. When the diameter of the thread reaches the correct diameter break the thread in several

pieces. Knead and reform the pieces into ellipsoidal masses and re-roll them. Continue this alternate rolling, gathering, kneading and re-rolling until the thread crumbles under the pressure required for rolling.

5. Gather the potions of the crumbled thread together and place the soil into moisture can and then cover it.
6. Place the can into the 110°C oven. Leave the moisture can in the oven for at least 16hrs.
7. Repeat the three steps before this one at least two more times.
   Data analysis
8. Determine the water content from each trial
   Water content = $\frac{Mws-Mds}{Mds-M} \times 100$
   Where Mwc is the mass of the container with wet soil, Mdc is the mass of the container with dry soil and Mc is the mass of the container.
9. Compute the average of the water contents to determine the plastic limit, PL

A.4 INDIRECT TENSILE TESTING

Draft August 2016. Compiled by BSM Laboratories

1. Firstly, ensure the testing temperature is 25 °C ±2 °C by placing the test specimens in a temperature chamber for a minimum of 4 hours prior to testing.
2. The height, diameter and weight of each test specimen is recoded to the nearest 0.1 mm. The height is measured at three different places around the circumference of the test specimen.
3. The loading apparatus is then placed on the shelf inside the Universal Testing Machine (UTM).
4. Upon recording specimens dimensions, it is placed on the bottom loading strip, ensure it is stable then place the top loading strip diametrically opposite the bottom strip, inspect for symmetry. Ensure the strips are parallel and centred on the vertical plane, appropriately sized loading strips should be used for specimens being tested, 20 mm loading strips for 150mm diameter samples.
5. Using the computer software; stress and strain program the shelf inside the UTM is then raised until the top of the loading apparatus contacts the bottom of the actuator, preventing any force from being applied to the core and loading apparatus. The same software is used to adjust the position of the actuator.

6. On the loaded test software program, input necessary parameters for the test specimen. These parameters include the specimen height, maximum load accurate to 0.1 kN, the loading rate of 50.8 mm per minute as well as the axial loading type (which is actuator displacement).
7. The test is then started and is stopped once the maximum load has been applied to the test specimen which fractures diametrically under applied loading.
8. Once the maximum load is achieved and the test stopped, the temperature at break is recorded; this is done by using the temperature gun with a laser point on the test specimen centre.
9. A moisture sample is taken, placed in a container of known mass, then its wet mass is recorded then placed in a 110 °C oven to achieve dry mass, this is done to determine moisture content at break. Moisture content determination procedure is detailed in (SANS 3001, Test Method GR 20)
10. The shelf is then lowered, and the loading apparatus removed, remnants of a broken test specimens are thoroughly cleaned in the UTM machine to keep the equipment clean and in preparation for further testing
11. The results from the test are also automatically captured by the testing software and used for further calculations.
12. The ITS value calculation is the calculated using the maximum force recorded and test specimen average dimensions.
13. This entire process is repeated for each core.

A.5 TRIAXIAL TEST: MONOTONIC

Draft August 2016. Compiled by BSM Laboratories

1. Firstly, ensure the testing temperature is 25 °C ±2 °C by placing the test specimens in a temperature chamber for a minimum of 4 hours prior to testing.
2. The height, diameter and weight of each test specimen is recorded to the nearest 0.1 mm. The height is measured at three different places around the circumference of the test specimen.
3. Carefully lift the test specimen off the mass balance and place it in the mid base plate without damaging its edges. Cautiously, fit the inflatable tube onto the specimen without damaging it, ensure the inflatable bladder is inflated so that it fits easily.
4. Cover the assembly with a metal casing and sufficiently fasten it to the base plate using

bolts to secure the setup while under loading. Ensure there is adequate spacing between the actuator and the base plate of the testing machine

5. The assembly is lifted on the base plate of the UTM, the top plate is then placed at the top of the specimen encased in a metal casing. Ensure the base plate of the UTM is at the selected reference point. The actuator is then lowered down using adjustment knobs until it barely contacts the depression of the top plate then locked in place.
6. Connect the air supply to the inflation valve from the confining cylinder and adjust the pressure gauge to the necessary amount of pressure. A total of 8 samples is tested under dry conditions with each per being tested at each confining pressure: 0 kPa,50 kPa,100 kPa,200 kPa.
7. Using the computer testing program, input the necessary test parameters, constant displacement rate, strain break percentage
8. Once the specimen has failed, the test is stopped, this is seen by the maximum applied load reducing from the maximum and declines steeply denoting the specimen cannot resist the load anymore.
9. The confining pressure is released, loading ram is adjusted back to its original position. Using the testing software, the position of the UTM loading plate is lowered to the bottom point, easily remove the confining cylinder assembly off the loading frame.
10. Unfasten the assembly and remove both the metal casing and the inflatable tube, immediately break the sample, measure the temperature using the temperature gun and record it. Take at least 1000 g of the deformed sample weigh it off to determine the moisture content at break following standard test method detailed in SANS 3001, Test Method GR 20.
11. This procedure is similar for all test specimens tested at both dry conditions and wet conditions. Wet specimens are tested at 100 kPa pressure and their results are used to determine retained strength. The maximum force recorded is used to calculate the applied stress at each confining pressure, a plot of applied stress and confining pressure is done to obtain the shear parameters of the tested material.

A.6 TRIAXIAL TEST: RESILIENT MODULUS

1. Firstly, the deviator stress ratios determined form the material cohesion and internal friction angle are captured into MTS software before testing, these are coded into testing profiles and retrieved during testing.

2. Test specimens are weighed off and mass recorded. The latex membrane is initially stretched using the metal membrane stretcher which is has an air tube connected to rid the assembly off entrapped air.

3. The test specimen is placed on the base disc underlain by a base plate, it is then sealed with the latex membrane, the air tube closing is released, allowing the latex membrane to return to its normalcy, then the membrane stretcher removed. The loading cap is placed at the top of the specimen, the membrane is then rolled down and up at the specimens top and bottom respectively, the two areas are then tightly fastened using two O-rings at each area to prevent air movement.

4. The LVDT holders are placed parallel to each other at 1/3 and 2/3 along the specimen height then tightly fastened around the sealed test specimen using rubber bands. LVDT probes are inserted and sufficiently secured by bolts, they are adjusted such that half end of movable part is visible. The steel brace is then placed on a clean lubricated surface, followed by a glass casing.

5. The LVDT cables are then connected to the corresponding cables on the pressure chamber top cover, which is also assembled on to the system using nuts and tie rots. A steel piston is aligned to the depression of the loading cap, care must be taken when placing the piston as it may cause a safety hazard or injury should it drop.

6. The assembly is then lifted to the base plate of the UTM, loading ram lowered to just above the steel piston top and pressure connected to the valve. A pressure test is the carried out to check for any air leakages, pressure gauge is adjusted to 200 kPa to check if it stays constant or declines signalling air leak.

7. A preload of 0.4KN is applied to seat the specimen, this, and other input parameters such as specimen dimensions are captured. The test is began starting at 200 kPa and the software automatically records all results.

8. The test goes through all stress levels per confining pressure and once done, the testing software program warns that the confining pressure be changed to 150 kPa until it requires an adjustment to 20 kPa at which testing is complete.

9. The data is recorded and retrieved to be used in resilient modulus determination.

A.7 HIGH PRESSURE PERMEABILITY

1. Firstly, the test apparatus should be thoroughly cleaned with a paint brush to ensure that the filter material does not create a pathway for a water leak or damage the silicone rubber mould of the inflatable seal.
2. Place the core inside the silicone rubber mould and then inflate the seal to 300 kPa.
3. Place the rubber between the top and bottom section of the apparatus and then place the top section of the apparatus on the rubber.
4. Tighten the bolts of the apparatus to lock the two sections of the apparatus together.
5. Close valve 2 and open valve 1 to fill the apparatus with water until the 0 ml mark is reached.
6. Tilt the apparatus to the side until all the water is out of the level indicator and then open valve 2. Slowly lower the apparatus back to its original position until water flows out of valve 2, which should then be closed. Lower the apparatus to its original position. This is done to force all air out of the system.
7. Close valve 1 and make sure that valve 3 is completely open.
8. Set the compressor to 100 kPa and apply this pressure by attaching the quick coupling nozzle to the apparatus. Record the water level and start the stopwatch for 1 minute. After 1 minute has passed, record the final water level and remove the pressure. This is done as an initial wetting of the core.
9. Leave the apparatus to settle for another minute and then apply 100 kPa pressure by attaching the quick coupling nozzle to the apparatus. Record the water level and start the stopwatch. Apply this pressure for 20 minutes and record the water level every 5 minutes.
10. After 20 minutes record the last reading and remove the pressure by disconnecting the compressor nozzle.
11. Repeat step 9 and 10 for 150 kPa as well as 200 kPa. Stellenbosch University https://scholar.sun.ac.za If the core is very permeable and water flows through before the 20 minute mark is reached, record the time it takes for the water level to reach 100 ml, 200 ml, 300 ml, etc. until it is completely empty.
12. Once the test has been conducted for 100 kPa, 150 kPa and 200 kPa the water can be drained from the apparatus, the seal can be deflated and thoroughly cleaned before the next test is conducted.

APPENDIX B

X-RAY DIFFRACTION

B.1 XRD MIX DESCRIPTION

Table B.1: XRD mix ID descriptions

	Laterite		**Kalumbila GCS**		**Kansanshi CS**
ID	Mix	ID	Mix	ID	Mix
1	Natural Aggregates	19	Natural Aggregates	2	Natural Aggregates
3	SS60NME	8	CSS60	14	SS60NME+ 1% Lime
4	SS60	9	SS60NME	15	CSS60
5	0.5%(Terrasil+and Zycobond)	10	SS60	16	SS60
6	CSS60	11	CSS60+0.5% Terrasil+	17	CSS60 + 1% Terrasil+
7	CSS60+0.5%(Terrasil+ and Zycobond)	12	CSS60+0.65kg/m3 (Terrasil+ and Zycobond)	18	SS60NME
		13	CSS60+0.5% Terrasil+		

B.2 UNTREATED SAMPLES

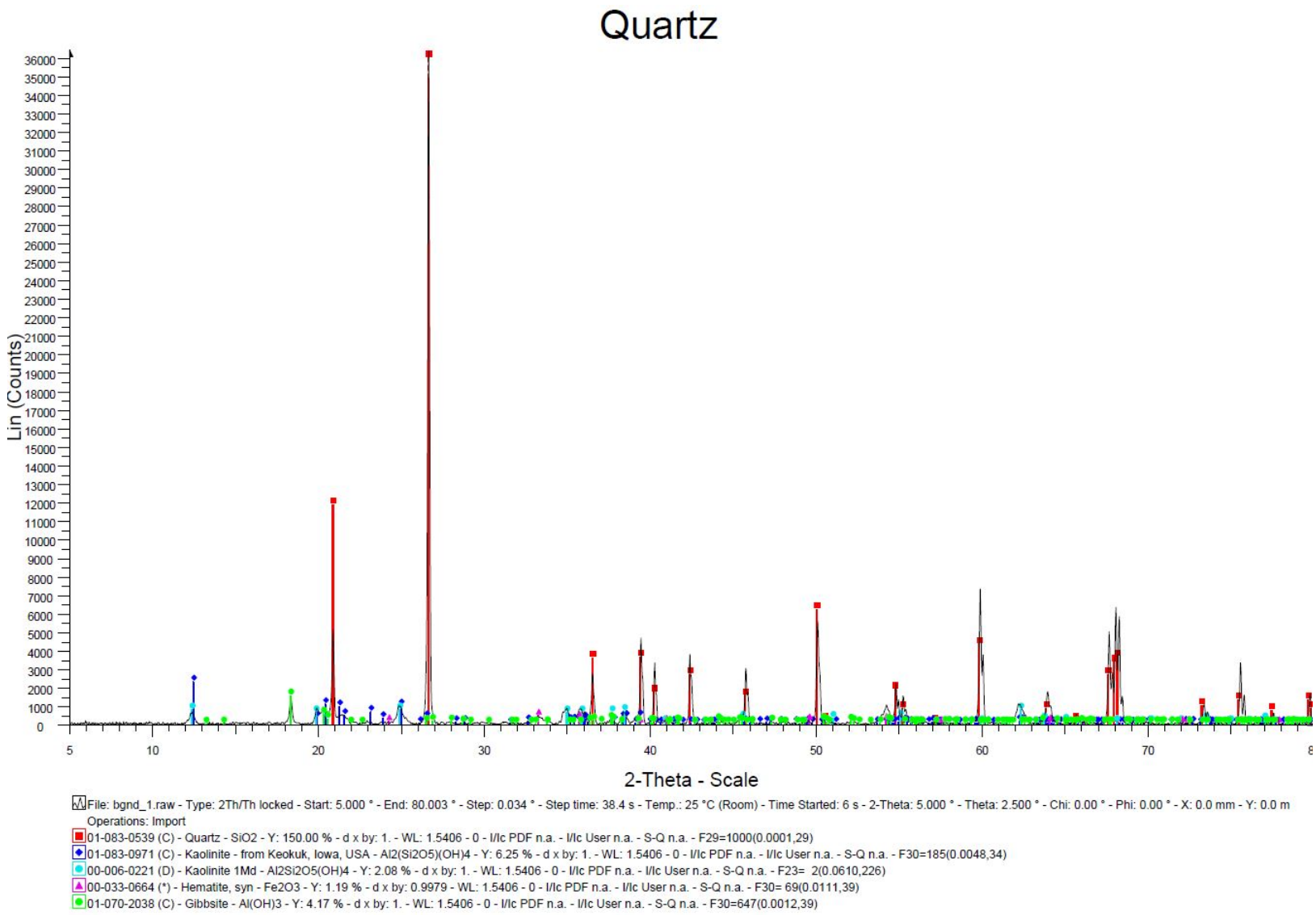

Figure B.1: Laterite XRD pattern

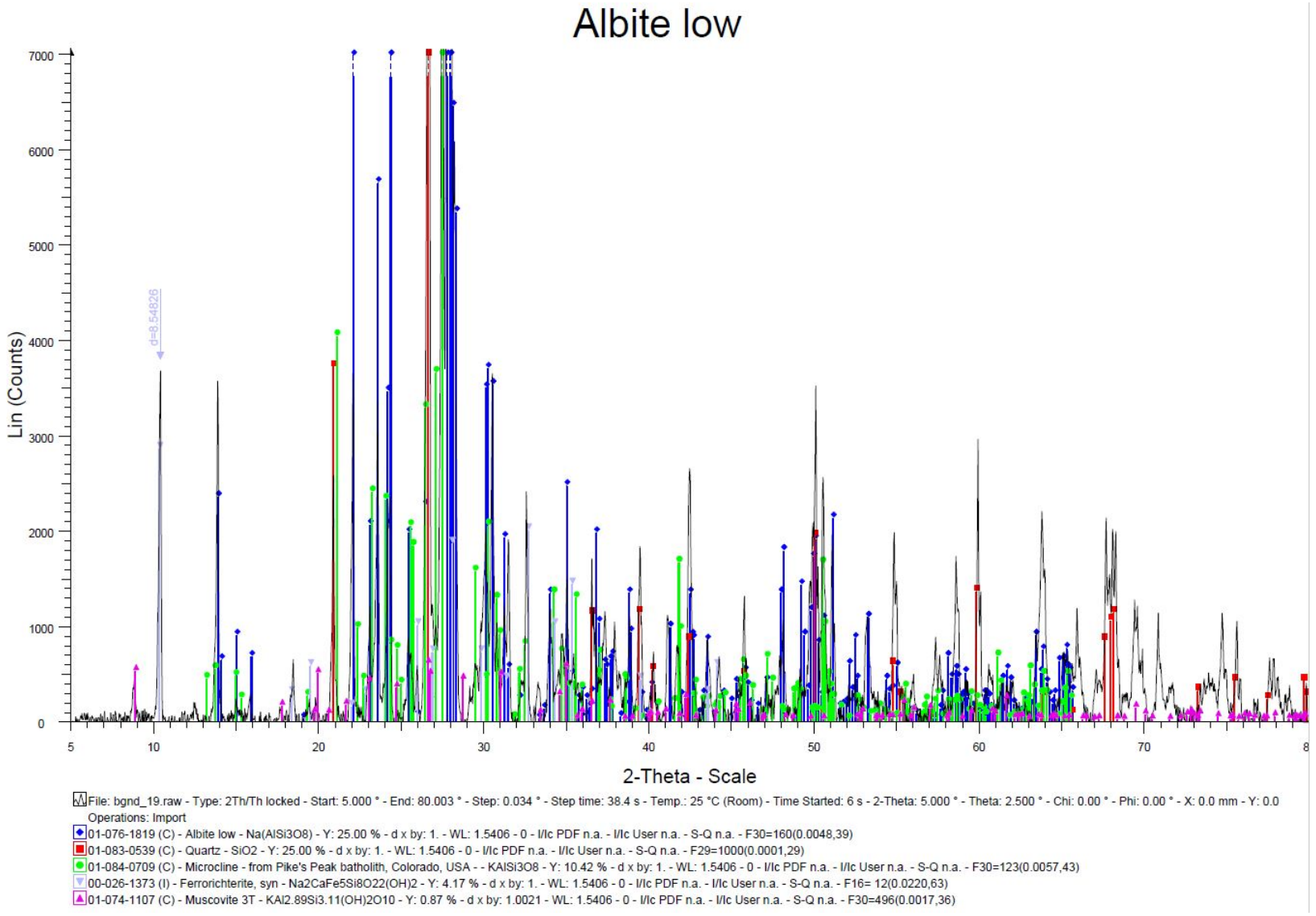

Figure B.2: Kalumbila GCS XRD pattern(close view)

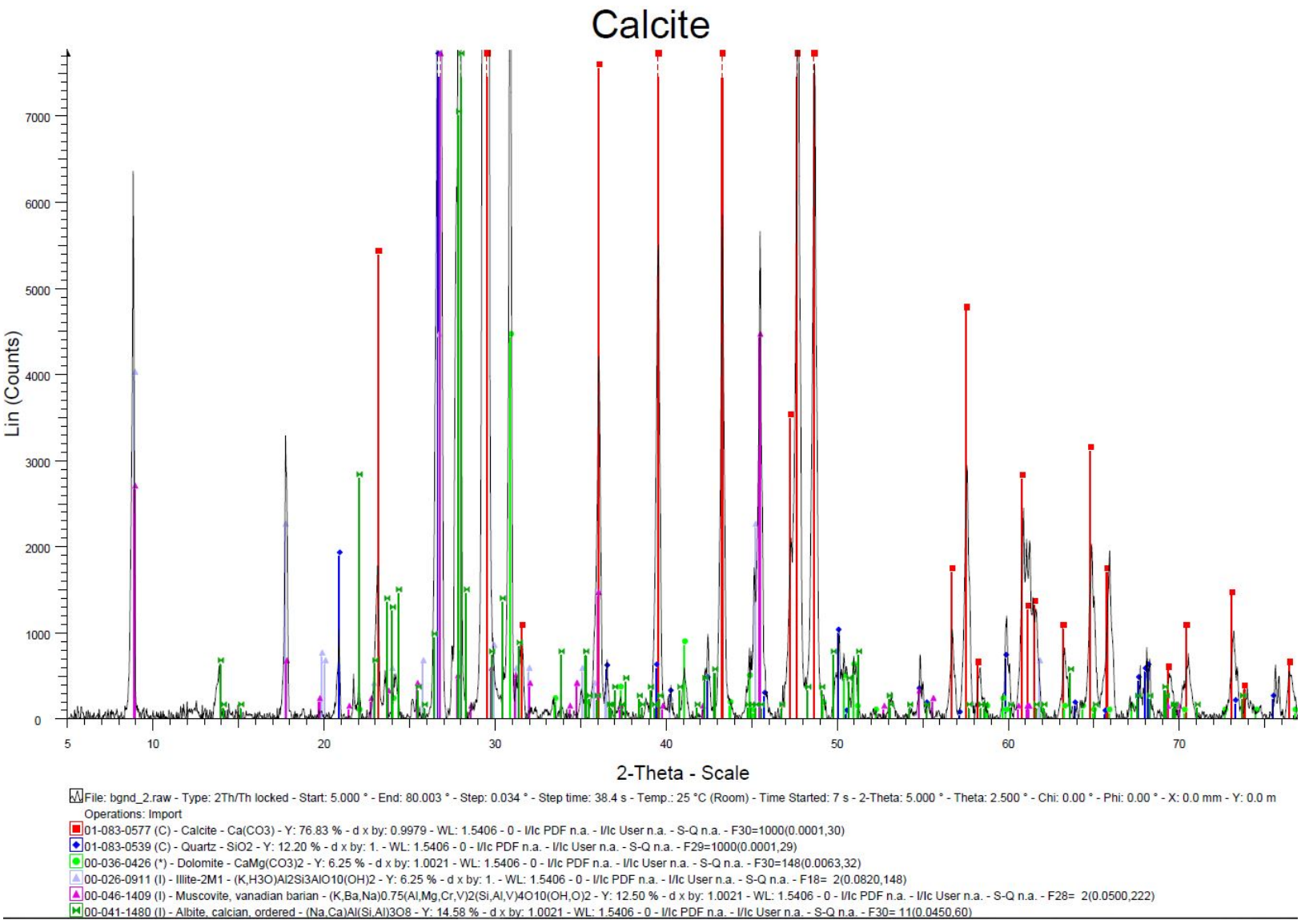

Figure B.3: Kansanshi CS XRD pattern(close view)

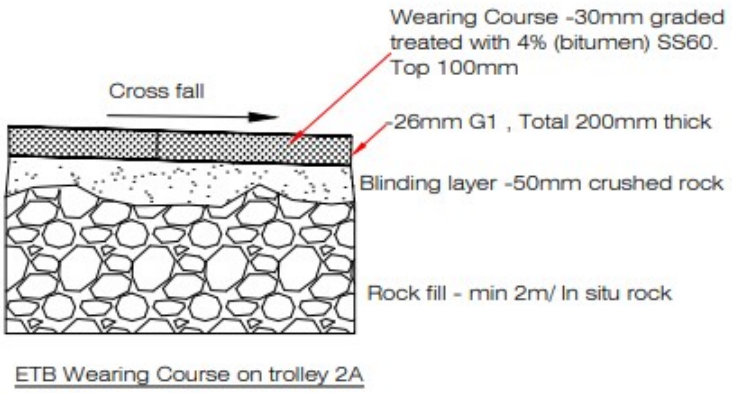

ETB Wearing Course on trolley 2A

Surfacing:

1. 200mm Unbound base - 26 G1 crushed rock
2. 4% SS60 mixed into 100mm layer of the base (8Litres SS60 per square metre)

Figure B.4: Pavement Structure on trolley 2A

B.3 TREATED SAMPLES

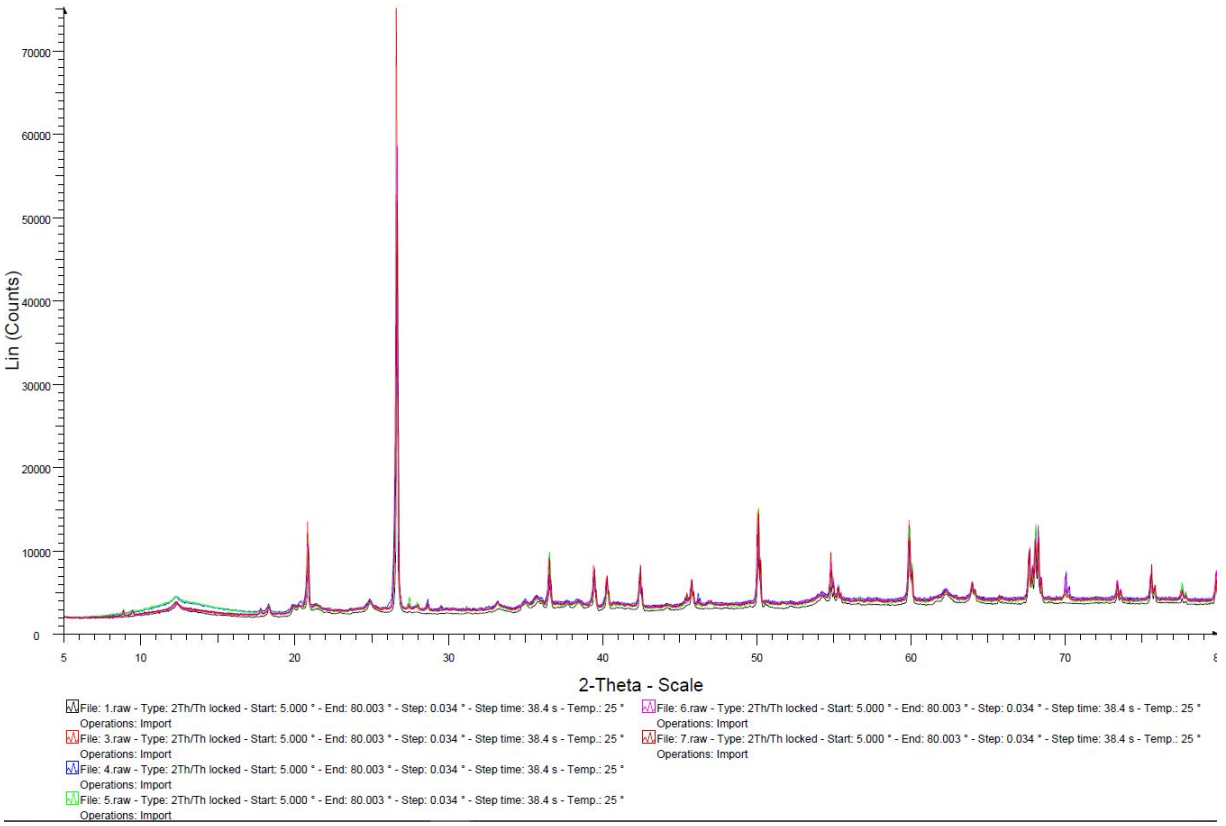

Figure B.5: All laterite Samples XRD patterns

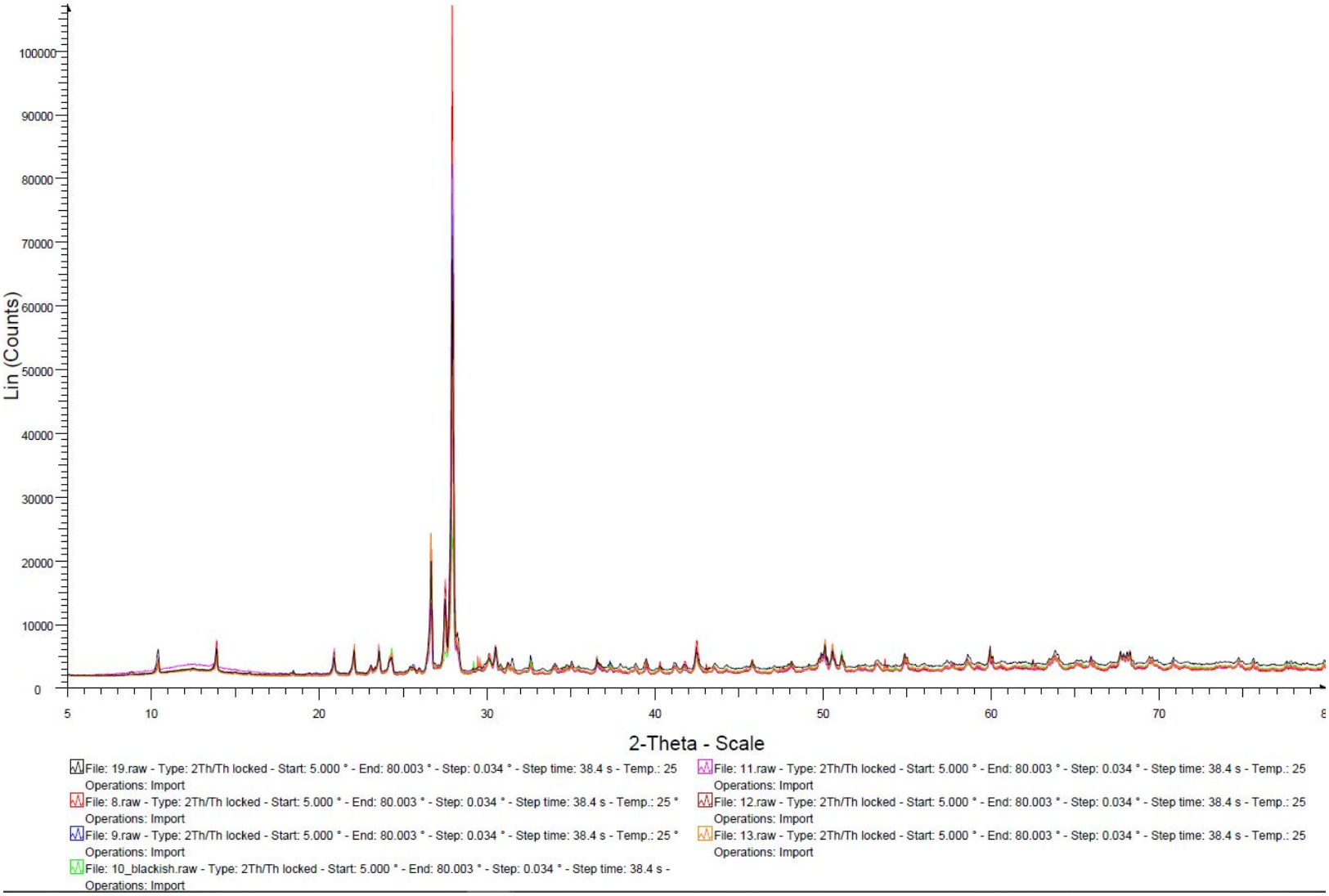

Figure B.6: All Kalumbila GCS Samples XRD patterns

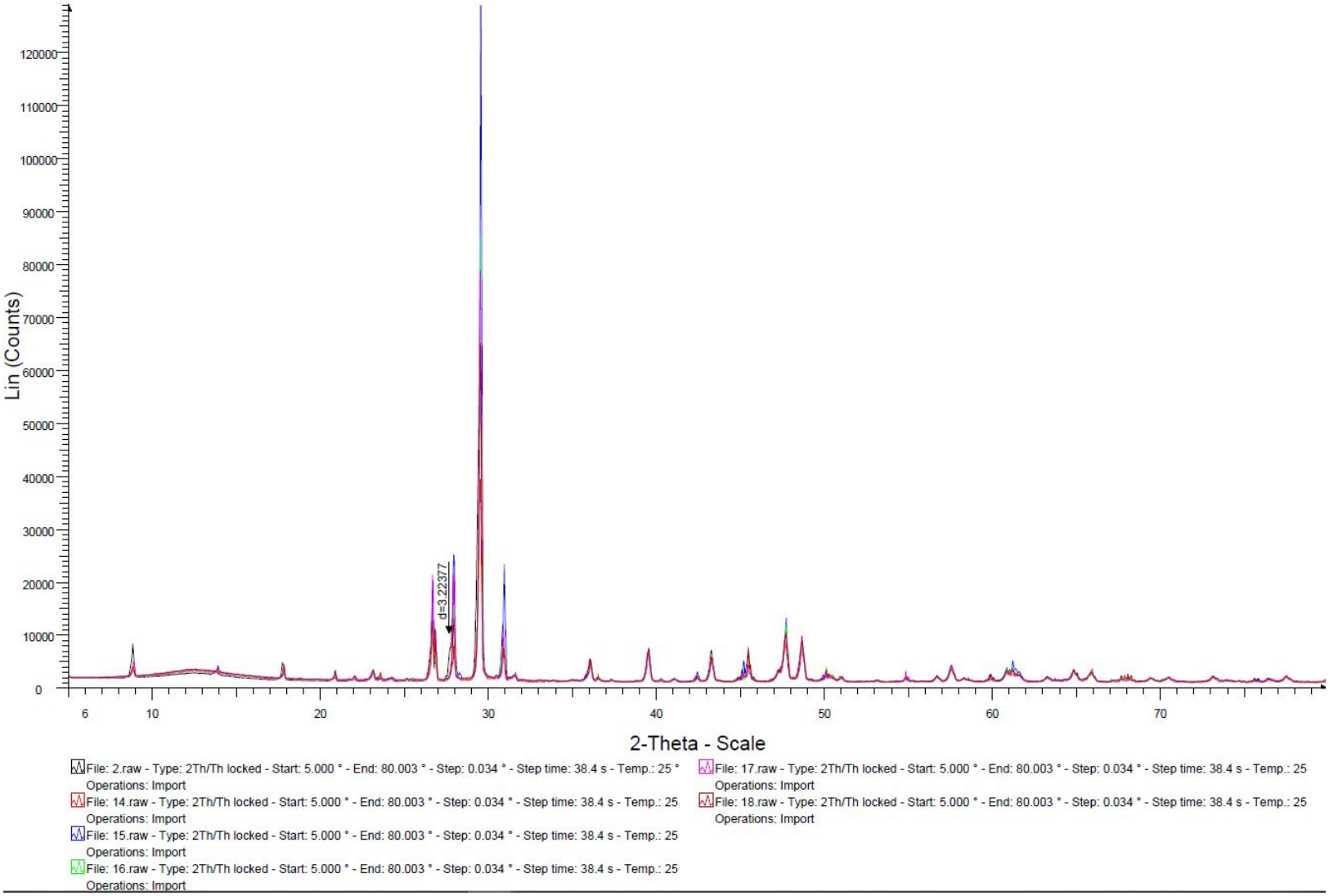

Figure B.7: All Kansanshi CS Samples XRD patterns

APPENDIX C

STRENGTH TEST

C.1 INDIRECT TENSILE STRENGTH

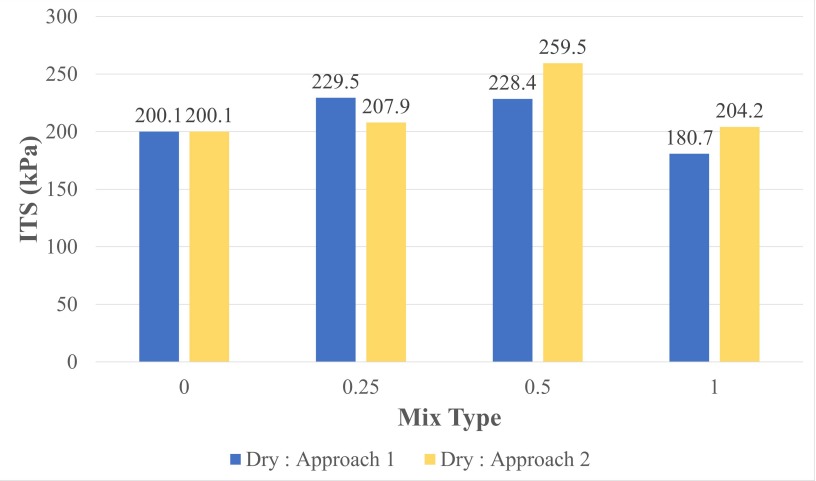

Figure C.1: CSS60NME treated dry laterite samples ITS

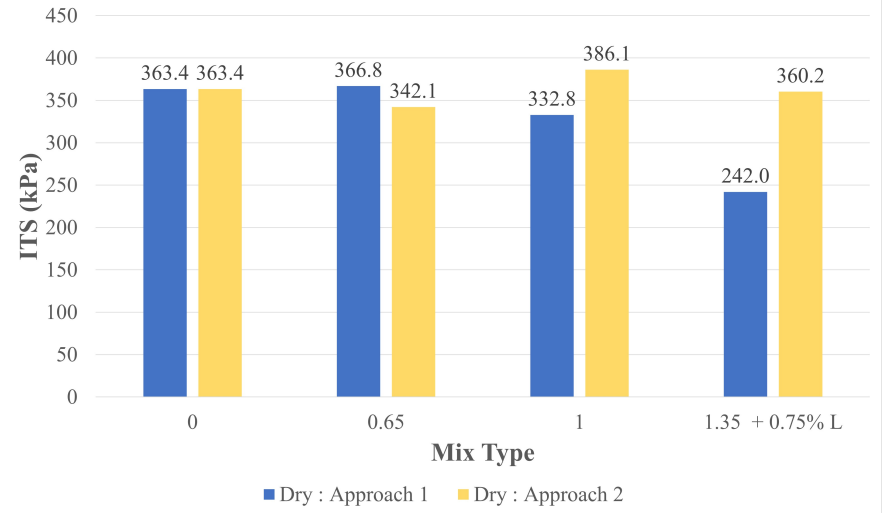

Figure C.2: CSS60NME treated dry Kalumbila GCS samples ITS

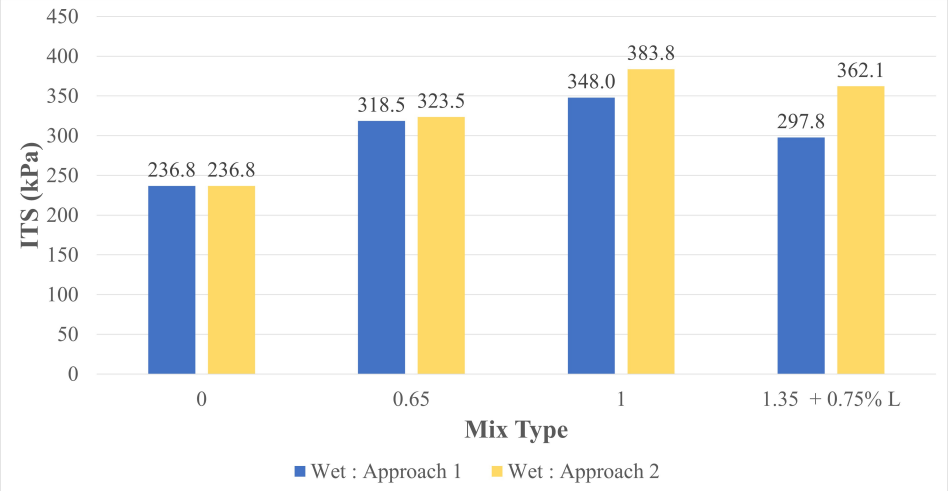

Figure C.3: CSS60NME treated wet Kalumbila GCS samples ITS

C.2 MONOTONIC TRIAXIAL TESTING

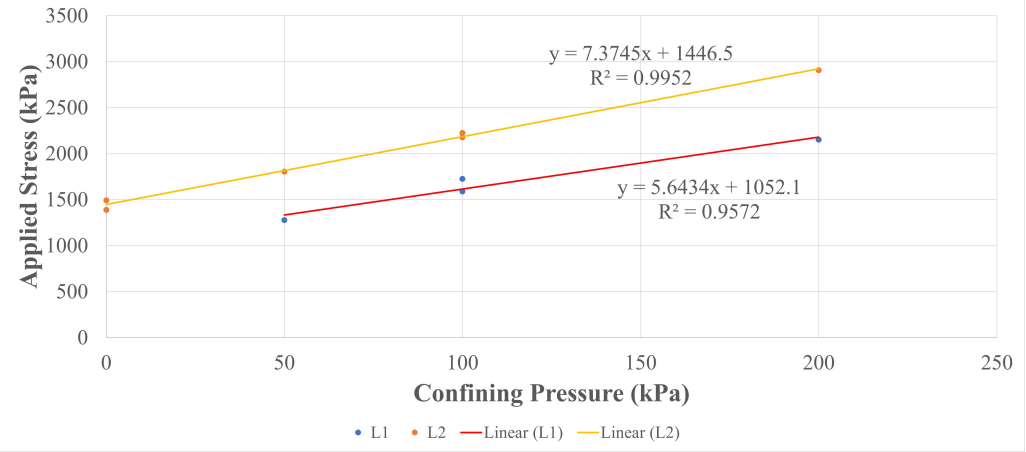

Figure C.4: Laterite triaxial test results regression lines

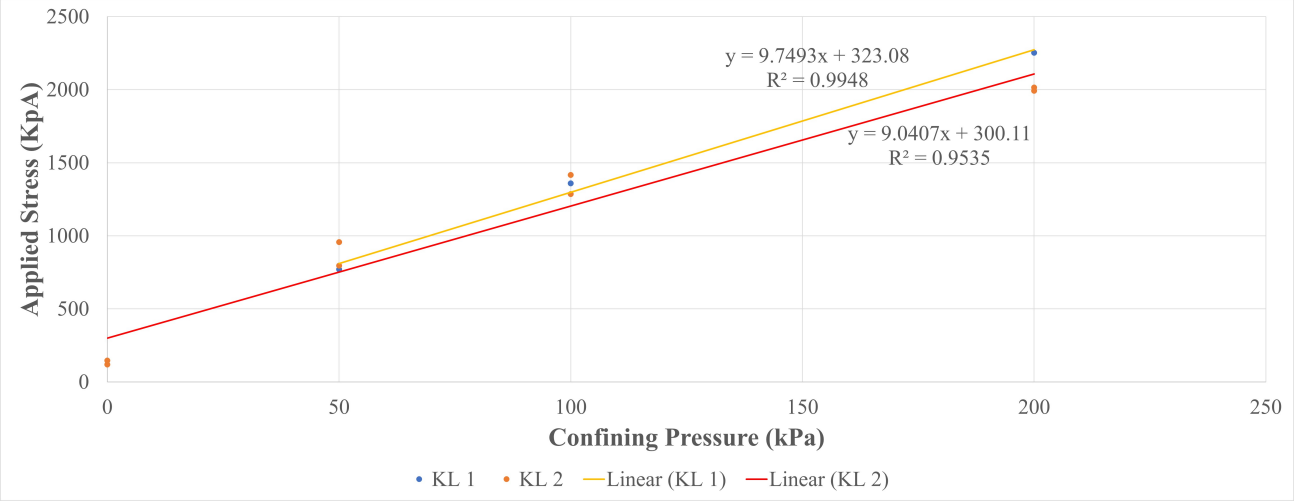

Figure C.5: Kalumbila GCS triaxial test results regression lines

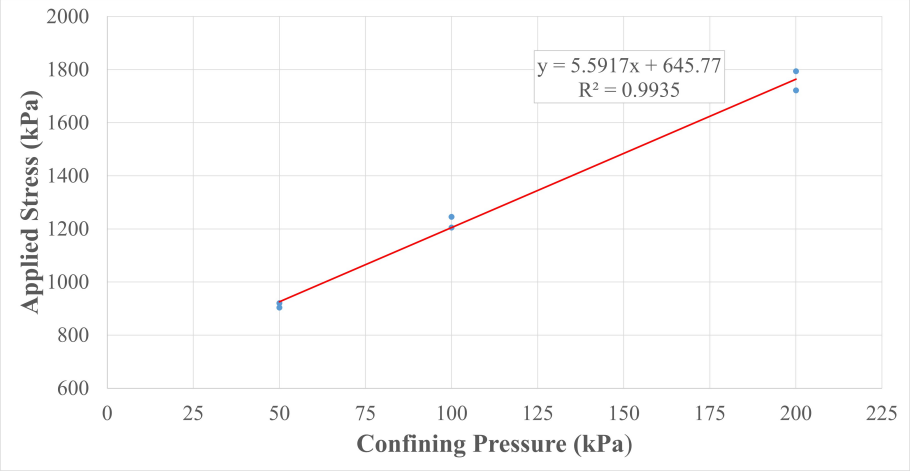

Figure C.6: Kansanshi CS triaxial test result regression line

APPENDIX D

TRIAXIAL TESTING

Laterite+ SS60 + 0.5% Lime

				Thickness (mm)						
							200			
Criteria	σ1	σ3	θ	Mr	σ1,f	σd	σd,f	DSR	C	ϕ°
1	610.7	322.0	1252.5	928.0	3825.8	288.7	3503.9	8.2	266.3	49.6
2	635.1	359.1	1345.2	961.1	4100.5	276.0	3741.4	7.4	266.3	49.6
3	636.4	395.0	1411.4	984.1	4365.6	241.4	3970.6	6.1	266.3	49.6
4	605.4	371.1	1333.3	956.9	4188.8	234.3	3817.8	6.1	266.3	49.6
5	627.6	501.4	1594.2	1044.9	5151.4	126.2	4650.0	2.7	266.3	49.6
6	631.3	470.8	1539.2	1027.0	4925.6	160.4	4454.8	3.6	266.3	49.6

				Thickness (mm)						
							300			
Criteria	σ1	σ3	θ	Mr	σ1,f	σd	σd,f	DSR	C	ϕ°
1	560.7	236.2	1027.8	841.9	3192.0	324.6	2955.9	11.0	266.3	49.6
2	595.3	271.1	1136.9	884.8	3450.5	324.1	3179.4	10.2	266.3	49.6
3	603.2	297.2	1193.1	906.0	3642.9	306.0	3345.7	9.1	266.3	49.6
4	554.7	260.9	1074.6	860.6	3375.0	293.7	3114.1	9.4	266.3	49.6
5	584.4	363.0	1292.2	942.3	4129.3	221.4	3766.3	5.9	266.3	49.6
6	596.0	344.3	1268.5	933.8	3990.9	251.7	3646.6	6.9	266.3	49.6

Kalumbila GCS + CSS60 +0.5% (Terrasil+ & ZycoBond)

				Thickness (mm)						
							200			
Criteria	σ1	σ3	θ	Mr	σ1,f	σd	σd,f	DSR	C	ϕ°
1	598.8	312.5	1221.2	1220.0	3124.3	286.3	2811.8	10.2	49.9	53.2
2	625.6	358.6	1333.6	1332.2	3540.5	267.0	3181.9	8.4	49.9	53.2
3	628.1	399.3	1409.7	1408.3	3908.4	228.8	3509.1	6.5	49.9	53.2
4	591.4	362.0	1300.7	1299.4	3571.2	229.4	3209.2	7.1	49.9	53.2
5	612.3	513.6	1600.6	1599.0	4941.5	98.7	4427.9	2.2	49.9	53.2
6	620.2	481.6	1546.5	1544.9	4651.8	138.6	4170.2	3.3	49.9	53.2

				Thickness (mm)						
							300			
Criteria	σ1	σ3	θ	Mr	σ1,f	σd	σd,f	DSR	C	ϕ°
1	550.5	230.2	1005.4	1004.4	2380.3	320.3	2150.1	14.9	49.9	53.2
2	583.4	267.0	1116.8	1115.6	2712.9	316.4	2445.9	12.9	49.9	53.2
3	590.6	294.4	1174.6	1173.4	2960.1	296.2	2665.8	11.1	49.9	53.2
4	543.0	254.2	1049.9	1048.8	2596.9	288.8	2342.7	12.3	49.9	53.2
5	567.8	362.2	1273.5	1272.2	3572.7	205.6	3210.5	6.4	49.9	53.2
6	581.4	342.9	1250.4	1249.2	3398.4	238.5	3055.6	7.8	49.9	53.2

Figure D.1: DSR values of laterite and Kalumbila GCS at 200mm and 300mm

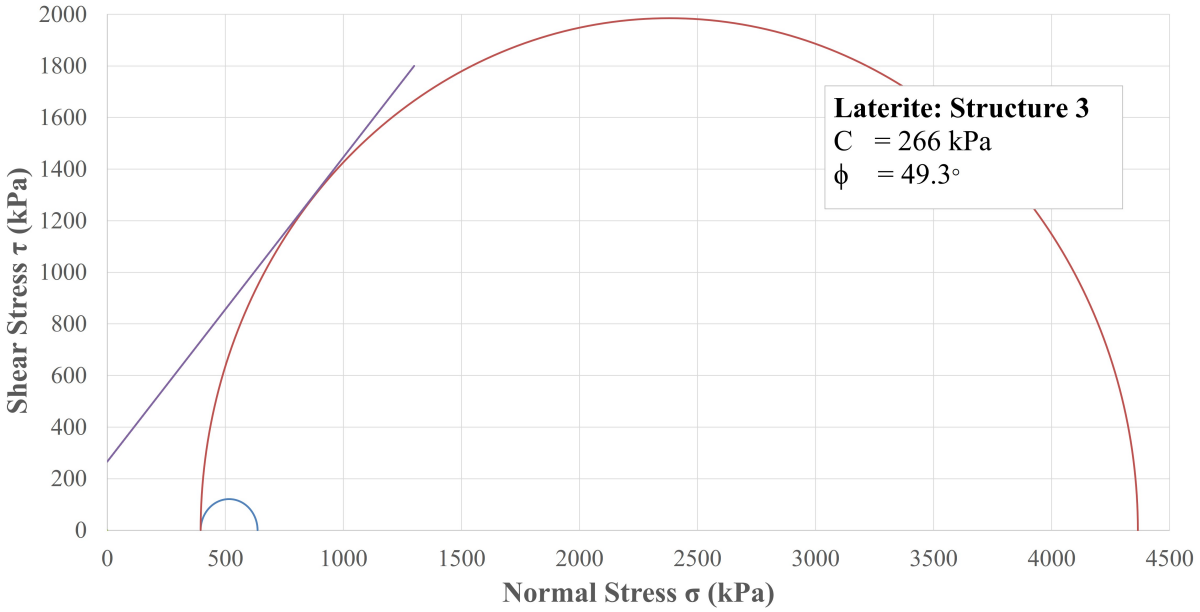

Figure D.2: Mohr circle of laterite structure 3

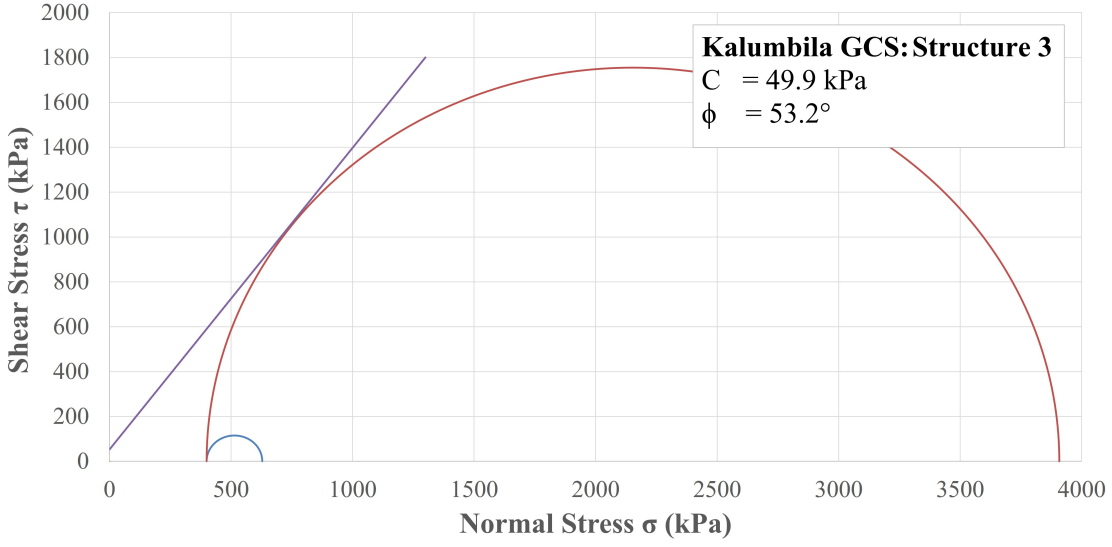

Figure D.3: Mohr circle of Kalumbila GCS structure 3

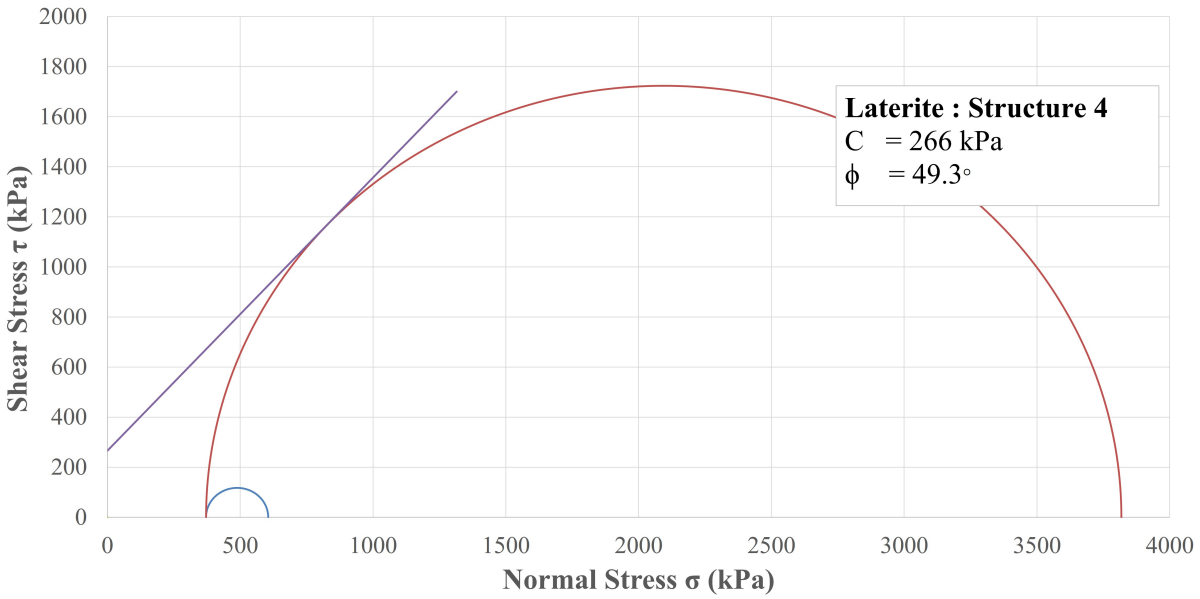

Figure D.4: Mohr circle of laterite structure 4

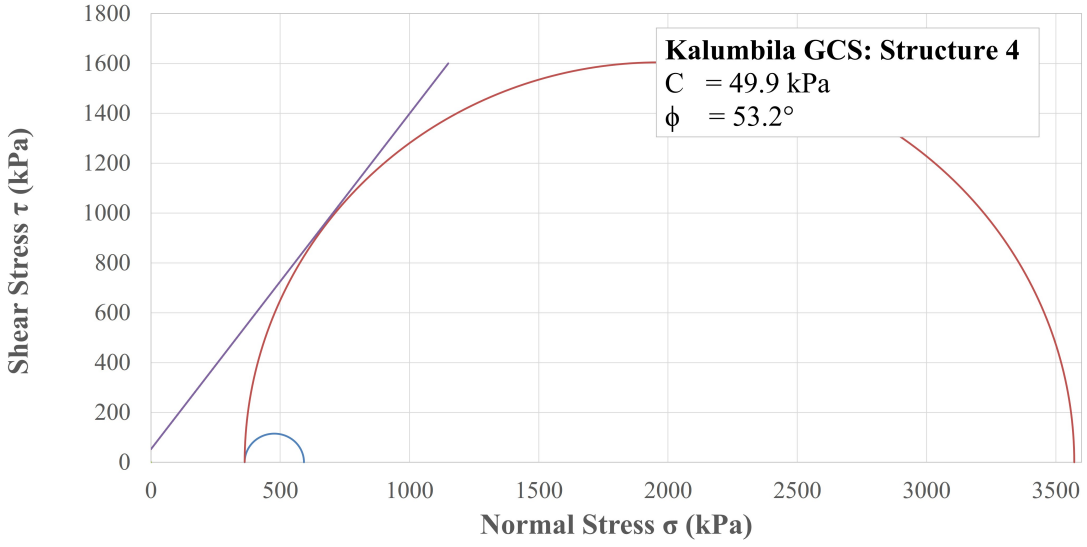

Figure D.5: Mohr circle of Kalumbila GCS structure 4